IMPROVING NUCLEAR DISASTER PREPAREDNESS THROUGH SYNOPTIC WEATHER ANALYSIS, THREE-DIMENSIONAL URBAN STRUCTURE INTEGRATION, AND POPULATION-LEVEL PUBLIC HEALTH CONSIDERATIONS FOR CASUALTY ESTIMATES AND SCARCITY OF HEALTH RESOURCES

by

MORGAN ASHLEY TAYLOR

(Under the Direction of Mark Ebell and Curt Harris)

ABSTRACT

Given the rare nature of nuclear disasters, researchers must continually expand upon existing methods to increase the accuracy and validity of nuclear models that better support the emergency management, health care, and public health communities in their preparedness efforts. This dissertation takes measured steps towards such a goal, by using simulated 15 kiloton (kt) improvised nuclear device (IND) detonations in Atlanta, Georgia (GA). An analysis of the simulated fallout radiation plumes throughout 2019 identified four clusters that captured the variation in the geospatial and population impacts. The medoids of the clusters were used in expanding upon the existing nuclear modeling framework by integrating building-specific attributes to account for thermal and radiation effects in an urban environment. Under the thermal attenuation model, approximately half of the buildings that would have previously been assumed to have been exposed to enough thermal fluence to cause either burns or mass fires were shadowed by the surrounding environment and therefore were no longer exposed to such levels of thermal radiation. Under a warned scenario, in which people would have time to seek

shelter in a basement or in the most interior room of a building, more than 90% of buildings that were externally exposed to more than 200 rads of fallout radiation received less than 200 rads internally due to the protection offered by building characteristics, such as construction material, height, and the presence of a basement. Across the four simulations, an estimated 185,896 to 196,537 individuals would not survive their injuries, and an additional 31,939 to 46,668 patients would require immediate health care. Another 454,015 to 1,060,235 individuals would require delayed or minimal care. While these estimates alone would overwhelm the health care infrastructure, the strain would be further exacerbated by losing health care facilities directly to the detonation. Even when surge capacity was considered, there would only be enough staffed beds in GA for approximately 25% of the patients requiring immediate health care. Multi-jurisdictional, innovative preparedness efforts to address these resource limitations, based on increasingly accurate models and simulations, will be imperative for a successful response to an IND detonation in the US.

INDEX WORDS: Nuclear model, Disaster preparedness, Casualty estimates, Public health, Health care resources

IMPROVING NUCLEAR DISASTER PREPAREDNESS THROUGH SYNOPTIC WEATHER ANALYSIS, THREE-DIMENSIONAL URBAN STRUCTURE INTEGRATION, AND POPULATION-LEVEL PUBLIC HEALTH CONSIDERATIONS FOR CASUALTY ESTIMATES AND SCARCITY OF HEALTH RESOURCES

by

MORGAN ASHLEY TAYLOR

AEMT, Emory University, 2013

BS, Emory University, 2016

MPH, University of Georgia, 2019

A Dissertation Submitted to the Graduate Faculty of The University of Georgia in Partial Fulfillment of the Requirements for the Degree

DOCTOR OF PHILOSOPHY

ATHENS, GEORGIA

2023

IMPROVING NUCLEAR DISASTER PREPAREDNESS THROUGH SYNOPTIC WEATHER ANALYSIS, THREE-DIMENSIONAL URBAN STRUCTURE INTEGRATION, AND POPULATION-LEVEL PUBLIC HEALTH CONSIDERATIONS FOR CASUALTY ESTIMATES AND SCARCITY OF HEALTH RESOURCES

by

MORGAN ASHLEY TAYLOR

Major Professor:	Mark Ebell
Co-Chair:	Curt Harris
Committee:	Kevin Dobbin
	Andreas Handel
	Michelle Ritchie

Electronic Version Approved:

Ron Walcott
Vice Provost for Graduate Education and Dean of the Graduate School
The University of Georgia
May 2023

DEDICATION

This work is dedicated to endless number of people who have supported me throughout my entire education. While there is not enough space to list each of you, I could not have completed this degree without your support and guidance. Thank you for making me see this adventure through to the end.

ACKNOWLEDGEMENTS

Thank you to Dr. Curt Harris for everything; for embarking on this process with me, for being supportive every step of the way, and for encouraging me to chase my dreams. Thank you to Dr. Mark Ebell for joining this project and for your guidance throughout the dissertation process. A debt of gratitude is particularly owed to Dr. William Bell for his time, energy, and mentorship. This project could not have been completed without his endless wisdom and support. Thank you to Dr. Kevin Dobbin, Dr. Andreas Handel, and Dr. Michelle Ritchie for serving on my committee and always answering my many questions. Lastly, to the entire team (former and current) at the Institute for Disaster Management, thank you for introducing me to the field of disaster management and for the endless encouragement and opportunities throughout all of my years at The University of Georgia.

TABLE OF CONTENTS

Page

LIST OF TABLES

Page

LIST OF FIGURES

Page

CHAPTER 1

INTRODUCTION

1.1. Statement of the Problem

On August 6th and 9th, 1945 the United States (US) nuclear weapons used on Hiroshima and Nagasaki in Japan,[1] causing an estimated 200,000 casualties, with approximately 105,000 fatalities and 95,000 injuries.[2] The dual bombings gave the world a glimpse of the devastating and expansive effects of this new warfare strategy, and a global arms race that has lasted decades immediately followed. Officials are now sounding the alarm that the world may be entering another arms race.[3] Despite the increasing risk of a nuclear attack on United States (US) soil, most organizations, local, state, and health care organizations, remain largely unprepared for a nuclear disaster.[4–6]

The detonation of a nuclear device has a trifecta of effects that impact the environment and people. The primary effect of a nuclear explosion is the blast effect, which is responsible for devastating infrastructure destruction. An estimated 50% of the energy from a nuclear explosion is released in the form of the blast wave.[7] Like any explosion, the rapidly expanding fireball is the origin point of the blast, generating a pressure wave extending in all directions.[8] The amount of light and heat generated by the explosion creates the secondary effect of a nuclear explosion, known as thermal radiation or heat.[8,9] An estimated 35% of the energy is released as thermal energy.[7] Measured by the thermal fluence, or radiant energy, deposited onto exposed surfaces,[9] thermal radiation causes burns to people, ignites flammable materials, and even causes mass fires.[8] Finally, the tertiary effect of a nuclear explosion is the radiation. Responsible for only

15% of the energy from the explosion[7], the radiation is categorized as prompt radiation and fallout radiation.[8] As the name suggests, prompt radiation occurs nearly instantaneously with the flash due to neutron activation.[8] Fallout radiation, alternatively, is created by the products of the fission process, known as radionuclides, which then irradiate various airborne particles and eventually "fall out" of the sky.[9] If the device is a larger yield, such as in a thermonuclear weapon, these particles are the products of the initial fission reaction to create the hydrogen fusion reactions in addition to the products from the fusion process.[10] Activation products, which are atoms of structural materials from the device itself or surrounding environment that absorb released neutrons from the detonation, further contribute to fallout radiation.[11] Accurate characterization of these effects through consideration of both amplifying and attenuating factors is a crucial step in establishing effective preparedness measures.

Each of the effects described above have the potential to individually cause devastating impacts, but when considered cumulatively, the impacts become catastrophic, as exemplified by the simulated detonation in Figure 1.1. Within the immediate area surrounding the detonation, few, if any, survivors and buildings are expected to remain.[8] The rubble in the streets would be impassable, and extremely high radiation levels would be present, increasing risk for any rescue efforts. Extending outward from the site of detonation,[9] the number of buildings destroyed would decrease, and the preponderance of structural damage would be with utility infrastructure damage, overturned cars, collapsed roofs, and fires.[8] However, this is the region of greatest opportunity for rescue efforts as radiation levels would be safe for rescuers with the appropriate personal protective equipment, dosimetry equipment, and standard operating procedures (SOPs). In particular, these SOPs should ensure the responders are aware of and implement time, distance, and shielding principles.[12] Following this region is the end of the visible damage after a

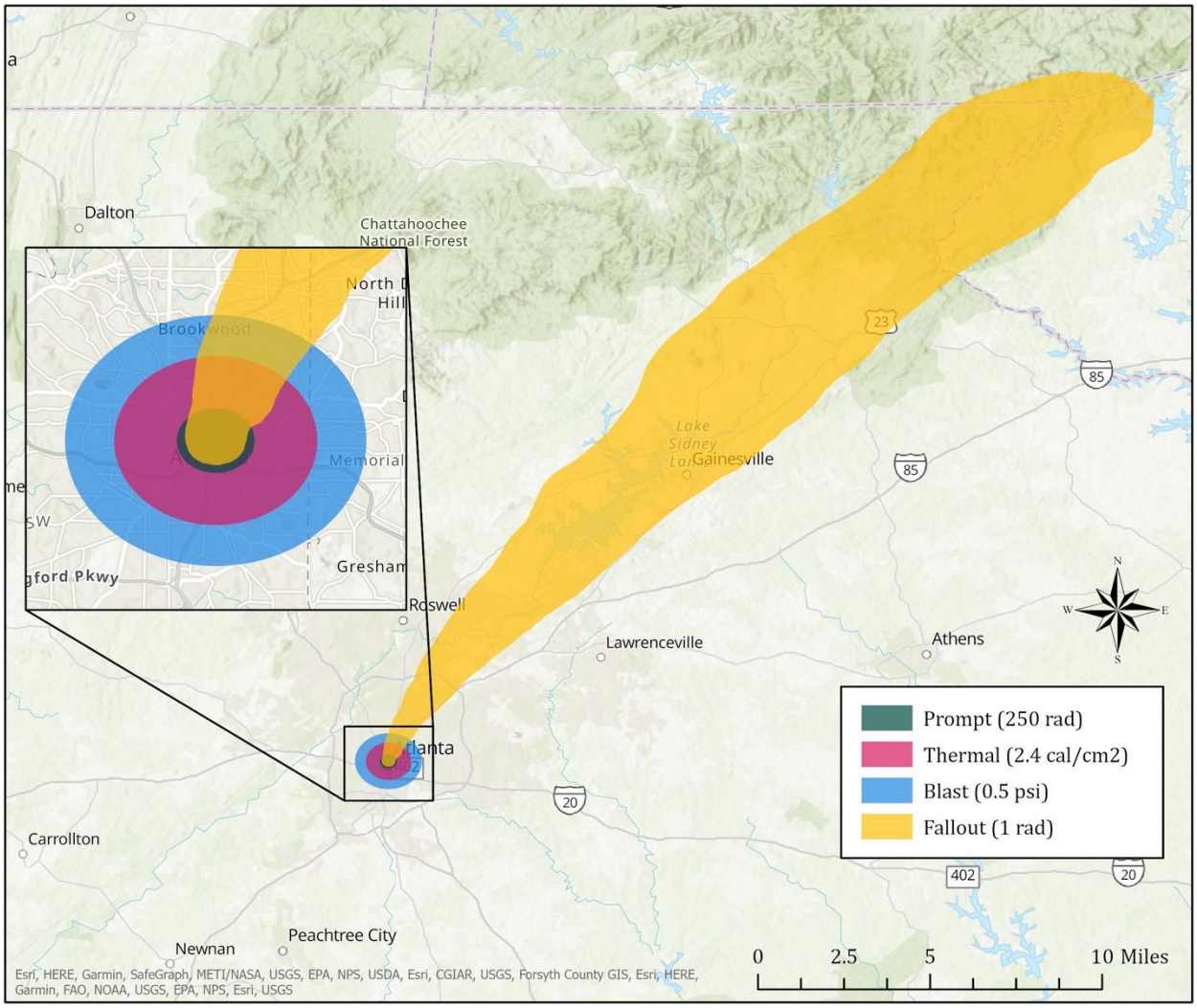

Figure 1.1. Simulated 15 kt detonation in Atlanta, Georgia on February 18, 2019, with a burst height of 40m. The values of each effect are provided as sample values to highlight the geographic spread of the incident.

detonation, mostly characterized by broken glass or blown out windows or doors.[8] Fallout radiation will extend well beyond this visible region of damage, carried by the upper atmospheric winds. The wide geographic footprint of these cumulative effects will cross traditional jurisdictions, and they will have rippling effects beyond the immediate destruction.

In particular, evidence suggests that the US health care system would not be able to handle a disaster on the scale of a nuclear device detonation. Gale and Armitage[13] go so far as to argue that existing medical preparedness efforts are "obviously useless" in the context of a nuclear device detonation. As of 2008, almost one third of the US population lives in counties where the number of staffed and unoccupied health care facility beds would be inadequate for a typical mass casualty event.[14] The coronavirus disease 2019 (COVID-19) pandemic illustrated this percentage has increased over time,[15] and the scale of a nuclear detonation would increase that fraction. Dallas et al.[16] estimated that a 15 kt (relatively small) weapon detonated in Beer Sheva, Israel would cause over 105,000 total fatalities, which is almost 50% of the population, and another 35,000 injuries. Bell and Dallas[17] further broke down casualty estimates by injury type for a 20 kt weapon in four major cities across the United States. In Atlanta, Georgia, they estimated that such a detonation would cause between 46,000 and 160,000 fatalities from fallout radiation alone,[17] a population size comparable to a large sports stadium. Within the model, the blast effect would cause approximately 2,000 fatalities and another 28,000 individuals vulnerable to injuries resulting from collapsing structures and debris.[8,17] An estimated 5,000 people were predicted to reside in the region associated with full-thickness thermal burns, and another 8,500 people would be found in the region associated with partial-thickness thermal burns.[17] While the fallout radiation potentially contributes to the greatest number of initial fatalities, the mortality rate among thermally burned patients will be significant, due to the severely limited resources available in the US burn care infrastructure.

Within the US health care system, burn center criteria indicate patients with significant burns or compounding injuries should be treated at a burn center with a specialized care team.[18] However, across the entire country, Kearns et al.[19] estimate the US burn care community could

manage approximately 2,000 patients if resources exist to treat and redistribute patients geographically. Within Bell and Dallas' model of an Atlanta detonation,[17] this leaves an estimated 11,500 individuals who could potentially need care at a burn center but would lack access. Beyond the burn care capacity, a disaster of such scope would incapacitate the Georgia health care system. A recent analysis[20] suggests in a no-notice event (such as a nuclear detonation), the Atlanta-area hospitals could treat 499 adult patients and 96 pediatric patients total. Of these patients, the system can only treat 55 adult and eight pediatric critical patients.[20] Furthermore, according to the American Hospital Directory,[21] 17 of the state's 113 non-federal, acute-care, short-term hospitals are in Atlanta, Georgia, comprising 30% of the staffed beds available in the state. In the event of a nuclear detonation in Atlanta, few if any of these facilities would be available to treat patients, leaving only 70% of the state's typical operating volume responsible for handling the possible tens of thousands of patients. Moreover, when Harris et al.[22] conducted a chemical release exercise with Atlanta-area hospitals, the researchers received significant pressure to modify the scenario in such a way to lower the severity and magnitude of the simulated event. This experience suggests that Atlanta-based health care providers are unprepared to respond to a severe chemical disaster, let alone a larger and more catastrophic nuclear disaster. As such, there exists a significant area of opportunity to inform local and state organizations about the estimated impacts of a nuclear device detonation and provide them with assistance in increasing preparedness for such an incident.

The governmental organizational structure as it relates to nuclear disasters historically defines the ownership of information and intelligence as well as the responsibilities for response to such an incident. Due to the nature of nuclear weapons, the US federal government retains the preponderance of knowledge and control surrounding nuclear disasters. The Department of

Defense (DOD) is the umbrella federal government organization ultimately responsible for nuclear mitigation, preparedness, and response.[23] Within the DOD, the Defense Threat Reduction Agency (DTRA) is the official combat support agency for countering weapons of mass destruction (WMD), which includes nuclear weapons.[24] DTRA has a Nuclear Enterprise Directorate that spearheads the federal government's efforts around education, training, and assessments of nuclear threats.[25] As the military is a branch of only the federal government, local governments lack an equivalent agency to liaise with DOD and DTRA. State governments have National Guard, but the juxtaposition of State National Guard and Federal National Guard assets creates further confusion. Moreover, the expectation is that the federal government will manage any nuclear event, with state and local agencies supporting their efforts. In 1987, Congress asked the US Government Accountability Office (GAO) to review the DOD's policies and practices for coordinating planning and response to nuclear disasters with state and local governments.[26] GAO recommended the DOD and Secretary of Navy share unclassified information around the potential hazards associated for these incidents, including notification policies and procedures, DOD response capabilities, and procedures for requesting assistance.[26] While these measures were implemented by the DOD, there remains a disconnect to this day with emergency management, health care, and public health organizations understanding their true vulnerability of a nuclear disaster.

Redlener[27] identified six US cities (New York City, Chicago, Washington, DC, Los Angeles, San Francisco, and Houston) that have the greatest likelihood of being the target of a nuclear weapon, but only two of their emergency management agencies directly address the possibility of a nuclear attack.[4] Moreover, in its document entitled "Planning Guidance for Response to a Nuclear Detonation",[8] the US federal government advises states and local agencies

that federal resources may take up to 72 hours to arrive following a nuclear disaster. This delay leaves local and state officials responsible for managing the aftermath for the first three days, when rescue and treatment efforts are the most urgent. As such, efforts to increase understanding of and preparedness for the threat and impacts of a nuclear disaster at local and state levels are essential for future successful responses.

Further complicating this immediate response requirement for state and local organizations is the difficulty surrounding accurately assessing the likelihood of a nuclear device detonation. A significant proportion of the information surrounding nuclear threat is classified information at the federal government level.[9] However, enough information publicly exists to paint an alarming picture. Following World War II, the US and Union of Soviet Socialist Republics (USSR) entered a nearly fifty-year period of geopolitical tension known as the Cold War, most known for the period of nuclear arsenal development.[28] The 1980s marked the beginning of a period of substantial de-proliferation of nuclear arsenals. The Federation of American Scientists[29] estimates there has been an 85% reduction in the global stockpile, which includes the US arsenal. However, this reduction effort has plateaued in the last several years, as the last significant arms control agreement was established more than a decade ago.[30] Some political scientists argue the world is entering a new arms race, citing the US' plan to spend more than $2 trillion over the next 30 years to rebuild its arsenal.[31] In July 2021, the US Pentagon disclosed its doctrinal publication on nuclear war fighting, which states, "there is an increased potential for regional conflicts involving nuclear-armed adversaries in several parts of the world and the potential for adversary nuclear escalation in crisis or conflict."[30] Moreover, Federal Emergency Management Agency's (FEMA's) Radiological Emergency Management training states an improvised nuclear device is "well within a terrorist's ability to employ."[32] The

culmination of these warnings is cause for concern for local and state organizations. While the public may not be able to quantitatively assess the risk of a nuclear device detonation on US soil, the increasing alarm at the federal government suggests actions to increase preparedness for these disasters should be taken immediately to increase the response capability if such event were to happen.

Finally, one of the largest challenges in accurately quantifying the effects and impacts of a nuclear explosion is the lack of available data. The atomic bombs dropped on Hiroshima and Nagasaki remain to this day the only real-world data for a nuclear explosion in an urban environment.[33] As these explosions occurred over 75 years ago, the data captured was extremely limited, and its accuracy is heavily debated.[9] The next potential source, from test explosions, also does not provide readily accessible and useable data. From the initial atomic bomb test for the Manhattan Project in 1945 until the Comprehensive Nuclear-Test-Ban Treaty (CBT) in 1996, an estimated 2,047 nuclear tests were conducted across the world.[28] Within the US, these tests were designed like any scientific experiment: focusing on specific elements while controlling for all other factors. Tests ranged from assessing new technology to determining the level of protection different building materials provide from radiation.[9] While these tests provide critical information to supplement data from Hiroshima and Nagasaki, there is potential for error due to the controlled environment. Moreover, the US military and federal government retain the results and data from these tests, the preponderance of which remain classified to this day.[9] As such, the federal government has extensive modeling capabilities for nuclear disasters, but little data exists for local and state agencies. Models that can be publicly distributed and accessed therefore must be built by integrating data from multiple sources, including those in the grey literature. This

burden thus lands upon local, state, and/or civilian organizations, many of whom do not have the training or capability to create such methodology.

Future research to clearly characterize the expansive impacts of nuclear disasters is imperative to increase awareness and preparedness, especially at the state and local levels. We can use methodologies well established in other, similar disciplines to take steps toward this goal. By incorporating multiple data sources into the existing models, we can begin to better understand the true impact of nuclear disasters. Furthermore, the inclusion of patient outcomes modeling will allow us to support emergency managers, health care providers, and other first responders in population-level patient management to save as many individuals as possible during catastrophic disasters.

1.2. Aims of the Dissertation

The primary goal for the following three aims is to better understand the geographic and health care impacts of a nuclear device detonation in a large US metropolitan city for the purposes of increasing nuclear disaster preparedness. The three aims are:

1. To characterize the possible distribution of, and cluster the fallout radiation plumes resulting from, and IND detonation in Atlanta, Georgia (GA).
2. To develop a framework for improving the methods to estimate the thermal and radiation effects resulting from an IND detonation in an urban environment.
3. To leverage the improved modeling framework to realistically characterize the estimated casualties in the aftermath of an IND detonation in Atlanta, GA and to understand the health care capacity in the state of GA to respond to such an incident.

To accomplish the first aim, we will utilize the Hazard Prediction and Assessment Capability (HPAC) software created by DTRA as a foundation for the fallout radiation model.

Additional data that captures key elements such as historical surface-level and three-dimensional (3D) weather data. Data from previously published studies conducted by the national laboratories[34] and academic researchers[9,16,35] will be leveraged to inform the improved thermal and radiation effect models in the second aim. The final aim will build upon the results of the first two aims to assess the capacity of the GA health care system to treat the patients created by a nuclear detonation.

Atlanta was chosen as the site of a simulated nuclear detonation for numerous reasons. Firstly, Atlanta's moderate climate[36] and lack of proximity to water allows for the consideration of meteorological factors without having to account for meteorological perturbations caused by large bodies of water.[37] Secondly, as a leader in commerce, industry, and transportation, particularly among southeastern US centers,[38] Atlanta is a plausible target for a nuclear attack. The city includes Hartsfield Jackson International Airport, the busiest airport in the world, as well as the headquarters for major businesses, such as Cable News Network (CNN) and The Coca-Cola Company, and a US Air Force reserve base. Other significant points of interest in the city include the Mercedes-Benz stadium, and the National Center for Civil and Human Rights, and Centennial Olympic Park, which was the location of a domestic terrorist pipe bombing attack during the 1996 Summer Olympics.[39] As far back as 1990, the FEMA has listed Atlanta as a potential target.[40,41] Lastly, Atlanta is a representative of a typical major city found in the US. With a population of almost 500,000 and even more commuters every day, it is the 38th most populous city in the US.[42] It has a relatively large urban sprawl, with a balanced mix of land uses, and a metropolitan area population of approximately six million.[42,43] Moreover, the health care resources in the state of GA are an average representation of all states in the US. According to an analysis conducted by the Kaiser Family Foundation,[44] the US averaged 2.40 total hospital

beds per 1,000 people in 2019. In that same analysis, the state of GA averaged 2.34 total hospital beds per 1,000 people and was the closest state to the national average.[44] The combination of these factors make Atlanta an ideal sample location to consider the weather, thermal, and radiation effects in an urban environment, as well as the population-level health care impacts in the aftermath of an IND.

1.3. Objectives of the Dissertation

Each aim has its own set of objectives and methods, which are described in detail in Chapters 3 - 5. The following is a brief description of the objectives, data sources, methods, and anticipated output for each aim, presented as Table 1.1.

Aim 1 focuses on characterizing the possible distribution of, and clustering the fallout radiation plumes resulting from, an IND detonation in a large city. We will first generate cumulative fallout radiation plumes for each day in the year 2019, which will then be clustered based on spatial patterns and affected population estimates using a partition around medoids (PAM) clustering algorithm. The medoids resulting from the chosen number of clusters will be used as the simulated dates of detonation in the remaining aims. We hypothesize that these medoids will provide an improved understanding of the possible geographic variation in nuclear detonation effects. The relationship between surface-level weather characteristics and fallout radiation plumes will then be examined using four different machine learning (ML) algorithms to determine significant surface-level weather variables in predicting fallout radiation. If significant, such predictions would be useful for assisting operational decision-making at a local level.

Aim 2 addresses the role of the urban environment in the context of thermal and radiation effects resulting from an IND detonation. Multi-source building data will be integrated to assign

Table 1.1. Brief description of the objectives, data sources, methods, and anticipated output for each aim.

Aim	Objective(s)	Data Sources	Methods
1	– To characterize the possible distribution of, and cluster the fallout radiation plumes resulting from, an IND detonation – To examine the relationship between surface-level weather characteristics and fallout radiation plumes – To identify representative days that can be used for simulation in future aims	– Weather Underground – weather.US – Spatial Synoptic Classification v3.0 – MDS Weather Archive (MERRA-2) – HPAC	– Synoptic weather analysis – Cluster analysis – Machine learning
2	– To develop a framework for improving the methods to estimate the thermal and radiation effects resulting from an IND detonation in an urban environment	– Output from Aim 1 – ONEGEO 3DBuildings – National Structure Inventory (NSI) – Literature	– Spatial data integration – 3D modeling (Blender)
3	– To leverage the improved modeling framework from Aim 2 to realistically characterize the estimated casualties in the aftermath of an IND detonation – To understand the health care capacity in GA to respond to such an incident	– Output from Aim 1 – Output from Aim 2 – LandScan USA – GA hospital bed capacity / availability – Literature	– Vectorized population modeling – Spatial data integration

prompt and fallout radiation protection factors on a building-by-building basis. An improved thermal effects model will be developed by combining a previously published thermal ignition prediction model[45] with a thermal attenuation model, derived from a 3D model of the city, to account for shadowing and reflections of the thermal energy. These improved attenuations will be incorporated into the existing nuclear modeling workflow, which leverages both HPAC and ESRI's ArcGIS Pro to integrate multiple sources of spatial data. We hypothesize that these

considerations will emphasize a way in which nuclear disaster modeling can transition from worst-case scenario to more realistic estimates of the true impact of these incidents.

Aim 3 builds on the results of the first two aims to create a simulation that realistically estimates the casualties resulting from an IND detonation in a large city. We will identify the injuries expected from the strength of the blast, thermal, and radiation effects, based on publicly available literature. A triage algorithm specifically designed for radiation incidents will be applied to understand the anticipated injury profiles within each disaster triage category. Lastly, we will examine the anticipated patients within the context of collected GA hospital data regarding staffed bed capacity and availability. We hypothesize the GA health care system will not have the capacity to treat the patients generated by a nuclear detonation and that this simulation will highlight the need for increased disaster preparedness within the health care community.

1.4. Dissertation Outline

Chapter 1 of this dissertation provides a brief introduction to the challenges faced in nuclear disaster preparedness. Chapter 2 describes the available literature surrounding nuclear devices, modeling nuclear disasters, patient management, and methods to predict patient outcomes during disasters. Chapters 3 through 5 are manuscripts prepared for publication representing each of the three aims. Each manuscript will be traditionally formatted, with an introduction, methods, results, and discussion section. Chapter 6 is a summary of the findings of each aim and conclusions with areas for future research.

CHAPTER 2

LITERATURE REVIEW

This chapter summarizes and analyzes information from publicly available, published literature pertinent to this dissertation. The review begins with a brief history and description of types of nuclear weapons, followed by a detailed explanation of the effects caused by nuclear detonations. A description and analysis of existing nuclear detonation models follows. The focus of this review then transitions to the health care impacts of a nuclear detonation, concluding with a particular emphasis on thermal burn patients.

2.1 History of Nuclear Weapons

The possibility of a nuclear weapon was first realized less than a hundred years ago, in 1938, when German nuclear physicists Otto Hahn, Lise Meitner, and Fritz Strassma first discovered nuclear fission.[46] In response to fears that the German scientists would begin developing nuclear weapons, the United States (US) President Franklin D. Roosevelt authorized the formation of the Manhattan Project on December 28, 1942.[47,48] The work conducted in Los Alamos, New Mexico blended the expertise of military officials and scientists to develop a functional atomic bomb.[47,49] The project was primarily conducted under the guidance of J. Robert Oppenheimer, a theoretical physicist now known as the "father of the atomic bomb."[50] Three years later, on July 16, 1945, the Trinity Test became the first successful atomic bomb detonation.[51] The newly appointed President Harry Truman soon issued the Potsdam Declaration, promising "prompt and utter destruction" if Japan did not surrender in continued World War II (WWII) conflict in the Pacific.[52,53] On August 6, 1945, the US dropped the first

nuclear bomb detonated in a civilian city on Hiroshima, Japan, killing an estimated 118,661 civilians and injuring another 82,807.[54] Just three days later, on August 9, 1945, the US dropped a second nuclear bomb on Nagasaki, Japan, with an estimated 73,884 dead and another 74,909 injured.[54]

In the aftermath of WWII, the US and the Union of Soviet Socialist Republics (USSR) entered an intense arms race, known as the Cold War, in which both countries endeavored to expand their nuclear weapon capabilities, including fusion technology and thermonuclear weapons.[55] The testing and research of nuclear bombs became the primary international focus for several decades, until the 1970 Non-Proliferation Treaty (NPT).[56] The five countries who were known to possess nuclear weapons at the time, the US, the USSR, Great Britain, France, and China, all agreed to not use nuclear weapons and to not assist other countries in developing their own nuclear arsenal.[57] The NPT also stipulated that these countries were to gradually reduce their respective nuclear stockpiles over time and should not acquire or develop additional nuclear weapons.[56] Testing of nuclear weapons, however, continued in various forms until the Comprehensive Nuclear-Test-Ban Treaty (CBT) in 1996, which banned all nuclear weapons tests and any other nuclear explosions in all environments, for both civilian and military purposes.[28] In the nearly fifty year period of tremendous research and development, an estimated 2,047 nuclear tests were conducted across the world, with the US alone conducting 1,030 tests.[51] The preponderance of the data and knowledge developed during this period is still relied upon in present-day research as the foundational information for predictive modeling and emergency management practices.[9]

2.2. Nuclear Reactions

The frenzied research on nuclear weapons in WWII and the Cold War led to the development of a variety of nuclear weapon types. Each type of weapon varies by chemical process, mechanism of action, and construction. This review will focus on the two primary chemical processes behind nuclear weapons: fission and fusion. Shubayr[58] and Bunn[59] cover nuclear weapon types in more detail, addressing the mechanisms and construction of the various types.

2.2.1. Fission

Colloquially known as atomic bombs, fission nuclear weapons were the first nuclear weapons created.[47] Uranium-235 (^{235}U) and plutonium-239 (^{239}P) are the most widely used radioisotopes for fission weapons.[60] As heavier elements with a larger nucleus diameter, the force holding onto neutrons is relatively low, so both isotopes release more neutrons per fission reaction than other radioisotopes.[61] Further, these radioisotopes are stable enough to be stockpiled in a nuclear device over significant periods of time, a critical consideration in nuclear arsenal development.[59]

In a fission reaction, a neutron is sent with force toward the nucleus of a radioisotope (^{235}U or ^{239}P), where it is absorbed to briefly create a new, extremely unstable radioisotope.[62] To achieve greater stability, the intermediate radioisotope then splits into two or more fission fragments, two or three neutrons, and gamma radiation (gamma-rays).[62,63] The fission fragments and any remaining starting material from the weapon undergo further radioactive decay, producing fission products.[64] As an exothermic reaction, the first fission reaction produces approximately 200 megaelectron volts (MeV), as detailed in Table 2.1.[65] As a point of reference, most chemical reactions are on the order of just a few electron volts (eV).[66] Additionally, the

fission neutrons initiate a chain reaction, which in turn generates more fission reactions.[64,65] Construction of fission weapons involves precisely calculating critical mass, which is the minimum amount of nuclear material required to sustain the fission chain reaction.[59] Without a sustained chain reaction, not all of the nuclear material present in the weapon will undergo fission, and thus the extent of effects will be less.[65] The two types of fission weapons, gun-type assembly and implosion-type, both condense the stored material to reach the critical mass required for an efficient detonation.[59,67] The gun-type weapon, which uses ^{235}U, achieves the supercritical mass by using a conventional explosive to shoot one piece of sub-critical material into another.[59,67] The implosion-type weapon contains a sphere of ^{239}P, which achieves super-critical mass after conventional explosives drive the sphere inward.[59,67] These designs are difficult to achieve precisely, as the conventional detonations must happen simultaneously to achieve the required critical mass.[59,67]

Table 2.1. Average distribution of energy produced in the entirety of a single fission reaction.[64]

Source	**Energy (MeV)**
Kinetic energy of fission fragments	165 ± 5
Kinetic energy of fission neutrons	5 ± 0.5
Instantaneous gamma-ray energy	7 ± 1
Beta-particles from fission products	7 ± 1
Gamma-rays from fission products	6 ± 1
Neutrinos from fission products	10
Total energy per fission	**200 ± 8.5**

The total amount of energy released by fission weapons is relatively small in comparison to modern thermonuclear weapons, which are described below in section 2.2.2. The amount of explosive power from a nuclear detonation, referred to as the yield, is most commonly measured

in units of kiloton (kt) of trinitrotoluene (TNT) equivalent.[8,9,58,64,65] More precisely, a one kt nuclear weapon produces an explosive yield equivalent to 1,000 tons of TNT,[8,64,65] and a one megaton (Mt) is the equivalent of 1,000 kt or 1,000,000 tons of TNT.[64,65] Figure 2.1 compares the yield of several historically significant nuclear weapon detonations, which are described in Table 2.2.[51,68] The Trinity Test has a yield that is just 6.25% of the yield of the smallest fusion weapon listed, Joe-4.

Table 2.2. Historically significant nuclear weapon detonations.[51,68]

Name	Location	Yield	Year	Weapon Type
Little Boy	Hiroshima	12.5 kt	1945	Plutonium Implosion-Type
Fat Man	Nagasaki	22 kt	1945	Highly Enriched Uranium Gun-Type
Trinity	New Mexico	25 kt	1945	Plutonium Implosion-Type
Joe-4	U.S.S.R	400 kt	1953	Fusion – Boosted Fission
Ivy Mike	Marshall Islands	10.4 Mt	1952	Thermonuclear
Castle Bravo	Marshall Islands	15 Mt	1954	Thermonuclear
Tsar Bomba	U.S.S.R.	50+ Mt	1961	Thermonuclear

2.2.2. Fusion

In the years of intense research in the Manhattan Project, a second chemical reaction, fusion, was leveraged to build higher yield nuclear weapons.[59,67] Naturally occurring in the sun, fusion is the chemical process in which two lighter nuclei fuse to form a heavier nucleus.[64,65] These reactions require exposure to extreme temperature and pressure in order to overcome the electromagnetic repulsion that naturally exists between two positively charged nuclei.[65,67] The deuterium-tritium fusion is the most energetic fusion reaction, which produces an alpha-particle (a helium nucleus) and a neutron.[64,65] Most of the energy produced in a fusion reaction is in the form of the neutron's kinetic energy, which accounts for 14 of the 17.6 MeV.[65]

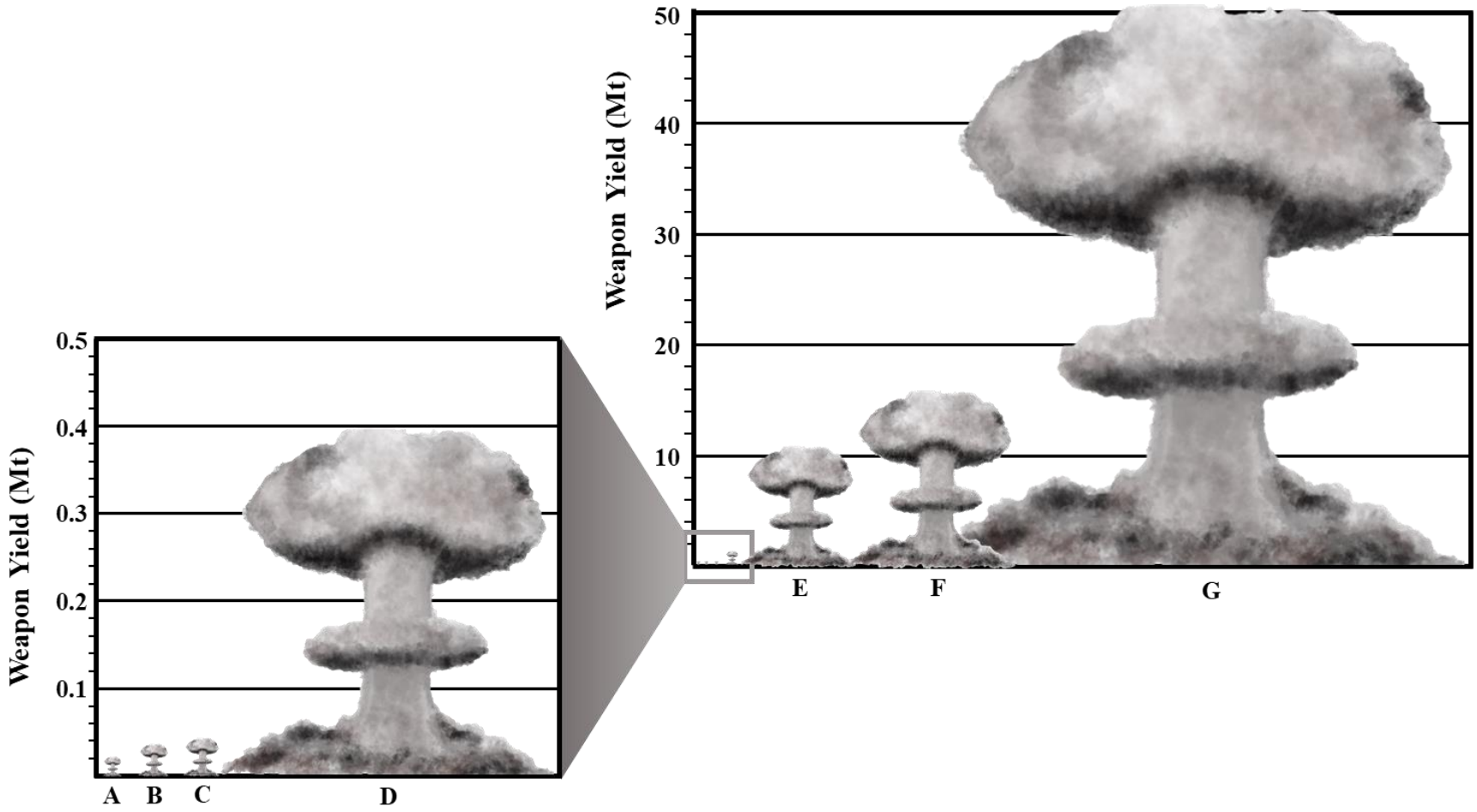

Figure 2.1. Comparison of yield for historically significant nuclear weapon detonations: (A) Hiroshima – 12.5 kt, (B) Nagasaki – 22 kt, (C) Trinity Test – 25 kt, (D) Joe-4 – 400 kt, (E) Ivy Mike – 10.5 Mt, (F) Castle Bravo – 15 Mt, and (G) Tsar Bomba – 50+ Mt. The plume height is scaled relative to the weapon yield for illustrative purposes only.

The extreme conditions required for a fusion reaction are not easily produced on earth, and thus, fusion nuclear weapons are preceded by a fission reaction.[67] Fusion-boosted weapons inject a small amount of tritium (a hydrogen atom with two neutrons and a proton) to trigger the reaction of the fission materials.[59] As the fission reaction occurs, the fusion material is exposed to extreme temperatures and pressures, thus causing a fusion reaction.[59] The only fusion-boosted weapon tested was the USSR's Joe-4, which achieved a yield of 400 kt.[51,68] Thermonuclear weapons employ a similar technique, although the process is begun by a conventional explosive detonation that increases the pressure around the fission material. The fission process then creates fusion reactions, which trigger a secondary fission reaction. The secondary fission reaction then produces a secondary fusion reaction, which ultimately creates a final fission reaction.[59,67] These sequential reactions are responsible for the significantly higher yield of fusion nuclear weapons in comparison to fission weapons. The US detonated the first thermonuclear weapon in 1952, but Castle Bravo in 1954 was the first test of a deliverable thermonuclear weapon.[51,68] To date, the largest nuclear weapon ever detonated is the USSR's Tsar Bomba, which had an estimated yield between 50 and 58 Mt.[51,68]

2.3 Effects of Nuclear Detonations

In this review, consistent with US federal government documentation, the term "nuclear effects" will refer to the outputs from the nuclear explosion, while the term "nuclear impacts" will be used to characterize the consequences to materials, people, or the environment as a result of the nuclear effects.[8] The nuclear effects can be further categorized into primary and secondary effects. The primary effects, blast, thermal (heat), and prompt radiation, occur immediately after the initial detonation.[64,65] The secondary effects, fallout radiation and the electromagnetic pulse (EMP), are considered to be side effects of the detonation.[8,64,65]

While certain elements are consistent across all nuclear weapons, the effects of a nuclear detonation are particularly sensitive to weapon yield, the type of chemical reaction(s), and the altitude of detonation. Glasstone and Dolan[64] discuss each parameter and its subsequent influence on each nuclear effect in depth. This review will use a low-yield, fusion weapon detonated as a near-surface burst to discuss the nuclear effects. These conditions are consistent with federal planning documents and combined represent a standardized fission weapon.[8,32,69] Table 2.3. describes the estimated energy distribution among the effects from this device. As the energy behind the EMP does not account for a significant percentage of energy released, it is not included in the table.[64]

Table 2.3. Energy distribution of a standard fission weapon.[64,65]

Effect	Percent of Energy Released
Blast	50%
Thermal Radiation	35%
Prompt Radiation	5%
Fallout Radiation	10%

2.3.1. Blast Effects

Nuclear explosions are similar to conventional explosions to the extent that the immediate impact is mainly due to the blast effect or shock.[8,32] The explosion results from a rapid release of energy within a limited space, which causes a tremendous increase of pressure and temperature.[64,70] Subsequently, all materials present in the immediate vicinity are vaporized into hot, compressed gasses.[65] The intense pressure and temperature cause the gasses to expand rapidly, thus creating the “shock wave” and the blast effect front.[9,54,64] The overall blast effect is

created by overpressure and dynamic pressure.[7,9,32,64] Responsible for the crushing mechanism associated with a blast effect, the overpressure is simply the pressure over and above the atmosphere pressure.[8,64,65] While it acts in all directions from the detonation source, it is highest closest to the detonation point and decays as the inverse cube of the distance from the detonation point.[7,9,64,65,69] After the initial dissipation, the blast wave expansion slows to approximately the speed of sound in ambient air, approximately 343 meters per second (m/s) or one mile in 4.7 seconds.[8,64,71] The dynamic pressure, meanwhile, creates high-speed winds that also exert force on structures in the aftermath of the initial shock wave.[7–9] It has a direct relationship to the density of the air through which it travels and the velocity of the shock front that precedes it.[64] The speed of these winds can peak at almost 1,000 miles per hour (mph) for a small, 10 kt explosion.[8,64] As would be expected, as distance from the detonation site increases, the peak overpressure and maximum dynamic pressure decrease.[64]

The full impact of the blast effect in a modern city is not currently known, but various models and guidance provide general estimates, as summarized in Table 2.4.[8,64,65,72] While dynamic pressure contributes to the blast effect, these thresholds are typically quantified by the overpressure alone in pounds per square inch (psi).[7,72,73] The exact value for such thresholds varies by source and interpretation, but the values listed in Table 2.4 are consistent with US federal government documentation.[72,73] In particular, there is some evidence to suggest that the severe damage zone will begin closer to 5.0 psi, rather than 8.0 psi.[7,8,64] The transition between these zones is not finite or clear, and determination is based upon ground-level observations and/or overhead imagery.[8,73] Given the complex nature of urban environments, the building damage will be irregular and anomalies or discrepancies should be anticipated. For example, an urban environment alters the geographic distribution of dynamic pressure. The winds will be

amplified between buildings in close proximity, due to the wind tunnel effect, and, due to the laws of conservation of energy and mass, therefore, the dynamic pressure does not have a uniform geographic distribution.

Table 2.4. Damage zone definitions caused by the blast effect.[8,72,73]

Damage Zone	Threshold (psi)	Description
Light	0.5 – 3.0	– Buildings sustain minor damage – Primarily broken windows
Moderate	3.0 – 8.0	– Buildings sustain significant structural damage – Concrete or reinforced buildings remain standing – Substantial rubble in streets – Blown out building interiors – Blown down utility lines – Broken water and gas lines – Overturned vehicles – Caved roofs
Severe	>8.0	– Few, if any, buildings left standing – Streets impassible – Rubble may be 30 feet high or more

Injuries caused by the blast are categorized as primary, secondary, tertiary, and quaternary blast injury.[35,74,75] Primary blast injury occurs when the overpressure wave hits the human body.[35] Air-filled organs, such as ears, stomach, intestines, and lungs, are particularly at risk for blast injuries, but organs surrounded by fluid, such as the brain and the spine, can be also affected.[74,75] As the overpressure wave passes through these organs, it can cause fragmenting and shearing of tissues.[35,75] The remaining categories of blast injury are caused by indirect effects of the blast wave.[76] Secondary blast injury occurs when shrapnel from the device or flying debris from the shock wave collides with the human body, causing either penetrating or nonpenetrating

injuries.[35,64,74,75] Secondary injuries will likely be the dominant complaint of patients seen in the aftermath of a nuclear detonation[8,77] Tertiary blast injury occurs when an individual is propelled through the air by the blast wave, often colliding against a rigid surface.[35,64,74] Tertiary blast injury can also occur when structure collapse causes casualties.[35,74,76] Lastly, quaternary blast injuries are defined as any additional injuries beyond those previously listed, examples of which include burns, toxidromes from chemical exposure, inhalation injury, respiratory distress from asthma or chronic obstructive pulmonary disease (COPD), acute coronary syndrome (ACS), acute myocardial infarction (AMI), and psychosocial or behavioral emergencies.[70,74–76]

Connecting the blast injuries to the physical characteristics of the explosion is challenging as injury correlates are confined to animal models.[64] Injuries seen in conflicts or terrorism incidents are used to supplement the results from animal models, but the existing literature cannot precisely establish the physical characteristics of these incidents to confirm specific thresholds.[35] Table 2.5 summarizes the effects of both the overpressure and the dynamic pressure on the human body, developed from weapons tests.[64,78] In the absence of additional trauma, the human body is relatively resilient to overpressure-induced primary blast injuries, as the minimum threshold for lung damage is 15.0 psi,[8,64,79] and the most vulnerable organ to pressure, the tympanic membrane, requires a minimum of 5.0 psi to rupture.[64] However, overpressure does not occur in a vacuum, which is why the dynamic pressure must be considered when estimating the blast effect on the human body. The strong winds resulting from the dynamic pressure cause the secondary and tertiary blast effects, which additionally further explains their increased incidence in the aftermath of an explosion.[64,77,78]

2.3.2 Thermal Effects

One of the most important distinctions between a conventional high-explosive weapon and a nuclear weapon is the proportion of energy released as thermal (or heat) radiation.[9,64,78] While a conventional weapon of comparable yield would release almost all of its explosive energy in the form of the blast effect, approximately 70-80% of the total energy from a fission weapon is released in the form of thermal radiation within a millisecond of detonation.[35,64,78] The enormous amount of energy released per unit mass in a nuclear weapon allows temperatures to

Table 2.5. Effect of various blast overpressures and dynamic pressures (represented as maximum wind speed) on the physical environment and the human body.[64,78]

Peak overpressure (psi)	Peak dynamic pressure (mph)	Physical environment effects	Human body effects
1.0	38	Broken windows	Minimal injuries, mostly from flying glass
2.0	70	Moderate damage to residential structures (especially windows, doors, and roofs)	Moderate injuries, mostly from flying glass and projectile debris
3.0	102	Severe damage to residential structures (collapse)	Serious injuries prevalent, fatalities may occur
5.0	163	Most buildings collapsed	100% injuries, widespread fatalities
10.0	294	Reinforced concrete buildings severely damaged or collapsed	Most people are killed
20.0	502	Heavy built concrete buildings severely damaged or collapsed	Almost 100% fatality

reach several tens of million degrees, whereas temperatures reach just a few thousand degrees in a conventional explosion.[35,64] Due to the extreme temperatures, most of the initial thermal

radiation is in the form of short wavelength light, mostly soft X-rays.[9,35,78] Unless the detonation occurs more than 50 miles into the atmosphere, the soft X-rays are efficiently absorbed by the surrounding air and superheat the air to extreme temperatures.[9,64,78] The superheated air creates a ball of intense heat, commonly called a fireball.[9,35,78] As the fireball expands, approximately half of the thermal energy is converted into the energy that drives the shock wave.[35,64,78] The remaining thermal energy is reradiated at lower temperatures, ranging between 6,000 – 7,000 kelvin (K), which produces light in the ultraviolet, visible, and infrared spectrums.[64,78] This reradiation constitutes the thermal radiation at distances from the explosion.[64,65] As the thermal radiation travels at the speed of light, time elapsing between the detonation and arrival at any distance is negligible.[64]

The extent of damage or injury caused by thermal radiation depends on the amount of thermal radiation energy received by the specified area, sometimes referred to as the radiant energy or thermal fluence.[45,64] The amount of thermal energy deposited decreases as distance from the detonation increases for two primary reasons. First, the thermal radiation is spread over an ever-increasing area as it travels away from the fireball. It has an inverse relationship with the square of distance from the explosion.[64] Second, the atmosphere significantly attenuates the thermal energy via absorption and scattering. Atoms and molecules in the air absorb, and thus remove, portions of the thermal radiation, particularly that in the ultraviolet region.[64,65] Scattering primarily results from the reflection and diffraction of rays by particles of dust, smoke, or fog in the atmosphere.[45] Both absorption and scattering reduce the amount of thermal energy that reaches a specified area.[45,64] Glasstone and Dolan[64] as well as Binninger et al.[45] provide in-depth analyses of the various atmospheric conditions, including cloud height, cloud

thickness, cloud type, atmospheric scattering, dust particles in the air, and humidity, that affect absorption and scattering, and thus thermal radiation transmission.

While a nuclear detonation can cause significant blast damage, the thermal radiation can cause serious additional damage by igniting combustible materials and causing extensive fires over urban and suburban areas.[9,64] These fires are most likely to occur in the moderate damage zone described in Table 2.4.[8,72] The dust and smoke from the blast and thermal effects, respectively, would result in a dense, low-visibility, fog-like environment.[9] Moreover, the thermal radiation would ignite any combustibles exposed by the blast effects, such as gas lines or electrical equipment, creating blast disruption fires.[9,35] There is significant debate as to whether these fires would coalesce into a mass fire in an urban environment or would remain as independent, secondary fires. Many nuclear scientists argue that the probability and range of a mass fire depends on too many unpredictable variables and therefore is essentially meaningless to model.[9,72] The "Planning Guidance for Response to a Nuclear Detonation",[8] a document developed by the US federal government to guide local and state planners, goes as far to specifically state, "experts suggest the nature of modern US city design and construction may make a raging firestorm unlikely." However, there is a significant contingent that argues otherwise, citing the mass fires in WWII.[9,35,45] Postol[35] argues that as the individual fires burn and intensify, the volume of heated and buoyantly rising air from the fire zone increases significantly. The expanding hot air could then begin to lift the vertical column of cooler air above it, and cool air from the periphery of the fire would be pulled in to replace it.[35] This pumping action would soon generate superheated ground winds of hurricane force that only further intensify the fire.[35] Eden[9] suggests that these winds would force combusting buildings horizontally toward the ground, filling city streets with hot flames, breaking doors and windows,

and causing the fire to jump to anything not yet combusting. Table 2.6 describes the levels of thermal fluence that may be required to ignite a mass fire for a 15 kt nuclear weapon detonation.[9,16,35,45] Models indicate the inclusion of mass fires increases the number of fatalities by two to four times those predicted from just blast injuries alone.[9,35] However, if a mass fire were to occur, evidence from WWII suggests that there would be fewer injured patients requiring medical attention, as many of those individuals would be consumed in the fires.[35]

Thermal radiation emitted by a nuclear detonation causes burn injuries in a number of ways.[8,58,64] The first occurs when exposed skin directly absorbs the thermal radiation energy, and the second is an indirect effect from the heating or ignition of clothing.[8,58] Either method causes flash burns, which are so named because the thermal energy is delivered so quickly that

Table 2.6. Thermal fluence thresholds for mass fire development from a 15kt nuclear weapon.[9,16,35,45]

Mass Fire Probability	**Thermal Fluence (cal/cm^2)**
Fires Highly Probable	23
Fires Probable	12
Mass Fires Likely	10

burn patterns, such as the side facing the fireball or the pattern of the clothing, will be evident.[54,64] The third mechanism is from secondary fires ignited by the burst or the mass fire phenomenon.[9,64] Individuals in this area are also at risk for inhalation injury, which is caused by thermal injury to the respiratory tract, chemical irritation of the respiratory tract, systemic toxicity due to agents such as carbon monoxide (CO) and cyanide (CN^-), or a combination of these insults.[80] Lastly, thermal radiation can also cause retinal burns for individuals who look

directly at the detonation, resulting in a permanent blind spot in their vision.[8,58,64] Depending on the distance from the detonation, these individuals may instead have temporary flash blindness, which typically resolves spontaneously after a few minutes without permanent damage.[54,58] Individuals remaining outside and within a direct line of sight to the explosion are most at risk for severe burn injury.[64]

Burn injury severity is typically described within the context of two parameters: burn depth and percent of total body surface area (%TBSA).[81] Burn depth is classified into three primary categories: superficial, partial thickness, and full thickness.[81,82] However, burn injuries tend to be a dynamic process such that the true depth of the burn may not be apparent for up to four days after the incident.[83] Superficial burns, known colloquially as 1st-degree burns, involve only the epidermis of the skin.[84,85] The burn appears red to pink, has no blisters, and is dry. On average, superficial burns heal without scarring within 5 to 10 days.[81,86] Partial thickness burns, known colloquially as 2nd-degree burns, penetrate the epidermis and involve part of the dermis.[81,83,85] Superficial partial-thickness burns involve only the superficial dermis.[86] The burn appears red (which blanches with pressure), has blisters, and is wet.[81,83] The pain associated with superficial partial-thickness burns is severe and healing typically occurs within three weeks with minimal scarring.[81,83,86] Deep partial-thickness burns penetrate deeper into the dermis.[81,84] The burn appears yellow or white, is dry, and does not blanch with pressure.[81,83,86] The pain associated with deep partial-thickness burns is minimal due to decreased sensation.[81,83,84,86] Healing typically occurs within three to eight weeks with scarring present.[81,83,84,86] Lastly, full thickness burns, known colloquially as 3rd-degree burns, involve the entirety of skin and subcutaneous structures.[84,86] The burn appears white or black/brown, does not blanch with pressure, is leathery, and is dry.[81,85,86] The pain associated with a full thickness burn is likely

nonexistent and healing requires surgical intervention.[81,86] Burn injuries frequently present with all three types, depending on the mechanism of injury, and classification accuracy to discern between partial thickness and full thickness is between 50 – 80% among experienced health care providers.[87–90]

The %TBSA reflects the percent of an individual's skin that is covered in either partial thickness or full thickness burns; it does not include superficial burns.[81,86,91] In practice, %TBSA is estimated by either the rule of nines, which divides a patient's body into regions that are approximately 9% of the surface area, or the palmar method, where a patient's palm is approximately 1% of their surface area.[81,86] These methods are notoriously subjective, especially if conducted by health care providers who do not routinely treat burn injuries.[92–94]

Similar to the blast effect, connecting the thermal injuries to the physical characteristics of a nuclear explosion is challenging and is rarely fully discussed in the literature. Frequently, literature sources will include only burn depth and thermal fluence and do not connect the injury to %TBSA. Table 2.7 provides thresholds of thermal fluence required to create each burn depth category for a 15kt nuclear detonation.[64] Interestingly, Glasstone and Dolan[64] suggest individuals with darker skin require less thermal fluence to be burned than individuals with lighter skin. Dallas et al.[16] assign fatality rate and survivor injury rate to thermal fluence thresholds, but it is

Table 2.7. Thermal fluence thresholds for burn injury for a 15kt nuclear weapon.[16,64]

Burn Depth	**Thermal Fluence (cal/cm^2)**
Superficial	2.4
Partial Thickness	4.8
Full Thickness	7.4

unclear how such estimations were made. Therefore, there remains a gap in the literature to integrate thermal fluence, burn depth, and %TBSA in casualty estimations from a nuclear detonation.

2.3.3. Radiation Effects

Perhaps the most notorious effect of a nuclear explosion is radiation, which is the process by which energy is emitted as particles or waves.[62,64] The three most frequently considered types of radiation are alpha, beta, and gamma (Appendix B).[95] Alpha radiation occurs when an alpha particle, a positively charged particle identical to a helium nucleus (two protons and two neutrons) is emitted from the radioactive decay of an unstable nucleus.[62,64] Because it moves at approximately one-tenth the speed of light, it can be easily stopped.[64,95] Materials such as a piece of paper or human skin are enough to stop the penetration of alpha-radiation.[54,95] However, if alpha particles are inhaled or ingested, alpha-radiation becomes the most dangerous of the three types and is virtually undectable.[64,95] Cell membranes are much thinner than a piece of paper, and as such, alpha particles can penetrate.[95] Moreover, the strong ionization ability of alpha particles means the dose equivalent of alpha-radiation is amplified by a factor of 20 inside the human body.[62,64,77,95] The second type of radiation, beta-radiation, occurs under either beta-negative decay or beta-positive decay.[62] The more common mechanism in fission reactions, beta-negative decay, occurs when an electron is emitted in the radioactive decay of an unstable nucleus.[62] The electron does not come from the electron cloud of an atom, but rather from the decomposition of a neutron.[62] Beta-positive decay occurs by a similar mechanism, except it produces a positron instead of an electron.[62] Regardless of the generation method, beta particles move approximately at the speed of light and have a penetrating power approximately 100 times greater than alpha particles.[62,64,95] As such, beta-radiation can penetrate a piece of paper or

human skin, but it can still be stopped by aluminum foil or a layer of clothing.[77,95] Depending on the sub-atomic nature of the beta particle, the moderate ionization ability of beta particles means the internal dose equivalent of beta-radiation is amplified by a factor ranging from five to 20 inside the human body.[62,64,77,95] As beta-radiation can partially penetrate skin, it causes a phenomenon known as "beta burns," which are shallow burns that appear similar to superficial burns.[64] The final type of radiation, gamma-radiation, causes the most concern due to its penetrating.[64] On a molecular level, it is an electromagnetic radiation with an extremely high frequency and energy in the form of a photon emitted by an excited nucleus.[62,64,96] Gamma rays also travel at the speed of light, but due to their extremely high energy, gamma radiation is the most penetrating of all radiation.[62,77,95] Lead is the primary material used to stop gamma rays, but it does not stop all gamma radiation.[62,77] However, the weak ionization ability of gamma rays means there is no amplification inside the human body.[95] Appendix B includes a tabular comparison of these types of radiation.

While less frequently considered, nuclear reactions also cause X-ray and neutron radiation.[65] X-rays behave identically to gamma-rays, and the difference between the two is the mechanism by which they are generated.[64,65] A gamma-ray is emitted when a nucleus transitions from an excited state to a lower-energy state or the ground state, while an X-ray is emitted when an excited electron transitions from an excited state to a lower-energy state or the ground state.[65] As a result, X-rays typically, but not always, are lower energy than gamma-rays.[64,65] Neutron radiation consists of a free neutron, which is typically emitted as a result of the initial fission reaction.[63,64] Because neutrons have no charge, they are indirectly ionizing, whereby they are absorbed into a stable atom, making it unstable and more likely to emit another type of ionizing radiation.[64,65] Neutron radiation can even penetrate lead and is only stopped by large quantities of

hydrogen-rich material, such as water.[63,64] When absorbed into the human body, neutron radiation can have an amplification factor as high as 50, making it the most dangerous type of radiation.[63,97,98]

In the aftermath of a nuclear detonation, the cumulative radiation effect is most commonly categorized either as prompt or fallout radiation.[8,64,72] Occurring within the first minute after detonation, prompt radiation occurs nearly instantaneously with the flash.[8,64] It consists mostly of the gamma rays and neutrons released as part of the initial fission reaction.[64,65] It is the largest proportion of the nuclear effect for smaller devices.[64,65] The concentration of prompt radiation is affected by absorption, scattering, and capture of radiation by the atmosphere and buildings.[64] As the thermal and prompt radiation effects occur simultaneously and first in a nuclear detonation, debris created from the blast effect will be radioactive for the areas that overlap with the prompt radiation effect.[8,72] Fallout radiation, on the other hand, occurs primarily from the fission products and as a result of the interaction between the fireball and the ground.[8,64,65] As such, fallout radiation only occurs for surface and near-surface bursts, not for air bursts.[64] In this phenomenon, large quantities of soil, debris, and other ground material are sucked into the fireball, along with the weapon casing.[7,64,65] The extreme temperatures within the fireball vaporize these materials, and they are drawn into the mushroom cloud.[64,65] As the temperature cools, the radioactive materials and dirt particles that were also vaporized condense.[64,65] As the cloud rises, winds transport these contaminated particles from the cloud and carry the fallout radiation over significant distances downwind.[8,64,65] However, in addition to the size and weight of the particles, fallout radiation is subject to atmospheric conditions that vary by height, so the fallout pattern cannot simply be predicted by surface-level winds.[17,64] All three types of radiation are seen in radioactive fallout, but gamma rays and beta particles compose the

preponderance of the radioactive materials in fallout.[64] Moreover, due to the nature of fallout, the most hazardous areas where fallout particles would likely land are on rooftops and the ground.[72]

Like the blast effect, the fallout radiation effect has two specified zones, as summarized in Table 2.8. Prompt radiation does not have widely accepted, similar zone definitions, due to significant levels of prompt radiation being contained within the severe damage zone and inaccessible.[64,72] Unlike the damage zones characterized by visible destruction, the fallout zones are characterized by radiation exposure.[8,72] The threshold between zones is measured as an exposure rate in roentgen per hour (refer to Appendix C for radiation measurement units).[8,72] Access to the Dangerous Fallout Zone (DFZ) will be restricted to time-sensitive, mission-critical actions, such as immediate life-saving operations.[69,72,99] Most of the longer-term rescue operations will occur in the hot zone.[8,72,99] While there is a low probability of acute radiation effects in the hot zone, each responder's exposure should be carefully monitored and controlled.[8,69,72,99] Due to the nature of fallout radiation, there will be regions in which the DFZ includes light and moderate damage zones. The DFZ takes precedence for restricting operations due to the risk to the responders and will require constant reassessment, due to its dynamic nature.[72] Additionally, it is important to note that fallout radiation rate decays rapidly, and thus there will never be an increase in fallout radiation.[64,72] Fallout radiation releases more than 50% of its energy within the first hour after explosion and approximately 90% of its energy within the first eight hours.[72] As such, the DFZ reaches its maximum extent within an hour after detonation, and the hot zone reaches its maximum extent 12-24 hours after detonation.[8,72]

Health impacts from fallout radiation can be mitigated either by evacuating an area before the fallout arrives or by sheltering in place from it.[64,72,100] Buildings provide protection by increasing the distance between fallout particles and individuals at risk as well as blocking the fallout

radiation as it travels through the building.[72,100] The protection a building provides is called a protection factor (PF), calculated as the ratio of the outside radiation exposure to the

Table 2.8. Fallout zone definitions caused by the radiation effect.[8,72]

Fallout Zone	Threshold (R/h)	Description
Dangerous Fallout Zone (DFZ)	≥10	– ARS likely – All operations restricted to time-sensitive, mission-critical actions – Reaches its maximum extent approximately one hour after detonation
Hot Zone	0.01 – 10	– Unlikely to cause ARS – Entrance requires appropriate personal protective equipment (PPE) – Reaches its maximum extent 12 – 24 hours after detonation

inside radiation exposure.[72] A higher PF suggests more protection, and adequate protection, defined as a PF ≥ 10, protects occupants against Acute Radiation Syndrome (ARS).[64,72] Table 2.9 describes sample shelters with PF ranges.[72] Basements offer the best protection, while vehicles and single-story structures offer the least protection. [72,100] Within a building, middle floors are more protective than top or bottom floors, except for in large office buildings, where the bottom floor is the most protective.[72] Recent research[72] suggests that more than 130,000 lives can be saved in the aftermath of a 10 kt detonation in Washington, DC by ensuring adequate shelter for the first four days.

Mortality from acute radiation exposure via ARS is tightly associated with whole-body dose and presentation of acute symptoms, as described in Table 2.10.[8] Due to the rapidly decaying nature of radiation, the acute effects listed are likely to be reduced by half if the

radiation exposure occurs over weeks.[8] The lethal dose for 50% of the exposed population at 60 days ($LD_{50/60}$) in untreated patients is approximately 450 rads, but with medical care, this threshold increases to 600 rads.[8,64] However, Stricklin et al.[101] found the lethal dose without medical treatment varies significantly with age (Table 2.11). It is plausible to assume a similar distribution of the lethal dose threshold for patients receiving medical treatment. Moreover, compounding injuries, or additional injuries resulting from the blast or thermal effects, which are a particular concern for individuals exposed to prompt radiation, worsen prognosis for irradiated patients.[35,64] The lethal dose for patients with compounding injuries drops to 250 rads for adults with acute radiation exposure.[8] Further research is needed to characterize the relationship between compounding injuries with acute radiation exposure and age. In practice, determining the absorbed dose of radiation is difficult, especially in the chaotic aftermath of a nuclear

Table 2.9. Shelter quality by associated PF with example shelters.[72]

Shelter Quality Category	PF	Example Shelters
Poor	< 4	– Vehicles – Wood single-story home – Brick-sided, single-story strip mall
Inadequate	≥ 4 to ≤ 10	– Stand-alone two-story home without a basement – Stand-alone, small-footprint four-story apartment building without a basement
Adequate	≥ 10 to ≤ 40	– Residential basements – Outer areas of high-rise building with brick walls – Outer areas of mid-rise building with concrete walls
Good	≥ 40	– Large basement or underground area – Inner area of high-rise building with brick walls – Inner area of mid-rise building with concrete walls

detonation. In the absence of a confirmed dose, onset of vomiting can be a vital tool to determine between compounding injuries with acute radiation exposure and age. In practice, determining the absorbed dose of radiation is difficult, especially in the chaotic aftermath of a nuclear detonation. In the absence of a confirmed dose, onset of vomiting can be a vital tool to determine survival likelihood (Table 2.12).[102,103] Almost 95% of individuals exposed will begin vomiting within an hour, which corresponds to a whole-body dose of 600 rads. Table 2.10 corroborates the fact that individuals with 600 rad or more are unlikely to survive.[8] Together, these tables emphasize the close relationship between acute radiation exposure and vomiting and may prove to be a key assessment tool for health care providers in the aftermath of a nuclear detonation. The syndrome that causes mortality from acute radiation exposure, ARS, is characterized by the development of a group of signs and symptoms that are manifestations of damage to tissues and organs by ionizing radiation.[102,104] However, individuals exposed to radiation will only develop ARS if the following four conditions are met: 1) the radiation dose was high, 2) the radiation was penetrating (i.e., only X-rays or gamma-rays), 3) the individual's entire body received the dose, and 4) the radiation was received over a short period of time.[99,102] The syndrome has four stages: prodromal, latent, manifest illness, and recovery or death.[104,105] The prodromal phase, which lasts up to the first 48 hours after exposure, results as the immediate effect of cell membrane damage.[104,105] In this phase, patients present with anorexia, nausea, vomiting, lymphopenia, diarrhea, fever, and granulocytosis.[104,105] As the patient transitions to the latent phases, which lasts between hours and 21 days, the prodromata becomes absent or diminished.[104,105] The manifest illness phase, which is the most critical phase, can begin just hours after exposure or can present up to 30 days after exposure.[104,105] In this phase, there are four subsyndromes of ARS that vary with dose and host factors: hematopoietic, gastrointestinal, cutaneous, and

Table 2.10. Death from acute radiation exposure as a function of whole-body absorbed doses (for adults)[8]

Short-Term Whole-Body Dose (rad)	Death from Acute Radiation Without Medical Treatment (%)	Death from Acute Radiation with Medical Treatment (%)	Acute Symptoms (nausea and vomiting within 4 h) (%)
1	0	0	0
10	0	0	0
50	0	0	0
100	< 5	0	5 – 30
150	< 5	< 5	40
200	5	< 5	60
300	30 – 50	15 – 30	75
600	95 – 100	50	100
1,000	100	> 90	100

Table 2.11. $LD_{50/60}$ values from acute radiation exposure for selected age categories.[101]

Age Category	Age (years)	$LD_{50/60}$ (rad)
Infant	0 – 1	328
Juvenile	> 1 – 18	353
Adult	> 18 – 50	410
Late Adult	> 50 – 65	353
Older Adult	> 65	291

Table 2.12. Role of time to vomiting in patient survival following acute radiation exposure.[102,103]

Dose (rad)	Time to Vomiting (h)	Victims with Vomiting (%)	Survivability
0	0	0	
100	N/A	19	
200	4.63	35	
300	2.62	54	
400	1.74	72	
500	1.29	86	
600	0.99	94	
700	0.79	98	
800	0.66	99	
900	0.56	100	
1,000	0.48	100	

neurovascular.[104,105] Table 2.13 summarizes the signs and symptoms associated with each subsyndrome, as well as the estimated dose thresholds.[105] It is important to note that Cutaneous Radiation Syndrome (CRS) can also result from exposure of skin to beta-radiation, causing beta burns.[105,106] Unlike ARS that results from the highly penetrating gamma-radiation, beta burns are rarely deeper than the skin, due to the reduced penetrating power of beta-radiation.[106] However, presentation of beta burns worsens prognosis for patients also presenting with ARS.[104–106]

2.3.4 Electromagnetic Pulse (EMP)

The EMP is perhaps the least understood effect from a nuclear detonation. It is an electromagnetic field generated from the detonation that produces a high-voltage surge.[8,64] The EMP is a major effect for high-yield weapons detonated at an extremely high altitude, but it is not well understood how the surge interacts with the environment in a surface or near-surface burst.[64] Posing no direct health threat, it predominantly impacts electronic equipment.[8] Currently, there are no widely accepted thresholds or estimates for impacts, and even the characterization of the impacts is heavily debated.[8,72] Scientists have postulated that an EMP could cause stalling of vehicles, destruction or disruption of communications equipment (e.g. cell towers), destruction of water and electrical control components, disruption of medical equipment (e.g. ventilators, cardiac monitors, etc.), and damage to other electronic devices.[8,72] Most nuclear weapon effect literature suggests that the extent of the EMP would be relatively close to the detonation site and thus dominated by other nuclear effects.[64,65]

2.3.5. Conclusion

In summary, the significant effects of a nuclear detonation include blast, thermal, and radiation effects. While the prompt and fallout radiation effects are well-known, the blast and thermal effects also cause significant impacts to the surrounding environment and people. The

Table 2.13. Subsyndromes of acute radiation sickness with associated thresholds.[104,105]

Subsyndrome	Threshold (rad)	Signs and Symptoms
Subclinical	0 – 100	– No detectable signs and symptoms
Hematopoietic	> 200	– Nausea / vomiting – Lymphocytopenia – Leukocytopenia – Pancytopenia – Immunodysfunction – Sepsis – Impaired wound healing – Gastrointestinal bleeding (20 – 30 days post-exposure)
Gastrointestinal	> 600	– Nausea / vomiting / diarrhea – Malabsorption – Ileus (obstruction) – Fluid and electrolyte imbalance – Hypovolemia – Acute renal failure – Cardiovascular failure (8 – 14 days post-exposure)
Cutaneous	> 600	– Erythema – Edema – Desquamation – Blistering – Ulcer / necrosis – Onycholysis – Hair loss – Abnormal sensation / itching
Neurovascular	> 1,000	– Nausea / vomiting – Anorexia – Fatigue – Headache – Confusion – Disorientation – Hypotension – Cerebral edema – Ataxia – Convulsions (1 – 2 days post-exposure) – Coma (1 – 2 days post-exposure)

EMP is less understood, but its impacts will likely be contained within the damage zones resulting from the other effects. It is imperative for emergency management personnel to understand the breadth and severity of impacts caused by nuclear effects to develop appropriate preparedness measures and response plans. A key mechanism to communicate these effects and impacts is through modeling nuclear detonations.

2.4. Modeling Nuclear Detonations

The rare occurrence of nuclear detonations necessitates the development of models and simulations to better inform emergency planners about the extent of impacts in such incidents.[107] However, the complex nature of nuclear detonations in conjunction with the relatively limited amount of publicly available data makes it extremely difficult to develop reliable models. The preponderance of existing models focus on a singular nuclear detonation effect, and few researchers attempt to develop a comprehensive model, at least in the public domain.

2.4.1. Upfront Challenges

Predicting the effects of a nuclear weapon detonation is particularly difficult as the majority of the publicly available data arises from the atomic weapons detonated in Hiroshima and Nagasaki in 1945. The atomic bombs dropped on Hiroshima and Nagasaki remain to this day the only real-world data for a nuclear explosion in an urban environment.[54] As these explosions occurred over 75 years ago, the data captured was extremely limited and its accuracy is heavily debated.[8] The next potential source, from test explosions, also does not provide readily accessible and useable data. From the initial atomic bomb test for the Manhattan Project in 1945 until the CBT in 1996, an estimated 2,047 nuclear tests were conducted across the world.[29] Within the US, these tests were designed like any scientific experiment: focusing on specific elements while controlling for all other factors. Tests ranged from assessing new technology to

determining the level of protection different building materials provide from radiation.[9] While these tests provide critical information to supplement data from Hiroshima and Nagasaki, there is potential for error due to the controlled environment. Moreover, this potential for error is further increased by the now-outdated data collection mechanisms. At the time of these tests, the technology to collect high resolution weather data did not exist, which increased the measurement error, especially in retrospective analyses.[108]

Furthermore, the US military and federal government retain the results and data from these tests, most of which remains classified.[9] As such, the federal government has extensive modeling capabilities for nuclear disasters, but limited data exist for local and state agencies. Publicly available and accessible models therefore must be built by integrating data from multiple sources, including those in the grey literature. This burden lands upon local, state, and/or civilian organizations, many of whom do not have the training or capability to create such methodology.

2.4.2. Nuclear Effect Models

In the published literature, it is far more common for a model to simulate one nuclear effect. The most studied nuclear effect is fallout radiation, which is modeled using atmospheric dispersion models. These models have applicability to all chemical, biological, radiological, nuclear, and explosive (CBRNE) incidents, which explains the volume of research. A report by the US Environmental Protection Agency (EPA)[109] identified 96 different dispersion models relevant to preparedness and response activities for CBRNE incidents for homeland security and emergency management personnel. Of these, 39 can be used to model fallout radiation.[109] Each model makes mathematical assumptions about how the particulates interact with the atmosphere and can be categorized by such assumptions. The two most common model types for fallout

radiation are Gaussian plume and Gaussian puff.[109,110] As the easiest to implement, Gaussian plume models assume conditions are horizontally homogeneous, the pollutant is released continuously, and the downwind concentration of the pollutant has a cross-section that resembles a normal distribution.[109] Gaussian puff models also assume a normally distributed cross-section of the downwind concentration of the pollutant, but unlike Gaussian plume models, do not assume homogeneous horizontal meteorological conditions.[109,111] They also do not assume a continuous release of the pollutant, which allows such models to capture near-instantaneous releases, such as in a nuclear detonation, more accurately.[109]

Similarly, countless models exist for a blast effect following an explosion, albeit mostly for conventional explosions.[112–116] Blast effect models first predict the blast loads and then evaluate the damage levels. The blast load predicts the overpressure pulse a specific location receives and is most commonly modeled using Computational Fluid Dynamics (CFD).[112,113,115] To accurately evaluate damage levels, the model must account for the time-dependent nature and non-linear behavior of the overpressure wave in addition to the fluid-structure interaction, the size and shape of the reflecting surface, afterburning, and the channeling effect.[116] Blast effect models range from equivalent single-degree-of-freedom (SDOF)[117] models to finite element (FEM)[118] representation. In SDOF models, only position and velocity are considered in a single, second-order differential equation.[116,117] FEM models discretize the space into numerous small, simple components (the finite elements) whose behavior is then described by partial differential equations with two or three space variables.[118] These models are often incorporated into other models, as the blast effect is the least debated nuclear effect.

Far fewer models have been created to simulate the thermal effects for a nuclear detonation, particularly regarding the development of a mass fire. Eden[9] extensively reviewed

the published and grey literature and interviewed key scientists to document the evolution of thermal effect models. Brode developed an initial model to predict fire and blast damage from a nuclear weapon by the late 1980s, but federal funding for his research was canceled by 1992.[9] Brode's work transformed the then-existing blast vulnerability system, which included a factor to indicate how fire and blast damage vary with weapon yield.[9] Much of Brode's work remains classified.[9] Almost concurrently, Martin developed the Nuclear Weapon Fires (NWFIRES) model, which incorporated fire-induced winds as a factor in fire spread.[9] However, the model lacked a physical basis for predicting fire spread; instead, the fire-induced winds were based on user input.[9,119] The developers insisted the uncertainties of weather and other local conditions made the prediction of mass fire and resulting fire damage infeasible, which proved to have a lasting influence in the fire modeling community.[8,9,72,119] Since then, Binninger et al.[45] built upon Brode's work to develop a thermal ignition model for an urban environment, further adjusted by data from the Nevada test site. This model incorporates weapon yield, a cloud attenuation factor, an enhancement factor for reflections from cloud and/or snow, an air scattering factor, an air absorption factor, ground range, height of burst, and visibility.[45] The number of uncertainties in an environment as complex as an urban environment in the aftermath of a nuclear detonation remains high and active debate continues surrounding the interaction between thermal fluence and the environment.

2.4.3. Nuclear Detonation Models

The most comprehensive, publicly available model of an improvised nuclear device (IND) detonation in a modern urban city was developed as a collaboration between the US federal government and multiple national laboratories.[72] As a further development of previous work by the Lawrence Livermore National Laboratory (LLNL)[120], it simulates a 10kt detonation

in downtown Washington, DC and uses the results to identify key planning recommendations related to an IND response.[72] However, the models used to simulate the blast and radiation effects were created by the national laboratories and cannot be used by local or state emergency management personnel unless they directly contract with the national laboratories due to security concerns. Moreover, the report focuses primarily on the blast and radiation effects, with minimal discussion of the thermal effects. The authors argue the thermal effect is uncertain and diminished for a low-yield, urban detonation due to urban shielding and a cooler fireball temperature compared to an air burst.[72] The model does, however, conduct a "block-by-block" analysis of the effects, which allows for increased accuracy in the assessment of the shelter quality and associated protection factors of the radiation exposure.[72] Due to these improvements, this report remains the most accurate and detailed modern nuclear detonation simulation publicly available more than a decade after its initial publication.

Developed as a mechanism to provide less-granular results but to more cities, the most comprehensive effort to provide modeling results to local and state agencies comes from FEMA's Improvised Nuclear Device City Planner Resource (iCPR) tool.[121] The developers of the tool pre-calculated improvised nuclear device (IND) effects for 60 major cities in the United States (US).[122] For each city, a one kt and 10 kt ground-level detonation is simulated in the downtown business district location at noon local time.[122] Users of the tool can choose one of five weather patterns for the city simulation, one representative pattern for each season and a representative pattern all year.[121] While this tool is an invaluable resource, access to it is restricted to government (i.e., federal, state, local, and tribal) emergency planners.[122] The results of the tool, and therefore the weather pattern analysis, are not available to civilian emergency management organizations or academic institutions.

Perhaps the most popular nuclear modeling software, NUKEMAP is a free, publicly available, web-based nuclear weapons effects simulator.[123] First released in 2012, it allows a user to simulate a nuclear detonation in any location with any weapon yield at any height of burst.[123] However, NUKEMAP was primarily developed to educate members of the public on the effects of nuclear weapons.[124,125] The underlying data are primarily derived from Glasstone and Dolan[64] and online mapping programs.[123] Numerous academic publications have utilized the software to make assessments about the health care[58,126–128] and policy[129,130] impacts due to its easy comprehension and limited technical knowledge required. However, it does not achieve the same level of precision as other models. For example, the estimated fatalities and injuries are provided in totality and are not elucidated by etiology. The link for further documentation of methods for casualty estimates yields a "Not Found" URL error.[131] Other publications have suggested NukeMap only considers blast effects, ignoring the thermal and radiation effects, in estimating acute casualties.[130] Additionally, the only weather-related variables a user can adjust are wind speed and origin; there is no inclusion of parameters such as cloud cover or precipitation, which significantly alter the thermal and radiation effects.[64] Furthermore, a user can only customize thresholds for prompt radiation exposure, which is provided as the dose equivalent. In contrast, fallout radiation is provided as the absorbed dose rate, and is subsequently easily misinterpreted. While NUKEMAP provides a foundational model of nuclear detonations, its broad assumptions suggest it should not be used by local and state emergency management personnel in the development of detailed plans or exercises.

2.4.4. Hazard Prediction and Assessment Capability (HPAC)

While there are other programs that model all of the effects of a nuclear detonation, Hazard Prediction and Assessment Capability (HPAC), created by the Defense Threat Reduction

Agency (DTRA), is widely agreed upon as the authoritative software for nuclear detonations.[7,8,16,17,132,133] Used for both civilian and military purposes, HPAC has both forward deployable and reachback modeling capacities, which allows it to be used in training and planning efforts as well as in real-time incidents.[133] First tasked with developing HPAC in 1991, DTRA has since iteratively improved the software, with the most current version being 6.7.[134] Access to HPAC is tightly controlled by DTRA for government, government-related, and academic uses, due to the classified and sensitive nature of certain aspects of the software. The preponderance of model development and analysis using HPAC occurs in the national research laboratories, with access to classified data and databases.[8,69] Much of the publicly available literature analyzes the accuracy of HPAC's dispersion model.[108,133,135–137] As such, published literature focusing on model development for a nuclear detonation, especially for simulating the impact on populations and health outcomes, is limited.

Of the available literature that comprehensively analyze a nuclear detonation, the methodology remains largely consistent. The fallout radiation is simulated using earlier versions of HPAC, and the blast and prompt radiation effects are supplemented, using either ESRI's ArcGIS or the Defense Nuclear Agency's Weapons Effects (WE) program.[7,16,17,132] Unlike previously discussed models, the authors do incorporate an array of models for the likelihood of mass fires, including the models put forth by Binninger, Postol, and Eden.[7,16] To address the variability in weather and climatological patterns, the authors repeated the simulations in various conditions or in conditions that represent estimated average conditions.[7,16,17,132] There is not a clear statistical methodology behind choosing these conditions. Moreover, earlier studies did not utilize fully three-dimensional weather data but rather inputted various variables at repeated levels in the atmosphere, essentially discretizing continuous variables.[17] Additionally, these

studies largely represent the worst-case scenarios and do not fully address the role of the urban environment in nuclear detonations. These existing models largely assume an open environment with few individuals sheltered inside buildings. The thermal effects contain a robust analysis of the weapon's interaction with the atmosphere but fail to fully address interaction with the urban environment. In an urban setting, tall buildings can cast shadows over nearby buildings, thus reducing the thermal fluence the latter receive. This ultimately reduces the number of individuals with burn injuries. The blast effect interaction with the urban environment is not included, even though the close proximity of buildings causes the wind tunnel effect, amplifying the velocity of the winds resulting from the dynamic pressure. The authors do partially address the interaction between the urban environment and the radiation effects by estimating protection factors corresponding to average building construction in the area of interest.[7,16] However, a more in-depth consideration of these variables is necessary to consider the true impacts of a nuclear detonation in an urban environment.

The methodology behind the casualty estimates in these studies[16,17,132] are primarily based on the thresholds for each effect previously discussed in this review. The most recently published study[7] applies the modified sort, assess, life-saving interventions, treatment and/or transport (modified-SALT) triage algorithm to estimate the volume of casualties by triage categories. This classification is an imperative step forward in the literature, especially for emergency management planning, as it further distinguishes the volume and severity of patients anticipated in the aftermath of a nuclear disaster. However, even the modified-SALT triage algorithm struggles to address the complexity of patients from a nuclear detonation. Many of these patients will have compounding injuries, which significantly alters survival likelihood and the treatment required, as well as the resources required to provide the required treatment.

Moreover, these models largely represent a worst-case scenario, so it is plausible that the casualties would be fewer in reality. Public health measures such as sheltering in place, evacuation, and communication will be imperative in minimizing radiation exposure.[138] Parikh et al.[139] found that such measures have a nonlinear and non-monotonic impacts on the number of casualties in the aftermath of a nuclear detonation, so incorporations of such measures into a more realistic model cannot simply assume a linear, monotonic relationship. As such, future studies focused on improving the methodology of nuclear detonation modeling should explore additional methods for estimating the volume and severity of casualties in an urban environment.

2.5. US Health Care Impacts from a Nuclear Detonation

2.5.1. Health Care Impact Models

The results from using both NUKEMAP and HPAC models suggest that the US health care system would not be able to handle a disaster on the scale of a nuclear device detonation.[17,126,128,132] Gale and Armitage[13] go so far as to argue existing medical preparedness efforts are "obviously useless" in the context of a nuclear device detonation. As of 2008, almost one third of the US population lives in counties where the number of staffed and unoccupied health care facility beds would be inadequate for a typical mass casualty event.[14] The COVID-19 pandemic illustrated that this percentage has likely increased over time,[15] and the scale of a nuclear detonation would likely increase that fraction. Sauer and Thakur[127] determined that "no society can ever be prepared for such a scenario" when analyzing the number of intensive care beds required in the aftermath of a nuclear detonation. It is worth noting the smallest weapon considered in their analysis had a yield of 45 kt.[127] Dallas et al.[16] estimated that a 15 kt weapon detonated on Beer Sheva, Israel would cause over 105,000 total fatalities, which is almost 50% of the population, and another 35,000 injuries. Bell and Dallas[132] further broke down casualty

estimates by injury type for a 20 kt weapon in four major cities across the US. In Atlanta, Georgia, they estimated that such a detonation would cause between 46,000 and 160,000 fatalities from fallout radiation alone,[17] a population size comparable to a large sports stadium. Within the model, the blast effect would cause approximately 2,000 fatalities and another 28,000 individuals vulnerable to injuries resulting from collapsing structures and debris.[17,74] An estimated 5,000 people were predicted to reside in the region associated with full-thickness thermal burns, and another 8,500 people would be found in the region associated with partial-thickness thermal burns.[17] While the fallout radiation potentially contributes to the greatest number of initial fatalities, the volume of thermal burn patients will likely overwhelm the existing burn care infrastructure in the US and subsequently increase the percentage of fatalities due to the thermal effects.

Kearns et al.[19] estimate the burn care community could manage approximately 2,000 patients if resources exist to treat and redistribute patients geographically. Within Bell and Dallas' model of an Atlanta detonation,[17] this leaves an estimated 11,500 individuals who would need care at a burn center but would lack access. Beyond the burn care capacity, a disaster of such scope would incapacitate the Georgia health care system. According to the American Hospital Directory,[21] 17 of the state's 113 non-federal, acute-care, short-term hospitals are in Atlanta, Georgia, comprising 30% of the staffed beds available in the state. In the event of a nuclear detonation in Atlanta, these facilities would likely be decimated, leaving only 70% of the state's hospitals responsible for handling the possible tens of thousands of patients. Analyses for the remaining cities in Bell and Dallas[17] yield a similar illustration of a strained health care system.

The complexity of nuclear detonations necessitates an extraordinarily complex response, with countless agencies and organizations responsible for just a small part of the overall response. The convoluted response infrastructure inevitably lends itself to easily passed over gaps. McDonald et al.[128] blended NUKEMAP and system dynamics to analyze how the entire US medical system, from local to federal resources, would respond to a CBRNE event. By analyzing plans for each involved agency and conducting interviews, sixteen gaps in the systematic response were identified.[128] These gaps ranged from cultural challenges, such as lack of willingness to prepare and lack of realistic operational training, to coordination challenges, such as different patient tracking software among local hospitals and reliance on electronics, to command challenges, such as confusion of jurisdictional responsibilities of each responding agency.[128] As more resources and systems are added to the medical response infrastructure, such as the Radiation Injury Treatment Network (RITN)[140] or regional burn disaster plans,[141] careful review of existing plans and coordination becomes even more imperative.

2.5.2 Thermal Burn Patient Considerations

Detonation of a nuclear device over an urban area would generate an unprecedented volume of patients, with injuries resulting from the blast itself, from the thermal energy and fires, and from the radiation emitted from the device. Of all of the injury etiologies, management of thermal burns may be the least understood, and treatment of such injuries has the greatest resource constraints. Every nuclear detonation simulation included in this review[7,8,17,72,120,132] exceeds the projected 2,000-patient threshold[19] by orders of magnitude, which suggests the burn health care infrastructure will be completely overwhelmed.

2.5.2.1. Burn Health Care

Even in non-disaster settings, burn injuries are relatively infrequent. Each year, there are approximately 129,974,000 visits to emergency departments in the US, but only 416,000 of them are for burns or corrosives.[142] As this is less than half a percent of all visits annually, it is evident why even experienced practitioners express discomfort or hesitation treating burn patients.[143] Burn patients are uniquely complex, as even a single patient with an extensive burn injury requires a greater commitment of supplies, personnel, and time to achieve optimal outcomes.[144] Patients with extensive burn injuries lose heat, plasma, and fluids that, if left uncorrected, can cause hypothermia, hypovolemic shock, and renal insufficiency.[145] Moreover, severely burned patients are particularly susceptible to infection, as skin is the primary line of defense in the immune response.[146,147] Care for these patients is intensive, prolonged, and costly.[148] The gold standard of care extends well beyond the immediate wound care to include the management of pain, nutritional deficiencies, immune system suppression consequences, and rehabilitation therapy.[81] Taylor et al.[149] note that the most resource-intensive burn patients are patients 50 – 70 years old with moderate-sized major burns (%TBSA 50 – 80%) and inhalation injury. Ryan et al.[150] supports these results, as the authors identified age greater than 60 years, %TBSA greater than 40%, and presence of inhalation injury as significant risk factors for mortality. To fully address all of the potential challenges and complications, burn patients are typically hospitalized approximately one day per %TBSA burned.[149] The average length of stay in a burn center is approximately 10 days,[151] but burn size and depth significantly affect the duration.[81,152,153] Lastly, treatment cost further exemplifies the intensity of resources required to treat burn patients. Carter et al.[154] recently determined the national average bed cost per day is $8,362 in a burn center. Comprehensive care also includes anesthesiology (on average $5,187) and surgical

operations ($4,844 per hour, on average).[154] Total charges average $268,435 for surviving patients and $354,560 for non-surviving patients.[151] In comparison, the average cost per stay across all health care etiologies is $9,700,[155] which suggests burn care is 27 - 36 times more expensive than the average hospitalization in the US.

Because of these challenges, burn injuries require a highly trained team for appropriate care. Specialized burn centers are designed to care for patients with burns as well as other skin and soft tissue injuries and disorders.[91,151] Highly specialized teams comprised of burn surgeon(s), nurses, anesthesiologist(s), respiratory therapists, physical therapists, dietitians, and psychosocial experts staff burn centers, but there is a severe shortage of trained personnel to supplement these locations.[18] Across the US, there are approximately 300 burn surgeons whose teams cover approximately 2,000 burn beds.[19] Similarly, there are 133 burn centers, only 72 of which are verified by the American Burn Association (ABA).[19] The ABA-verified designation is equivalent to accreditation, with stringent requirements surrounding personnel training, programmatic infrastructure, resources, and long-term follow-up capacity.[151] Moreover, the sparse nature of these burn centers dictates that there are several locations in the US that are hundreds of miles from the closest facility.[156] Eight states do not have a burn center, and another 11 lack an ABA-verified burn center.[156] Therefore, in addition to the patient management complexities, the broader systemic infrastructure for thermal burn patients is severely limited.

2.5.2.2. Burn Mass Casualty Incidents (BMCI)

In a disaster setting, the needs of the response overwhelm the available resources. Disasters causing burn injuries are of particular concern, due to the extremely limited available resources. The average burn center in the US has just 15 beds,[19,151] and recent research suggests burn centers operate at 95% capacity on average.[154] Therefore, a typical burn center has, on

average, 0.75 beds available for incoming patients. Even if the burn center implements their surge plan and expands their bed capacity by a factor of 1.5,[86] a typical burn center may only be able to take eight patients before becoming overwhelmed. Incidents with multiple burn injuries often present with more than eight patients, so burn centers in other states would be called upon to treat additional patients. However, at any given moment in the US, there are approximately 90 available burn beds across the entire country on average.[154] The bed capacity challenges described above for an individual burn center also apply to the entire burn care system in the US. Even if every burn center in the US could increase their bed capacity by a factor of 1.5 in a no-notice event, there would only be 3,000 burn beds available. Furthermore, the US National Bioterrorism Hospital Preparedness Program states that a burn center should plan to care for at least 50 burn cases per million people in a facility's service area in the event of a disaster.[157] However, Dai et al.[158] found that few, if any, centers responding to BMCIs occurring between 1990 – 2015 had this capacity, let alone capability.

In such circumstances, it will be imperative to transition to population patient care by employing triage practices. It is well documented that medical providers struggle to transition from the mentality of providing optimum patient care to focusing on population-level care in the aftermath of a disaster,[159,160] and this phenomenon is particularly pronounced in burn care. Current burn care is so successful that the idea of altering support for any patient is seldom practiced.[144,161] Modern burn care focuses on the foundational principle that all patients are potentially salvageable, and burn surgeons are becoming increasingly unfamiliar and uncomfortable with anything less than the most aggressive treatments.[144]

Coming from the French word "trier," which means "to sort," a health care provider triages potential patients by using an established system or plan to determine a treatment priority

for each patient.[162] Historically, triage systems are tailored to trauma etiologies, as the preponderance of mass casualty care is derived from military experiences.[163,164] For example, one of the most widely used systems, simple triage and rapid treatment (START), had poor specificity when used in response to a powder explosion in Taiwan that produced more than 500 burn patients.[165] Moreover, the most commonly used triage systems are not evidence-based and can be highly subjective.[166] Extensive research has documented poor interrater reliability among providers triaging the same group of patients in the same setting.[167–169]

To address the lack of evidence-based triage guidance for burn patients, Saffle et al.[144] constructed a triage decision table for burn patients by first tabulating mortality rate based on age group and total %TBSA. The table was then divided into six sections based on the likelihood of survival with aggressive treatment.[144] While the triage table begins to provide insight into prioritizing patients, it assumes all patients will be treated at a burn center with unlimited, aggressive treatment. In a disaster setting, these conditions are unlikely to be true, making it challenging for first responders to implement such a system in a pre-hospital environment when they are attempting to prioritize patients for transport.

To determine the appropriate health care destination, a system based on triage tables for burn health care sorts patients to a facility (outpatient or non-burn-center hospital, burn center, and comfort care) based on age and %TBSA.[19] The study, which has been adopted by the ABA, adjusts the destinations based on the environment of care (i.e. conventional, contingency, crisis, and catastrophic) and has associated guidelines for treatment in each of these categories.[19] These tables are static and heavily caveated to be adjusted at the discretion of a burn surgeon or other subject matter expert.[19] These triage tables do not integrate with the previously established, patient-level triage systems. As such, Robertson-Steel[170] calls for “an integrated triage,

prioritization, and streaming system or concept" that identifies patient need and the most appropriate resources and end point of care.

2.6. Gaps in the Literature

Nuclear detonations remain among the least understood disasters, due to the high degree of complexity and the lack of readily available data. Recent publications have made great strides in estimating the health care impacts from such an incident, but the accuracy of such predictions remains restricted by the limitations of the source models. The publicly available models have yet to consider synoptic climatological analyses to capture typical weather patterns for the detonation site. Moreover, the continued debate around the predictability of mass fires from a nuclear detonation has caused a lack of emphasis on, and preparedness for, thermal effects. Furthermore, the models in academic literature have yet to incorporate a building-specific analysis of radiation PFs. Finally, the lack of focus on thermal burn injuries from a nuclear detonation in conjunction with a severely constrained burn health care system suggests there is a tremendous gap in plans to manage burn patients in the aftermath of a nuclear disaster. Prior examinations into the role of the health care infrastructure in the aftermath of a nuclear detonation have also not addressed staffed bed capacity and availability, either total beds or by specialty treatment needs, such as beds in burn centers. Addressing these gaps will aid local and state emergency management personnel in better understanding the effects and impacts of a nuclear detonation.

These gaps in the literature will be addressed through the three aims of this dissertation. The first aim will utilize a synoptic weather analysis to characterize the variation in fallout radiation distribution. The second aim will increase the accuracy of existing nuclear detonation models by addressing shadowing and reflectance from the thermal effect in the urban

environment and by leveraging publicly available data to address building-specific protection factors. The third and final aim will combine the results of the previous two aims by estimating the casualties resulting from an IND and examining the response capacity of the health care infrastructure.

CHAPTER 3

CHARACTERIZING FALLOUT RADIATION PATTERNS FOLLOWING A SIMULATED NUCLEAR DETONATION IN ATLANTA, GEORGIA

3.1. Introduction

3.1.1. Background

The growing likelihood of the use of weapons of mass destruction (WMD), including nuclear weapons, on civilian populations has been increasingly described over the last two decades.[3,5,6,17] The detonation of a nuclear weapon would release blast, thermal, and ionizing radiation effects that woud result in a catastrophic number of casualties. The fallout radiation alone has the potential to injure or kill tens to hundreds of thousands (or more) of people.[17,72,171] However, the rare occurrence of such detonations necessitates the development of models and simulations to better inform emergency planners about the extent of impacts in such incidents.[107]

3.1.2. Fallout Radiation Models

A number of models have been used to simulate the explosion and ionizing fallout radiation from a nuclear weapon with varying degrees of complexity.[172] This effect is modeled using atmospheric dispersion models that have applicability to all chemical, biological, radiological, nuclear, and explosive (CBRNE) incidents, which explains the volume of research. A report by the United States (US) Environmental Protection Agency (EPA)[109] identified 96 different dispersion models relevant to preparedness and response activities for CBRNE incidents for homeland security and emergency management personnel. Of these, 39 can be used to model fallout radiation.[109] Each model makes mathematical assumptions about how the

particulates interact with the atmosphere and can be categorized by such assumptions. The two most common model types for fallout radiation are Gaussian plume and Gaussian puff.[109,110] Gaussian plume models assume conditions are horizontally homogeneous, the pollutant is released continuously, and the downwind concentration of the pollutant has a cross-section that resembles a normal distribution.[109] Gaussian puff models also assume a normally distributed cross-section of the downwind concentration of the pollutant, but unlike Gaussian plume models, do not assume homogeneous horizontal meteorological conditions.[109,111] They also do not assume a continuous release of the pollutant, which allows such models to capture near-instantaneous releases, such as in a nuclear detonation, more accurately.[109]

3.1.3. Impact of Weather Conditions

Regardless of the exact model used to predict the distribution of fallout radiation, the specified weather conditions are a critical component, as weather and climate significantly affect the distribution of fallout radiation.[173] Wind strength and direction are major factors, as the wind transports the radioactive particles from the mushroom cloud and carries the fallout radiation over significant distances downwind.[64,65] Atmospheric stability affects the height of the cloud as well as the behavior of the fallout plume.[64,65] The amount, thickness, and height of clouds affect scattering, reflection, and absorption of the radiation.[45,64] Detonations occurring below the cloud level have a significantly greater effect on thermal radiation, as the radiation is reflected back to the ground.[45] In contrast, detonations above the clouds reflect the radiation out to space and therefore reduce the radiation present on the ground.[45] A nuclear detonation model cannot be run for every possible permutation of these parameters and therefore representative weather conditions should be utilized to capture the most likely distribution of fallout radiation.

3.1.4. Selection of Simulation Date

Prior nuclear detonation models have primarily utilized a "typical" day for the city of interest[16,37] or have chosen weather conditions that optimize the nuclear weapons effects for the study objectives.[7,17,37,174] One study involving simulation of a nuclear war between Israel and Iran[16] chose median three-dimensional climates from 30 years of data for a typical mid-September day. In an effort to illustrate possible fallout patterns in the Washington, DC area, Buddemeier and Dillon[37] used weather data from nearby airports and weather stations on the 15th of each month in the year 2006. In their full simulation, however, the authors chose a weather profile from May 23rd, 2005 such that the effects would be similar to National Planning Scenario #1.[37] Similarly, a study of nuclear detonations in New Delhi, India[7] utilized weather data from May, as the minimal precipitation and cloud coverage typical for May in New Delhi optimized the dispersion of fallout radiation and thermal energy. An investigation of the climatological impacts of a regional nuclear weapon exchange[174] similarly selected weather conditions to optimize fire storm and other thermal effects. Rather than focusing explicitly on the optimization of effects, an analysis of the health care implications of a nuclear detonation in four major US cities[17] examined three years of twice daily skew-T, log-P thermodynamic diagrams to identify days in which winds typically ran in a direction with a major impact on the health care system.

The most comprehensive effort to consider the statistical variance for possible fallout patterns was conducted for the Federal Emergency Management Agency's (FEMA)'s Improvised Nuclear Device City Planner Resource (iCPR) tool.[121] The developers of the tool pre-calculated improvised nuclear device (IND) effects for 60 major cities in the United States (US).[122] For each city, a one kiloton (kt) and 10kt ground-level detonation is simulated in the downtown business district location at noon local time.[122] To parameterize the representative

weather conditions for the city, the developers examined ten years of vertical weather data, mapping characteristics across layers of the atmosphere, to determine each city's predominant weather pattern for each of the four seasons over a 12-month period.[121] Users of the tool can choose one of five weather patterns for the city simulation, one representative pattern for each season and a representative pattern all year.[121] While this tool is an invaluable resource, access to it is restricted to government (i.e., federal, state, local, and tribal) emergency planners.[122] The results of the tool, and therefore the weather pattern analysis, are not available to civilian emergency management organizations or academic institutions. As such, there remains a gap in the published literature in identifying and using truly representative weather conditions in a nuclear detonation model.

3.1.5. Study Objective

The purpose of this study was to characterize the possible distribution of, and cluster the fallout radiation plumes resulting from, an IND detonation in Atlanta, Georgia (GA). This study also aimed to examine the relationship between surface-level weather characteristics and fallout radiation plumes to determine significant surface-level weather variables in predicting fallout radiation. If significant, such predictions would be useful for assisting operational decision-making at a local level.

3.2. Materials & Methods

To characterize the variation in fallout radiation distribution following an IND detonation in Atlanta, GA, the following tasks were performed: (a) collect and process historical surface-level and three-dimensional weather data; (b) generate and characterize simulated fallout radiation plumes; (c) classify the plumes based on spatial patterns and affected population; and

(d) construct prediction models for the fallout radiation plume classification based on surface-level weather conditions (Figure 3.1).

3.2.1. Study Area and Time Period

This study focuses specifically on simulated accumulated fallout radiation 48 hours post-detonation in Atlanta, GA for each day in the year 2019. Atlanta was used as the site of a simulated nuclear detonation for numerous reasons. Firstly, Atlanta's moderate climate[36] and lack of proximity to water allows for the consideration of meteorological factors without having to account for meteorological perturbations caused by large bodies of water.[37] Secondly, as a leader for commerce, industry, and transportation, particularly among southeastern US centers,[38] Atlanta is a plausible target for a nuclear attack. The city includes Hartsfield Jackson International Airport, the busiest airport in the world, as well as the headquarters for major businesses, such as Cable News Network (CNN) and The Coca-Cola Company, and a US Air Force reserve base. Other significant points of interest in the city include the Mercedes-Benz stadium, and the National Center for Civil and Human Rights, and Centennial Olympic Park, which was the location of a domestic terrorist pipe bombing attack during the 1996 Summer Olympics.[39] As far back as 1990, FEMA has listed Atlanta as a potential target.[40,41] Lastly, Atlanta is a representative of a typical major city found in the US. With a population of almost 500,000 and even more commuters every day, it is the 38th most populous city in the US.[42] It has a relatively large urban sprawl, with a balanced mix of land uses, and a metropolitan area population of approximately six million.[42,43] The combination of these factors make Atlanta an ideal sample location to characterize the potential patterns of fallout radiation.

3.2.2. Historical Weather Data

Data describing surface-level daily weather conditions and weather conditions at the time

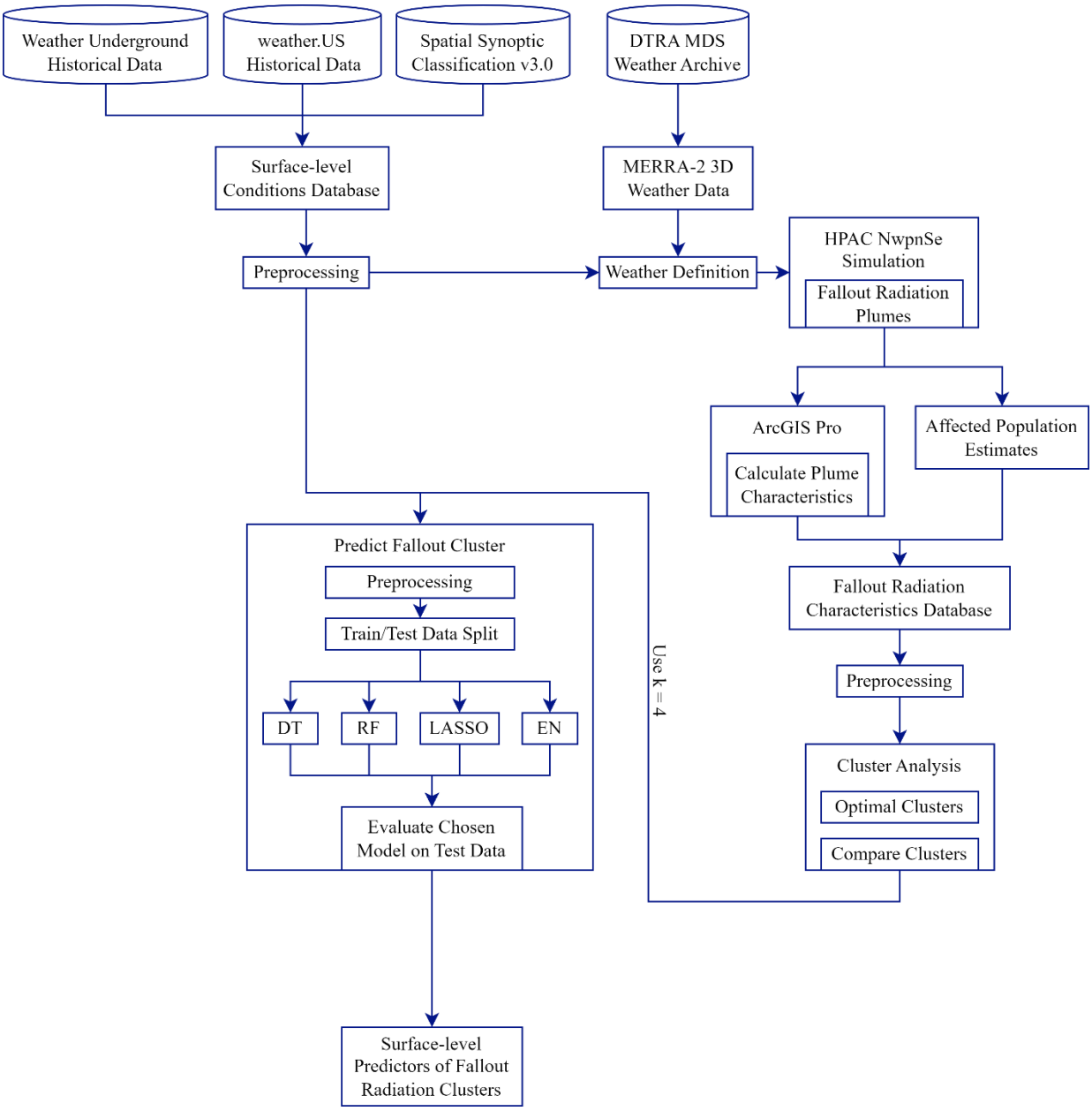

Figure 3.1. Overall workflow to characterize fallout radiation patterns. Abbreviations: DTRA = Defense Threat Reduction Agency; MDS = Meteorological Data Server; MERRA-2 = Modern-Era Retrospective analysis for Research and Applications, Version 2; HPAC = Hazard Prediction and Assessment Capability; NwpnSe = Nuclear Weapon Single Event; DT = Decision Tree; RF = Random Forest; LASSO = Least Absolute Shrinkage and Selection Operator; EN = Elastic Net

of the simulated detonation (10:00 am local time) were generated using Weather Underground's historical data for each date of the simulated detonation.[175] As the closest station to the simulated

detonation location, the Hartsfield Jackson International Airport weather station (KGAATLAN528) was used. This station is located at (33.63°N, 84.44°W), and has an elevation of 1,005 feet.[175] To supplement the data available in Weather Underground's historical weather database, percent cloud coverage at time of detonation at the same weather station was queried from the publicly available weather.us historical database.[176] If cloud coverage observations were not available at precisely 10:00 am local time, the observations recorded at the next closest time were used as an estimate of the cloud coverage.

Once these data were combined into a single database of all surface-level weather conditions, cloud coverage, hourly precipitation, and surface moisture were discretized for use in the nuclear weapon detonation simulation. Cloud coverage was categorized into clear (0% – 9.9%), scattered (10% – 50%), broken (51% – 90%), and overcast (91% – 100%). Hourly precipitation was categorized into none (0 in/hr), light rain (< 0.1 in/hr), moderate rain (0.12 – 0.3 in/hr), and heavy rain (> 0.3 in/hr). Within this time frame, there were no days in which hourly precipitation at time of detonation included snow. Surface moisture was defined as wet if the cumulative prior 24-hour precipitation was greater than zero. Otherwise, surface moisture was categorized as normal.

To further elucidate relevant factors in the surface-level conditions, hours of sunlight before simulated detonation, saturation pressure, vapor pressure, and absolute humidity at time of detonation were also calculated. Hours of sunlight before the simulated detonation was calculated as the difference between 10:00 am local time and time of sunrise. It was included in the analysis to account for any atmospheric perturbations caused by the increasing UV index. Saturation pressure (P_s) in kilopascals (kPa) was calculated using Teten's equation (Equation 3.1), where the *T* represents the temperature at time of detonation in degrees Celsius.[177]

$$P_s = 0.61078 \exp\left(\frac{17.2694 * T}{T + 237.3}\right) \quad (3.1)$$

Vapor pressure (P_v) in kPa was then calculated using P_s and the relative humidity (RH) at the time of detonation (Equation 3.2).[177]

$$P_v = \left(\frac{RH}{100}\right) * P_s \quad (3.2)$$

Lastly, a variation of the ideal gas law was used to calculate the absolute humidity (AH) in g/m^3 (Equation 3.3), where *M* represents the molecular weight of water (18.01528 g/mol), *R* represents the universal gas constant (8.3145 J/mol*k), and *T* represents the temperature at time of detonation in Kelvin.[177]

$$AH = \left(\frac{P_v * M}{R * T}\right) * 1000 \quad (3.3)$$

3.2.3. Spatial Synoptic Classification Patterns

Spatial synoptic classification (SSC)[178] was used to describe the synoptic environment in Atlanta area for each day during the study period. This synoptic weather-typing tool employs

four-times daily observations of temperature, pressure, dew point, and cloud cover to delineate different weather types that characterize the daily air mass at a particular location.[178] It does not take into account upper-level atmospheric conditions, but is a hybrid classification scheme that uses both manual assignment by subject matter experts and algorithm imputation based on typical days within each weather type.[178] SSC classifies each day at a particular location into one of seven main weather types: dry polar (DP), dry moderate (DM), dry tropical (DT), moist polar (MP), moist moderate (MM), moist tropical (MT), or transition (TR).[179] DP days are characterized by cool or cold dry air, with typically northerly winds and little or no cloud cover.[178] DM days are mild and dry, while DT days are associated with the hottest, sunniest, and driest conditions for a particular location.[178] MP days are typically cool, cloudy, and humid, often with light precipitation.[178] MM days are also cloudy but are warmer and more humid than MP air.[178] MT days are warm and extremely humid, and convective precipitation is relatively common, especially in the summer.[178] These days are typically cloudy in the winter and partly cloudy in the summer.[178] Lastly, TR days are those in which one weather type yields to another, based on large shifts in pressure, dew point, and wind throughout the course of the day.[178] The most recent version, SSC v3.0, also reports expanded weather types, which are based on one or more standard deviations from the mean apparent temperature within each weather type.[179]

For the purposes of this study, SSC v3.0 data was collected from the "ATL" station for each day within the study period. For each day, the weather type was recorded for the date in question (day 1) and the following day (day 2), as the fallout radiation simulation extends 48 hours. The expanded weather types were merged into the main weather type, per discussions with subject matter experts and the SSC v3.0 documentation.[179] The weather type for day 1 and

day 2 were also combined into a single variable (SSC Pattern) to capture the two-day weather typing pattern.

3.2.4. Three-Dimensional Weather Data

The Defense Threat Reduction Agency's (DTRA's) Meteorological Data Server (MDS) Weather Archive was queried to retrieve the Modern-Era Retrospective analysis for Research and Applications, version 2 (MERRA-2) data to generate the three-dimensional weather data for the nuclear weapon simulations. MERRA-2 is a global atmospheric reanalysis that assimilates historical atmospheric observational data spanning an extended period, using a single consistent analysis scheme.[180] It includes data for upper air observations, global models, surface observations, and mass consistent winds for urban models.[134] The reanalysis generates data with 0.625° × 0.5° spatial resolution at 42 levels, with the top level occurring at 0.1 hPa.[180] For the purposes of this study, the MERRA-2 data were used to capture the three-dimensional meteorological data for each day in 2019, beginning at 10:00 am local time and including the following 48-hour time period. These data for the study's spatial and temporal domain were then exported for use in the fallout radiation simulations within the Hazard Prediction and Assessment Capability (HPAC) software.[134]

3.2.5. Fallout Radiation Simulations

A tactical nuclear weapon with a predicted explosive yield of 15 kilotons (kt) detonated at 40 meters was simulated for each day in the year 2019 using DTRA's HPAC software. The height of the burst was chosen during a sensitivity analysis to optimize the nuclear effects while still maintaining realistic conditions. At such a height, the blast effect is greater at the detonation site, but the extent of damage is likely restricted since much of the shock wave is absorbed by the ground.[64] By detonating the device slightly above the ground, the fireball is absorbed less by the

ground and thus the radiant energy expands to further distances.[64] Fallout radiation only results when the fireball interacts with the ground, so the height was constrained to ensure fallout radiation occurs.[64]

While the yield of modern nuclear weapons can be much larger, the emergency management community emphasizes that a low yield weapon is the most useful for planning scenarios.[8,72,78,120] Most planning documents focus on a 10 kt weapon, but some experts argue this yield may be too low.[181] A 15 kt yield was also chosen to reflect a weapon size between those detonated in Hiroshima and Nagasaki.[54]

The simulated detonation occurred at 10:00 am local time each day to allow for the influx of the commuter population while minimizing meteorological changes. Lastly, the coordinates of the detonation location were +33.7566667, -84.38833333, which closely approximates the center of downtown Atlanta. Its proximity to significant points of interest, including the CNN headquarters, the Mercedes-Benz stadium, and the National Center for Civil and Human Rights, suggests that it is a plausible location to be targeted. Moreover, this area also includes Centennial Olympic Park, the location of a domestic terrorist pipe bombing attack during the 1996 Summer Olympics.[39]

Under these parameters, the atmospheric dispersion of ionizing radiation was calculated using the Second-order Closure Integrated PUFF (SCIPUFF) model, which is a Lagrangian puff dispersion model using Gaussian puffs to represent a three-dimensional, time-dependent concentration.[134,182,183] The fallout radiation dose was then estimated as the total effective dose equivalent (TEDE), ranging from 1 rem to 1,000 rem, 48 hours post-detonation. Due to the constraints of the HPAC workflow, the fallout radiation effects were estimated by modeling the detonation as if there were no obstructions (i.e., in a desert) and then subsequently adjusted by an

assumed average protection factor. For the purposes of this cluster analysis, an average protection factor of 7 was assumed. This value likely marginally overestimates typical stand-alone residential buildings while under-estimating mid-rise and high-rise buildings.[72] Additionally, due to the constraints of the population data available within HPAC, daytime population data from 2016[184] was suitably proportioned and used to estimate the population within each plume contour.

The simulated fallout radiation plumes were then exported as shapefiles for analysis in ArcGIS Pro.[185] Each plume was dissolved to calculate the total population at risk for fallout radiation dose greater than 1 rem at 48 hours post-detonation. The dissolved plume was also used to calculate the total area, and the centerline of each merged plume was used to estimate the maximum distance of the simulated plume. Lastly, the angle of the plume was determined by measuring the angle of the centerline from due North. However, as the angle is a circular variable, it cannot easily be included with other non-circular variables in statistical analysis. As such, it was broken into its x and y radian components, which could be treated as linear variables.

The resulting data from these simulations were then joined to create a database for fallout radiation characteristics that was used for the cluster analysis. Prior to beginning the cluster analysis, the likelihood of survival from the fallout radiation dose was based on data from the Hiroshima bombing in 1945,[186] further supplemented by additional guidance from the Centers for Disease Control and Prevention's (CDC's) toxicological profile for ionizing radiation[187] (Table 3.1). Fujita, Kato, and Schull[186] estimated the probability of death by radiation dose inside a wooden Japanese house, which is higher than other sources.[101–103,105,188] However, such sources are predominantly based on animal models and the minimally available human data. The

Hiroshima probability of mortality estimations were used to reflect the real-world likelihood of additional ionizing radiation (in the form of alpha and beta particles) and compounding injuries, both of which lower the likelihood of survival. Given that this cluster analysis only includes the fallout radiation, it was important to at least partially account for these additional factors in estimating mortality and survival.

Table 3.1. Estimated probability of survival by acute radiation dose.[186,187]

Dose Range (rad)	Estimated Probability of Death	Estimated Probability of Survival
0 - 99	0.10	0.90
100 - 199	0.33	0.67
200 - 299	0.50	0.50
300 - 599	0.67	0.33
600 – 799	0.80	0.20
800+	0.90	0.10

3.2.6. Statistical Methods

3.2.6.1. Exploratory Data Analysis

A preliminary descriptive analysis of the surface-level weather conditions was first conducted to assess the range of weather conditions included in the spatial and temporal domain of the study. A similar exploratory analysis was performed to assess the distribution of fallout radiation characteristics, particularly focusing on plume area, maximum extent, and angle, as well as affected population estimates within each survivability category. As a preliminary assessment of relationships between the surface-level conditions and the fallout radiation

characteristics, univariate regressions were conducted for each surface-level condition and repeated with each fallout radiation characteristic as the outcome of interest.

3.2.6.2. Cluster Analysis

The second part of this study aims to classify the fallout radiation plumes based on spatial patterns and affected population. Clustering analyses provide an objective way to create such classifications.

3.2.6.2.1. Parameters Considered

The following parameters were considered in the cluster analysis: plume area, plume distance, plume angle, the total population at risk, and the population proportion within each survivability category. All parameters were scaled prior to application of the algorithm to avoid disproportionate weight by any singular variable.

3.2.6.2.2. Clustering Algorithm

While a variety of methods for classifying data are available, this study used the Partition Around Medoids (PAM) algorithm, which was first introduced by Kaufman and Rousseeuw.[189] The objective of this approach is to minimize the average dissimilarity of data points to their closest selected points by identifying a sequence of points (e.g. medoids) that are centrally located in the clusters.[190] The algorithm accomplishes that objective by mapping a distance matrix into the specified number of clusters.[191] It begins by randomly selecting *k* data points in the data, to act as the initial medoids.[190,192] For all other data points, the algorithm then determines the medoids to which they are closest and assigns points to the representative clusters.[190] The "quality" of these cluster assignments is defined as the average distance from each data point to its cluster center (or medoid).[192] Then, different data points are tested as medoids.[190,192] If a different point reduces the total within cluster distance, the medoid is

swapped that point.[190] This process continues until no single swap improves the "quality" of the final cluster assignment.[192]

The PAM algorithm was chosen for this study for two reasons. First, it is more robust than the more commonly known *k*-means cluster approach, as PAM uses actual points in the data sample, while *k*-means randomly generates one using a Gaussian distribution.[190,193] Second, PAM enables clustering relative to any specified distance or dissimilarity matrix.[189,194] Instead of the traditional Euclidean distance, which calculates the shortest distance between two points, this study used the Manhattan distance, which calculates the absolute sum of distances between all attributes.[195,196] For two data points *x* and *y* in *d*-space dimensions, the Manhattan distance between those two points is defined in Equation 3.4.

$$d_{man}(x, y) = \sum_{k=1}^{d} |x_j - y_j| \tag{3.4}$$

The Manhattan distance was used for this study primarily because it is more robust to outliers than Euclidean distance.[196] Given the relatively small sample (n = 365), it was imperative to avoid methods that were sensitive to outliers. Furthermore, for clustering analyses involving weather applications, the Manhattan distance has been shown to outperform other distance metrics.[195]

3.2.6.2.3. Cluster Number Optimization

The PAM algorithm requires a user-assigned number of clusters (*k*). To determine the optimal number of clusters, three metrics were used: the elbow method, the silhouette method, and the gap statistic.

The elbow method is perhaps the most well-known and oldest method for determining the optimal numbers of clusters.[193] Beginning with a cluster value $k = 2$, the Within-Sum-of-Squares (WSS) is calculated (Equation 3.5), where x_i is the data point and c_i is the center point of the cluster (or the medoid).[197] The cluster value is then increased at each step by a value of 1.[197] In this method, the optimum number of clusters is the value of *k* in which the WSS most rapidly declines. This can easily be visualized by plotting the k-WSS curve, as it has a clear inflection point at the optimal number of clusters that looks like an elbow.[196,197]

$$WSS = \sum_{i=1}^{m} (x_i - c_i)^2 \tag{3.5}$$

Originally proposed by Hubert and Levin,[198] the silhouette method calculates with silhouette coefficient (s(*i*)), by measuring how similar a point is to its own cluster (cohesion), compared to other clusters (separation).[199] Values of s(*i*) range from -1 to 1, where the optimal number of clusters corresponds to the highest value of s(*i*).[193] A negative value of s(*i*) suggests an inappropriate number of clusters was chosen.[193] The silhouette coefficient for each data point *i* is defined in Equation 3.6, where $|C_I|$ is the number of points belonging to cluster I.[189,199] The

coefficient equals zero when *i* is the only point in the cluster, which prevents the number of clusters increasing significantly with many single-point clusters.[199]

$$s(i) = \frac{b(i) - a(i)}{\max\{a(i), b(i)\}}, \text{if } |C_I| > 1 \tag{3.6}$$

$$s(i) = 0, if\ |C_I| = 1$$

As defined in Equation 3.7, where $d(i,j)$ is the distance between data points *i* and *j* in the cluster, *a(i)* is the average distance between *i* and all other entities of the cluster to which *i* belongs. It can be interpreted as a measure of how well *i* is assigned to its cluster.[199]

$$a(i) = \frac{1}{|C_I| - 1} \sum_{j \in C_I, i \neq j} d(i,j) \tag{3.7}$$

Conversely, *b(i)* is the minimum of the average distances between *i* and all points in other clusters, as defined in Equation 3.8, where C_J represents some other cluster. In other words, it is a measure of dissimilarity of *i* from points in other clusters.[42]

$$b(i) = \min_{J \neq I} \frac{1}{|C_J|} \sum_{j \in C_J} d(i,j) \tag{3.8}$$

The last method to determine the optimal number of clusters in this study is the gap statistic, which was introduced by Tibshirani, Walther, and Hastie.[200] It compares the total within intra-cluster variation for different values of *k* with their expected values under a null reference distribution of the data.[196] The optimal number of clusters is the value that maximizes the gap statistic.[200] In this method, the normalized within-cluster sum of squares around the cluster mean (W_k) is first calculated (Equation 3.9), where D_r is the sum of the pairwise distances for all points in cluster r and n_r is the number of clusters.

$$W_k = \sum_{r=1}^{k} \frac{1}{2n_r} D_r \tag{3.9}$$

The gap statistic standardizes the graph of $\log(W_k)$ by comparing it with its expectation under a null distribution of the data (i.e., a distribution with no obvious clustering).[200] This null distribution is obtained by the Monte-Carlo sampling method, and the optimal number of clusters is the value for which $\log(W_k)$ falls the farthest below the null reference curve.[201] Mathematically, this is defined in Equation 3.10, where $E_n^*(\log(W_k))$ refers to the $\log(W_k)$ expectations (i.e., the null distribution), *P* is the number of samplings, and *s(k)* is the standard

deviation.[200] The optimal number of clusters is the smallest value of *k* such that the gap statistic is within one standard deviation of the gap at k+1: $Gap_k \geq Gap_{k+1} - s_{k+1}$.[201]

$$Gap_n(k) = E_n^*(\log(W_k)) - \log W_k E_n^*(\log(W_k))$$
$$= \left(\frac{1}{P}\right)\sum_{b=1}^{P}\log(W_{kb}^*) \approx \left(\frac{1}{P}\right)\sum_{b=1}^{P}\log(W_{kb}^*)\, s(k) \qquad (3.10)$$
$$= \sqrt{\frac{1+P}{P}}\, s(k)$$

3.2.6.3. Cluster Prediction

Following evaluation of the cluster analysis to determine the most appropriate cluster assignments, the final portion of this study endeavored to construct prediction models for the fallout radiation plume classification, based on surface-level weather conditions.

3.2.6.3.1. Parameters Considered

In addition to the cluster assignment, parameters for month, season, SSC weather type and pattern, temperature, precipitation, dew point, wind direction and speed, pressure, humidity, cloud coverage, visibility, and hours of sunlight before detonation were included in the cluster prediction analysis.

3.2.6.3.2. Model Development

Four machine learning models were considered for the cluster prediction analysis. The data were split such that 66.7% were used for training the models and the remaining 33.3% were used for testing the final chosen model. Cross-validation was used for all models, using a 10-times repeated, five-fold resampling structure. Using the tidymodels framework, all predictors with zero variance were removed, as well as variables with a Pearson correlation coefficient greater than 0.75. Lastly, due to the irregular variances across the variables included in the model, a Yeo-Johnson Power Transformation was applied to all predictors. In meteorological applications, the Yeo-Johnson Transformation has improved accuracy and performance in comparison to the standard Box-Cox transformation.[202] This transformation created a more uniform dataset by reducing the skewness and approximating normality in the remaining variables included in the analysis.[203]

3.2.6.3.3. Model Definition

There are numerous machine learning (ML) models that could be applied to this portion of the study, but this analysis focused primarily on two major types of models: tree-based and regularization-based. The tree-based models were chosen as the primary users of the prediction algorithms are non-statisticians, and such models are among the easiest machine learning models to interpret and understand.[204] However, to robustly consider the potentially relevant machine learning methods applicable to this study, two regularization-based methods were also included in the analysis. Broadly, regularization allows variables to be included in a model with less weight than other variables by reducing the value of the variable's coefficient.[205] The hyperparameters of each model were tuned to optimize the performance of each model.

Also known as a classification and regression tree (CART), the Decision Tree (DT) model examines each predictor and splits the outcome at a value of the predictor that leads to the best performance increase in the model.[206,207] The tree development continues until a certain threshold criterion is met, such as number of observations in each leaf of the tree.[207] A DT model is often the most intuitive machine learning algorithm, but it also typically has a reduced performance compared to other models.[208]

A slightly more sophisticated model, a Random Forest (RF) model aims to reduce the variance by building a tree for each re-sampling of the existing data.[208,209] However, instead of considering all possible predictors at each decision tree split, the split occurs based on the best predictors of a random sample of all predictors.[209] This method allows for de-correlation in the trees by avoiding the default nature of decision trees that aim to include as many predictors as possible.[209,210] Each individual tree is then averaged to find the final model. RF models are also more difficult to interpret than standard DT models.[209]

As a regularization-based model, Least Absolute Shrinkage and Selection Operator (LASSO) balances the goodness of fit with a penalty for the coefficients, calculated by the respective absolute value.[211] This methodology allows coefficients to go to zero and thus be dropped from the model.[211] The disadvantage of the LASSO model comes predominantly in the form of selection of just one variable from highly correlated variables, ignoring the rest entirely.[208,211]

Lastly, for particular use in circumstances with correlations between predictor variables, an Elastic Net (EN) model further adds to a LASSO model by incorporating a mixture parameter in addition to the overall weight given of the penalty.[208,212] The mixture parameter determines the distribution of the penalty, which is the sum of the LASSO regularization component as well as a

new regularization component, which is calculated by squaring the magnitude of the coefficient, and then all coefficients are shrunk by the same factor.[212]

3.2.6.3.4. Model Performance Evaluation

To compare the performance of each model, a confusion matrix was calculated for each model, and the accuracy, sensitivity, specificity, and area under the receiver operating curve (AUC ROC) of the models were calculated and compared. These standardized metrics are widely used in evaluation of classification models, particularly for models that predict multiclass variables.[213–216] The confusion matrix compares the assigned clusters (from the cluster analysis) and predicted cluster assignments (from the ML model). The information in this matrix was used to calculate the classification performance metrics accuracy, sensitivity, and specificity (Equations 3.11 – 3.13),[217–219] where *TP* represents the true positives, *TN* represents the true negatives, *FP* represents the false positives, and *FN* represents the false negatives. While interpretation of these measures is relatively straightforward for binary outcomes, it is slightly more complex for multi-class outcomes, as is the case in this study for the cluster assignments.[217] Using the example of cluster 1, TP are instances in which days in the observed (assigned) cluster 1 are correctly predicted as cluster 1. Similarly, TN are instances in which days in the observed cluster 1 are incorrectly predicted as any other cluster. FP occur when days in any other observed cluster are predicted as cluster 1, while FN occur when days in the observed cluster 1 are predicted as any other class.

$$Accuracy = \frac{TP + TN}{TP + TN + FP + FN} \tag{3.11}$$

$$Sensitivity = \frac{TP}{TP + FN} \tag{3.12}$$

$$Specificity = \frac{TN}{TN + FP} \tag{3.13}$$

Accuracy, sensitivity, and specificity were calculated for each cluster and then averaged with equal weight assigned to each class. In the context of this study, the accuracy metric represents the proportion of correctly predicted clusters within the training dataset. Sensitivity corresponds the average proportion of observed cluster assignments that were correctly predicted, averaged across each cluster. Similarly, specificity corresponds to the average proportion of correct instances in which the observations not assigned to a cluster were predicted to not belong to that cluster.

Lastly, the AUC ROC was also calculated for each model. The AUC ROC is a measure of the two-dimensional area underneath the entire ROC, which was created by plotting the sensitivity versus the false positive rate (1 – specificity) at different classification thresholds.[220] The AUC ROC represents the degree of separability and is an indicator of how well the model can distinguish between classes.[221] Possible values of AUC ROC range between 0 and 1, where a higher value is desirable and a null model has a value of 0.50.[220] For the multi-class outcome, the AUC ROC was calculated using the method proposed by Hand and Till.[221] In this approach, the

AUC for each pair of clusters is calculated, and then the AUC values are averaged over all possible pairs.[221]

3.2.7. Software

The nuclear weapon detonation simulation and fallout radiation plumes were generated in HPAC (v6.8),[134] and the spatial characteristics of the plumes were analyzed in ArcGIS Pro (v3.0).[185] All data processing and statistical analyses were performed using R Statistical Software (v.4.2.2), via RStudio Desktop on a Windows Server operating system.[222] The following R packages were utilized: broom,[223] broom.mixed,[224] circular,[225] cluster,[226] doParallel,[227] extrafont,[228] factoextra,[229] GGally,[230] ggpubr,[231] glmnet,[232] gtsummary,[233] here,[234] lubridate,[235] ranger,[236] readxl,[237] rpart.plot,[238] scales,[239] skimr,[240] tidyverse,[241] tidymodels,[242] vip,[243] viridis,[244] and writexl.[245]

3.3. Results

3.3.1. Surface-level Weather Characteristics

Daily weather conditions (Table 3.2) and weather conditions at the time of the simulated detonation (10:00 am local time) (Table 3.3) for each day in the year 2019 (N = 365) were included in this study. Throughout the course of the year, the ambient air temperature ranged from 22°F to 99°F, with a daily average of 65.63°F. The ambient air temperature at the time of simulated detonation similarly averaged to 63.28°F. Congruently, the dew point each day ranged from 7°F to 75°F, with a daily average of 51.66°F. The dew point at the time of simulated detonation similarly averaged to 52.17°F. At 10:00 am local time, conditions were typically mild, with an average temperature of 63.28°F, a mean relative humidity of 68.38%, and relatively limited precipitation (0.01 in/hr). These conditions are in alignment with the most frequent SSC weather types: MT (n = 122; 33%) and DM (n = 95; 26%). The wind direction at

the time of the simulated detonation varied significantly (Figure 3.2). Winds originating from the northwest (n = 95; 16%) and blowing in a southeasterly direction were the most common, along with winds originating from the east (n = 54; 15%) and blowing in a western direction.

Figure 3.3 depicts the distribution of daily average temperature, cumulative 24-hour precipitation, and maximum wind speed throughout the year. Similarly, Figure 3.4 illustrates the distribution of the temperature, relative humidity, cloud coverage, and wind speed at the time of simulated detonation throughout the year. Both the daily average air temperature and air temperature at time of simulated detonation followed typical seasonal patterns throughout the year, with the highest temperatures occurring June through October. Both wind speed distributions were relatively noisy, with significant variation throughout the year. However, the daily maximum wind speed has notable peaks in the summer months, whereas the highest wind speeds at time of detonation occurred in the spring months. The cumulative 24-hour precipitation, relative humidity, and cloud coverage do not have any clear changes in distribution throughout the year.

Figure 3.5 illustrates the SSC weather type distribution for each day in 2019. MT and DM were the most common days, with MT occurring more frequently in the spring and summer months, and DM occurring more frequently in the winter months. This pattern aligns with the temporal distribution of temperature and cloud coverage discussed above. However, MT days are characterized by extreme humidity, and the temporal distribution of relative humidity in Figure 3.4 does not appear to match the temporal distribution of MT days in Figure 3.5, plausibly because relative humidity peaks later in the day, typically in the afternoon, rather than in the morning, as captured by the data in this analysis.

Table 3.2. Summary statistics for daily weather conditions in Atlanta, GA, January 1, 2019 – December 31, 2019.

Daily Weather Conditions	N = 365[1]	Mean	Std Dev	Median	Min	Max
Season						
Fall	89 (24%)					
Spring	93 (25%)					
Summer	94 (26%)					
Winter	89 (24%)					
Spatial Synoptic Classification						
Dry Moderate	95 (26%)					
Dry Polar	10 (2.7%)					
Dry Tropical	59 (16%)					
Moist Moderate	37 (10%)					
Moist Polar	7 (1.9%)					
Moist Tropical	122 (33%)					
Transition	35 (9.6%)					
Air Temperature - High [F]		74.80	15.12	76.00	43.00	99.00
Air Temperature - Low [F]		57.20	14.77	59.00	22.00	78.00
Air Temperature - Average [F]		65.63	14.58	67.24	32.50	87.48
Cumulative 24hr Precipitation [in]		0.12	0.34	0.00	0.00	3.06
Dew Point - High [F]		56.41	14.31	61.00	16.00	75.00
Dew Point - Low [F]		46.38	16.45	50.00	7.00	71.00
Dew Point - Average [F]		51.66	15.22	55.71	10.00	72.83
Maximum Wind Speed [mph]		15.04	5.58	14.00	7.00	41.00
Visibility [mi]		9.92	0.68	10.00	0.50	10.00
Sea Level Pressure [in]		29.05	0.15	29.04	28.67	29.98

[1]n (%)

Table 3.3. Summary statistics for weather conditions at simulated time of detonation in Atlanta, GA, January 1, 2019 – December 31, 2019.

Weather at Time of Detonation	**N = 365[1]**	**Mean**	**Std Dev**	**Median**	**Min**	**Max**
Temperature [F]		63.28	16.00	65.00	24.00	87.00
Precipitation Rate [in/hr]		0.01	0.05	0.00	0.00	0.60
Dew Point [F]		52.17	16.09	57.00	9.00	74.00
Wind Speed [mph]		8.29	4.17	8.00	0.00	21.00
Wind Direction						
N	7 (1.9%)					
NNE	2 (0.5%)					
NE	12 (3.3%)					
ENE	16 (4.4%)					
E	54 (15%)					
ESE	11 (3.0%)					
SE	11 (3.0%)					
SSE	9 (2.5%)					
S	19 (5.2%)					
SSW	15 (4.1%)					
SW	16 (4.4%)					
WSW	16 (4.4%)					
W	28 (7.7%)					
WNW	24 (6.6%)					
NW	59 (16%)					
NNW	31 (8.5%)					
CALM	23 (6.3%)					
VAR	12 (3.3%)					
Wind Gust [mph]		1.82	6.52	0.00	0.00	33.00
Cloud Coverage [%]		69.85	34.26	75.00	0.00	100.00
Relative Humidity [%]		68.38	13.82	67.00	34.00	97.00
Absolute Humidity [g/m^3]		11.19	5.20	11.93	1.84	20.31
Sea Level Pressure [in]		29.01	0.14	29.01	28.43	29.44
Sunlight Before Detonation [hr]		2.80	0.44	2.73	2.03	3.53

[1]n (%)

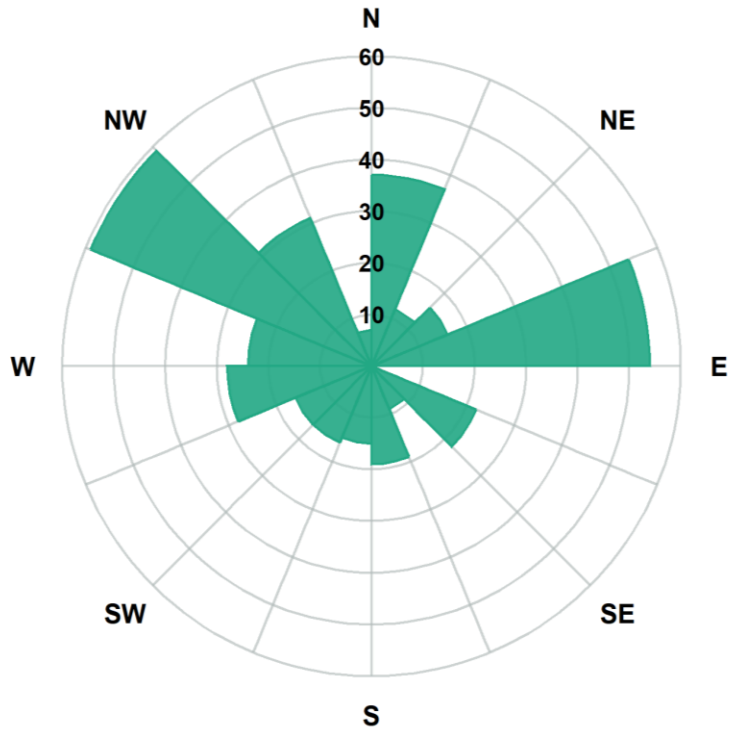

Figure 3.2. Distribution of wind direction origin at 10:00 am local time in Atlanta, GA, January 1, 2019 – December 31, 2019.

The two-day SSC weather type patterns exhibit a similar prevalence of MT and DM weather types (Figure 3.6). For a consecutive two-day period, the most common weather type pattern was MT to MT (20%), followed by DM to DM (15.34%), suggesting a relatively stable environment across the 48-hour temporal domain for the fallout radiation simulations.

3.3.2. Fallout Radiation Plume Characteristics

A low-yield, IND detonation was simulated in downtown Atlanta, GA for each day in the year 2019 (N = 365). The summary statistics for these fallout radiation plumes are described in Table 3.4. Across the sample, the mean plume extended 160.25 kilometers (km) east from the detonation site, covering 3,174.44 km^2 and placing nearly 3.7 million people at risk for radiation exposure.

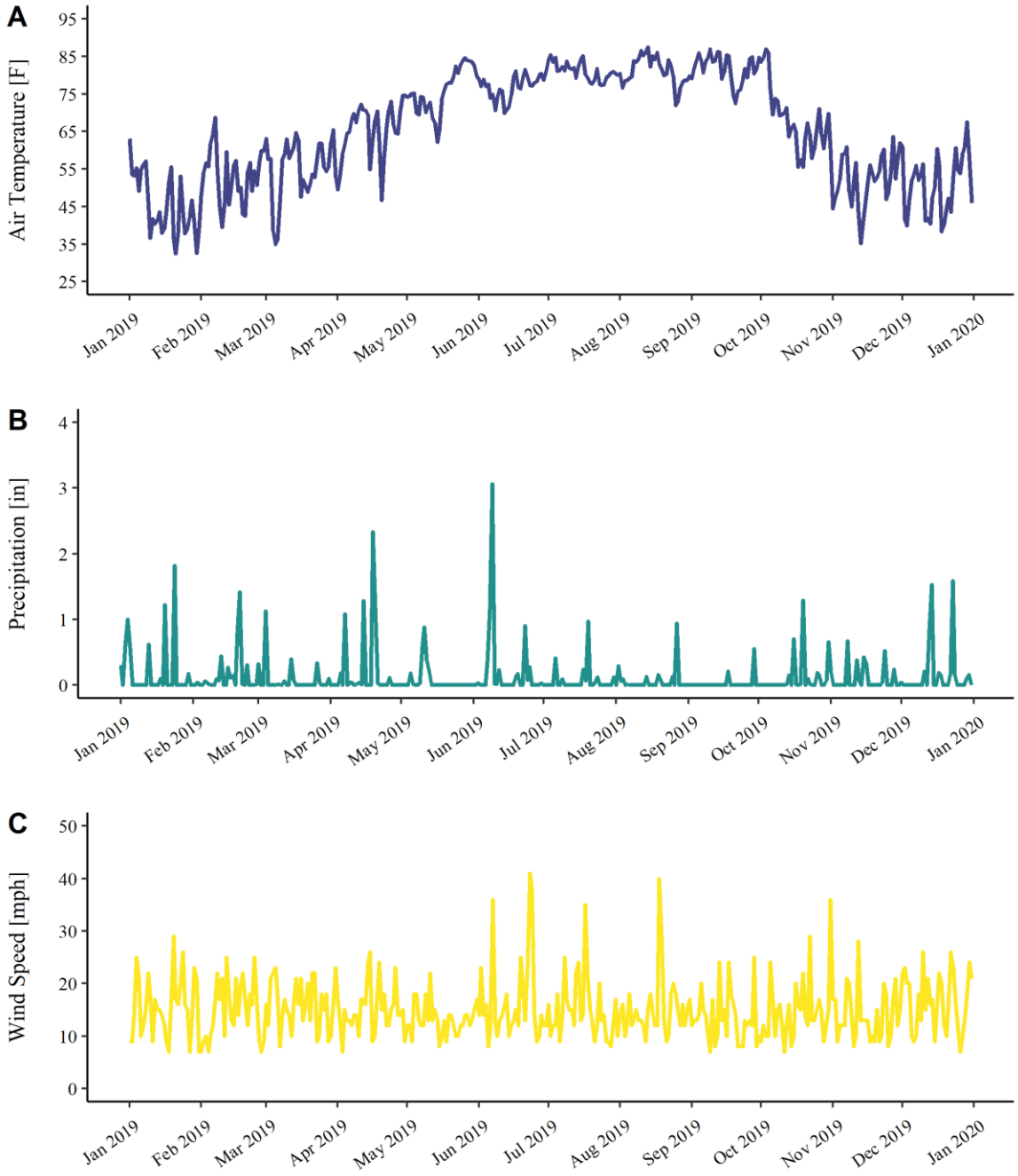

Figure 3.3. Time-series distribution of daily weather conditions in Atlanta, GA in 2019. A) average ambient air temperature, in degrees Fahrenheit; B) cumulative 24-hour precipitation, in inches; C) maximum wind speed, in miles per hour.

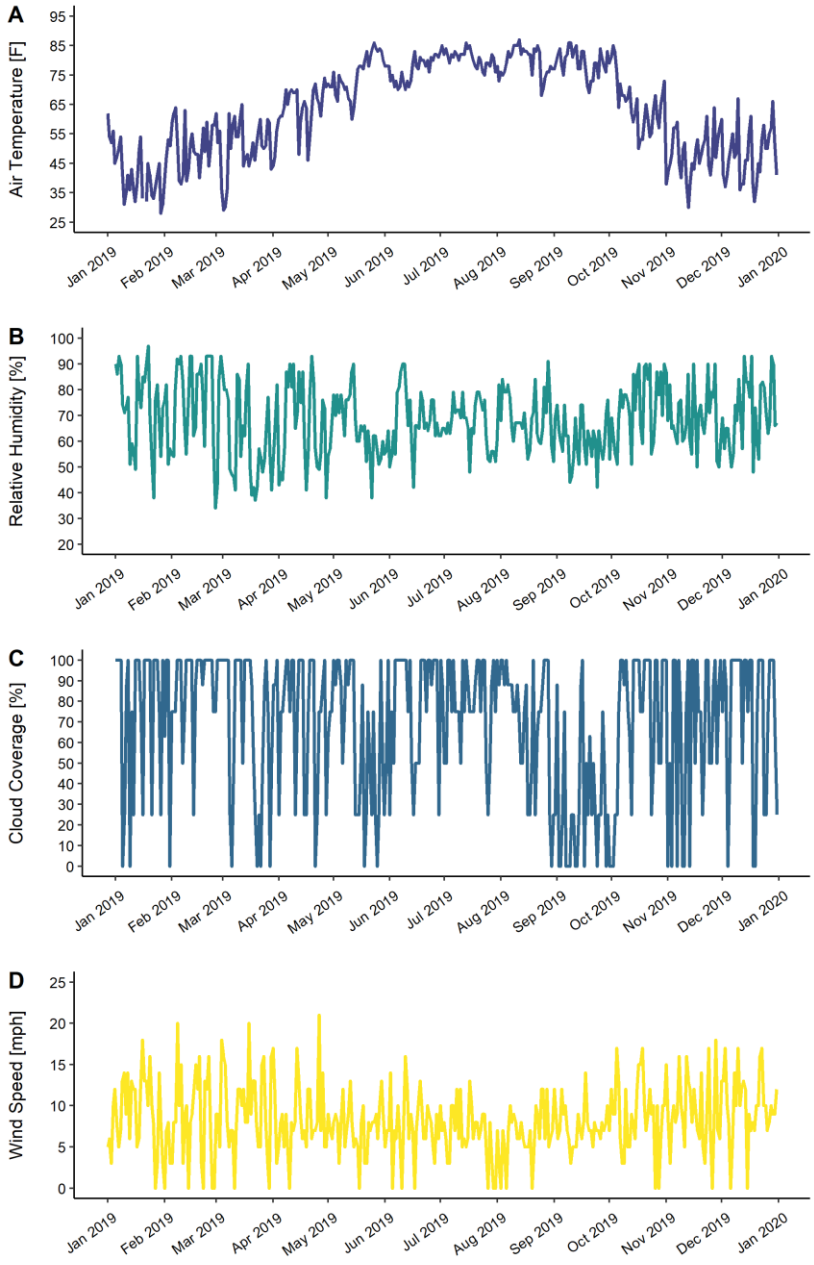

Figure 3.4. Time-series distribution of weather conditions at 10:00 am local time in Atlanta, GA in 2019. A) ambient air temperature, in degrees Fahrenheit; B) percent relative humidity; C) percent of sky covered by clouds; D) wind speed, in miles per hour.

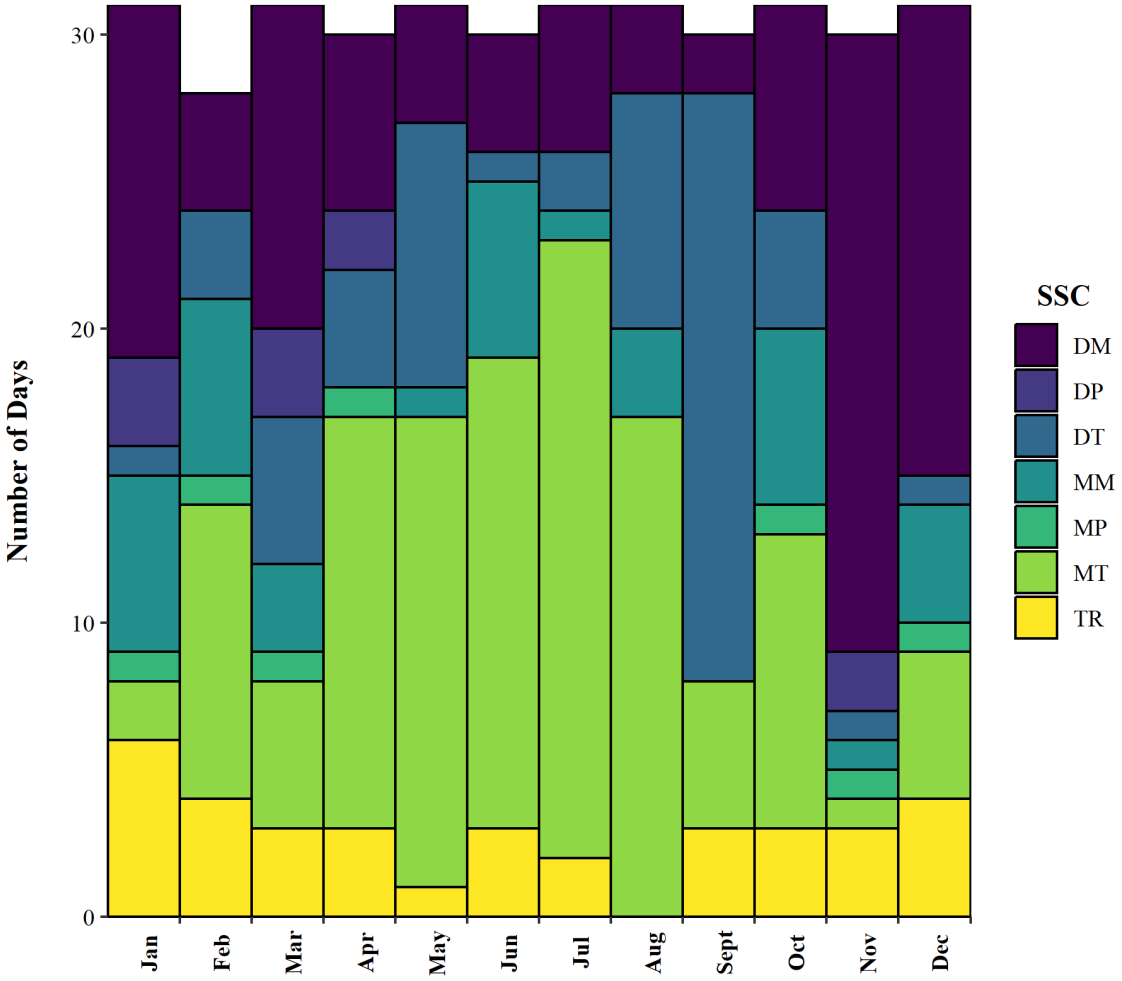

Figure 3.5. Time-series distribution of SSC weather type in Atlanta, GA in 2019.

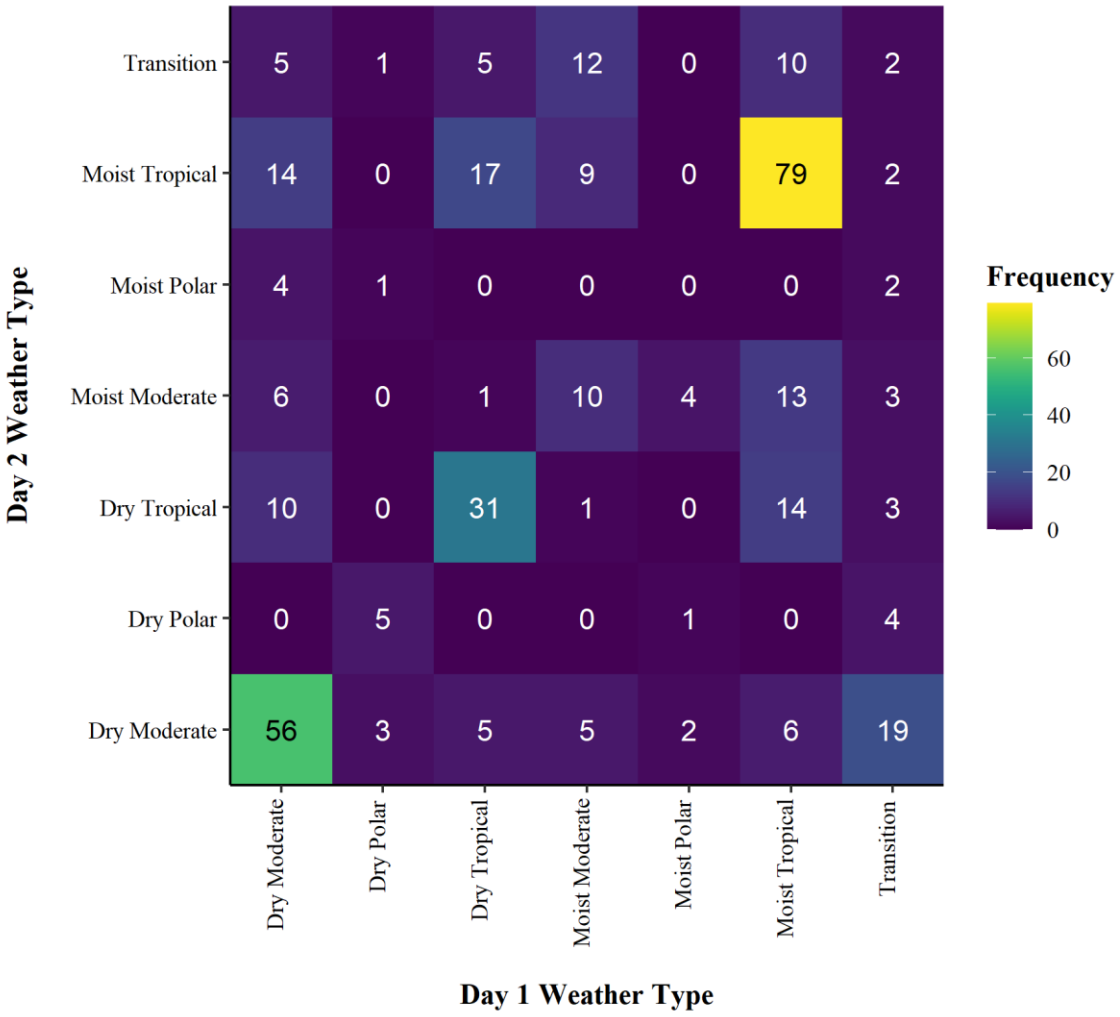

Figure 3.6. Distribution of two-day SSC weather type pattern in Atlanta, GA, January 1, 2019 – December 31, 2019. The lighter color denotes a higher frequency in the pattern.

The distribution of the plume area followed a relatively normal distribution in the study sample, but the distance of the plume 48 hours after the simulated detonation had a slightly right-skewed distribution (Figure 3.7). The total population at risk had a more pronounced right-skewed distribution than plume distance. Despite the inter-related nature of these variables, there was minimal pairwise correlation between total population at risk, plume distance, and plume area (Figure 3.7). The angle of the plume had a relatively normal distribution, with the preponderance of plumes extending in the northeast to southeast direction (Figure 3.8). There is a small secondary peak for plumes extending southwest from the detonation site.

The preponderance of the population at risk resided within the lowest radiation dose range (0 – 100 rad), or the dose range with the highest likelihood of survival (Figure 3.9). The distribution within each survivability category is relatively normal, with slight perturbations in the ~66% survival and ~50% survival categories.

Table 3.4. Summary statistics for simulated, cumulative fallout radiation plumes 48 hours post-detonation in downtown, Atlanta, GA (N = 365).

Plume Characteristic	Mean	Std Dev	Median	Min	Max
Plume Angle [°]	83.5	0.96	83.36	2.22	357.63
Plume Distance [km]	160.25	66.75	153.68	40.47	337.58
Plume Area [km^2]	3,174.44	663.94	3,147.61	1,588.68	5,218.11
Total Population at Risk	3,668,172	1,482,405	3,307,195	1,540,808	8,112,067
Absorbed Dose (% Survival)	**Population Proportion With Dose Range**				
[0 - 100 rad] (90%)	0.61	0.09	0.6	0.4	0.79
[100 - 199 rad] (66%)	0.12	0.02	0.12	0.07	0.17
[200 - 299 rad] (50%)	0.08	0.02	0.08	0.04	0.13
[300 - 599 rad] (33%)	0.13	0.04	0.13	0.05	0.23
[600 - 799 rad] (20%)	0.03	0.01	0.03	0.01	0.06
[>800 rad] (10%)	0.03	0.01	0.03	0.01	0.07

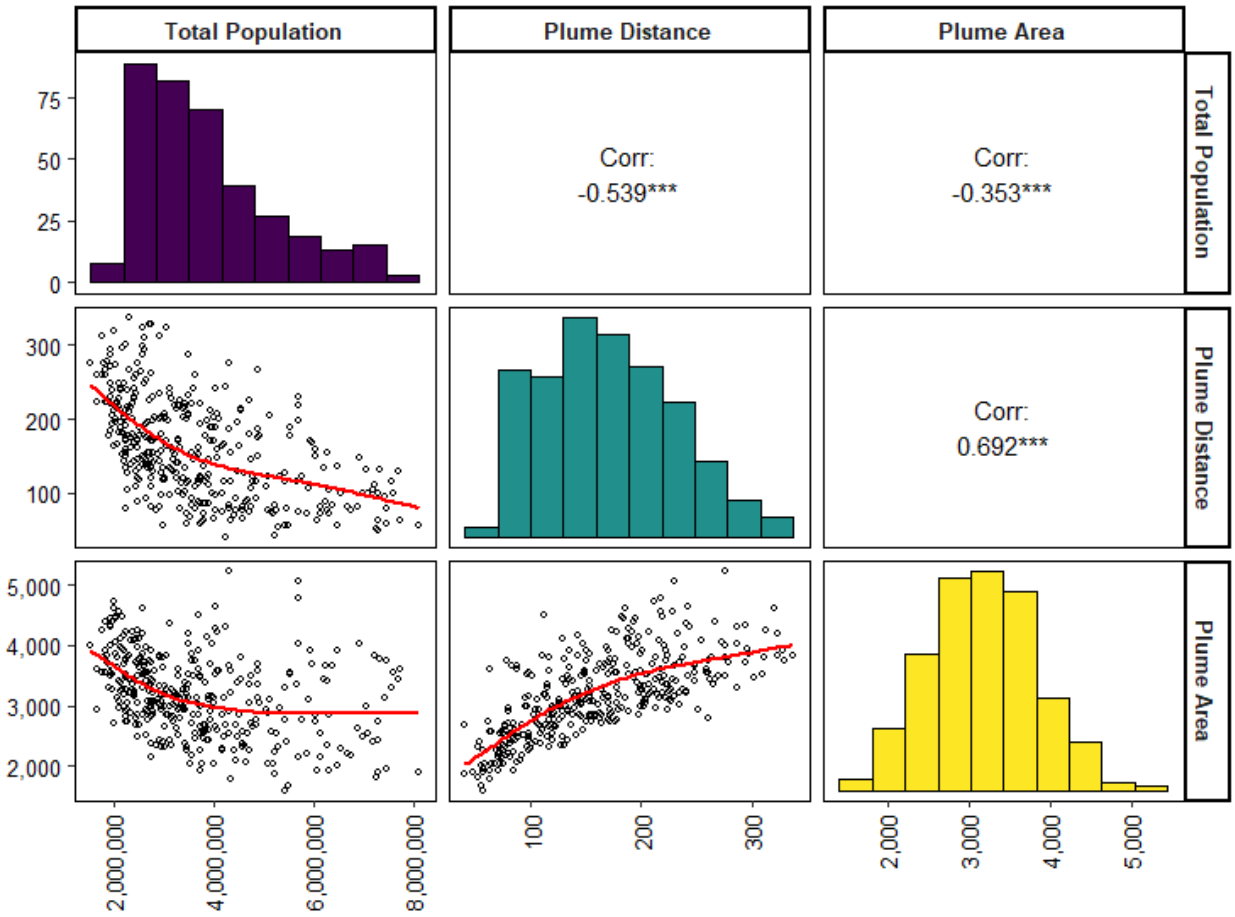

Figure 3.7. Correlation matrix of fallout radiation plume distance (km), plume area (km^2), and total population at risk, 48 hours post-detonation. The diagonal of the matrix represents the distribution of each variable, visualized via a histogram. The lower corner of the matrix creates a pairwise scatterplot, with the red line represents a fitted linear model. Pearson correlation coefficients are reported in the upper corner of the matrix, where *** denotes a p-value < 0.001.

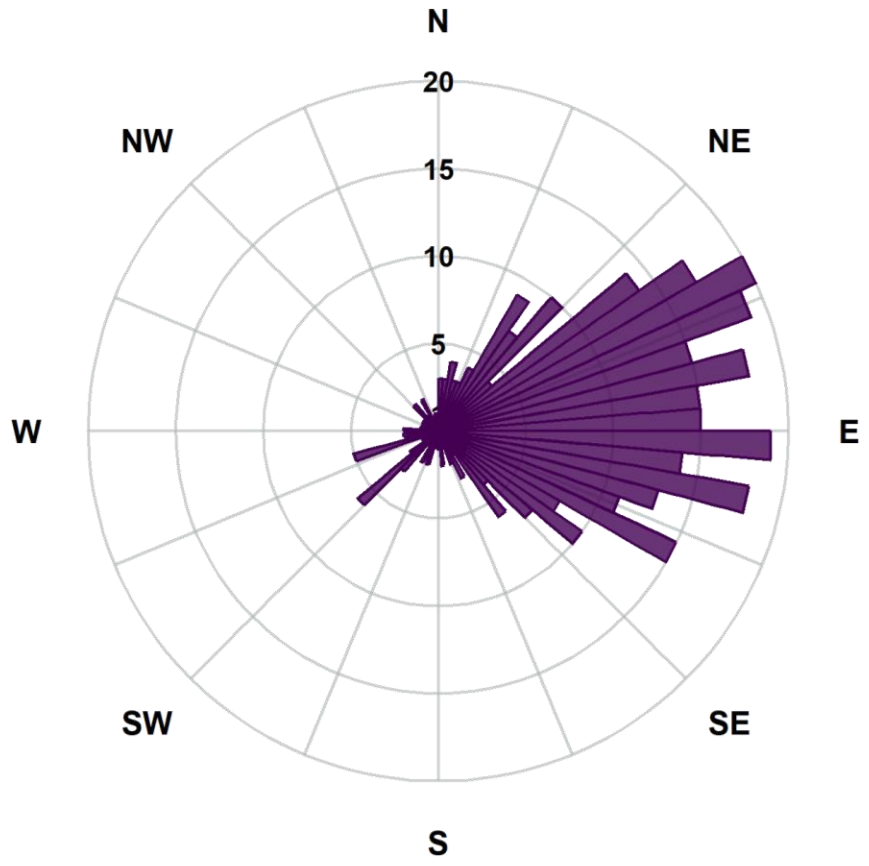

Figure 3.8. Distribution of fallout radiation plume angle in the sample.

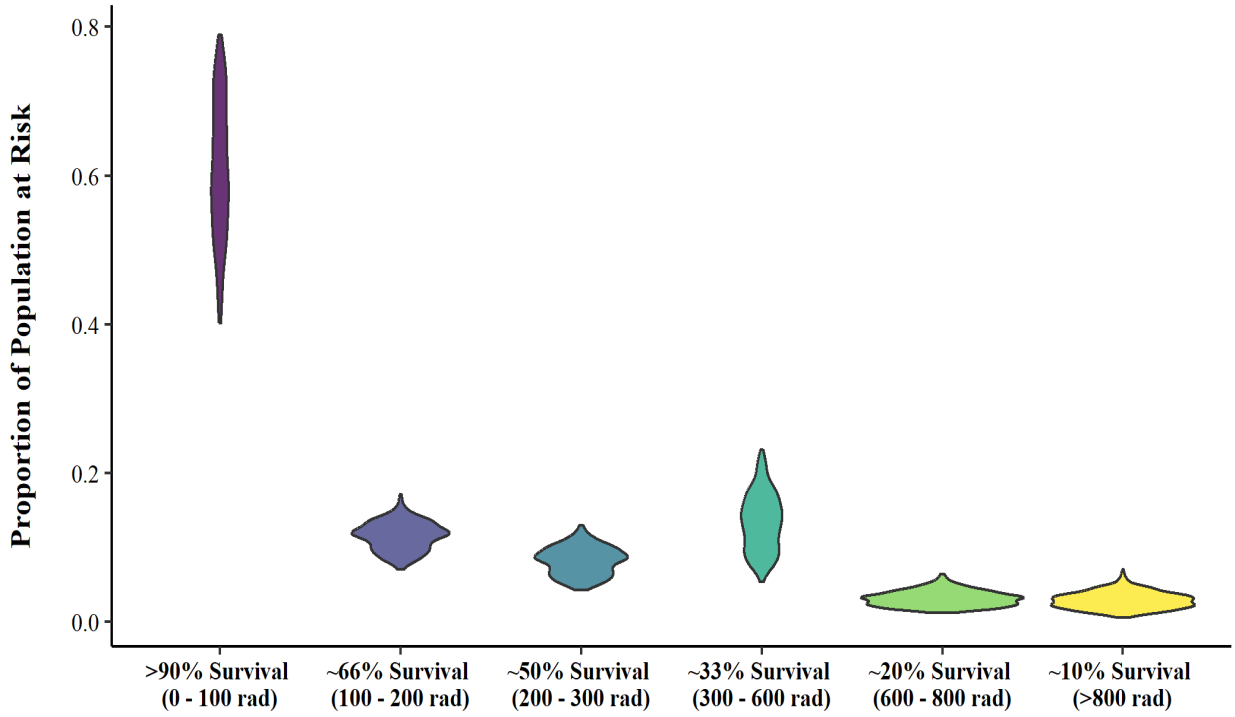

Figure 3.9. Proportion of population within each survivability category of the cumulative fallout radiation plume, 48 hours post-detonation in downtown Atlanta, GA. The data are presented as violin plots, where the width of the shaded area represents the proportion of the data.

3.3.3. Optimal Number of Clusters

The characteristics of the fallout radiation plume were used in a PAM clustering algorithm to classify the plumes based on spatial patterns and affected population. The calculated Manhattan distance matrix (Figure 3.10) was used as the distance in determining the optimal number of clusters, based on the elbow method, silhouette method, and gap statistic (Figure 3.11). Each method yielded a different number of optimal clusters. The elbow method suggests either $k = 3$ or $k = 5$ would optimize the clusters, while the silhouette method suggests the clusters would be optimized with $k = 2$. The gap statistic suggests $k = 9$ is the optimal number of clusters for this dataset.

3.3.4. Cluster Comparison

Due to the lack of agreement among cluster optimization methods, subject matter experts (SMEs) were consulted to determine the appropriate number of clusters for the study. Figure 3.12 conducts a basic visualization of the clusters using principal components to examine 2, 3, 4, 5, and 9 clusters. The SMEs advised including $k = 4$ to plausibly represent the seasonal patterns. The first component of the principal component accounts for 60.9% of the variation in the dataset, while the second component accounts for 19.5% of the variation in the dataset. Cumulatively, the PAM algorithm accounts for 80.4% of the variation present in the dataset.

To further compare the possible number of clusters, the medoids for each value of k are represented in Table 3.5. In review with SMEs, it was determined that $k = 4$ clusters most appropriately captured the variations in the fallout radiation plumes included in this study. Selecting fewer clusters did not accurately capture the variation in plume angle and distance, while affected population estimates overlapped significantly with additional clusters. Figure 3.13 maps the plumes for each medoid for $k = 4$ clusters.

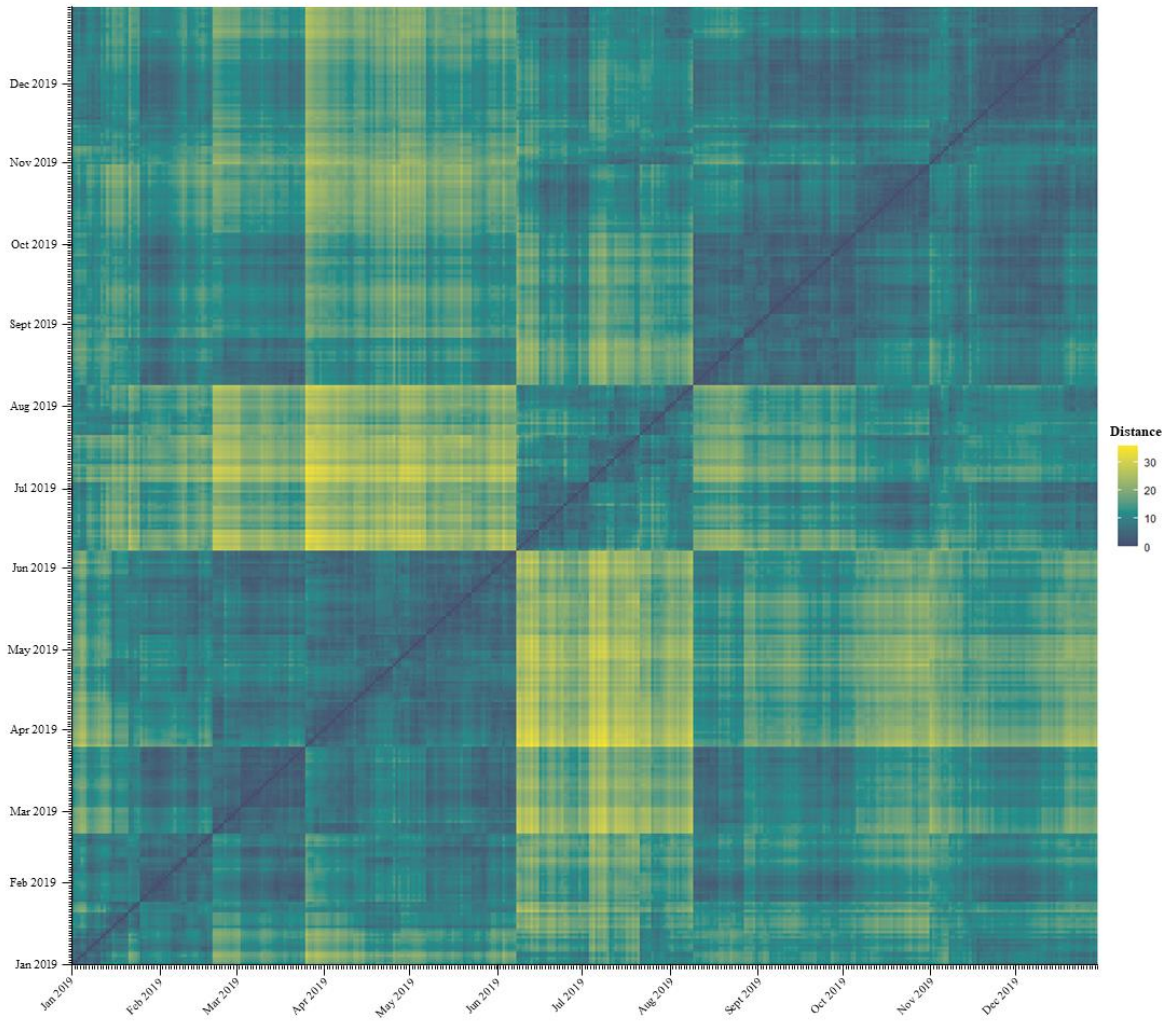

Figure 3.10. Manhattan distance matrix for the sample. High similarity between points is represented by the darker colors, while the lighter colors indicate low similarity.

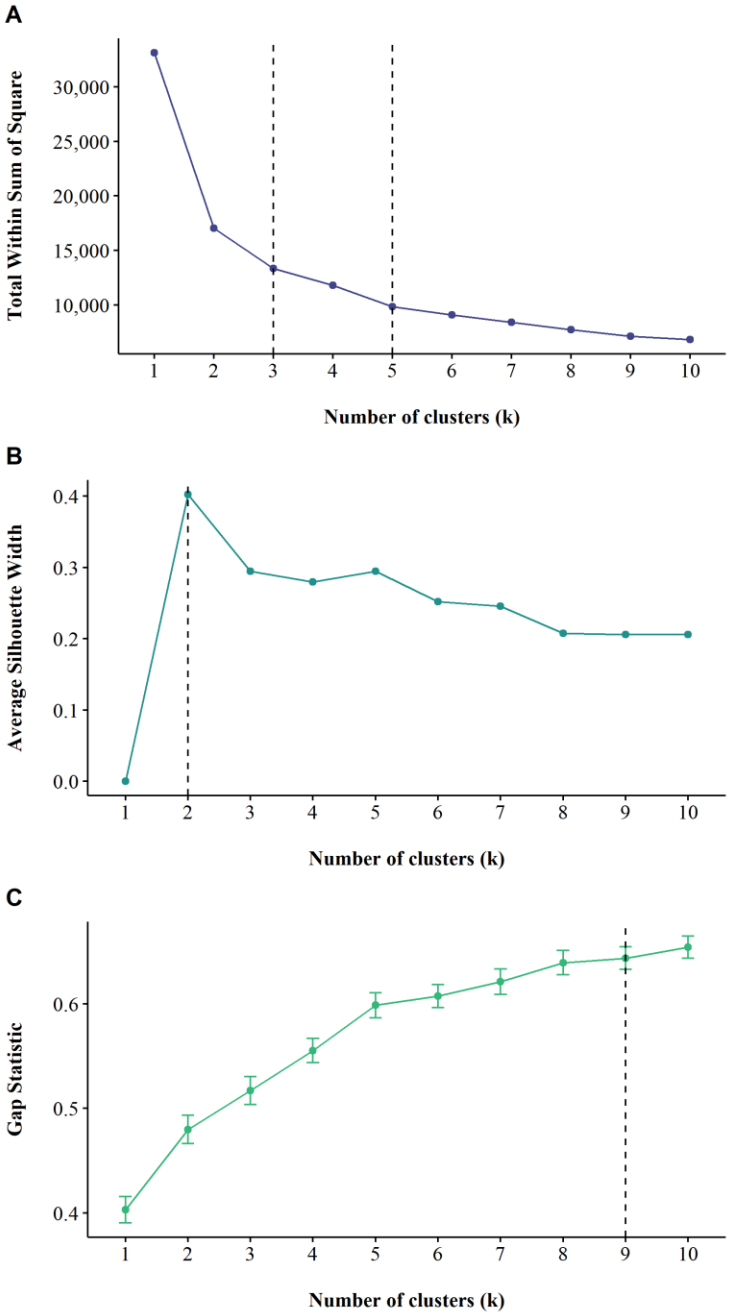

Figure 3.11. Cluster number optimization methods: a) elbow method; b) silhouette method; c) gap statistic. The vertical dotted line corresponds to the optimal number of clusters for the PAM algorithm.

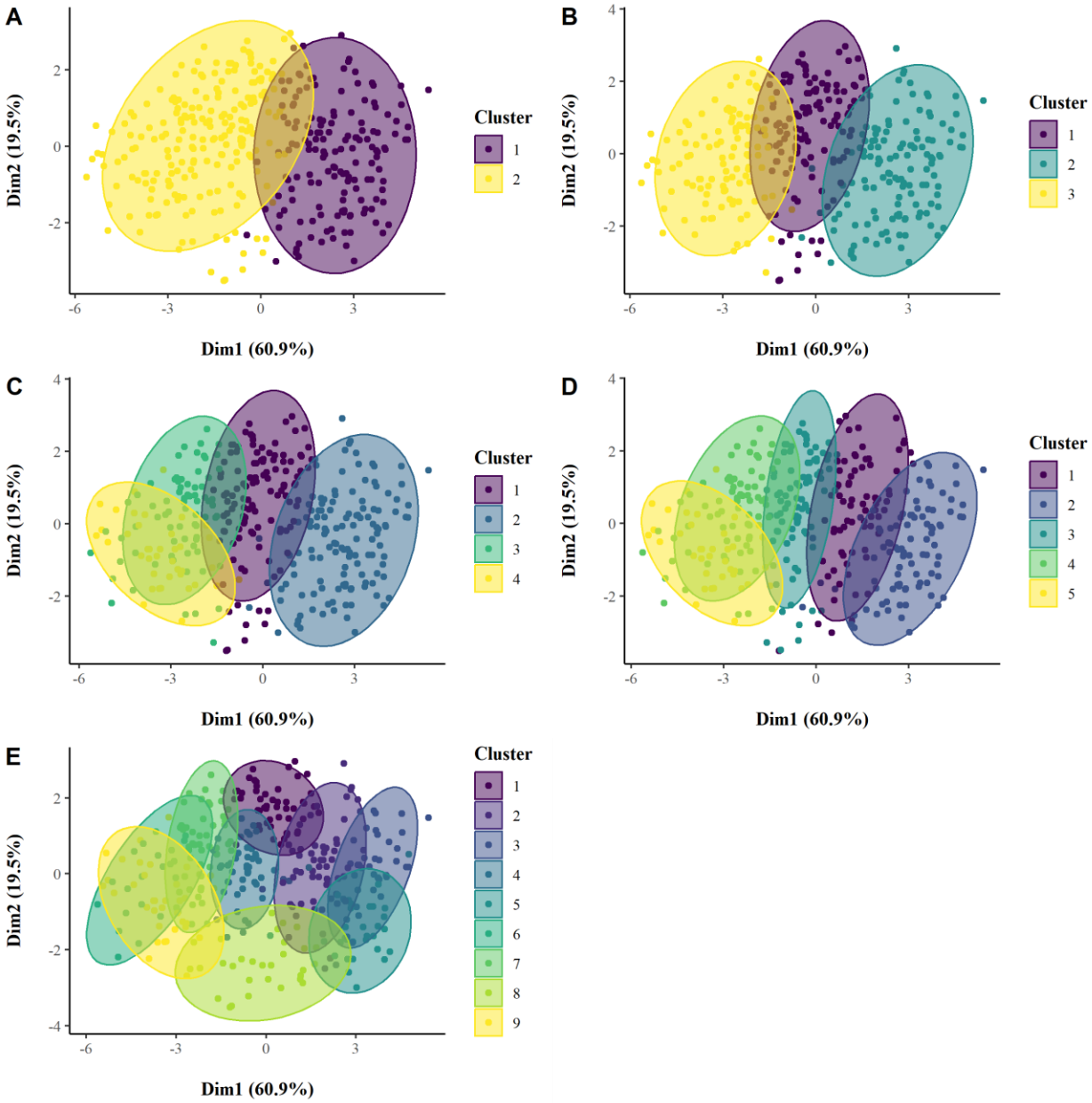

Figure 3.12. Cluster visualization using principal components for k = 2 (A), k = 3 (B), k = 4 (C), k = 5 (D), and k = 9 (E). Each point represents an individual plume.

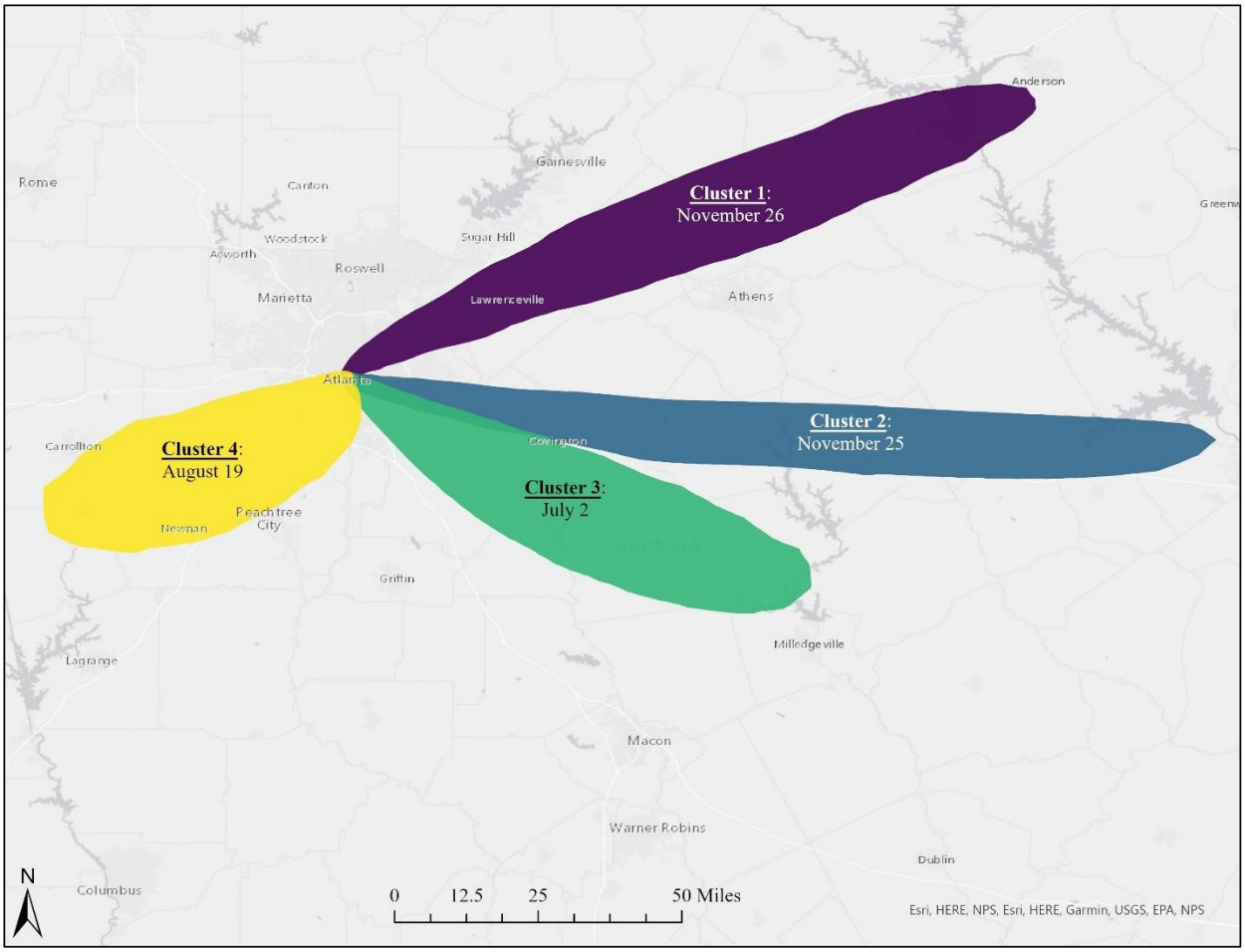

Figure 3.13. Simulated fallout radiation plumes 48 hours post-detonation in downtown, Atlanta, GA, for each medoid in $k = 4$ clusters.

Table 3.5. Selected medoids for each considered value of *k*.

Cluster	Date	Plume Distance [km]	Plume Area [km^2]	Plume Angle [°]	Total Population at Risk	Population Proportion Within Absorbed Dose Rage (rad)					
						0 - 100	100 - 200	200 - 300	300 - 600	600 - 800	800+
k = 2											
1	11/26	187.01	3,661.25	63.7	4,306,849	0.70	0.10	0.06	0.10	0.02	0.02
2	1/6	145.65	2,813.89	105.05	2,735,524	0.55	0.12	0.09	0.16	0.04	0.04
k = 3											
1	11/26	187.01	3,661.25	63.7	4,306,849	0.70	0.10	0.06	0.10	0.02	0.02
2	11/25	209.15	3,214.92	94.41	2,309,531	0.59	0.12	0.09	0.15	0.03	0.03
3	9/8	95.61	2,982.86	127.3	3,126,846	0.51	0.13	0.10	0.17	0.04	0.05
k = 4											
1	11/26	187.01	3,661.25	63.7	4,306,849	0.70	0.10	0.06	0.10	0.02	0.02
2	11/25	209.15	3,214.92	94.41	2,309,531	0.59	0.12	0.09	0.15	0.03	0.03
3	7/2	126.49	3,043.22	117.98	2,260,651	0.51	0.13	0.10	0.17	0.04	0.04
4	8/19	84.56	2,450.55	242.86	3,798,307	0.48	0.14	0.11	0.19	0.04	0.04
k = 5											
1	3/24	178.31	3,042.04	51.62	4,714,100	0.73	0.09	0.06	0.09	0.02	0.02
2	4/7	202.17	3,183.94	83.36	2,957,573	0.65	0.11	0.07	0.12	0.03	0.03
3	9/26	167.60	3,194.55	106.19	2,420,309	0.59	0.12	0.08	0.14	0.03	0.03
4	7/2	126.49	3,043.22	117.98	2,260,651	0.51	0.13	0.10	0.17	0.04	0.04
5	8/19	84.56	2,450.55	242.86	3,798,307	0.48	0.14	0.11	0.19	0.04	0.04
k = 9											
1	2/11	221.69	3,745.62	57.56	3,568,499	0.75	0.08	0.05	0.08	0.02	0.02
2	5/22	134.51	3,422.77	27.18	6,196,096	0.75	0.10	0.05	0.07	0.02	0.01
3	7/17	206.56	3,191.89	65.42	3,011,517	0.68	0.10	0.07	0.10	0.02	0.02
4	9/23	133.28	2,899.77	97.25	2,693,953	0.59	0.12	0.09	0.15	0.03	0.03
5	2/2	98.19	2,525.96	65.67	7,109,010	0.60	0.12	0.08	0.14	0.03	0.02
6	6/4	122.00	2,650.14	101.75	3,751,783	0.44	0.14	0.11	0.21	0.05	0.05

Cluster	Date	Plume Distance [km]	Plume Area [km^2]	Plume Angle [°]	Total Population at Risk	Population Proportion Within Absorbed Dose Rage (rad)					
						0 - 100	100 - 200	200 - 300	300 - 600	600 - 800	800+
k = 9 (con't)											
7	3/4	216.37	4,080.65	88.54	2,334,529	0.61	0.12	0.08	0.13	0.03	0.03
8	8/9	138.38	3,203.13	129.3	2,329,156	0.51	0.13	0.10	0.18	0.04	0.04
9	8/19	84.56	2,450.55	242.86	3,798,307	0.48	0.14	0.11	0.19	0.04	0.04

Table 3.6 further elucidates this point by providing the summary statistics for each of the fallout radiation plume characteristics. While the distribution of population proportions within each survivability category are relatively similar between clusters 3 and 4, the two clusters differ in their plume distances and angles. Clusters 1 and 2 have similar plume distances but the plume angles differ slightly. Cluster 1 has the largest proportion of the affected population within the lowest radiation dose range, while clusters 3 and 4 have larger proportions of affected population within the survivability categories corresponding to a radiation dose greater than 300 rad (Figure 3.14).

3.3.5. Predicting Clusters from Surface-level Weather

Four models were fit to predict the fallout radiation plume classification, based on surface-level weather conditions: DT, RF, LASSO, and EN. Table 3.7 shows the model comparison for predicting the cluster, including comparison to the null model, where no surface-level weather conditions were fit to the model. While all four models performed better than the null model, no model was able to correctly predict the cluster assignment with greater than approximately 50% accuracy. The DT model had the poorest performance, with 44.30% accuracy, and an AUC ROC of 0.65. There was no meaningful difference in the performance of the RF, LASSO, and EN models. In examining the confusion matrices (Figure 3.15), all four models were able to predict cluster 1 the best. The RF, LASSO, and EN models captured approximately 70% of the plumes assigned to cluster 1, while the DT captured only 60% of the plumes assigned to cluster 1. Additionally, all four models had difficulty in differentiating between clusters 2 and 3. More specifically, cluster 3 was incorrectly predicted as cluster 2 more often than it was correctly predicted as cluster 3 in all four models.

Table 3.6. Summary statistics for simulated fallout radiation plumes 48 hours post-detonation in downtown, Atlanta, GA, assigned to $k = 4$ clusters.

	Cluster (k = 4)			
Fallout Radiation Characteristics	**Cluster #1**, N = 131	**Cluster #2**, N = 121	**Cluster #3**, N = 74	**Cluster #4**, N = 39
Plume Angle [°]				
Mean	51.12	97.40	113.25	251.13
Std Dev	0.39	0.58	0.42	0.66
Median	56.03	94.41	115.06	251.18
Min	2.22	4.48	59.32	171.59
Max	357.63	331.81	227.3	322.53
Plume Distance [km]				
Mean	177.65	179.42	135.28	89.72
Std Dev	67.91	63.04	51.02	28.66
Median	177.91	177.26	136.31	83.98
Min	61.96	47.47	51.89	40.47
Max	337.58	312.85	260.13	175.79
Plume Area [km^2]				
Mean	3,347.29	3,326.98	2,941.70	2,562.23
Std Dev	633.83	635.36	619.95	409.71
Median	3,353.40	3,270.79	2,905.97	2,538.16
Min	1,922.59	1,888.57	1,588.68	1,867.57
Max	5,218.11	4,712.04	4,472.88	3,601.23
Total Population at Risk				
Mean	4,433,997.80	2,941,302.64	3,286,474.31	4,075,196.51
Std Dev	1,451,361.54	1,396,117.79	1,221,373.36	815,375.66
Median	4,074,368	2,505,778	2,982,827	3,906,101
Min	2,003,389.00	1,540,808	1,841,791	2,640,467
Max	7,736,996	8,112,067	7,275,472	6,476,671
Population Proportion Within [0 - 100 rad]				
Mean	0.71	0.60	0.50	0.50
Std Dev	0.04	0.03	0.04	0.05
Median	0.71	0.59	0.51	0.50
Min	0.62	0.54	0.40	0.40
Max	0.79	0.66	0.56	0.60
Population Proportion Within [100 - 200 rad]				
Mean	0.1	0.12	0.13	0.14
Std Dev	0.01	0.01	0.01	0.01
Median	0.1	0.12	0.13	0.14
Min	0.07	0.1	0.11	0.11
Max	0.14	0.15	0.14	0.17

Fallout Radiation Characteristics	Cluster (k = 4)			
	Cluster #1, N = 131	**Cluster #2**, N = 121	**Cluster #3**, N = 74	**Cluster #4**, N = 39
Population Proportion Within [200 - 300 rad]				
Mean	0.06	0.08	0.10	0.11
Std Dev	0.01	0.01	0.01	0.01
Median	0.06	0.08	0.10	0.10
Min	0.04	0.07	0.09	0.08
Max	0.09	0.11	0.12	0.13
Population Proportion Within [300 - 600 rad]				
Mean	0.09	0.14	0.18	0.18
Std Dev	0.02	0.01	0.02	0.02
Median	0.09	0.14	0.18	0.18
Min	0.05	0.11	0.15	0.13
Max	0.13	0.17	0.23	0.22
Population Proportion Within [600 - 800 rad]				
Mean	0.02	0.03	0.04	0.04
Std Dev	0	0	0.01	0.01
Median	0.02	0.03	0.04	0.04
Min	0.01	0.02	0.03	0.02
Max	0.03	0.04	0.06	0.05
Population Proportion Within [>800 rad]				
Mean	0.02	0.03	0.04	0.04
Std Dev	0.01	0.01	0.01	0.01
Median	0.02	0.03	0.04	0.04
Min	0.01	0.01	0.03	0.02
Max	0.03	0.04	0.07	0.05

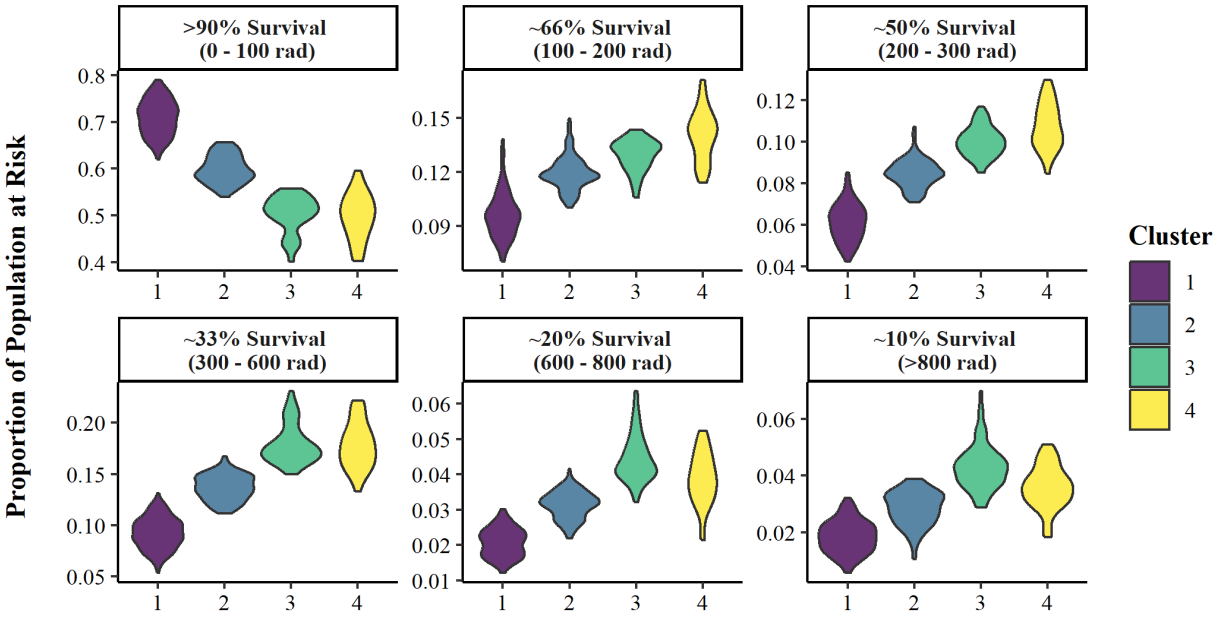

Figure 3.14. Proportion of population within each survivability category presented as violin plots, among $k = 4$ clusters. The width of the shaded area represents the proportion of the data.

Table 3.7. Machine learning model comparison for predicting fallout radiation plume classification.

Model	Accuracy [%]	Sensitivity [%]	Specificity [%]	AUC ROC
Null	25.00	-	-	0.50
Decision Tree	44.30	40.76	79.96	0.65
Random Forest	51.16	46.36	82.18	0.76
LASSO	50.91	47.72	82.69	0.76
Elastic Net	51.16	47.65	82.77	0.75

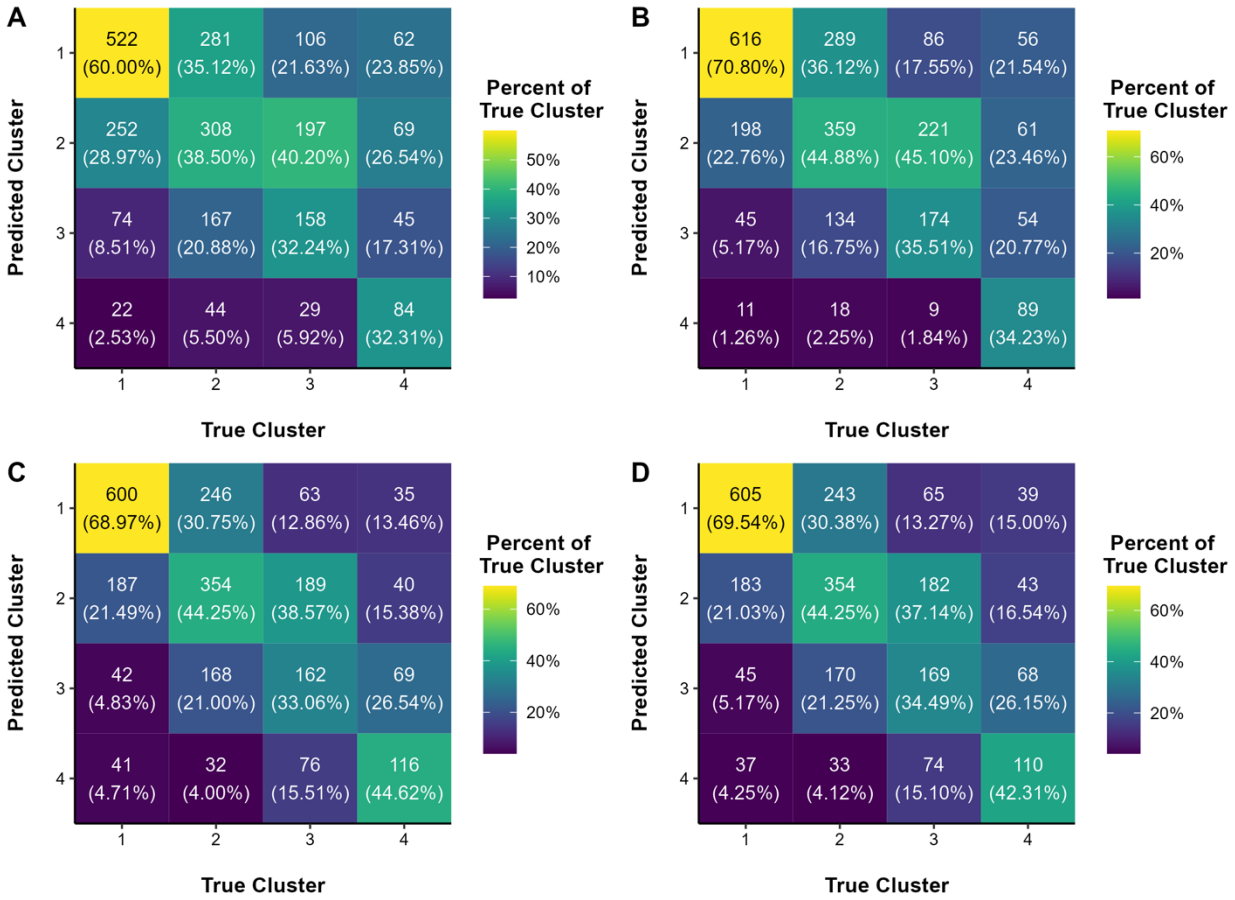

Figure 3.15. Confusion matrices for each model: A) decision tree; B) random forest; C) LASSO; D) elastic net.

Figure 3.16 indicates the variables with greatest importance among the three best performing models. Variables included in the RF model had greater relative importance than those included in the LASSO and EN models. All three models included cloud coverage, dew point range, and wind with a northwest or west-northwest origin. However, the LASSO and EN models placed greater importance on the SSC weather typing and two-day patterns, which were binary variables, while the RF model placed greater importance on relative humidity, sea level

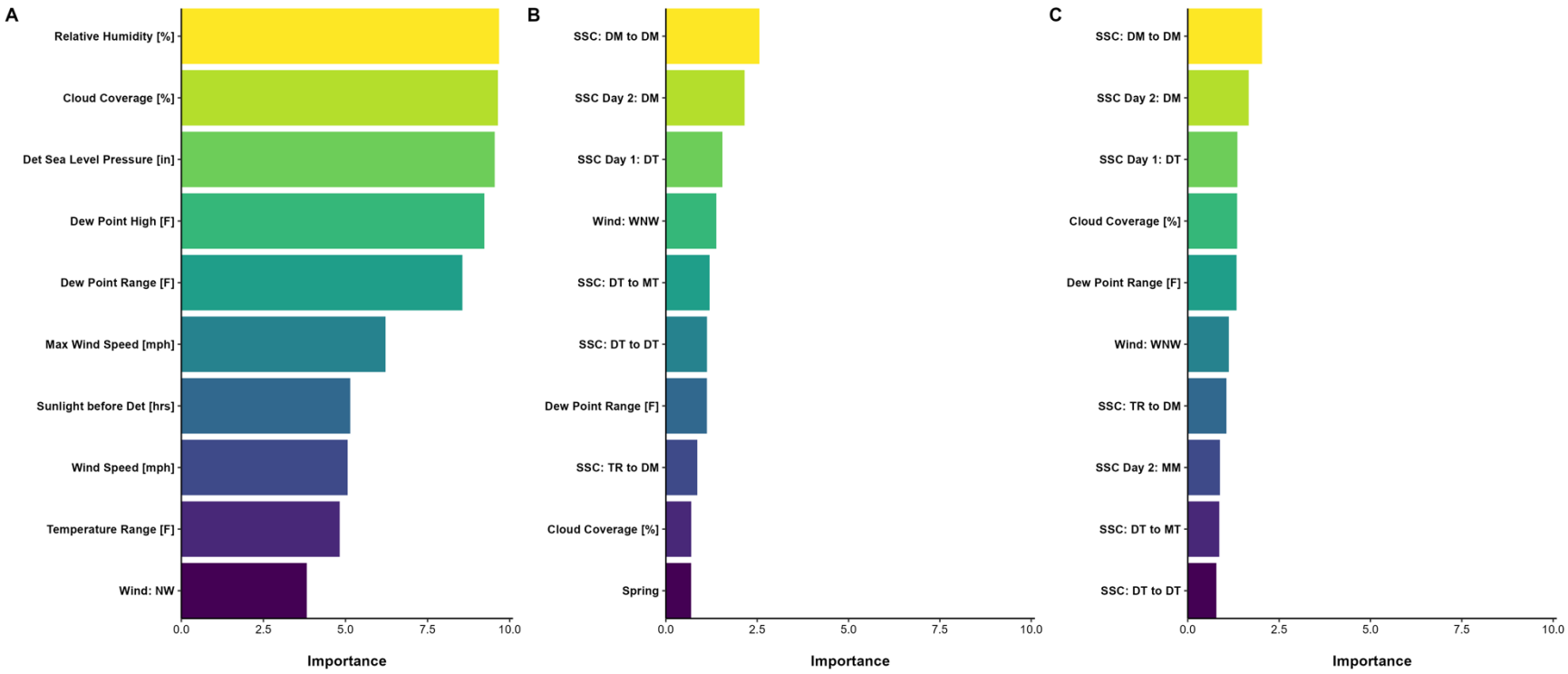

Figure 3.16. Variable importance plots for the ten most important parameters in the A) random forest, B) LASSO, and C) elastic net models.

Table 3.8. Random forest model comparison for test/train data for predicting fallout radiation plume classification.

Data Set	Accuracy [%]	Sensitivity [%]	Specificity [%]	AUC ROC
Train	51.16	46.36	82.18	0.76
Test	57.72	52.80	84.52	0.80

pressure at detonation, and dew point, all of which were continuous variables. While the difference in performance of these three models is nearly indistinguishable, the RF model was chosen as the most appropriate model for this study. The variables with the greatest importance in the RF model, especially relative humidity and cloud coverage, are known to have a close relationship with fallout distribution.

The RF model was fit to the reserved, test data sample to evaluate the fit of the model using data that was not used to initially train the model. Table 3.8. compares the fit of the random forest model between the test and train data sample. The model fit the test data better than the training data, as all four metrics for evaluation were improved. In examining the confusion matrices for each data set (Figure 3.17), under the test data, the model was better able to differentiate between clusters 2 and 3, in comparison to the training data.

3.4. Discussion

This study characterized the variation in fallout radiation distribution following an IND detonation in Atlanta, GA in 2019. The fallout radiation plumes 48 hours post-detonation were clustered into four groups, based on spatial patterns and affected population estimates. While accuracy in predicting the assigned clusters from surface-level weather conditions was limited, the RF model illustrated relative humidity, cloud coverage, sea level pressure, and dew point were among the most important conditions in predicting the cluster assignments.

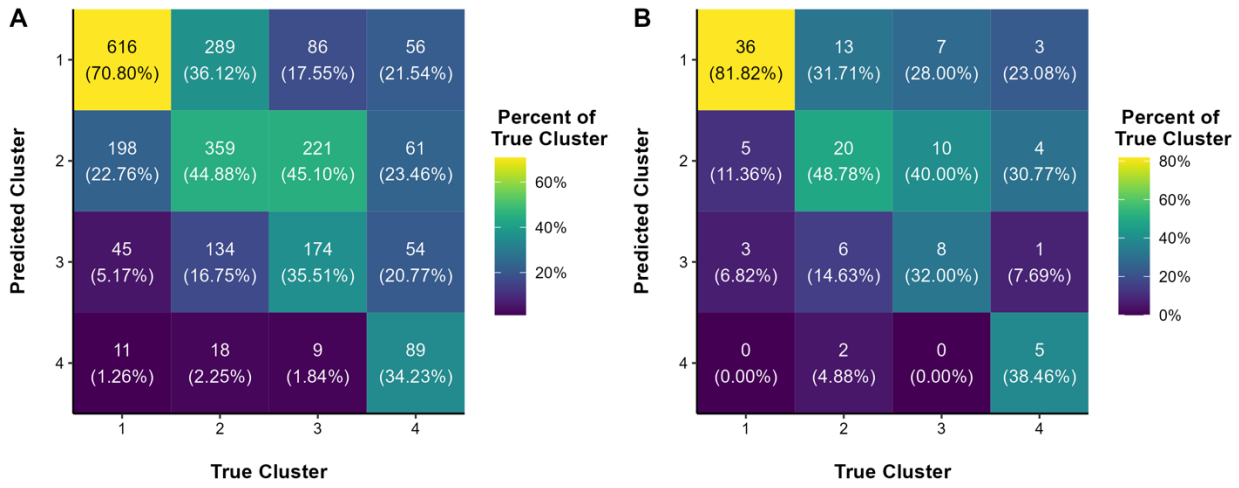

Figure 3.17. Confusion matrices for the random forest model under the a) training dataset and b) testing dataset.

The study period focused specifically on the year 2019, in which average daily weather conditions had a high temperature of 74.80°F (SD = 15.12°F), 9.92 miles (SD = 0.68) of visibility, 0.12 inches (SD = 0.34) of precipitation in the previous 24 hours, and maximum wind speeds of 15.04 miles per hour (SD = 5.58). At 10:00 am local time, conditions were typically comparable, with an average temperature of 63.28°F, a mean relative humidity of 68.38%, and relatively limited precipitation (0.01 in/hr). While this study period only includes one year of data, these conditions were largely comparable but more humid than those reported in previous studies characterizing Atlanta weather over multiple years. Tasian et al.[246] reported the meandaily temperature ranging from 23°F to 87.8°F (-5°C to 31°C) in their analysis of Atlanta weather in 2005 to 2011, while the mean daily temperature ranged from 32.50°F to 87.49°F. The authors also reported a median relative humidity of 54%, ranging from 13% to 100%, in contrast to this study, which found a median relative humidity of 67%, ranging from 34% to 97% in the year 2019. In their analysis of the warm season (May through September) in Atlanta, using data

from 1993 to 2012, Winquist et al.[247] reported a maximum ambient air temperature of 105.08°F (40.6°C), while the maximum air temperature in Atlanta in 2019 was 99°F. The authors reported 0.19 inches (4.8 mm) of mean total daily precipitation, which is slightly greater than this study's reported 0.12 inches mean cumulative 24-hour precipitation. Similarly, the authors reported 7.16 mph (3.2 meters per second (m/s)) average daily wind speed, which is similar to the 8.29 mph (SD = 4.17) mean wind speed at 10:00 am local time reported in this study. In 2019, winds most commonly originated in the northwest and east, blowing to the southeast and west, respectively. McLeod et al.[248] found the prevailing winds originated most commonly from the southwest to northwest direction in Atlanta during the summer in their analysis of data from 2002 to 2015. In evaluation of the SSC distribution, MT and DM were the most common weather types in 2019. This distribution is in alignment with other studies that have characterized SSC weather types in Atlanta over multiple years,[249–252] suggesting the temporal domain of this study is largely representative of typical meteorological conditions over time in Atlanta, GA.

A low-yield, IND detonation was simulated in downtown Atlanta, GA. The mean fallout radiation plume 48 hours after the simulated IND detonation extended 160.25 km almost directly east from the detonation site, covering 3,174.44 km^2 and placing nearly 3.7 million people at risk for radiation exposure. Within the fallout radiation plume, nearly two-thirds (61%) of the affected population resided within the lowest risk cumulative radiation dose category (0 – 100 rad) over 48 hours.

Based on similarities in plume angle, distance, and area, as well as affected population estimates, this study described four clusters derived from a PAM clustering algorithm. Cluster 1 was comprised of plumes extending a mean 177.65 km (SD = 67.91) northeast, covering approximately 3,347.29 km^2 (SD = 633.83) on average and placing nearly 4.5 million people on

average at risk for radiation exposure. Cluster 2 was comprised of plumes extending a mean 179.42 km (SD = 63.04) east, covering approximately 3,326.98 km^2 (SD = 635.36) on average and placing approximately 2.9 people on average at risk for radiation exposure. Cluster 3 was comprised of plumes extending a mean 135.28 km (SD = 51.02) east-southeast, covering approximately 2,941.70 km^2 (SD = 619.95) on average and placing approximately 3.3 million people on average at risk for radiation exposure. Lastly, cluster 4 was comprised of plumes extending a mean 89.72 km (SD = 28.66) west-southwest, covering approximately 2,562.23 km^2 (SD = 409.71) on average and placing nearly 4.1 million people at risk for radiation exposure.

In the published literature, nuclear detonation simulations in GA featuring fallout radiation plumes most commonly reflect plumes in cluster 1. Bell and Dallas[17] modeled 20kt and 550kt detonations in Atlanta, and the featured plume was almost identical to the medoid presented for cluster 1. Further, FEMA's "Risks and Hazards: A State-by-State Guide,"[40] included two sample fallout plumes in GA. The first, centrally located in the state, extended northeast, following a pattern similar to cluster 1. The second example the guide provided, located near Columbus, GA, was far shorter than the first and extends southeast, reflecting a similar plume to that of the medoid in cluster 3. This preference for cluster 1 can be explained through analysis of the wind patterns in Atlanta. The vast majority of the upper-atmospheric winds in Atlanta blow east/northeast, thus creating the plumes characterized in cluster 1.[17,253] Due to the restricted nature of FEMA's iCPR tool, the authors of this study were not able to compare the results of the cluster analysis against the determined seasonal patterns for fallout radiation in the iCPR tool.

To identify the most important surface-level weather characteristics in predicting the cluster assignment, four machine learning algorithms were fit to the surface-level weather

conditions data: DT, RF, LASSO, and EN. Of the four models, the RF demonstrated best performance, with the highest accuracy and AUC ROC. The RF model identified relative humidity, cloud coverage, sea level pressure at time of simulated detonation, daily dew point high, and daily dew point range as the five most important predictors. These variables were hypothesized to be significant predictors, as relative humidity and cloud coverage have a documented effect on fallout radiation distribution.[17,45,64,65,108,173] The amount, thickness, and height of clouds affect scattering, reflection, and absorption of the fallout radiation.[45,64] It is plausible the dew point variables are also capturing a similar phenomenon, as the dew point can be an absolute measure of the water vapor in the air within a given air mass.[177] Interestingly, Khajure and Mohod[254] found humidity, temperature, pressure, wind speed, dew point, and visibility were among the most important variables for predicting future weather conditions, using a neural network. In conjunction with the results from the RF model, this potentially suggests the chosen RF model was most accurate when the atmospheric conditions were relatively stable (and by proxy, the fallout radiation plume) and thus were predictable from surface-level weather conditions.

The confusion matrices for both the training and testing data fits suggest further attenuation of the model is required to accurately predict the fallout radiation clusters. In particular, the RF model, as well as all of the other models considered, struggled to differentiate between clusters 2 and 3. As discussed below, future research is warranted to discern whether this inaccuracy is due to the variance within clusters or the surface-level weather data included in this study. Such research should endeavor to increase the accuracy of these prediction models far beyond the 50% accuracy found in this study for such models to be applicable in practical settings.

The generalizability of this study is limited, as the data only included a single year of observations focused on a single city using a single low-yield weapon. Given the relative similarity of the surface-level weather conditions found in this study in comparison to previously published studies with longer temporal domains, it is plausible to assume the year 2019 is an effective illustrative example of fallout distributions in Atlanta. Not only should future studies examine a longer period and/or alternative cities, but they should also include upper-level atmospheric data for predicting the fallout radiation plume cluster assignments. Such a data source should be easily accessible and interpretable, perhaps using data available to non-commercial pilots. Future studies could also consider an air mass classification system that captures upper-level atmospheric conditions in place of SSC. Lastly, this study is limited by the assumption of Gaussian puffs to represent the fallout radiation within SCIPUFF and HPAC. Buddemeier and Dillon[37] argue that a non-Gaussian distribution of fallout radiation caused by wind shear is far more likely. Efforts were made to reduce the likelihood of such a phenomenon by choosing a city away from a coastal area, and therefore choosing a city less likely to experience extensive wind shear. However, future studies should examine higher-fidelity atmospheric dispersion models, once they become available to academic institutions not affiliated with the national research laboratories.

In conclusion, the fallout radiation plumes from a low-yield IND detonation in Atlanta, GA vary in plume direction, distance, and area, as well as in proportion of affected population. This study highlights a larger range of plume direction and distance than those previously included in the published literature. This study also identified four representative days for fallout radiation conditions to be used in the following aims of this dissertation. Classifying the possible fallout radiation plumes into clusters can assist emergency managers in more fully assessing the

potential impacts from fallout radiation following an IND detonation. Future research to develop more accurate prediction algorithms from surface-level conditions will better position emergency management and all partner organizations to proactively understand the potential effects and impacts resulting from fallout radiation.

CHAPTER 4

A METHODOLOGICAL FRAMEWORK FOR MODELING THERMAL AND RADIATION EFFECTS FROM A NUCLEAR WEAPON DETONATION IN AN URBAN ENVIRONMENT

4.1. Introduction

4.1.1. Background

Threats to national security via detonation of a nuclear device have placed a renewed emphasis on accurately understanding the potential consequences of such an incident.[27,120,122,255] Models and simulations provide the only feasible mechanism to aid such comprehension efforts, given the rare nature of such incidents. It is imperative that researchers continually expand upon existing modeling methodology to increase the accuracy and validity of nuclear models in order to better support the emergency management community in preparing for a nuclear detonation.

4.1.2. Nuclear Effects and Impacts

The detonation of a nuclear device has three primary effects (blast, thermal, and radiation) impacting the environment and people. The blast effect is responsible for devastating infrastructure destruction.[64] Like any other explosion, the rapidly expanding fireball is the origin point of the blast, generating a pressure wave extending in all directions.[8,64] The amount of light and heat generated by the explosion creates the secondary effect of a nuclear explosion, known as thermal radiation or heat.[8,9,64] Measured by the thermal fluence, or energy, deposited onto exposed surfaces,[9] thermal radiation causes burns to people, ignites flammable materials, and causes mass fires.[8] Finally, the third major effect of a nuclear explosion is the radiation, which is categorized as prompt radiation and fallout radiation.[7,8,64] As the name suggests, prompt radiation

occurs nearly instantaneously with the flash due to neutron activation.[64] Fallout radiation, alternatively, is created by the products of the fission process, known as radionuclides, which then irradiate various airborne particles and eventually "fall out" of the sky.[64,65] Activation products, which are atoms of structural materials from the device itself or surrounding environment that absorb released neutrons from the detonation, further contribute to fallout radiation.[11] Accurate characterization of these effects through consideration of both amplification and attenuation factors is crucial to establish effective preparedness measures.

Each of the effects described above has the potential to individually cause devastating impacts, but when considered cumulatively, the impacts become catastrophic. Within the immediate area surrounding the detonation, few, if any, survivors and buildings are expected to remain.[8] The rubble in the streets would be impassable, and extremely high radiation levels would be present, increasing risk for any rescue efforts.[73] Extending outward from the site of detonation, the number of buildings destroyed would decrease, and the preponderance of structural damage would be related to utility infrastructure damage, overturned cars, collapsed roofs, and fires.[8,9,64] However, this is the region of greatest opportunity for rescue efforts as radiation levels would be safe for rescuers with the appropriate personal protective equipment, dosimetry equipment, and standard operating procedures (SOPs).[8] In particular, SOPs should ensure the responders are aware of and implement time, distance, and shielding principles.[12] Beyond this region is the end of the visible damage after a detonation, mostly characterized by broken glass or blown out windows or doors.[8,64] Fallout radiation will extend well beyond this visible region of damage, carried by the upper atmospheric winds. The wide geographic footprint of these cumulative effects will cross jurisdictional boundaries and will have rippling effects beyond the immediate destruction.

4.1.3. Modeling Nuclear Effects

The rare occurrence of nuclear detonations necessitates the development of models and simulations to better inform emergency planners about the extent of impacts in such incidents.[107] However, the complex nature of nuclear detonations in conjunction with the relatively limited amount of publicly available data makes it extremely difficult to develop reliable models. The preponderance of existing models focuses on a singular nuclear detonation effect, and few researchers have attempted to develop a comprehensive model, at least in the public domain. While there are some criticisms regarding the accuracy of the blast effect models in an urban environment, blast effect models are often incorporated into other models, such as Hazard Prediction and Assessment Capability (HPAC), as the blast effect is the least debated nuclear effect.[112–116,134] The preponderance of the published literature on modeling nuclear radiation focuses on fallout radiation, rather than prompt radiation. Most studies assume prompt radiation will largely be contained within the other nuclear effects,[7,16,17,37,58] while fallout radiation is frequently modeled by a wide swath of atmospheric dispersion models. Though there remain multiple opportunities to improve individual effects models, the scope of this study focuses specifically on improving methods for simulating the thermal effects and protection from radiation effects in an urban environment, within the context of the overall workflow for modeling an improvised nuclear device (IND) detonation.

4.1.3.1. Modeling Thermal Effects in an Urban Environment

In general, models of thermal effects of nuclear weapons are not as well developed as the modeling of blast and radiation effects, yet it is recognized that casualties resulting from fires and burns in a nuclear detonation would be of major impact for civil defense[9] and emergency health care.[17] In urban environments, a large number of variables can affect the intensity and

impact of the thermal pulse, including the weapon yield, fraction of the total yield emitted as thermal radiation, the distance between the weapon and point of interest and the thermal radiation transmissivity through the immediate atmosphere.[17,64,65] The atmosphere significantly attenuates the thermal energy via absorption and scattering. Atoms and molecules in the air are absorbed, and thus remove, portions of the thermal radiation, particularly that in the ultraviolet region.[64,65] Scattering primarily results from the reflection and diffraction of rays by particles of dust, smoke, or fog in the atmosphere.[45] Both absorption and scattering reduce the amount of thermal energy that reaches a specified area.[45,64] Previous studies[7,9,16,17,45,132] have conducted an in-depth analysis of the various atmospheric conditions that affect absorption and scattering, including cloud height, cloud thickness, cloud type, atmospheric scattering, dust particles in the air, and humidity. These parameters, therefore, also affect thermal radiation transmission and casualties from thermal radiation.

However, no study has comprehensively considered the role buildings play in the urban environment in estimating casualties from the thermal effect. As the thermal pulse expands from the fireball, buildings will create a shadow opposite the fireball, thus shielding a region from the potential thermal fluence.[64] Depending on the construction materials, buildings within the line of sight of the fireball may reflect the thermal radiation, which would increase the thermal fluence an area may receive.[64] This attenuation and amplification dichotomy likely influences the quantity and distribution of thermally burned patients and fires in the aftermath of a nuclear detonation and, therefore must be addressed when developing models to inform planning efforts.

4.1.3.2. Modeling Protection from Radiation in an Urban Environment

Buildings provide varying degrees of protection from the prompt and fallout radiation effects, due to construction materials and location. This level of protection, referred to as a

protection factor (PF), depends on the construction material, the roof and wall type and thickness, number of floors, and location in relation to other floors (e.g. single story, basement, top floor, etc.).[35,64] The PF indicates the protective value of the structure and provides a measure of how much less the radiation level would be at a given point inside the structure rather than outside in an unprotected area (Equation 4.1).[256,257] The open field dose is modeled at 1 meter (m) above an infinite flat plane uniformly contaminated with radioactive materials.[256] Like Sun Protection Factor (SPF) in sunscreen, a larger PF implies more protection from radiation. While it is more commonly used in discussion of nuclear power plant incidents, a reduction factor (RF), also referred to as the transmission factor (TF), is occasionally used to describe the protection offered by buildings from radiation.[34,256] The RF is simply the inverse of the PF (Equation 4.2),[256,257] and is typically expressed either as a proportion or as a percentage.

$$PF = \frac{D_0}{D} = \frac{Unsheltered\ (Open\ Field)\ Dose}{Sheltered\ Dose} \tag{4.1}$$

$$RF = \frac{D}{D_0} = \frac{Sheltered\ Dose}{Unsheltered\ (Open\ Field)\ Dose} = \frac{1}{PF} \tag{4.2}$$

Damage from the blast effect greatly reduces the PFs via various mechanisms, such as breaking windows, blowing in doors, and damaging the roof.[64] Additionally, accounts from previous disasters suggest that individuals may run from buildings due to fear of collapse, thus

increasing their exposure to fallout radiation.[17] Recent research[258–260] also suggests that buildings, even in their optimal condition, fail to provide adequate filtration of radioactive particles, through the heating, ventilation, and air conditioning (HVAC) system, in the 1 - 10 micron range, where the greatest health threat exists. Even if a building has a high efficiency particulate air (HEPA) filter installed, HEPA filters have reduced efficiency for radioactive materials on the 100 – 300 nanometer (nm) size range, which correspond to the aerosols responsible for inhaled, internal radiation doses.[261] While these perturbations can affect prediction of PFs, a greater need exists to include a more granular approach to estimating the PFs in a nuclear detonation model.

4.1.3.2.1. Fallout Radiation Protection Factors

In prior academic studies, PFs for fallout radiation have either been assumed to be uniform across the spatial domain or ignored altogether. In an analysis of nuclear war between Israel and Iran, Dallas et al.[16] applied a 50% RF, or a PF of 2 across the entire spatial domain. When examining planning implications for a nuclear detonation in Riyadh, Saudi Arabia, Shubayr[58] used a RF of 0.09 (PF = 11.11) to represent a typical concrete blockhouse shelter within the study domain. In contrast, Desai et al.[7] argued that PFs could not be considered in their analysis of casualties following multiple nuclear detonations in New Delhi, due to "the significant diversity in the type of structures (e.g., slums, single-story houses, skyscrapers) that exist within the affected areas." Even with the Defense Threat Reduction Agency's (DTRA's) Hazard Prediction and Assessment Capability (HPAC) software designed for modeling all chemical, biological, radiological, nuclear, and explosive (CBRNE) incidents, the specificity for fallout PFs is limited.[134] There are six shelter categories (five building types and open terrain), the geographic distribution of which are provided by the Oak Ridge Global Protection Type

Database.[34] However, this shelter analysis is not available in all areas and cannot be adjusted to become more granular than the casualties estimated to result from assuming the entire population is in the open or sheltered within the shelter types.[134]

However, a recent effort has been made by scientists at the Lawrence Livermore National Laboratory (LLNL) to develop a world-wide fallout shelter database, as part of a larger Regional Shelter Analysis (RSA) methodology.[34] The RSA methodology combines individual, location-specific PFs and population fractions into a regional shelter quality distribution.[34] The fallout shelter database is based on the Prompt Assessment of Global Earthquakes for Response (PAGER) database as well as the Hazards-United States (HAZUS) database.[34] PAGER provides worldwide coverage but has lower resolution, while HAZUS has higher fidelity but only covers the United States (US).[34] For the US, the fallout shelter database estimates fallout PFs for 42 building types in the HAZUS database at a census-tract resolution. A preliminary form of the RSA methodology used in developing the most comprehensive, publicly available model of an IND detonation in a modern urban city conducts a block-by-block analysis of the radiation effects.[72] However, the published report does not discuss more than a specific block as an example of how such methodology could be used.[72] Additionally, the supplemental information for the RSA methodology that contained detailed information for incorporating it into the HPAC workflow can no longer be found.[262] As such, there remains an opportunity to leverage the fallout shelter database and apply it on a building-by-building basis within the affected region to more accurately assess the effects of fallout radiation resulting from a nuclear detonation.

4.1.3.2.2. Prompt Radiation Protection Factors

In contrast to fallout radiation PFs, virtually no studies consider prompt radiation PFs within the context of a nuclear detonation. Prior studies have typically assumed the maximum

extent of the prompt radiation would be contained within the most severely damaged areas from the blast and therefore would not be significant within the larger context of managing the response to a nuclear detonation.[7,16,17,132] However, a recent technical report prepared by the Technical Reachback Division at DTRA evaluated prompt radiation PFs based on simulated data from the propagation of prompt gamma rays and neutrons emitted from a low-yield thermonuclear device.[255] This report calculates prompt radiation PFs for 95 building types, based on exterior wall density, roof/floor density, interior wall mass densities, and percent of exterior walls that were covered by doors or windows. While this study has yet to be incorporated into any publicly available nuclear detonation model, it was designed to fold into the next generation RSA, supporting its relevance to accurate assessment of prompt radiation following a nuclear detonation in an urban environment.

4.1.4. Study Objective

The goal of this study was to develop a framework for improving the methods to estimate the thermal and radiation effects resulting from an IND detonation in an urban environment.

4.2. Materials & Methods

To improve current methods for estimating the thermal and radiation effects resulting from an IND detonation in Atlanta, Georgia (GA), multi-source building data were integrated to assign prompt and fallout radiation PFs on a building-by-building basis. An improved thermal effects model was developed by combining a previously published thermal ignition prediction model[45] with a thermal attenuation model to account for shadowing and reflections of the thermal energy. These components were then integrated into the existing nuclear detonation modeling workflow (Figure 4.1).

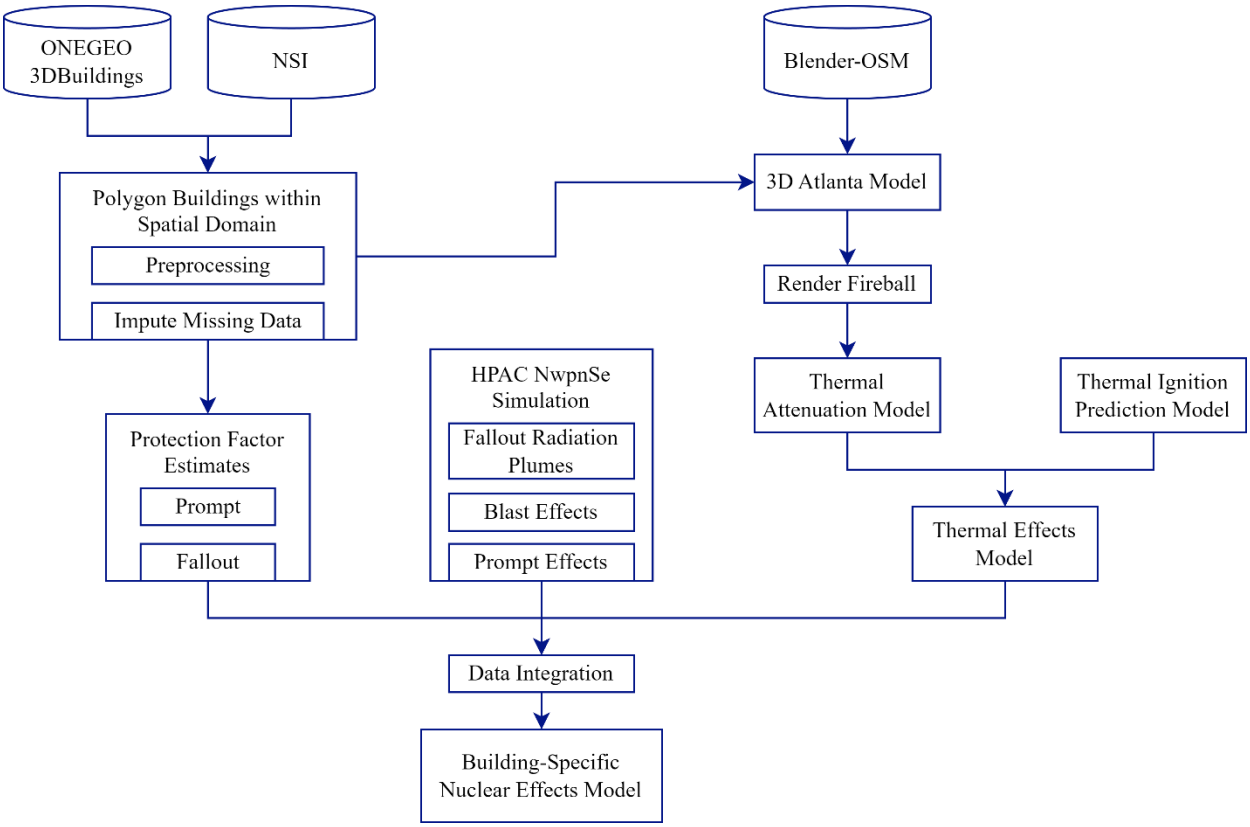

Figure 4.1. Overall workflow to model a nuclear detonation in an urban environments. Abbreviations: NSI = National Structure Inventory; OSM = OpenStreetMaps; 3D = three-dimensional; HPAC = Hazard Prediction and Assessment Capability; NwpnSe = Nuclear Weapon Single Event.

4.2.1. Study Area and Time Period

This study focuses on a simulated IND detonation at 10:00 am local time on four days in 2019 in Atlanta, Georgia (GA). The four days for this study (Table 4.1) are the four medoids identified in the cluster analysis described in Chapter 3: November 26 (Medoid 1), November 25 (Medoid 2), July 2 (Medoid 3), and August 19 (Medoid 4). Atlanta was chosen as the site of a simulated nuclear detonation for numerous reasons. Firstly, Atlanta's moderate climate[36] and lack of proximity to water allows for the consideration of meteorological factors without having to account for meteorological perturbations caused by large bodies of water.[37] Secondly, as a

leader in commerce, industry, and transportation, particularly among southeastern US centers,[38] Atlanta is a plausible target for a nuclear attack. The city includes Hartsfield Jackson International Airport, the busiest airport in the world, as well as the headquarters for major businesses, such as Cable News Network (CNN) and The Coca-Cola Company, and a US Air Force reserve base. Other significant points of interest in the city include the Mercedes-Benz stadium, and the National Center for Civil and Human Rights, and Centennial Olympic Park, which was the location of a domestic terrorist pipe bombing attack during the 1996 Summer Olympics.[39] As far back as 1990, the FEMA has listed Atlanta as a potential target.[40,41] Lastly, Atlanta is a representative of a typical major city found in the US. With a population of almost 500,000 and even more commuters every day, it is the 38th most populous city in the US.[42] It has a relatively large urban sprawl, with a balanced mix of land uses, and a metropolitan area population of approximately six million.[42,43] The combination of these factors make Atlanta an ideal sample location to consider the thermal and radiation effects in an urban environment.

4.2.2. Building Data

The polygon shapes of all buildings within the spatial domain of each medoid were provided by the 3DBuildings database.[263] 3DBuildings supplements the base OpenStreetMap data with more than 40 additional sources, including the US Geological Survey (USGS), ordinance surveys, and Microsoft building footprints.[263] This base map was then spatially joined with data from the National Structure Inventory (NSI),[264] which is a point-based structure database developed by the US Army Corps of Engineers specifically designed to support evaluation of consequences from both natural and human-made hazards.[265] This repository is used as the source database for HAZUS, among other applications in the federal government,[265] and it includes data for each building regarding construction materials, occupancy and use types,

Table 4.1. Conditions at 10:00am local time (time of simulated detonation) for dates of simulated IND detonation in Atlanta, GA.

Medoid	Date	Condition	Temperature [F]	Precipitation [in/hr]	Cloud Coverage [%]	Relative Humidity [%]	Visibility [mi]
1	11/26/2019	Mostly Cloudy	47	0	88	77	10
2	11/25/2019	Fair	41	0	50	79	10
3	7/2/2019	Fair	85	0	50	63	10
4	8/18/2019	Cloudy	82	0	100	71	10

height, number of stories, foundation type and height, and value estimates for the structure, contents, and vehicles associated with the structure, among other variables.

During the joining process of these two data sources for each medoid domain, there was a proportion of buildings present in the 3DBuildings dataset that were not present in the NSI database (Table 4.2). For each of these buildings, values for the NSI variables were imputed, using *k*-nearest average ($k = 5$) space time pattern mining.

Table 4.2. Percent of buildings present in the 3DBuildings data that were not included in the NSI database within the spatial domain of each medoid.

Medoid	Detonation Date	Missing Rate
1	11/26/2019	11.62%
2	11/25/2019	11.71%
3	07/02/2019	11.02%
4	08/19/2019	14.13%

4.2.3. Protection Factor Estimates

4.2.3.1. Fallout Radiation Protection Factors

Fallout radiation PFs were assigned to each building based on the preliminary work in RSA methodology, which assigned fallout PFs to buildings available in the HAZUS database.[34] However, the building data reported on a census-tract level resolution in HAZUS do not match the data included in NSI. Therefore, the fallout PFs identified in RSA were mapped to NSI buildings included in this study, based on construction type, building rise, foundation type, typical height, and range of stories (Table 4.3). The identified unwarned fallout PF reflects the median PF estimate in RSA, assuming the individuals within the building did not have the opportunity to take any protective actions. The identified warned fallout PF, however, assumes

Table 4.3. Assigned protection factors for fallout radiation, based on building construction characteristics. Unwarned assumes a median estimate for the entire building, while warned specifically refers to the location with the highest protection.

Construction Type	Building Rise	Basement Specific?	Typical Height (m)	Number of Stories			Protection Factor	
				Typical	Min	Max	Unwarned	Warned
Concrete	Low	No	6.1	2	1	3	20	50
	Mid	No	15.24	5	4	7	25	100
	High	No	36.58	12	8	–	33.3	200
Masonry	Low	No	6.1	2	1	3	20	50
	Mid	No	15.24	5	4	7	25	100
	High	No	36.58	12	8	–	33.3	200
Steel	Single	No	4.57	1	1	1	2.5	3.3
	Single	Yes	4.57	1	1	1	5	25
	Low	No	7.32	2	1	3	20	50
	Mid	No	18.29	5	4	7	25	100
	High	No	47.55	13	8	–	33.3	200
Wood	Low	No	4.27	1	1	2	2.5	6
	Low	Yes	4.27	1	1	2	2.5	20
Manufactured	Low	No	3.05	1	1	1	2.5	5

individuals within the building had enough warning from the detonation to take protective actions, such as sheltering-in-place in the basement or most interior room in the building.

4.2.3.2. Prompt Radiation Protection Factors

The prompt radiation PFs similarly leveraged previously identified prompt radiation PFs for simulated typical buildings.[255] The exterior wall density, roof/floor density, and interior wall mass density were estimated by NSI construction type, using the base data included in the simulations[255] and estimations for building attributes within the Global Earthquake Model (GEM) database[171] (Table 4.4). The percent of the exterior walls covered by doors or windows, referred to as the apertures, was estimated by mapping the use and occupancy type of the NSI buildings to previously published estimates for architectural features within the GEM database.[171] These aperture estimates were then discretized based on the possible values of apertures included in the simulations for estimating prompt PFs (Table 4.5).[33] The prompt radiation PFs for each building were then assigned based on the closest available approximation to the simulated buildings (Appendix D). Due to the HPAC modeling workflow, it is not feasible to model the prompt radiation PFs for all possible values resulting from this process. Therefore, the prompt radiation PFs were categorized into 22 possible values (Tables 4.6 – 4.9), which were then assigned to each building within the model spatial domain, based on construction type, number of stories, presence of a basement, and occupancy type. Like the fallout PF estimates, the unwarned prompt PF assumes the individuals within the building did not have the opportunity to take any protective actions, while the warned prompt PF assumes individuals within the building had enough warning from the detonation to take protective actions, such as sheltering-in-place in the basement or most interior room in the building.

Table 4.4. Estimated building material densities by construction type.[171,255]

Construction Type	Exterior Wall Density (psf)	Roof/Floor Density (psf)	Interior Wall Density (psf)
Concrete	100	100	100
Masonry	50	10	100
Steel	30	30	30
Wood	10	10	10
Manufactured	1.5	5	10

Table 4.5. Estimated percent area of exterior walls covered by doors or windows, based on prior estimates for simulated buildings[255] and buildings in the GEM database.[171]

Use Type	Occupancy Type	Description	Aperture %
Residential	RES1_1SNB	Single Family Residential, 1 story, no basement	10
	RES1_1SWB	Single Family Residential, 1 story, with basement	10
	RES1_2SNB	Single Family Residential, 2 story, no basement	10
	RES1_2SWB	Single Family Residential, 2 story, with basement	10
	RES1_3SNB	Single Family Residential, 3 story, no basement	10
	RES1_3SWB	Single Family Residential, 3 story, with basement	10
	RES1_SLNB	Single Family Residential, split-level, no basement	10
	RES1_SLWB	Single Family Residential, split-level, with basement	10
	RES2	Manufactured Home	10
	RES3A	Multi-Family housing 2 units	10
	RES3B	Multi-Family housing 3-4 units	25
	RES3C	Multi-Family housing 5-10 units	25
	RES3D	Multi-Family housing 10-19 units	25
	RES3E	Multi-Family housing 20-50 units	25
	RES3F	Multi-Family housing 50 plus units	25
	RES4	Average Hotel	25
	RES5	Nursing Home	25
	RES6	Nursing Home	25
Commercial	COM1	Average Retail	10
	COM2	Average Wholesale	10
	COM3	Average Personal & Repair Services	25
	COM4	Average Professional Technical Services	25
	COM5	Bank	25
	COM6	Hospital	25
	COM7	Average Medical Office	25
	COM8	Average Entertainment/Recreation	25
	COM9	Average Theater	25
	COM10	Garage	25
Industrial	IND1	Average Heavy Industrial	10
	IND2	Average light industrial	10
	IND3	Average Food/Drug/Chemical	10

Use Type	Occupancy Type	Description	Aperture %
Industrial	IND4	Average Metals/Minerals processing	10
	IND5	Average High Technology	10
	IND6	Average Construction	10
Commercial	AGR1	Average Agricultural	10
	REL1	Church	10
Public	GOV1	Average Government Services	25
	GOV2	Average Emergency Response	10
	EDU1	Average School	25
	EDU2	Average College/University	10

Table 4.6. Estimated prompt radiation protection factors for concrete buildings, based on number of stories, presence of a basement, and occupancy types.

Building Rise	Number of Stories		Basement Specific?	Qualifying Occupancy Types	Protection Factor	
	Min	Max			Unwarned	Warned
Single	1	1	Yes	All	6	125
	1	1	No	All	6	6
Low	2	3	Yes	All	6	85
	2	3	No	All	6	10
Mid	4	7	Yes	RES1_1SWB, RES1_2SWB, RES1_3SWB, RES3A, RES3B, RES3C, RES3E, COM3, IND2, IND6, AGR1	10	105
	4	7	No	RES3C, RES4, RES6, COM3, COM4, COM5, COM6, COM7, COM8, COM9, GOV1, EDU1	10	15
	4	7	No	RES1_1SNB, RES1_2SNB, RES1_3SNB, COM1, COM2, IND1, IND2, IND6, AGR1, REL1, EDU2, GOV2	10	25
High	8	30	Yes	RES1_1SWB, RES1_2SWB, RES1_3SWB	6	65
	8	30	No	COM1, COM2, IND6, AGR1, EDU2	6	10
	8	30	No	RES3B, COM3, COM4, COM7, COM8, COM9, GOV1	10	20
Skyscraper	30	–	No	All	10	30

Table 4.7. Estimated prompt radiation protection factors for masonry buildings, based on number of stories, presence of a basement, and occupancy types.

Building Rise	Number of Stories		Basement Specific?	Qualifying Occupancy Types	Protection Factor	
	Min	Max			Unwarned	Warned
Single	1	1	Yes	RES3B, RES3C, RES3E, RES6, COM3, COM4, COM5, COM7, COM8, EDU1, GOV1	3.3	10
	1	1	Yes	RES1_1SWB, RES1_2SWB, RES1_3SWB, RES2, RES3A, COM1, COM2, IND2, IND5, IND6, AGR1, REL1, EDU2	5	15
	1	1	No	RES3B, RES3C, RES3E, RES4, RES5, RES6, COM3, COM4, COM5, COM6, COM7, COM8, COM9, COM10, GOV1, EDU1	3.3	3.3
	1	1	No	RES1_1SNB, RES1_2SNB, RES1_3SNB, RES2, RES3A, COM1, COM2, IND1, IND2, IND3, IND4, IND5, IND6, AGR1, REL1, GOV2, EDU2	5	5
Low	2	3	Yes	RES3B, RES3C, RES3E, RES4, RES6, COM3, COM4, COM5, COM7, COM8, COM9, COM10, EDU1, GOV1	3.3	15
	2	3	Yes	RES1_1SWB, RES1_2SWB, RES1_3SWB, RES2, RES3A, IND1, IND2, IND3, IND5, IND6, COM1, COM2, AGR1, REL1, EDU2	5	30
	2	3	No	RES3B, RES3C, RES3E, RES4, RES5, RES6, COM3, COM4, COM5, COM6, COM7, COM8, COM9, COM10, GOV1, EDU1	3.3	5
	2	3	No	RES1_1SNB, RES1_2SNB, RES1_3SNB, RES3A, COM1, COM2, IND1, IND2, IND3, IND4, IND5, IND6, AGR1, REL1, GOV2, EDU2	5	6
Mid	4	7	Yes	RES3B, RES3C, RES3E, RES6, COM3, COM4, COM8	10	55
	4	7	Yes	RES1_1SWB, RES1_2SWB, RES1_3SWB, RES3A, COM1, COM2, IND1, IND6, REL1	10	75

Building Rise	Number of Stories		Basement Specific?	Qualifying Occupancy Types	Protection Factor	
	Min	Max			Unwarned	Warned
Mid	4	7	No	RES3B, RES3C, RES3E, RES4, RES5, RES6, COM3, COM4, COM5, COM6, COM7, COM8, COM9, COM10, GOV1, EDU1	10	15
	4	7	No	RES1_1SNB, RES1_2SNB, RES1_3SNB, RES3A, COM1, COM2, IND1, IND2, IND3, IND4, IND5, IND6, REL1, GOV2, EDU2	10	20
High	8	30	Yes	RES1_1SWB, RES1_2SWB, RES1_3SWB, RES3A, COM1	6	65
	8	30	Yes	COM4	10	115
	8	30	No	RES1_1SNB, RES1_2SNB, RES1_3SNB, RES3A, COM1, COM2, GOV2, EDU2	6	10
	8	30	No	RES1_3SWB, RES3C, RES3E, COM3, COM4, COM6, COM8, COM9	10	20
Skyscraper	30	–	No	COM3, COM4, COM8	6	20
	30	–	No	RES1_SNB, RES1_1SNB, COM1	10	25

Table 4.8. Estimated prompt radiation protection factors for steel buildings, based on number of stories, presence of a basement, and occupancy types.

Building Rise	Number of Stories		Basement Specific?	Qualifying Occupancy Types	Protection Factor	
	Min	Max			Unwarned	Warned
Single	1	1	Yes	COM7, COM8	2.5	10
	1	1	Yes	COM1, COM2, IND6, REL1	2.5	15
	1	1	No	All	2.5	2.5
Low	2	3	Yes	All	2.5	30
	2	3	No	All	2.5	3.3
Mid	4	7	Yes	RES3B, RES3C, RES3E, RES6, COM3, COM4, COM5, COM8	5	35
	4	7	Yes	RES1_2SWB, RES1_3SWB, RES3A, COM1, IND6, REL1	5	40
	4	7	No	RES3B, RES3C, RES3E, RES4, RES6, COM3, COM4, COM5, COM6, COM7, COM8, COM9, COM10, GOV1, EDU1	5	6
	4	7	No	RES1_2SNB, RES1_3SNB, RES3A, COM1, COM2, IND1, IND2, IND3, IND5, IND6, AGR1, REL1, GOV2, EDU2	5	10
High	8	30	Yes	RES1_1SWB	5	40
	8	30	Yes	RES3E, RES6, COM4	15	165
	8	30	No	RES1_3SNB, RES3A, COM1, COM2, IND1, IND2, IND3, IND4, IND5, IND6, AGR1, REL1, GOV2, EDU2	5	6
	8	30	No	RES3E, RES4, RES6, COM3, COM4, COM5, COM6, COM7, COM8, COM9, COM10, GOV1, EDU1	15	25
Skyscraper	30	–	No	All	3.3	10

Table 4.9. Estimated prompt radiation protection factors for wood and manufactured buildings, based on number of stories, presence of a basement, and occupancy types.

Construction Type	Building Rise	Number of Stories		Basement Specific?	Qualifying Occupancy Types	Protection Factor	
		Min	Max			Unwarned	Warned
Wood	Single	1	1	Yes	All	1.7	5
		1	1	No	All	1.7	1.7
	Low	2	3	Yes	All	1.7	5
		2	3	No	All	1.7	1.7
	Mid	4	7	Yes	All	2.5	15
		4	7	No	All	2.5	3.3
	High	8	30	Yes	RES1_1SWB, RES1_2SWB, RES1_3SWB, RES3A	2.5	15
		8	30	Yes	RES3B, COM4	3.3	25
		8	30	No	RES1_1SNB, RES1_2SNB, RES3A, COM1, COM2, IND2, AGR1, GOV2	2.5	3.3
		8	30	No	RES3B, RES4, RES6, COM3, COM4, COM5, COM7, COM8	3.3	5
	Skyscraper	30	–	No		1.7	3.3
Manufactured	Single	1	1	No	RES2	1.7	1.7
	Low	2	3	No	RES2	1.7	1.7

4.2.4. Nuclear Weapon Detonation Simulation

A tactical nuclear weapon with a predicted explosive yield of 15 kilotons (kt) detonated at 40 meters was simulated at 10:00 am local time on each of the four chosen days, using DTRA's HPAC software. The height of the burst was chosen during a sensitivity analysis to optimize the nuclear effects while still maintaining realistic conditions. At such a height, the blast effect is greater at the detonation site, but the extent of damage is likely restricted since much of the shock wave is absorbed by the ground.[64] By detonating the device slightly above the ground, the fireball is absorbed less by the ground and thus the radiant energy expands to further distances.[64] Fallout radiation only results when the fireball interacts with the ground, so the height was constrained to ensure fallout radiation occurs.[64]

While the yield of modern nuclear weapons is much larger, the emergency management community emphasizes that a low yield weapon is the most useful for planning scenarios.[8,72,78,120] Most planning documents focus on a 10 kt weapon, but some experts argue this yield may be too low.[181] A 15 kt yield was also chosen to reflect a weapon size between those detonated in Hiroshima and Nagasaki.[54]

The simulated detonation occurred at 10:00 am local time each day to allow for the influx of the commuter population while minimizing meteorological changes. Lastly, the coordinates of the detonation location were +33.7566667, -84.38833333, which closely approximates the center of downtown Atlanta. Its proximity to significant points of interest, including the CNN headquarters, Mercedes-Benz stadium, and the National Center for Civil and Human Rights, suggests that it is a plausible location to be targeted. Moreover, this area also includes Centennial Olympic Park, the location of a domestic terrorist pipe bombing attack during the 1996 Summer Olympics.[39]

Under these parameters, the overpressure resulting from the blast effect was modeled to reflect predicted damage zones (Table 4.10). The exact value for such thresholds varies by source and interpretation, but the values listed in Table 4.10 are consistent with US federal government documentation.[72,73] Similarly, the prompt radiation effect was modeled to reflect the thresholds listed in the Environmental Protection Agency Protective Action Guide (EPA PAG) for radiation: 1 – 100 rad; >100 – 200 rad; >200 – 600 rad; >600 rad – 800 rad; >800 rad.[266] Due to the constraints of the HPAC workflow, the prompt radiation effects were estimated by modeling the open field dose as the product of the possible prompt PFs (Tables 4.6 – 4.9) multiplied by the desired values for sheltered dose.

The atmospheric dispersion of ionizing radiation was then calculated using the Second-order Closure Integrated PUFF (SCIPUFF) model, which is a Lagrangian puff dispersion model using Gaussian puffs to represent a three-dimensional (3D), time-dependent concentration.[134,182,183] The fallout radiation dose was then estimated as the total effective dose equivalent (TEDE), ranging from 1 rem to 1,000 rem, 48 hours post-detonation. Given the focus on sheltering in this study, it was assumed that the preponderance of ionizing radiation permeating building structures would be gamma radiation; therefore, the absorbed fallout radiation dose was assumed to be equivalent to the TEDE. Due to the constraints of the HPAC workflow, the fallout radiation effects were estimated by modeling the open field dose as the product of the possible fallout PFs (Table 4.3) multiplied by the desired values for sheltered dose. For the purposes of this study, five dose ranges were modeled: 1 – 50 rad; >50 – 200 rad; >200 – 600 rad; >600 – 1,000 rad; and >1,000 rad, based on the estimates for clinically significant categories of fallout radiation doses in the Radiation Triage, Treat, and Transport (RTR) system.[267] To understand the implications for evacuation and shelter-in-place guidelines,

the EPA PAG thresholds for evacuation (5 rem) and protective actions (shelter-in-place or evacuation; 1 – 5 rem)[266] were also modeled as TEDE, 48 hours post-detonation.

Table 4.10. Damage zone definitions caused by the blast effect.[8,72,73]

Damage Zone	Threshold (psi)	Description
Light	0.5 – 3.0	– Buildings sustain minor damage – Primarily broken windows
Moderate	3.0 – 8.0	– Buildings sustain significant structural damage – Concrete or reinforced buildings remain standing – Substantial rubble in streets – Blown out building interiors – Blown down utility lines – Broken water and gas lines – Overturned vehicles – Caved roofs
Severe	>8.0	– Few, if any, buildings left standing – Streets impassible – Rubble may be 30 feet high or more

4.2.5. Thermal Effect Model

4.2.5.1. Thermal Attenuation Model

To account for the shadow and reflection effects resulting from the thermal energy released from an IND detonation, a thermal attenuation model was developed in the 3D modeling software Blender.[268] The terrain and imagery within the spatial domain of the immediate effects were first queried from Esri. The building data created for this study from the 3DBuildings and NSI databases were then imported into the modeling environment. Sample materials for buildings and other infrastructure were applied to mimic a generic urban

environment. Based on previous studies,[269] 80% of the windows were lit to represent approximately 80% building occupancy (Figure 4.2).

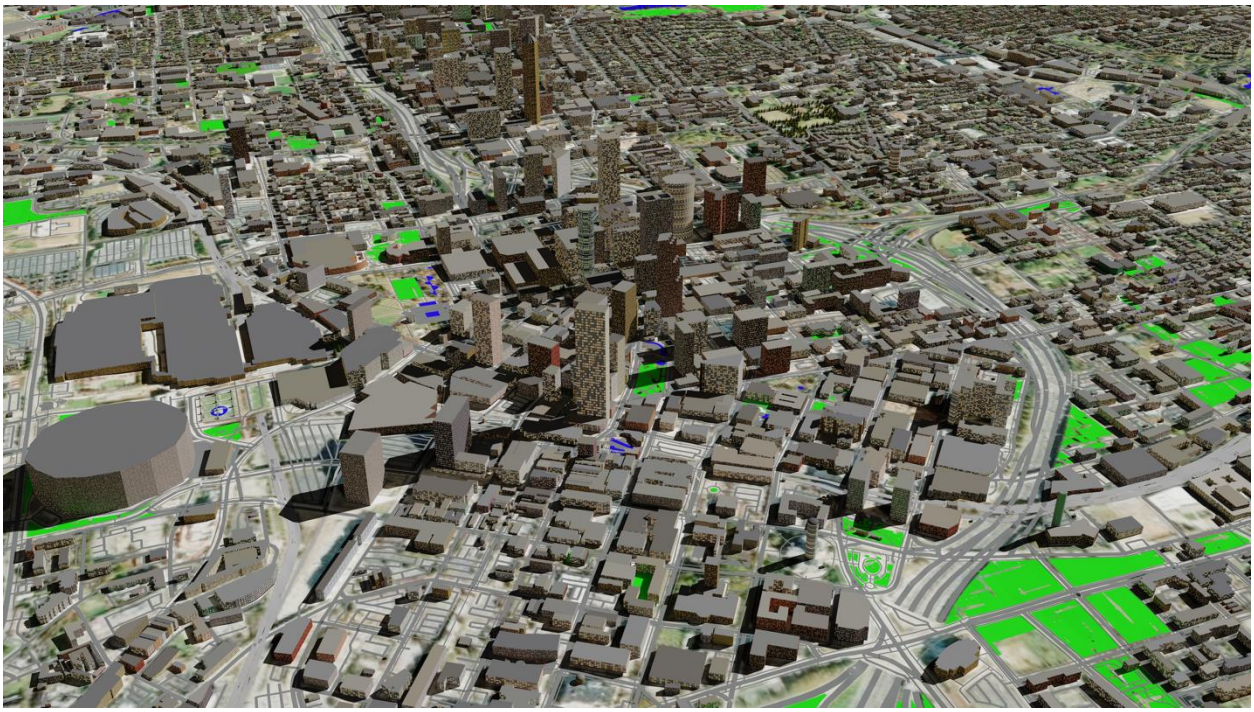

Figure 4.2. 3D model of downtown Atlanta, GA. The shadows are resulting from the sun position at 10:00 am local time. The green material represents grass areas, and the blue material represents water.

A point light was then created to represent the fireball resulting from the detonation. The light was set to a height of 40 m to reflect the height of detonation. The radius, derived from Glasstone and Dolan,[64] was specified to be 130.6 m, to reflect the fireball radius at the breakaway point. The power at the second maximum was calculated by Equation 4.3,[270] where W represents the yield in megatons (MT) and η is the air density ratio. The air density ratio is calculated by Equation 4.4, where B is the lapse rate (0.00650 K/m), z is the altitude in meters, T_0

is the standard temperature (288.16 K), g is the gravitational acceleration (9.81 m/s^2), and R is the ambient air gas constant (287 J/kg*K).[270] As a result, under the parameters of this study, the power at the second maximum of the fireball (and therefore the power of the light source in the model) was 96,724.65 gigawatts (GW).

$$power_{2nd\ max} \cong (1.2\ \times 10^{15}) W \eta^{-0.42} \tag{4.3}$$

$$\eta = \left(1 - \frac{Bz}{T_o}\right)^{\frac{g}{RB}} \left(\frac{T_0}{T_o - Bz}\right) \tag{4.4}$$

The model was then rendered using the Cycles Render Engine, as the engine calculates the physics of light distribution to account for any refraction of light between buildings (Figure 4.3). An orthogonal camera was set directly above the detonation site and captured the full thermal attenuation effects without being distorted by perspective (as normally occurs in a typical camera) (Figure 4.4). The rendered output was then imported into ArcGIS as a raster, using bilinear resampling. The image was georeferenced with a spline transformation before being vectorized for incorporation into the rest of the IND detonation model.

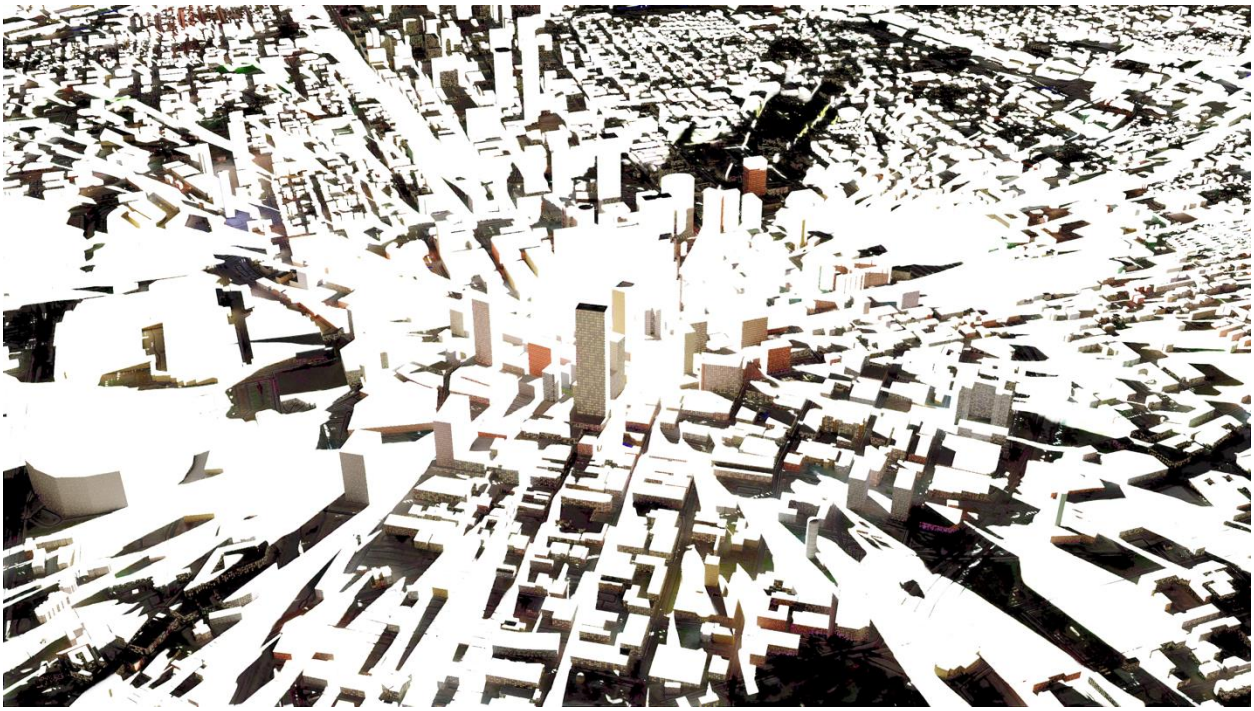

Figure 4.3. Rendered 3D model of fireball resulting from a 15kt IND detonation in downtown Atlanta, GA.

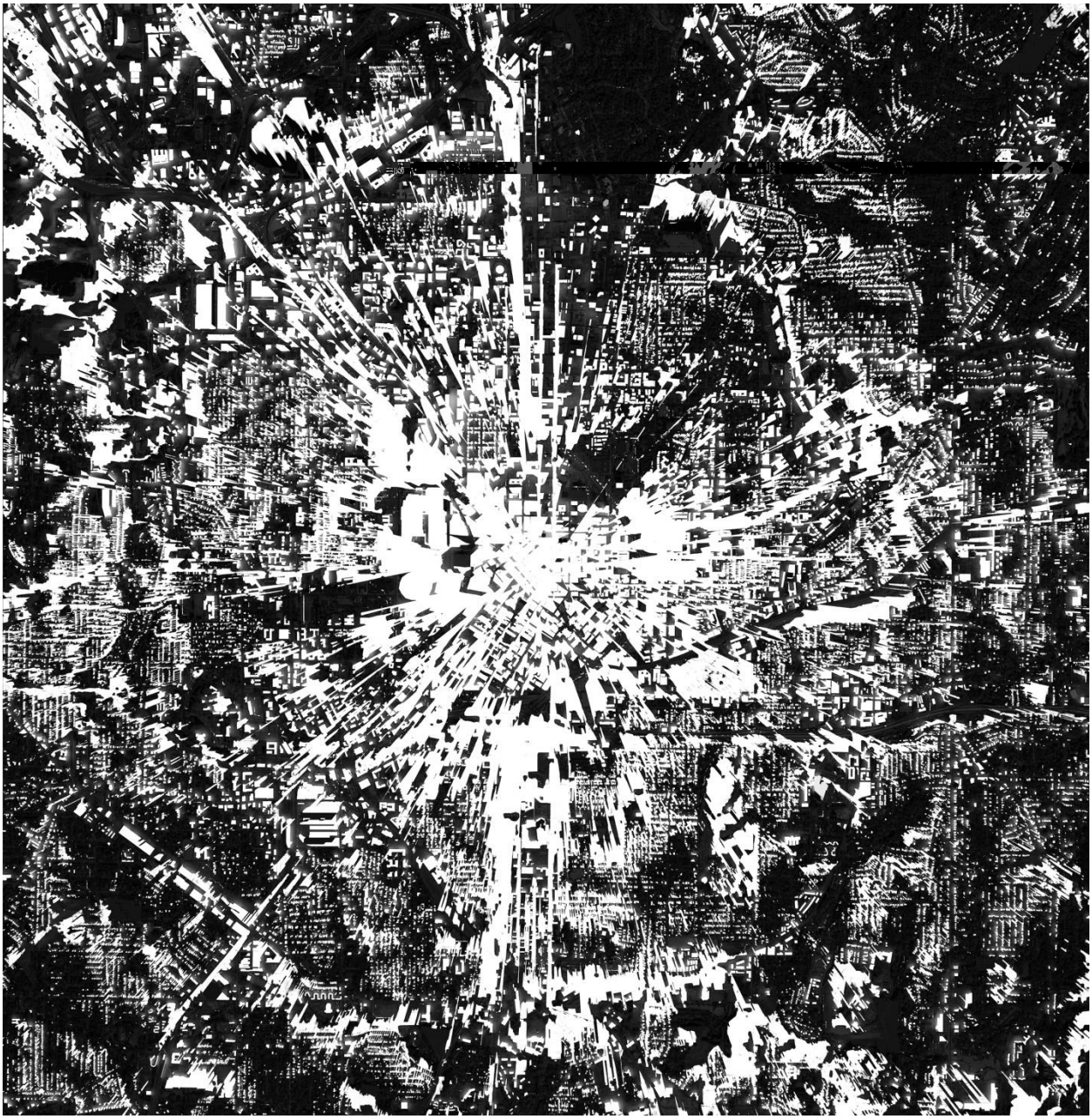

Figure 4.4. Orthogonal capture of the rendered model of a fireball resulting from a 15kt IND detonation in downtown Atlanta, GA.

4.2.5.2. Thermal Ignition Prediction Model

Preliminary model development suggested HPAC does not account for height of burst or weather conditions in the thermal effect estimates. Therefore, the actual thermal fluence, or radiant energy, distributed by the nuclear device was derived from Binninger et al.'s[45] thermal ignition prediction model developed specifically for use within HPAC (Equation 4.5). This model accounts for visibility, absorption and scattering by air, cloud attenuation, and cloud-snow enhancement, as each of these parameters influence the distribution of thermal fluence.

$$Q = W * C_{atm} * S_{cref} * T_{frac} * \left(\frac{\left(1 + \frac{\varphi}{\nu} r\right) e^{\left(\frac{-\delta r}{\nu}\right)}}{4\pi^2} \right) \tag{4.5}$$

Where:

Q = thermal fluence $\left(\frac{\text{cal}}{\text{cm}^2}\right)$

W = weapon yield (kt)

r = straight line slant distance from center of blast (m)

ν = visibility (km)

φ = air scattering factor

δ = clear air absorption factor

C_{atm} = clound attenuation factor

S_{cref} = cloud − snow enhancement factor

T_{frac} = thermal fraction

However, this equation cannot be solved directly for the radius of the thermal effect circle (r). Therefore, a custom goal-seek function was developed to backsolve Equation 4.3 for r, based on desired values for Q. Like the modeling process for radiation, the actual thermal fluence was estimated by modeling the open field thermal fluence as the product of the proportion of light distributed to a location (Figure 4.4) multiplied by the desired values for the attenuated thermal fluence. For the purposes of this study, thermal effects for burn severity were modeled to approximate the thresholds for 50% likelihood of 1st degree burns (2.4 cal/cm^2), 2nd degree burns (4.77 cal/cm^2), and 3rd degree burns (7.37 cal/cm^2). Thresholds for the likelihood of mass fire development were also modeled: 10-50% probability (10 cal/cm^2), >50% (12 cal/cm^2), and >90% (23 cal/cm^2).[9,16,35,45]

4.2.6. Data Integration

Once each component of the model was created, the components were then integrated to wholistically capture the effects from the IND detonation. For each detonation date simulated, the building database was first spatially joined with the fallout radiation plumes, and the absorbed dose from fallout radiation was calculated for each building, under the conditions of no assigned PF, the unwarned PF, and the warned PF. The resulting database was then joined with the blast effect circles, followed by the prompt radiation effect circles. The absorbed dose from prompt radiation was also calculated for each building, under the conditions of no assigned PF, the unwarned PF, and the warned PF. This database was next spatially joined with the vectorized thermal attenuation model and subsequently the thermal effect circles from the thermal ignition prediction model. The thermal fluence was calculated for each building under the conditions of no thermal attenuation model and the application of the thermal attenuation model.

4.2.7. Software

The nuclear weapon detonation simulation, blast effects, prompt radiation effects, and fallout radiation plumes were generated in HPAC (v6.8).[134] The thermal attenuation model was developed in Blender,[268] using the Blender-OSM[271] and Blender-GIS addons.[268] All spatial data integration and analysis was conducted in ArcGIS Pro (v3.0).[185]

4.3. Results

4.3.1. Overview of Simulated IND Detonations

An IND detonation with a predictive explosive yield of 15 kt in downtown, Atlanta, GA was simulated for four representative days in 2019 (Table 4.1). An overview of the spatial distribution of the effects are illustrated in Figures 4.5 – 4.8. Only maximum extent of each of the immediate effects is displayed to highlight the overlapping nature of the immediate effects. In all four simulations, the prompt radiation was completely contained within the thermal effects, which were completely contained within the blast effects. The fallout radiation plume in medoid 1 (November 26) extended 187.01 km in the ENE direction, spanning approximately 3,660 km^2. The fallout radiation plume for medoid 2 (November 25) extended 209.15 km in the E direction, covering approximately 3,215 km^2. The fallout plume for medoid 3 (July 2) extended 126.49 km in the ESE direction, spanning 3,043.22 km^2. Lastly, the fallout radiation plume in medoid 4 (August 19) extended only 84.56 km in the WSW direction, covering approximately 2,450 km^2.

4.3.2. Affected Buildings

The characteristics of the buildings within the affected regions for each simulated detonation are described in Tables 4.11 – 4.16. Even though it was the second longest plume, medoid 1 affected the largest number of buildings (N = 474,401). However, even though it was the largest plume, medoid 2 affected the least number of buildings (N = 29,302), likely because

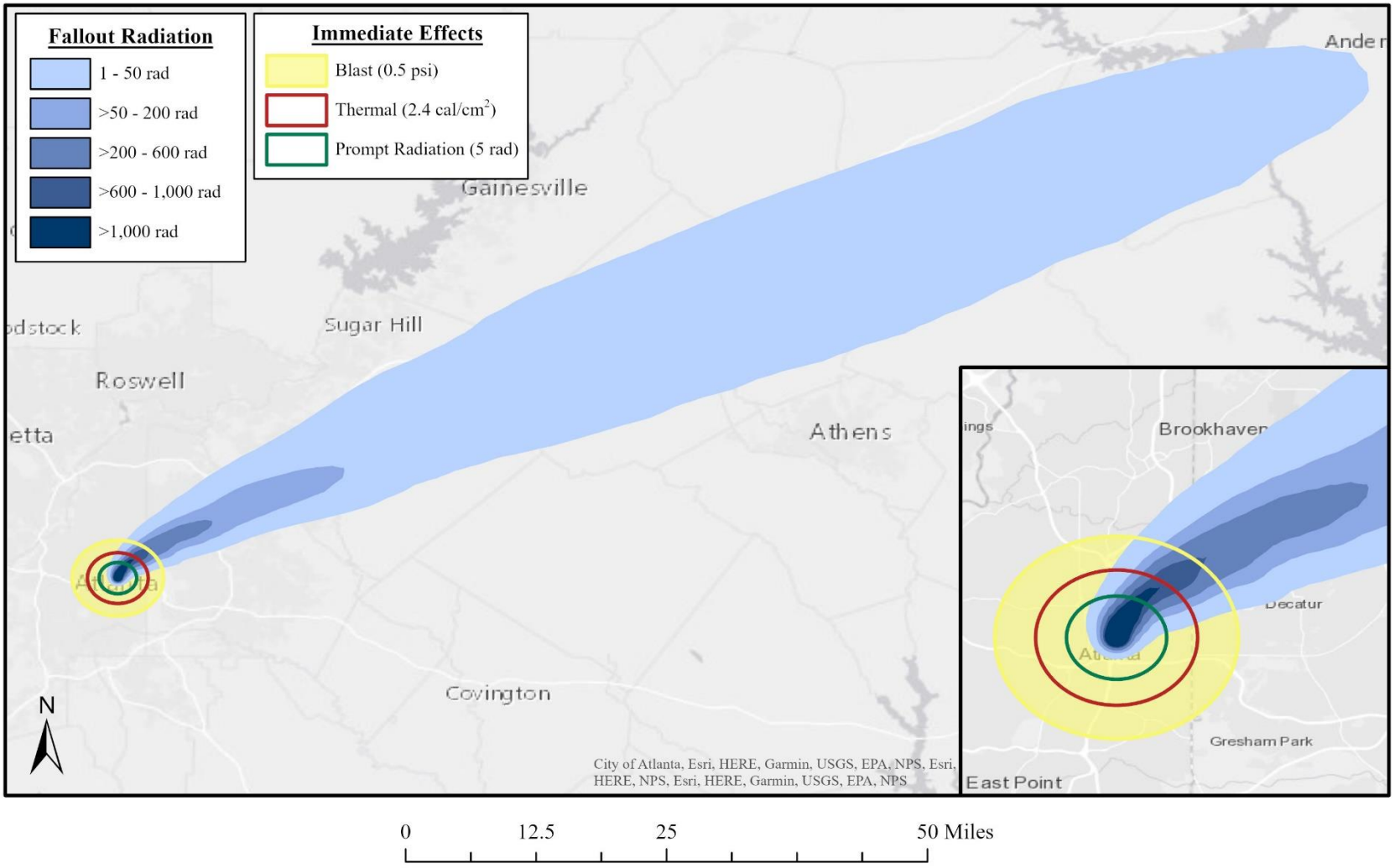

Figure 4.5. Overview of simulated 15 kt IND detonation in downtown Atlanta, GA on November 26, 2019 (Medoid 1) at 10:00 am local time.

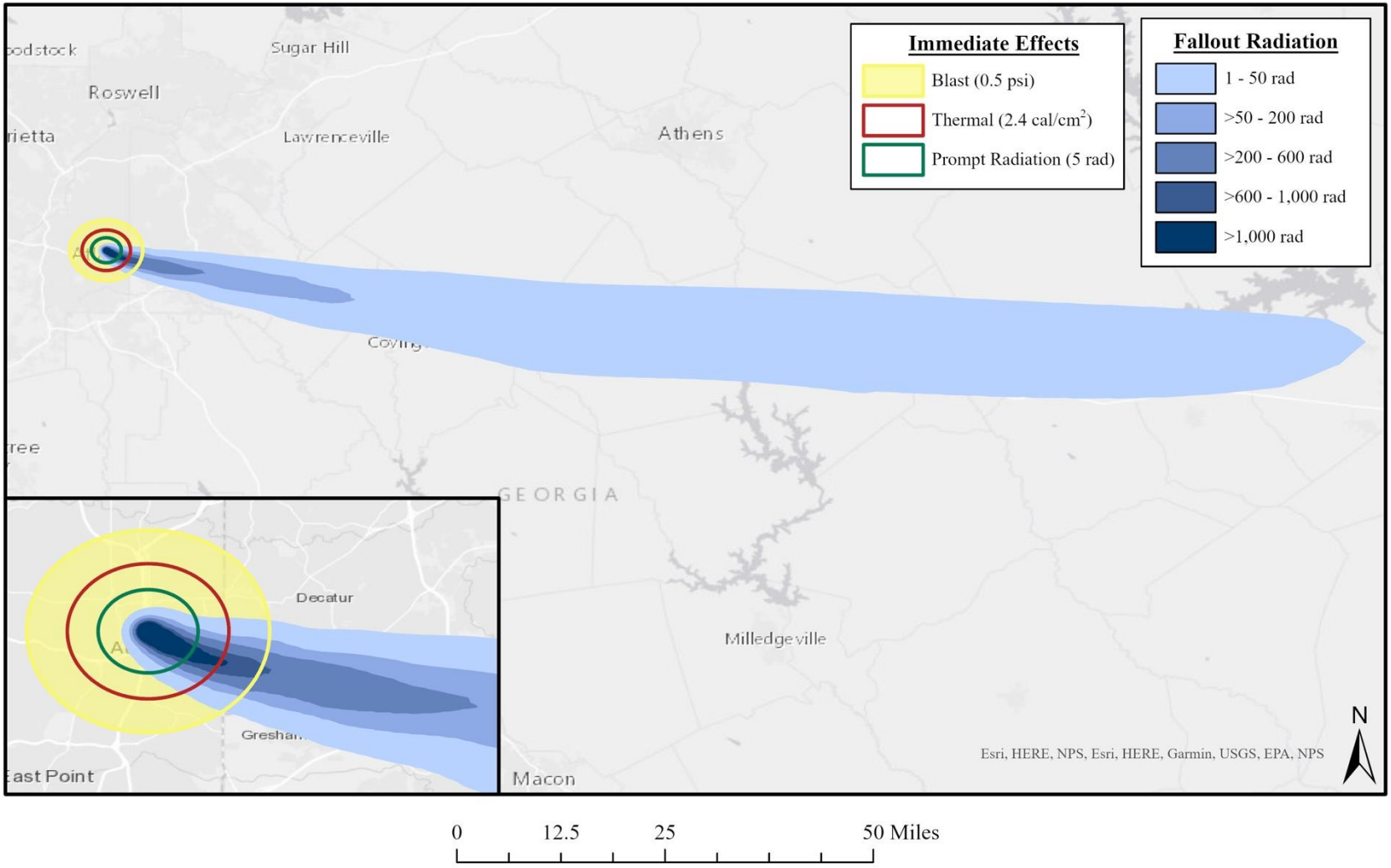

Figure 4.6. Overview of simulated 15 kt IND detonation in downtown Atlanta, GA on November 25, 2019 (Medoid 2) at 10:00 am local time.

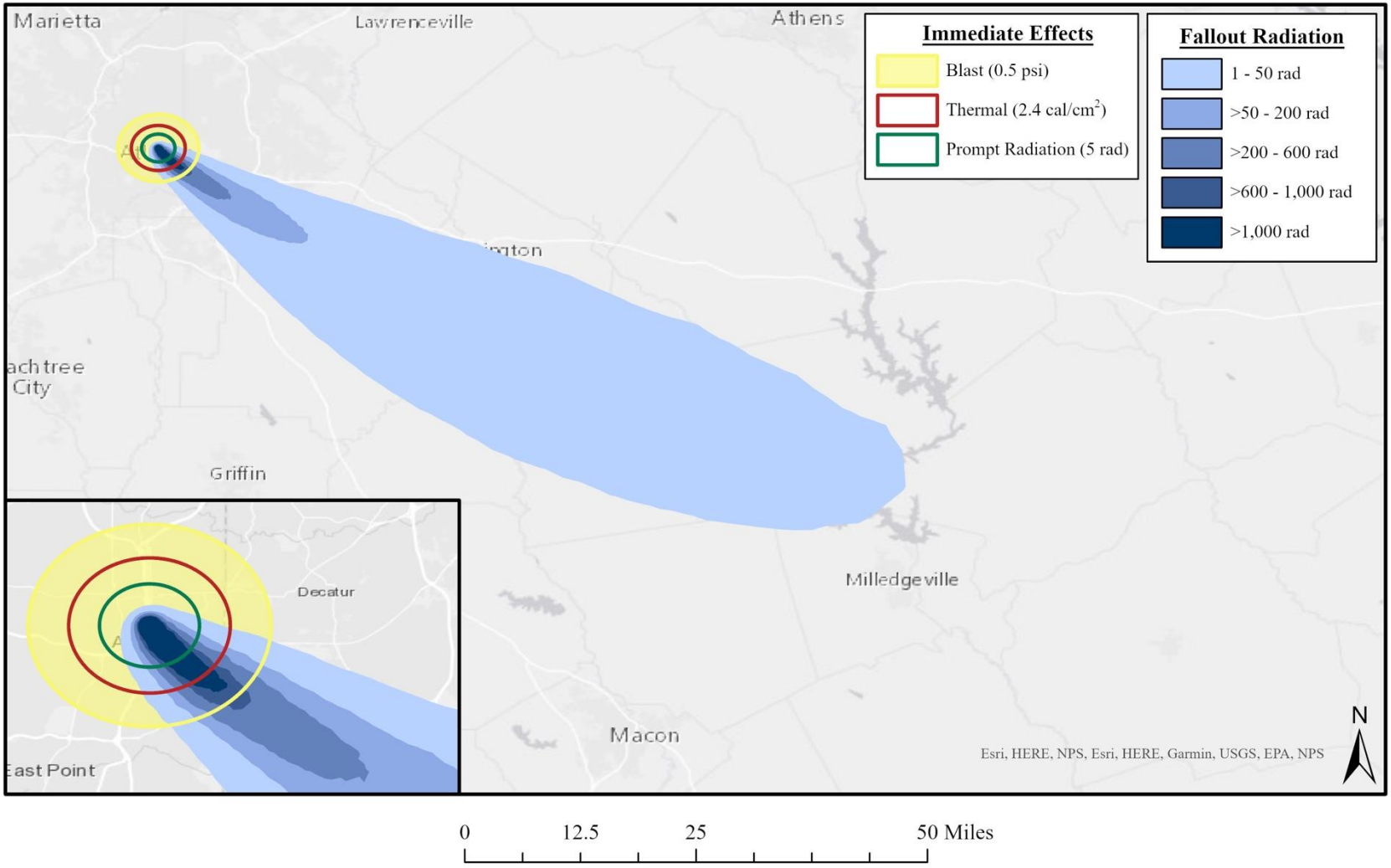

Figure 4.7. Overview of simulated 15 kt IND detonation in downtown Atlanta, GA on July 2, 2019 (Medoid 3) at 10:00 am local time.

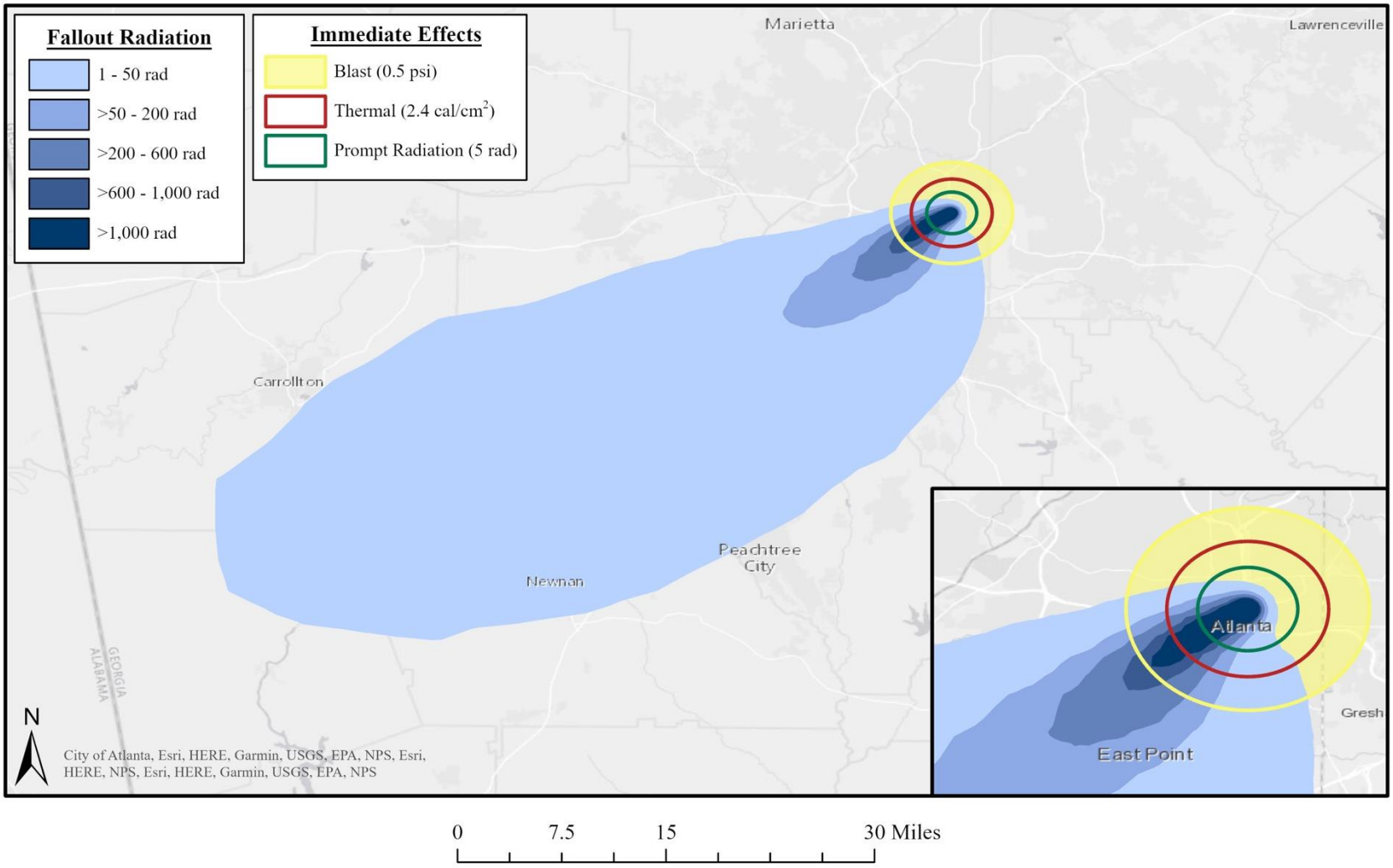

Figure 4.8. Overview of simulated 15 kt IND detonation in downtown Atlanta, GA on August 19, 2019 (Medoid 4) at 10:00 am local time.

the plume covered more rural regions of GA than the other medoids. The tallest building in all the models is the 55-story Bank of America Plaza, which is 1,023 feet (311.81 m) tall. Across all models, wood and masonry were the most common construction materials, and nearly 90% of all buildings in each model were designated as residential. The average unwarned fallout PF in all four medoids was approximately 10, while the average warned fallout PF ranged between 26.77 (Medoid 1) and 29.91 (Medoid 2). The average prompt PF for both unwarned and warned circumstances remained relatively constant across all four medoids; however, this is likely because the prompt PFs were only estimated for buildings within the immediate effect domain. This further suggests that the discrepancies in average fallout radiation PFs is due to the variation in buildings further downwind from the detonation site.

4.3.3. Blast Effects

The spatial extent of the overpressure wave resulting from the blast effect is depicted in Figure 4.9. As the blast effect does not vary with atmospheric or weather conditions, the simulated blast effect remained consistent across all four simulated detonation dates. The full extent of the blast effect, including the light damage zone, spanned approximately 7.5 miles. The moderate damage zone was contained to slightly more than 2 miles across, while the severe damage zone was contained to the downtown area, spanning approximately 1.25 miles. While significant points of interest such as the CNN headquarters and the Mercedes-Benz Stadium would be directly affected by the blast, crucial transportation access points, including Hartsfield Jackson International Airport, were not directly affected. Table 4.17 estimates the damages within each zone by estimated value of each structure, the contents within each structure, and any vehicles associated with each structure. As the light damage zone is primarily characterized by broken glass and other minor damage, only 10% of the structure's value was included in the

Table 4.11. Characteristics of the affected buildings following a simulated 15 kt IND detonation in Atlanta, GA on November 26, 2019 (Medoid 1).

Building Characteristic	**Medoid 1: Detonation on November 26, 2019**				
	Mean	**Std. Dev.**	**Median**	**Min.**	**Max.**
Area (m^2)	511.99	1,992.51	205.29	0.00	169,927.80
Number of Stories	1.55	1.65	1.00	0.00	55.00
Building Height (m)	5.43	5.47	3.91	1.60	311.81
Foundation Height (m)	1.37	0.79	1.50	0.50	8.00
Median Year Built	1982	18.60	1987	1939	2017
Value of Contents ($)	416,118	3,530,725	117,127	0.00	484,902,721
Value of Structure ($)	514,718	3,287,286	227,892	0.00	323,268,480
Value of Vehicle ($)	52,718	443,1867	27,000	0.00	60,615,000
Fallout PF Unwarned	9.12	8.62	2.50	2.50	33.30
Fallout PF Warned	26.77	22.64	20.00	3.30	200.00
Prompt PF Unwarned	3.48	1.96	2.50	1.70	15.00
Prompt PF Warned	15.71	26.93	5.00	1.70	165.00

Table 4.12. Characteristics of the affected buildings following a simulated 15 kt IND detonation in Atlanta, GA on November 25, 2019 (Medoid 2).

Building Characteristic	**Medoid 2: Detonation on November 25, 2019**				
	Mean	**Std. Dev.**	**Median**	**Min.**	**Max.**
Area (m^2)	526.09	1,775.28	184.52	0.00	140,739.49
Number of Stories	1.58	1.49	1.00	1.00	55.00
Building Height (m)	5.49	4.92	3.91	2.00	311.81
Foundation Height (m)	1.28	0.85	1.50	0.50	8.00
Median Year Built	1975	20.59	1979	1939	2017
Value of Contents ($)	365,319	2,226,078	94,848	0.00	484,902,721
Value of Structure ($)	446,175	1,959,975	185,924	0.00	323,268,480
Value of Vehicle ($)	52,879	355,458	27,000	0.00	60,615,000
Fallout PF Unwarned	10.53	8.89	2.50	2.50	33.30
Fallout PF Warned	29.91	23.93	20.00	3.30	200.00
Prompt PF Unwarned	3.49	1.97	2.50	1.70	15.00
Prompt PF Warned	15.72	26.91	5.00	1.70	165.00

Table 4.13. Characteristics of the affected buildings following a simulated 15 kt IND detonation in Atlanta, GA on July 2, 2019 (Medoid 3).

Building Characteristic	Medoid 3: Detonation on July 2, 2019				
	Mean	**Std. Dev.**	**Median**	**Min.**	**Max.**
Area (m^2)	456.76	1,568.49	190.89	0.00	87,530.57
Number of Stories	1.54	1.54	1.00	0.00	55.00
Building Height (m)	5.39	5.07	3.91	1.20	311.81
Foundation Height (m)	1.33	0.87	1.50	0.50	8.00
Median Year Built	1980	20.83	1988	1939	2017
Value of Contents ($)	310,005	1,948,829	101,699	0.00	484,902,721
Value of Structure ($)	402,924	1,814,085	199,918	0.00	323,268,480
Value of Vehicle ($)	48,123	338,482	27,000	0.00	60,615,000
Fallout PF Unwarned	9.43	8.71	2.50	2.50	33.30
Fallout PF Warned	27.21	23.33	20.00	3.30	200.00
Prompt PF Unwarned	3.50	1.96	2.50	1.70	15.00
Prompt PF Warned	15.74	26.88	5.00	1.70	165.00

Table 4.14. Characteristics of the affected buildings following a simulated 15 kt IND detonation in Atlanta, GA on August 19, 2019 (Medoid 4).

Building Characteristic	Medoid 4: Detonation on August 19, 2019				
	Mean	**Std. Dev.**	**Median**	**Min.**	**Max.**
Area (m^2)	508.40	2,026.95	186.34	0.00	203,571.14
Number of Stories	1.58	2.19	1.00	1.00	55.00
Building Height (m)	5.51	7.22	3.91	1.20	1,023.00
Foundation Height (m)	1.40	0.74	1.50	0.50	8.00
Median Year Built	1980	20.94	1985	1939	2017
Value of Contents ($)	464,373	3,029,544	105,161	0.00	484,902,721
Value of Structure ($)	550,757	2,844,245	205,520	0.00	323,268,480
Value of Vehicle ($)	53,801	413,451	27,000	0.00	60,615,000
Fallout PF Unwarned	10.18	8.83	2.50	2.50	33.30
Fallout PF Warned	29.61	23.16	20.00	3.30	200.00
Prompt PF Unwarned	3.53	1.99	2.50	1.70	15.00
Prompt PF Warned	15.51	26.68	5.00	1.70	165.00

Table 4.15. Building construction type, foundation type, and use designations for affected buildings within the spatial domain of each simulated date.

	Medoid 1		Medoid 2		Medoid 3		Medoid 4	
Building Designation	**N**	**(%)**	**N**	**(%)**	**N**	**(%)**	**N**	**(%)**
Construction Type	**474,401**		**269,302**		**305,347**		**376,669**	
Concrete	18,248	(3.85)	15,659	(5.81)	15,238	(4.99)	33,683	(8.94)
Manufactured	3,994	(0.84)	1,688	(0.63)	928	(0.3)	716	(0.19)
Masonry	151,922	(32.02)	102,153	(37.93)	100,248	(32.83)	123,809	(32.87)
Steel	21,199	(4.47)	9,688	(3.6)	8,026	(2.63)	12,486	(3.31)
Wood	279,038	(58.82)	140,114	(52.03)	180,907	(59.25)	205,975	(54.68)
Foundation Type	**474,401**		**269,302**		**305,347**		**376,669**	
Basement	198,604	(41.86)	105,084	(39.02)	118,650	(38.86)	185,567	(49.27)
Crawl	63,290	(13.34)	20,423	(7.58)	18,562	(6.08)	43,720	(11.61)
Pier	6,561	(1.38)	3,264	(1.21)	4,476	(1.47)	2,024	(0.54)
Slab	165,064	(34.79)	117,435	(43.61)	120,481	(39.46)	125,783	(33.39)
Solid Wall	40,882	(8.62)	23,096	(8.58)	43,178	(14.14)	19,575	(5.2)
Use Type	**474,401**		**269,302**		**305,347**		**376,669**	
Residential	412,981	(87.05)	233,382	(86.66)	273,234	(89.48)	327,518	(86.95)
Commercial	46,601	(9.82)	26,917	(10.00)	23,751	(7.78)	36,577	(9.71)
Industrial	7,856	(1.66)	3,744	(1.39)	3,545	(1.16)	5,296	(1.41)
Public	6,963	(1.47)	5,259	(1.95)	4,817	(1.58)	7,278	(1.93)

Table 4.16. Occupancy type designations for affected buildings within the spatial domain of each simulated date.

Occupancy Type	Medoid 1 (N = 474,401)		Medoid 2 (N = 269,302)		Medoid 3 (N = 305,347)		Medoid 4 (N = 376,669)	
	n	**(%)**	**n**	**(%)**	**n**	**(%)**	**n**	**(%)**
RES1-1SNB	133,522	(28.15)	79,836	(29.65)	99,710	(32.65)	82,805	(21.98)
RES1-1SWB	82,522	(17.39)	50,164	(18.63)	60,049	(19.67)	103,617	(27.51)
RES1-2SNB	59,861	(12.62)	35,387	(13.14)	43,607	(14.28)	49,368	(13.11)
RES1-2SWB	83,225	(17.54)	36,210	(13.45)	40,316	(13.2)	56,022	(14.87)
RES1-3SNB	3,094	(0.65)	2,545	(0.95)	2,146	(0.7)	2,605	(0.69)
RES1-3SWB	9,372	(1.98)	5,102	(1.89)	5,051	(1.65)	5,905	(1.57)
RES2	12,234	(2.58)	3,964	(1.47)	5,448	(1.78)	3,118	(0.83)
RES3A	16,558	(3.49)	12,823	(4.76)	10,782	(3.53)	15,767	(4.19)
RES3B	4,567	(0.96)	2,665	(0.99)	2,278	(0.75)	3,874	(1.03)
RES3C	2,854	(0.6)	1,836	(0.68)	1,361	(0.45)	1,552	(0.41)
RES3E	611	(0.13)	354	(0.13)	338	(0.11)	375	(0.1)
RES4	506	(0.11)	319	(0.12)	260	(0.09)	536	(0.14)
RES5/RES6	3,666	(0.77)	1,974	(0.73)	1,485	(0.49)	1,719	(0.46)
COM1	7,496	(1.58)	4,481	(1.66)	3,933	(1.29)	6,173	(1.64)
COM2	4,830	(1.02)	2,451	(0.91)	2,153	(0.71)	3,439	(0.91)
COM3	6,357	(1.34)	4,074	(1.51)	3,607	(1.18)	5,490	(1.46)
COM4	14,498	(3.06)	8,917	(3.31)	8,269	(2.71)	12,714	(3.38)
COM5	1,362	(0.29)	787	(0.29)	676	(0.22)	1,008	(0.27)
COM6	224	(0.05)	174	(0.06)	149	(0.05)	248	(0.07)
COM7	2,325	(0.49)	1,281	(0.48)	1,005	(0.33)	1,554	(0.41)
COM8	5,067	(1.07)	3,479	(1.29)	2,882	(0.94)	4,141	(1.1)
COM9	161	(0.03)	158	(0.06)	153	(0.05)	158	(0.04)
COM10	285	(0.06)	176	(0.07)	177	(0.06)	272	(0.07)
IND1	1,188	(0.25)	406	(0.15)	251	(0.08)	500	(0.13)
IND2	2,168	(0.46)	1,344	(0.5)	1,281	(0.42)	2,217	(0.59)
IND3	209	(0.04)	117	(0.04)	98	(0.03)	191	(0.05)
IND4	88	(0.02)	78	(0.03)	53	(0.02)	102	(0.03)
IND5	284	(0.06)	127	(0.05)	156	(0.05)	282	(0.07)
IND6	4,106	(0.87)	1,887	(0.7)	1,902	(0.62)	2,203	(0.58)
AGR1	3,627	(0.76)	562	(0.21)	547	(0.18)	909	(0.24)
REL1	3,228	(0.68)	2,409	(0.89)	2,289	(0.75)	3,027	(0.8)
GOV1	2,176	(0.46)	1,872	(0.7)	1,532	(0.5)	2,928	(0.78)
GOV2	238	(0.05)	197	(0.07)	173	(0.06)	247	(0.07)
EDU1	1,375	(0.29)	701	(0.26)	794	(0.26)	1,057	(0.28)
EDU2	517	(0.11)	445	(0.17)	436	(0.14)	546	(0.14)

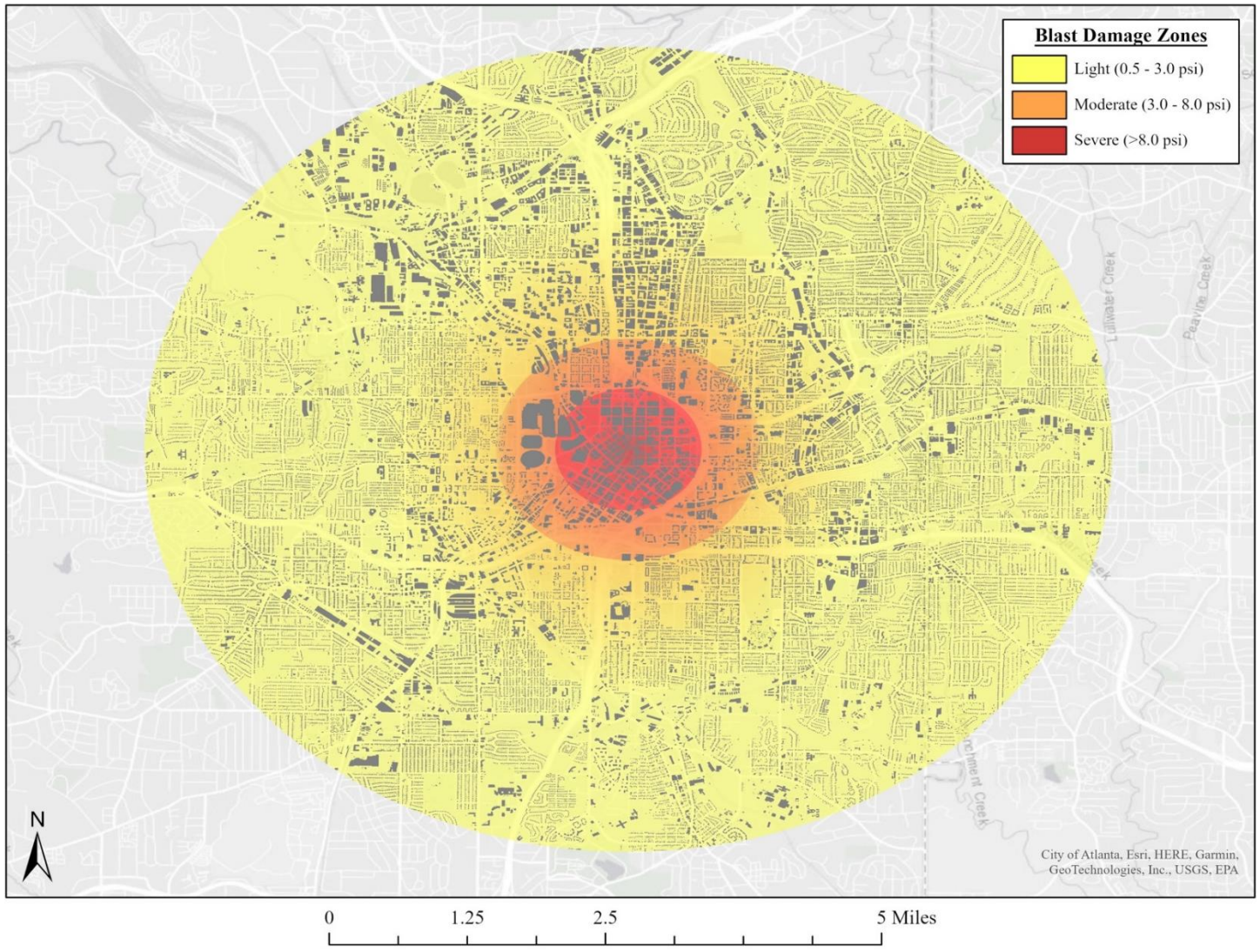

Figure 4.9. Estimated blast effects for the simulated 15 kt IND detonation in Atlanta, GA at 10:00 am local time. The colored regions represent the damage zones, and the grey polygons represent the affected buildings.

Table 4.17. Estimated damages resulting from the blast effects within each damage zone.

	Estimated Damages			
Damage Zone	**Structures**	**Building Contents**	**Vehicles**	**Total**
Light	$ 3,098,649,014	$ -	$ -	$ 3,098,649,014
Moderate	$ 2,915,165,912	$ 3,125,772,123	$ 414,703,800	$ 6,455,641,835
Severe	$ 3,908,842,391	$ 3,632,368,993	$ 916,740,900	$ 8,457,952,285
Total Damages	**$ 9,922,657,318**	**$ 6,758,141,116**	**$ 1,331,444,700**	**$ 18,012,243,134**

damage estimation. In the moderate damage zone, however, the entire value of the vehicles associated with, and contents within, each structure were included in the damage estimates, as any vehicles or contents are unlikely to remain undamaged. For the structures themselves, 75% of the structure's value was included in the damage estimation to account for the widespread but not complete destruction. However, in the severe damage zone, the entire value of each structure, the contents within each structure, and any vehicles associated with each structure were included in the damage estimates. The blast effect alone would cause an estimated $18B in damages within a 3.75-mile radius.

4.3.4. Thermal Effects

Figures 4.10 and 4.11 display the results of the thermal attenuation model and the thermal ignition probability model for medoid 3 (July 2, 2019) as an illustrative example. The spatial extent of the thermal effect circles derived from the thermal ignition model did not vary significantly across the four medoids, as the detonation was simulated below the cloud height for all days. The slight perturbations (<500 m in the estimated radius) were a result of the differences in cloud coverage. Tables 4.18 – 4.21 describe the affected buildings within each thermal effect of interest in this study. Across all four simulations, the thermal attenuation model significantly reduced the number of buildings affected by each thermal effect. Within the regions for 50% probability of burns, nearly half of the buildings (approximately 45% across all four simulations) no longer received enough thermal fluence to cause 50% probability of burns of any severity. A similar phenomenon occurred within the mass fire regions, with more than half of the buildings (Medoid 1: 54.19%; Medoid 2: 53.64%; Medoid 3: 53.63%; Medoid 4: 50.89%) no longer receiving enough thermal fluence to cause mass fires. Comparing the different simulations, Medoid 4 yielded the largest reduction in buildings affected by the thermal fluence

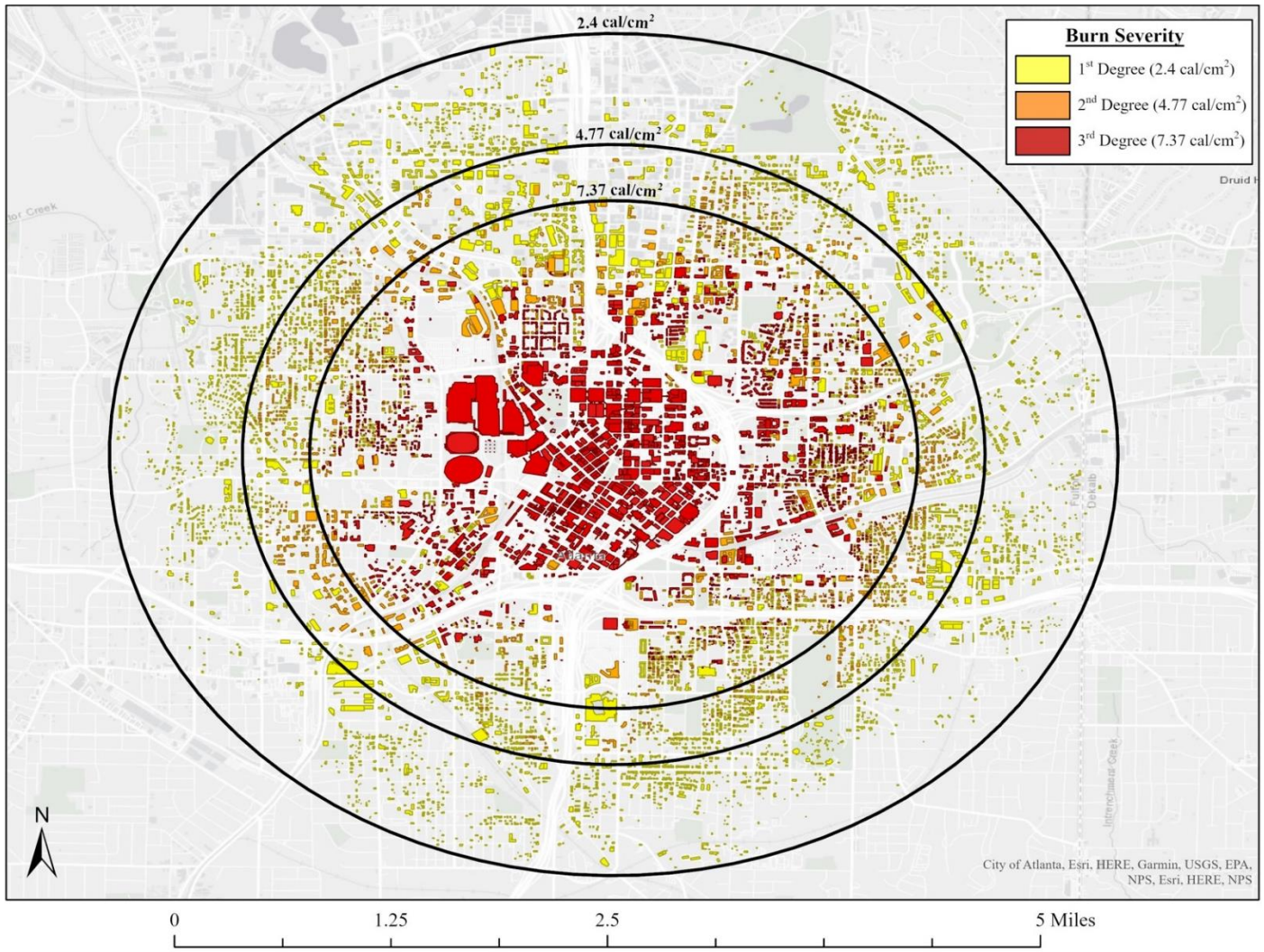

Figure 4.10. Estimated burn severity from a 15 kt detonation in downtown Atlanta, GA on July 2, 2019 (Medoid 3). The circles represent the thermal fluence effect circles from the thermal ignition prediction model, without accounting for the thermal attenuation model. The colors of the buildings represent the inclusion of the thermal attenuation model for the same thermal fluence thresholds to cause an estimated 50% probability of burns at each degree of severity.

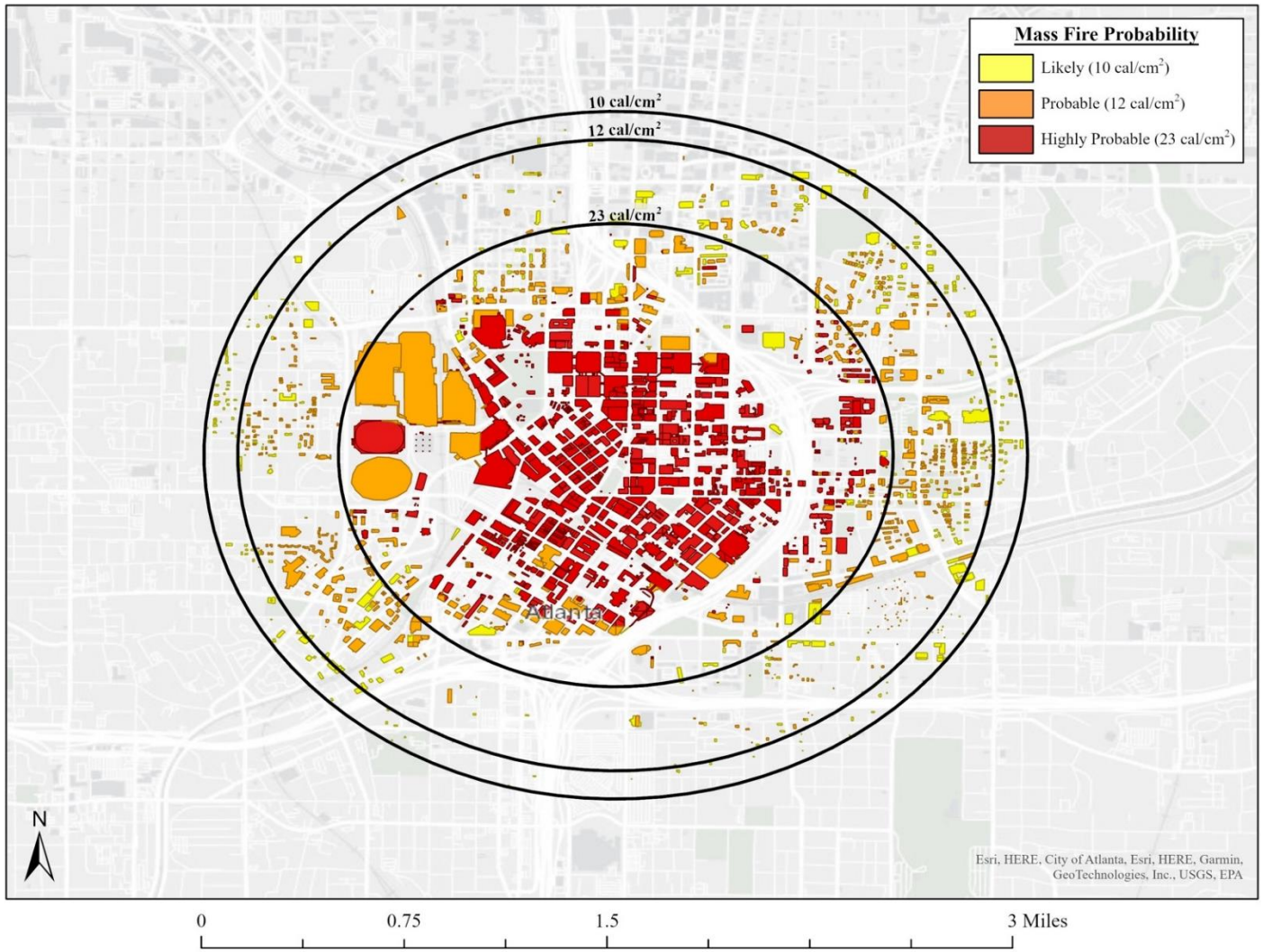

Figure 4.11. Estimated likelihood of mass fires resulting from a 15 kt detonation in downtown Atlanta, GA on July 2, 2019 (Medoid 3). The circles represent the thermal fluence effect circles from the thermal ignition prediction model, without accounting for the thermal attenuation model. The colors of the buildings represent the inclusion of the thermal attenuation model for the same thermal fluence thresholds to cause mass fires.

Table 4.18. Estimated number of affected buildings within each thermal effect region of interest, following a 15 kt IND detonation in downtown Atlanta on November 26, 2019 (Medoid 1).

			Thermal Model (Estimated Number of Buildings)	
Thermal Effect	**Probability**	**Thermal Fluence (cal/cm^2)**	**No Attenuation**	**Attenuation Model**
Burn Severity				
1st Degree	50%	2.40	34,167	15,287
2nd Degree	50%	4.77	14,166	5,403
3rd Degree	50%	7.37	22,946	11,207
Total			**71,279**	**31,897**
Mass Fire Likelihood				
Likely	10 - 50%	10.00	2,793	1,685
Probable	>50%	12.00	6,012	2,647
Highly Probable	>90%	23.00	8,098	4,827
Total			**16,903**	**9,159**

Table 4.19. Estimated number of affected buildings within each thermal effect region of interest, following a 15 kt IND detonation in downtown Atlanta on November 25, 2019 (Medoid 2).

			Thermal Model (Estimated Number of Buildings)	
Thermal Effect	**Probability**	**Thermal Fluence (cal/cm^2)**	**No Attenuation**	**Attenuation Model**
Burn Severity				
1st Degree	50%	2.40	34,808	15,302
2nd Degree	50%	4.77	14,653	5,471
3rd Degree	50%	7.37	22,941	11,282
Total			**72,402**	**32,055**
Mass Fire Likelihood				
Likely	10 - 50%	10.00	2,824	1,722
Probable	>50%	12.00	6,097	2,558
Highly Probable	>90%	23.00	8,036	4,816
Total			**16,957**	**9,096**

Table 4.20. Estimated number of affected buildings within each thermal effect region of interest, following a 15 kt IND detonation in downtown Atlanta on July 2, 2019 (Medoid 3).

			Thermal Model	
Thermal Effect	**Probability**	**Thermal Fluence (cal/cm^2)**	**No Attenuation**	**Attenuation Model**
Burn Severity				
1st Degree	50%	2.40	34,666	15,306
2nd Degree	50%	4.77	14,780	5,428
3rd Degree	50%	7.37	22,829	11,198
Total			**72,275**	**31,932**
Mass Fire Likelihood				
Likely	10 - 50%	10.00	2,780	1,651
Probable	>50%	12.00	6,041	2,581
Highly Probable	>90%	23.00	8,055	4,819
Total			**16,876**	**9,051**

Table 4.21. Estimated number of affected buildings within each thermal effect region of interest, following a 15 kt IND detonation in downtown Atlanta on August 19, 2019 (Medoid 4).

			Thermal Model (Estimated Number of Buildings)	
Thermal Effect	**Probability**	**Thermal Fluence (cal/cm^2)**	**No Attenuation**	**Attenuation Model**
Burn Severity				
1st Degree	50%	2.40	35,882	17,074
2nd Degree	50%	4.77	15,742	5,630
3rd Degree	50%	7.37	24,357	11,481
Total			**75,981**	**34,185**
Mass Fire Likelihood				
Likely	10 - 50%	10.00	2,863	1,685
Probable	>50%	12.00	7,309	2,743
Highly Probable	>90%	23.00	7,973	4,806
Total			**18,145**	**9,234**

for mass fires, while Medoid 1 yielded the lowest reduction in buildings affected by mass fires. Though these differences are small, it does suggest that the weather conditions occurring on November 26, 2019 (Medoid 1) were likely to cause the fewest fires, while weather conditions occurring on August 19, 2019 (Medoid 4) were likely to cause more mass fires.

4.3.5. Radiation Effects

4.3.5.1. Prompt Radiation Effects

The spatial extent of the prompt radiation effect circles generated in the HPAC simulation did not vary significantly across the four medoids, so Figure 4.12 displays the spatial extent of the prompt radiation effect circles for medoid 2 (November 25, 2019) as an illustrative example. Tables 4.22 – 4.25 describe the affected buildings within each radiation range of interest in this study. Across all four simulations, the number of buildings affected by prompt radiation were significantly reduced when considering the PFs under either the unwarned or warned scenario. When considering the unwarned scenario for prompt radiation, number of buildings exposed to prompt radiation decreased by approximately 1,900 (Medoid 1: 1,909; Medoid 2: 1,868; Medoid 3: 1,861; Medoid 4: 1,943). Considering the prompt PFs under the warned scenario further increased this reduction (Medoid 1: 2,158; Medoid 2: 2,177; Medoid 3: 2,136; Medoid 4: 2,211). In comparing the simulations, Medoid 4 yielded the largest reduction in buildings exposed to prompt radiation, among both the unwarned and warned scenarios, suggesting the urban environment contained within the spatial domain of medoid 4 offers the best protection from radiation. Conversely, medoid 3 yielded the smallest reduction in buildings exposed to prompt radiation when considering either the unwarned or warned scenario.

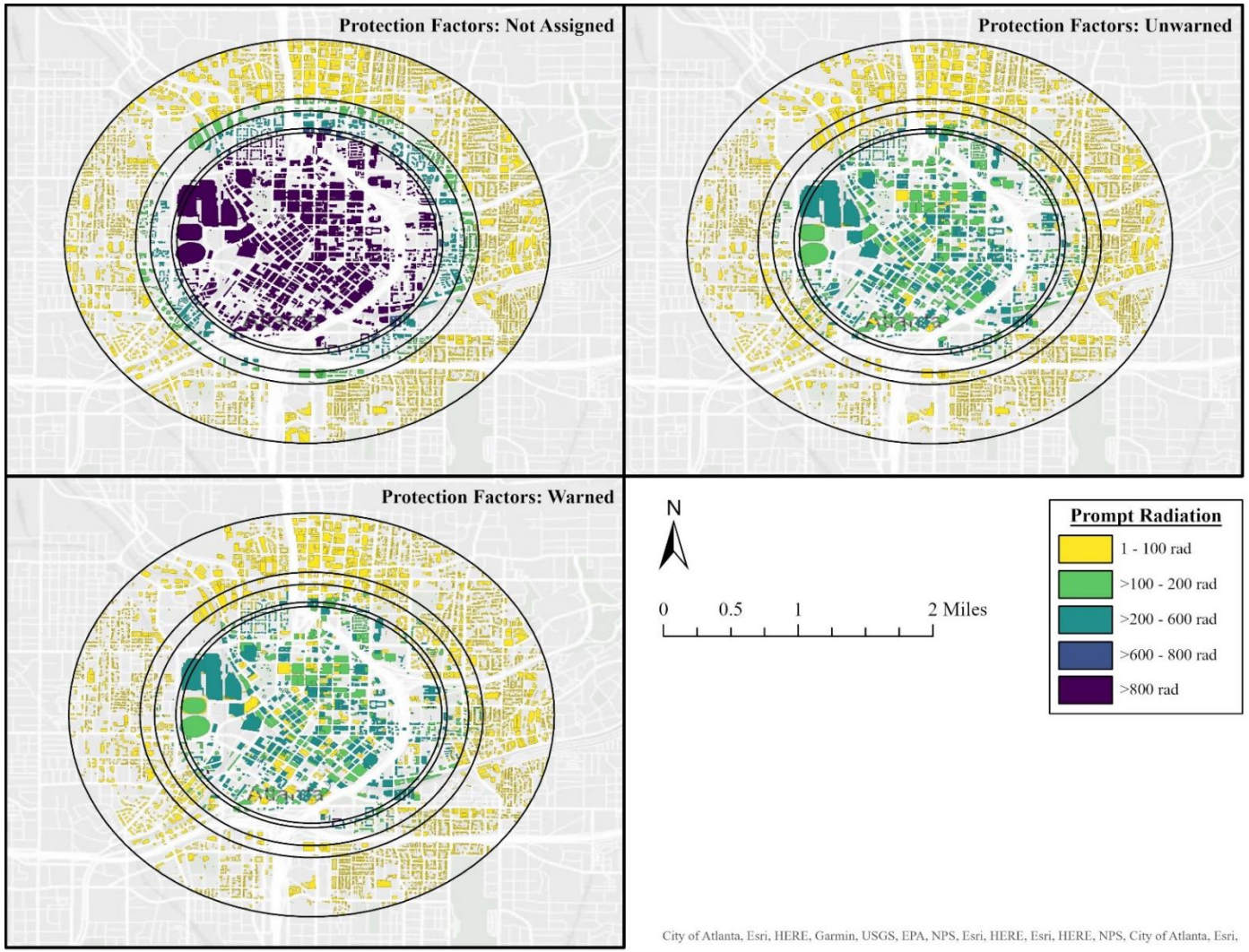

Figure 4.12. Simulated prompt radiation from a 15 kt IND detonation in downtown Atlanta on November 25, 2019 (Medoid 2), under the following conditions: PFs were not assigned; unwarned PFs were assigned; and warned PFs were assigned. The isolines from the contours represent the prompt radiation ranges with no PFs considered.

Table 4.22. Estimated number of affected buildings within each radiation dose range of interest, following a 15 kt IND detonation in Atlanta, GA on November 26, 2019 (Medoid 1).

	Protection Factors		
Prompt Radiation Dose Range (rad)	**Not Assigned**	**Unwarned**	**Warned**
1 – 100	13,185	14,132	15,069
>100 – 200	1,637	4,292	3,221
>200 – 600	1,657	4,136	4,021
>600 – 800	357	-	-
>800	7,633	-	-
Total	**24,469**	**22,560**	**22,311**
Fallout Radiation Dose Range (rad)			
1 – 50	305,888	245,614	168,948
>50 – 200	42,788	11,025	3,443
>200 – 600	21,711	4,551	660
>600 – 1,000	7,831	211	255
>1,000	8,342	520	218
Total	**386,560**	**261,921**	**173,524**
EPA PAG Recommendation			
Protective Actions (1 – 5 rem)	186,949	169,304	140,952
Evacuation Required (>5 rem)	208,217	101,189	42,326
Total	**395,166**	**270,493**	**183,278**

Table 4.23. Estimated number of affected buildings within each radiation dose range of interest, following a 15 kt IND detonation in Atlanta, GA on November 25, 2019 (Medoid 2).

	Protection Factors		
Prompt Radiation Dose Range (rad)	**Not Assigned**	**Unwarned**	**Warned**
1 – 100	13,108	14,146	15,010
>100 – 200	1,620	4,270	3,212
>200 – 600	1,724	4,095	3,980
>600 – 800	376	-	-
>800	7,551	-	-
Total	**24,379**	**22,511**	**22,202**
Fallout Radiation Dose Range (rad)			
1 – 50	112,377	109,186	92,697
>50 – 200	34,240	11,640	5,774
>200 – 600	16,488	7,107	706
>600 – 1,000	5,331	435	164
>1,000	6,457	589	320
Total	**174,893**	**128,957**	**99,661**
EPA PAG Recommendation			
Protective Actions (1 – 5 rem)	64,372	65,352	64,776
Evacuation Required (>5 rem)	119,353	73,271	45,876
Total	**183,725**	**138,623**	**110,652**

Table 4.24. Estimated number of affected buildings within each radiation dose range of interest, following a 15 kt IND detonation in Atlanta, GA on July 2, 2019 (Medoid 3).

	Protection Factors		
Prompt Radiation Dose Range (rad)	**Not Assigned**	**Unwarned**	**Warned**
1 – 100	13,067	14,040	14,941
>100 – 200	1,610	4,267	3,209
>200 – 600	1,654	4,108	3,990
>600 – 800	354	-	-
>800	7,591	-	-
Total	**24,276**	**22,415**	**22,140**
Fallout Radiation Dose Range (rad)			
1 – 50	159,089	115,531	84,663
>50 – 200	25,046	12,324	6,391
>200 – 600	12,810	7,485	1,206
>600 – 1,000	4,668	2,009	162
>1,000	9,445	743	363
Total	**211,058**	**138,092**	**92,785**
EPA PAG Recommendation			
Protective Actions (1 – 5 rem)	109,775	85,781	61,041
Evacuation Required (>5 rem)	110,470	63,796	43,897
Total	**220,245**	**149,577**	**104,938**

Table 4.25. Estimated number of affected buildings within each radiation dose range of interest, following a 15 kt IND detonation in Atlanta, GA on August 19, 2019 (Medoid 4).

	Protection Factors		
Prompt Radiation Dose Range (rad)	**Not Assigned**	**Unwarned**	**Warned**
1 – 100	13,863	15,216	16,122
>100 – 200	2,057	4,527	3,467
>200 – 600	1,951	4,054	3,940
>600 – 800	349	-	-
>800	7,520	-	-
Total	**25,740**	**23,797**	**23,529**
Fallout Radiation Dose Range (rad)			
1 – 50	228,299	142,176	96,524
>50 – 200	30,902	11,376	3,273
>200 – 600	16,364	7,179	1,216
>600 – 1,000	8,150	758	225
>1,000	7,922	747	467
Total	**291,637**	**162,236**	**101,705**
EPA PAG Recommendation			
Protective Actions (1 – 5 rem)	164,902	106,738	77,691
Evacuation Required (>5 rem)	138,577	68,218	38,175
Total	**303,479**	**174,956**	**115,866**

4.3.5.2. Fallout Radiation Effects

The spatial extent of the fallout radiation effects for each date of simulation are displayed in Figures 4.13 – 4.16, and Tables 4.22 – 4.25 describe the affected buildings within each radiation range of interest in this study. Across all four simulations, the number of buildings affected by fallout radiation after 48 hours were significantly reduced when considering the PFs under either the unwarned or warned scenario. For the unwarned scenario, the proportion of buildings no longer affected by fallout radiation varied across the simulations. Nearly 45% of the buildings within the spatial domain of Medoid 4 blocked all fallout radiation after considering the unwarned PFs. Approximately one third of the buildings within the spatial domains of Medoids 1 (32%) and 3 (34%) blocked all fallout radiation after consideration of PFs in the unwarned scenario, and Medoid 2 had the smallest reduction, with approximately 25% of buildings blocking all fallout radiation. In Medoids 1, 2, and 4, more than 90% of buildings that were exposed to more than 600 rads after 48 hours actually received less than 600 rads inside the buildings, once the PFs were considered in the unwarned scenario.

When considering the PFs associated with the warned scenario, similar trends occurred. Nearly two thirds (65%) of the buildings within the spatial domain of Medoid 4 blocked all fallout radiation after considering the PFs in the warned scenario, and approximately half of the buildings in Medoids 1 (55%) and 3 (56%). Medoid 2 also had the smallest reduction, with approximately 43% of buildings blocking all fallout radiation after consideration of the PFs in the warned scenario. Across all simulations, more than 90% of buildings that were exposed to more than 200 rads after 48 hours actually received less than 200 rads inside the buildings, once the PFs associated with the warned scenario were considered.

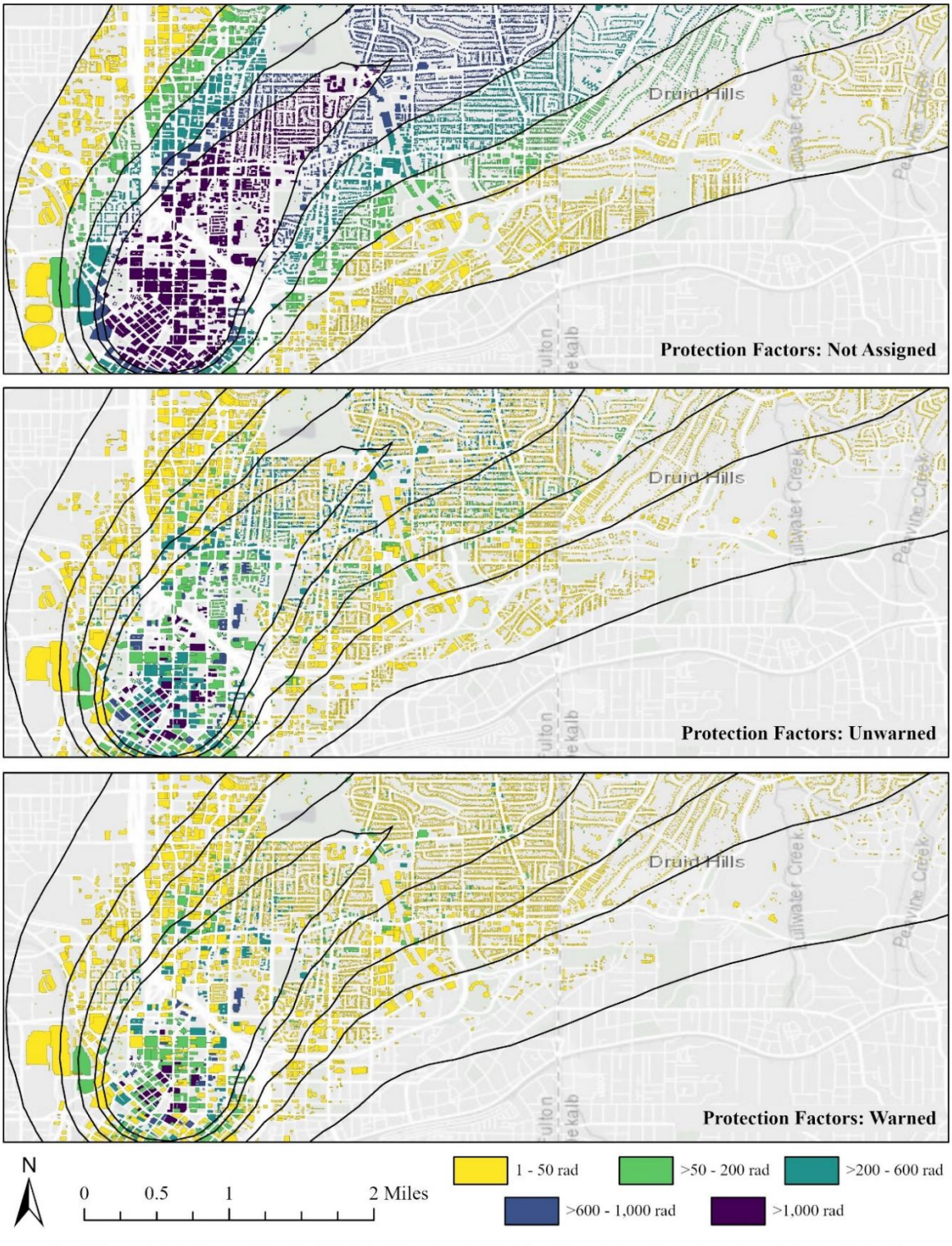

Figure 4.13. Simulated fallout radiation from a 15 kt IND detonation in downtown Atlanta on November 26, 2019 (Medoid 2), under the following conditions: PFs were not assigned; unwarned PFs were assigned; and warned PFs were assigned. The isolines from the contours represent the fallout radiation ranges with no PFs considered.

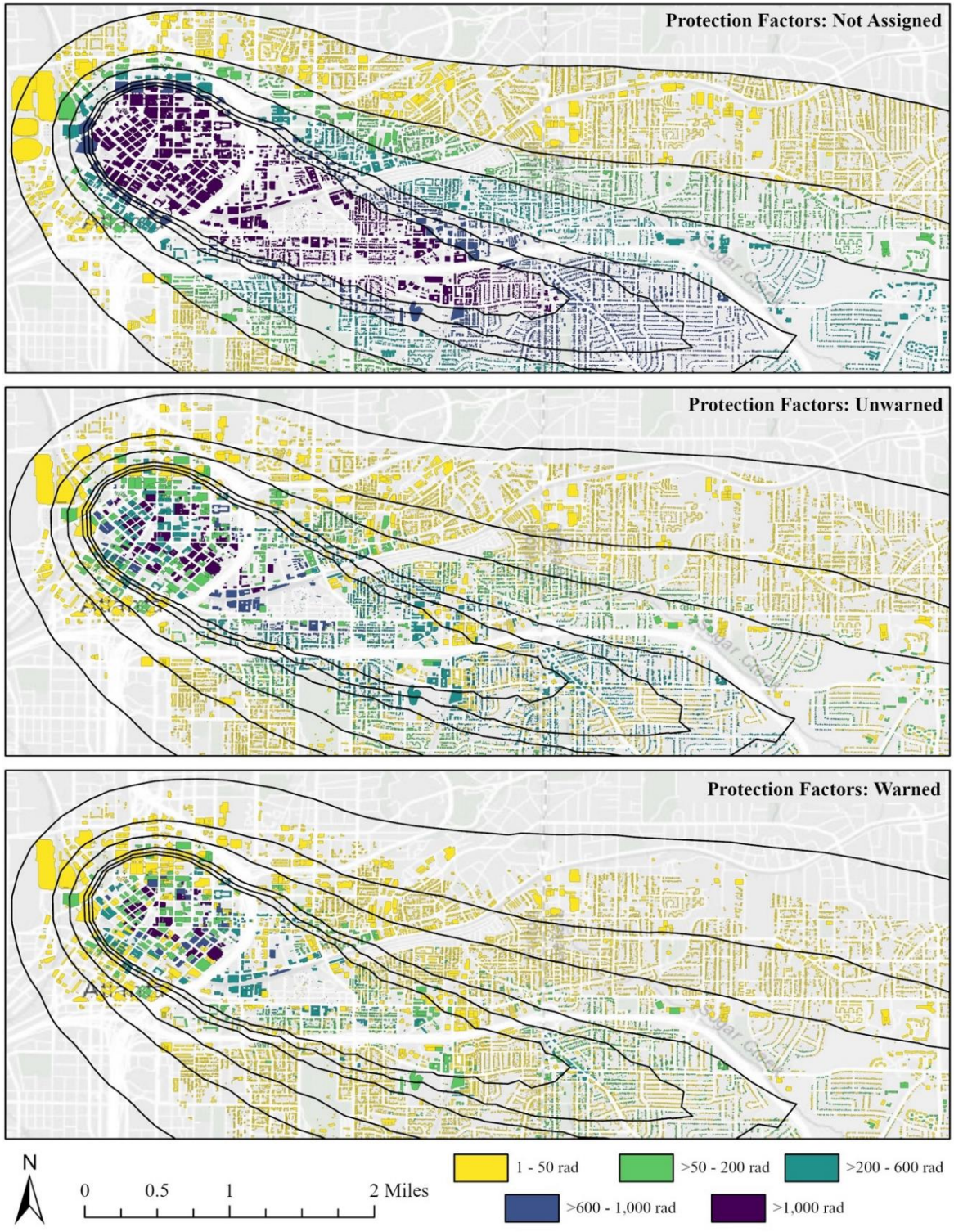

Figure 4.14. Simulated fallout radiation from a 15 kt IND detonation in downtown Atlanta on November 25, 2019 (Medoid 2), under the following conditions: PFs were not assigned; unwarned PFs were assigned; and warned PFs were assigned. The isolines from the contours represent the fallout radiation ranges with no PFs considered.

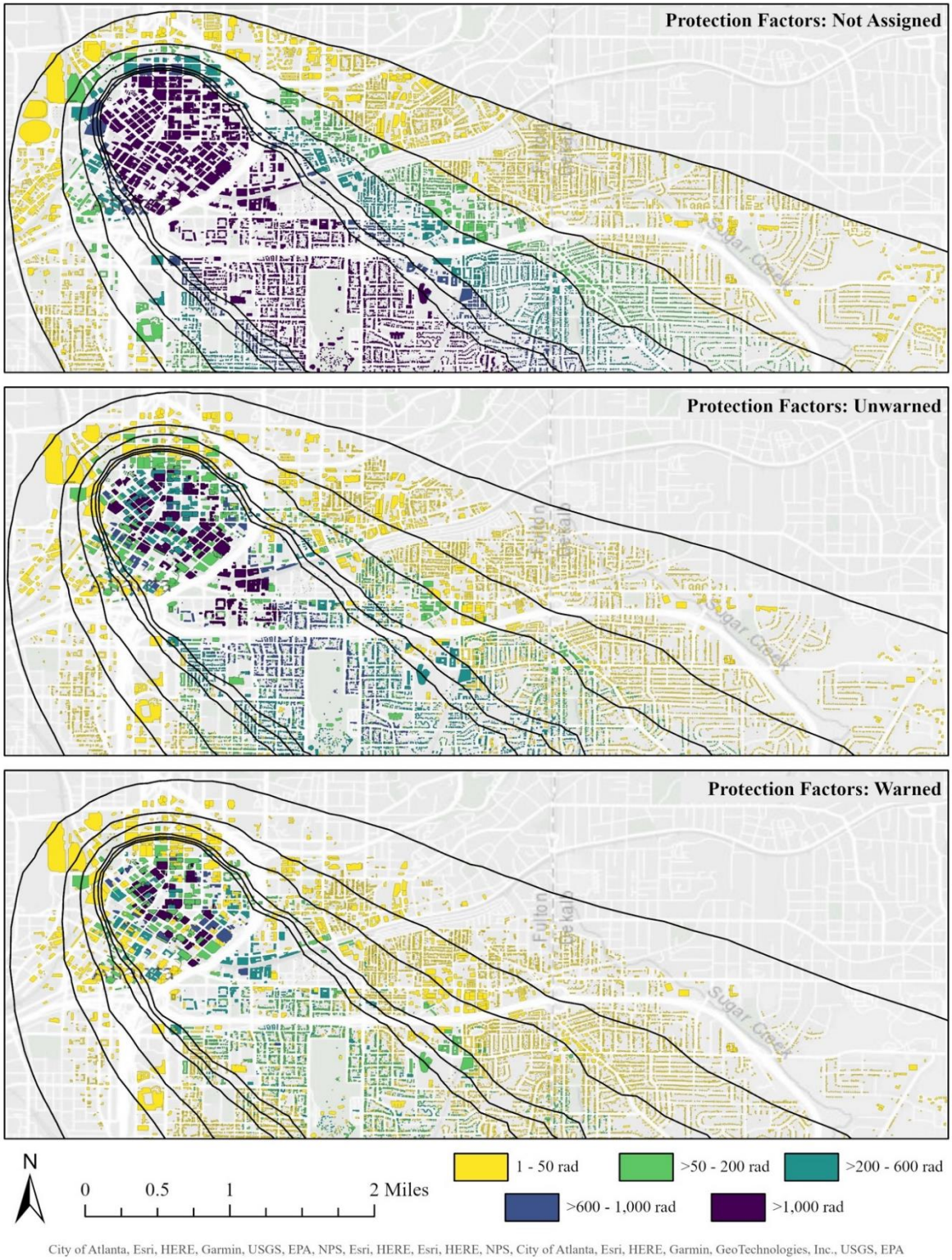

Figure 4.15. Simulated fallout radiation from a 15 kt IND detonation in downtown Atlanta on July 2, 2019 (Medoid 3), under the following conditions: PFs were not assigned; unwarned PFs were assigned; and warned PFs were assigned. The isolines from the contours represent the fallout radiation ranges with no PFs considered.

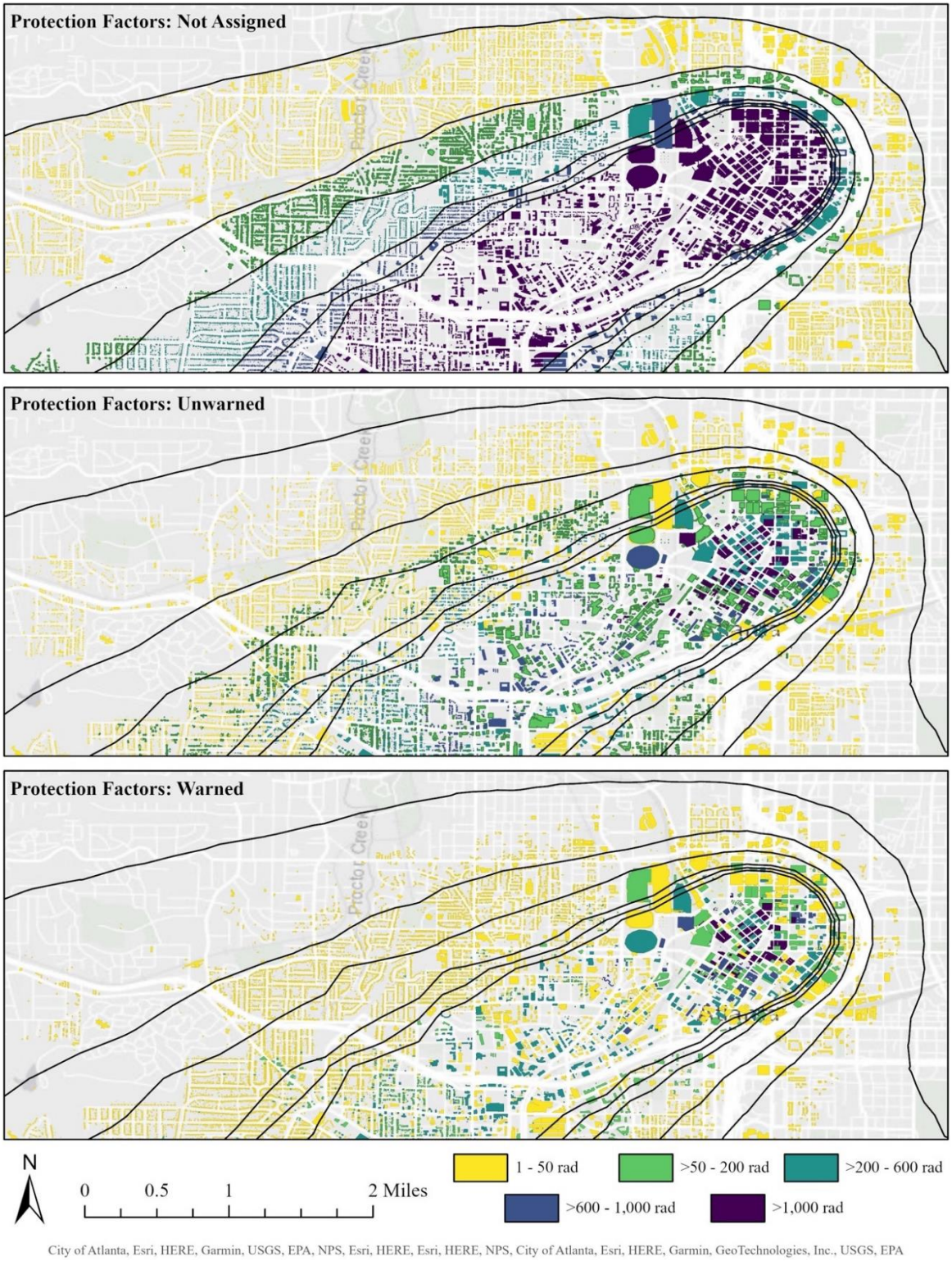

Figure 4.16. Simulated fallout radiation from a 15 kt IND detonation in downtown Atlanta on August 19, 2019 (Medoid 4), under the following conditions: PFs were not assigned; unwarned PFs were assigned; and warned PFs were assigned. The isolines from the contours represent the fallout radiation ranges with no PFs considered.

When considering the fallout PFs in the context of evacuation and shelter-in-place guidance, the number of buildings that would be required to evacuate varied across medoids. Approximately half (51%) of the buildings in Medoids 1 and 4 that were included in the evacuation region when no PFs were considered fell under the protective actions (i.e., evacuation or shelter-in-place) threshold when PFs associated with the unwarned scenario were considered. Medoid 2 had the smallest percent of buildings (39%) of buildings that were reduced from required evacuation to protective actions under the unwarned scenario.

The warned scenario had the greatest impact on Medoid 1, where 80% of the buildings that were included in the evacuation region when no PFs were considered fell under the protective actions threshold when PFs associated with the warned scenario were considered. Similarly, nearly three-quarters (72%) of the buildings that were included in the evacuation region when no PFs were considered fell under the protective actions threshold under the warned scenario. The smallest reduction in buildings under the evacuation region occurred in Medoids 2 (62%) and 3 (60%) under the warned scenario. As these reductions are on the tens to hundreds of thousand orders of magnitude, these reductions have tremendous implications for evacuation and shelter-in-place guidelines.

4.4. Discussion

This study introduced the integration of building-specific architectural attributes to account for the protection offered by buildings from prompt and fallout radiation as well as the for the attenuation of the thermal effects released by the fireball following an IND detonation. The results of this adaptation of the modeling workflow highlight the importance of building-specific characterizations. Under the thermal attenuation model, approximately half of the buildings that would have previously been assumed to have been exposed to enough thermal

fluence to cause either burns or mass fires were shadowed by the surrounding environment and therefore were no longer exposed to such levels of thermal radiation. This suggests the thermal effects in an urban environment can neither be assumed to be uniform nor be ignored in comprehensive nuclear models, as has been done in prior studies and federal guidance documents.[7,8,16,17,37,73,120] Even with the thermal attenuation model, more than 30,000 buildings would be exposed to enough thermal fluence to cause at least 50% probability of second or third degree burns, more than a quarter of which would likely receive enough thermal fluence for the occurrence of mass fires. Such effects would easily overwhelm the existing firefighting and burn health care resources,[19] further emphasizing the need for preparedness efforts among the emergency management, health care, and public health communities.

This study also improved upon the existing RSA methodology[34] for PFs by incorporating building-specific PF estimates for both fallout and prompt radiation. The introduction of building-by-building evaluation of protection factors further highlighted the importance of preparedness measures by showing the efficacy of sheltering from radiation. In all four simulations under a warned scenario, more than 90% of buildings exposed to more than 200 rads of fallout radiation over 48 hours actually received less than 200 rads inside the buildings. While some argue that any warning is unlikely to be feasible in such a scenario,[272] even the unwarned PFs demonstrated significant reductions in radiation dose. In three of the four simulations under an unwarned scenario, more than 90% of buildings that were exposed to more than 600 rads of fallout radiation after 48 hours actually received less than 600 rads inside the buildings. These results emphasize the need for widespread public education and preparedness efforts, in line with the “Get Inside, Stay Inside, Stay Tuned” awareness campaign.[273]

Under the EPA PAG recommendations[266] and across the simulated dates in this study, between 38,175 and 101,189 buildings would need to be evacuated, depending on the whether or not the population was warned and able to seek the most interior room of the building. Such a no-notice evacuation incident would likely be impossible given the large range of the affected area. In 2014, Atlanta experienced a near no-notice evacuation when snow suddenly began to fall on a Tuesday afternoon and all schools and employers closed nearly simultaneously.[274] When the commuters in the Atlanta area tried to leave simultaneously, the roads were jammed for more than 24 hours in deteriorating conditions.[274] The event, known colloquially as "snowpocalypse," demonstrated that the Atlanta metropolitan area cannot evacuate simultaneously, even when all of the roads are open and functional. In the aftermath of a nuclear detonation, where significant proportion of roads would be impassible, due to the damage from the immediate effects or the risk of fallout plumes, wide-spread evacuation would be significantly more difficult. Therefore, to better support emergency management planners, future studies should examine plausible shelter-in-place and evacuation strategies.

As with any complex model for an unprecedented incident, there are many sources of uncertainty in the input parameters and inherent limitations in the various models included in this analysis. The sources of uncertainty in the existing workflow from the HPAC model and the thermal ignition probability model, as well as the relevant validation and verification processes, have been carefully elucidated by others.[16,17] The most notable limitation of this study is the degree of uncertainty in the input parameters. Data that informs the nuclear detonation effects is based on the detonations in Hiroshima and Nagasaki, in addition to the nuclear tests conducted by the US until 1992. As of March 2023, no nuclear weapon has been detonated in a near-surface burst in a modern urban environment. Moreover, the exact evaluation of PFs remains an active

debate in the nuclear modeling community. Most notably, the PFs included in this study assume a uniform deposition of radioactive particles and are calculated for a gamma ray energy of 1 MeV. However, radiation varies by isotope and time, as the radiation energy (and therefore the degree to which radiation can penetrate a building) depends on the type and amount of radioactive isotopes present.[257] The unclassified workflow of HPAC prohibits the explicit designation of isotopes included in the detonation, so this study was unable to further specify the PFs beyond the assumption of a gamma ray energy of 1 MeV. Further experiments should be conducted to validate the PFs and sensitivity analyses should be conducted to better understand the health implications of minor perturbations in PF estimates. Given the resolution of the model, this study was also unable to account for minor variations in fallout distribution, such as a higher accumulation on window sills or leaves and branches, as some argue would occur in a real-world detonation.[58] However, future studies should consider the PFs of vehicles as well as the variation of PFs within a building and perhaps apply the RSA methodology to a building-level resolution to estimate distribution within a building. On a broader level, the warned PFs assume members of the public know how to shelter-in-place appropriately for a nuclear detonation and will comply with such recommendations. While the latter is more difficult to characterize, future studies should focus on the former and identify ways in which the public might engage with preparedness for such a rare incident.

The accuracy of thermal prediction models also remains highly contested and debated, particularly with regard to mass fires.[8,9,16,35,45,64] Relevant to this study, prior sensitivity analyses have been conducted to estimate the importance of each variable in the thermal ignition probability model.[16,45] The thermal attenuation model produces its own potential sources of error, particularly with the assumed general building materials and facades and their role in thermal

fluence reflection. Future studies should explore developing more accurate 3D models for the city of interest, to account for any particularly unique architectural features. Future studies should also consider the thermal protection offered by buildings once the data becomes available. Currently, only data for US military structures and vehicles are available to quantify the thermal protection offered by structures. Ultimately, however, the new additions to the modeling workflow in this study, including building-specific PFs and attenuation of the thermal effect, introduce a previously unobtainable level of accuracy for the thermal and radiation effects in an urban environment.

In conclusion, this study developed a methodological framework for improving the accuracy of models for the thermal and radiation effects of nuclear detonation in an urban environment. The introduction of building-specific architectural attributes to account for the protection offered by buildings from prompt and fallout radiation as well as the for the attenuation of the thermal effects released by the fireball highlight the role shelters play in health outcomes. Future studies should incorporate this framework into casualty estimates, as improving the methodology to estimate these effects will allow for an increased accuracy, which will subsequently better support emergency management agencies in their preparedness efforts for nuclear disasters.

CHAPTER 5

POPULATION-LEVEL HEALTH CARE CONSIDERATIONS FOR CASUALTY ESTIMATES AND SCARCITY OF HEALTH RESOURCES IN THE AFTERMATH OF A NUCLEAR DETONATION

5.1. Introduction

5.1.1. Background

On August 6th and 9th, 1945 the United States (US) nuclear weapons used on Hiroshima and Nagasaki in Japan,[1] causing an estimated 200,000 casualties, with approximately 105,000 fatalities and 95,000 injuries.[2] The dual bombings gave the world a glimpse of the devastating and expansive effects of this new warfare strategy, and a global arms race that has lasted decades immediately followed. Officials are now sounding the alarm that the world may be entering another arms race.[3] Despite the increasing risk of a nuclear attack on the US, most organizations, but especially local and state agencies, remain largely unprepared for a nuclear disaster.[4–6]

5.1.2. Nuclear Weapon Effects and Impacts

The detonation of a nuclear device has three primary effects (blast, thermal, and radiation) impacting the environment and people. The blast effect is responsible for devastating infrastructure destruction.[64] Like any other explosion, the rapidly expanding fireball is the origin point of the blast, generating a pressure wave extending in all directions.[8,64] The amount of light and heat generated by the explosion creates the secondary effect of a nuclear explosion, known as thermal radiation or heat.[8,9,64] Measured by the thermal fluence, or energy, deposited onto exposed surfaces,[9] thermal radiation causes burns to people, ignites flammable materials, and

even causes mass fires.[8] Finally, the third major effect of a nuclear explosion is the radiation, which is categorized as prompt and fallout radiation.[7,8,64] As the name suggests, prompt radiation occurs nearly instantaneously with the flash due to neutron activation.[64] Fallout radiation, alternatively, is created by the products of the fission process, known as radionuclides, which then attach to various airborne particles and eventually "fall out" of the sky.[64,65] Activation products, which are atoms of structural materials from the device itself or surrounding environment that absorb released neutrons from the detonation, further contribute to fallout radiation.[11] Accurate characterization of these effects through consideration of both amplification and attenuation factors is a crucial step in establishing effective preparedness measures.

Each of the effects described above has the potential to individually cause devastating impacts, but when considered cumulatively, the impacts become catastrophic. Within the immediate area surrounding the detonation, few, if any, survivors and buildings are expected to remain.[8] The rubble in the streets would be impassable, and extremely high radiation levels would be present, increasing risk for any rescue efforts.[73] Extending outward from the site of detonation, the number of buildings destroyed would decrease, and the preponderance of structural damage would be with utility infrastructure damage, overturned cars, collapsed roofs, and fires.[8,9,64] However, this is the region of greatest opportunity for rescue efforts as radiation levels would be safe for rescuers with the appropriate personal protective equipment, dosimetry equipment, and standard operating procedures (SOPs).[8] In particular, SOPs should ensure the responders are aware of and implement time, distance, and shielding principles.[12] Following this region is the end of the visible damage after a detonation, mostly characterized by broken glass or blown out windows or doors.[8,64] Fallout radiation will extend well beyond this visible region of damage, carried by the upper atmospheric winds. The wide geographic footprint of these

cumulative effects will cross traditional jurisdictions, and they will have rippling effects beyond the immediate destruction.

5.1.3. US Health Care Impacts from a Nuclear Detonation

Evidence suggests that the US health care system would not be able to handle a disaster on the scale of a nuclear device detonation.[17,126,128,132] Gale and Armitage[13] go so far as to argue existing medical preparedness efforts are "obviously useless" in the context of a nuclear device detonation. As of 2008, almost one third of the US population lives in counties where the number of staffed and unoccupied health care facility beds would be inadequate for a typical mass casualty event.[14] The closure of community hospitals as a consequence of the COVID-19 pandemic, confounded by pre-existing economic strains, suggests that this percentage has likely increased over time,[15] and the scale of a nuclear detonation would increase that fraction. Sauer and Thakur[127] determined that "no society can ever be prepared for such a scenario" when analyzing the number of intensive care beds required in the aftermath of a nuclear detonation. It is worth noting the smallest weapon considered in their analysis had a yield of 45 kt.[127] Dallas et al.[16] estimated that a 15 kt weapon detonated on Beer Sheva, Israel would cause over 105,000 total fatalities, which is almost 50% of the population, and another 35,000 injuries. Bell and Dallas[132] further broke down casualty estimates by injury type for a 20 kt weapon in four major cities across the US. In Atlanta, Georgia, they estimated that such a detonation would cause between 46,000 and 160,000 fatalities from fallout radiation alone,[17] a population size comparable to a large sports stadium. In their model, the blast effect would cause approximately 2,000 fatalities and another 28,000 individuals would be vulnerable to injuries resulting from collapsing structures and debris.[17,74] An estimated 5,000 people were predicted to reside in the region associated with full-thickness thermal burns, and another 8,500 people would be found in

the region associated with partial-thickness thermal burns.[17] While the fallout radiation potentially contributes to the greatest number of initial fatalities, the volume of thermal burn patients will overwhelm the existing burn care infrastructure in the US and subsequently increase the percentage of fatalities due to the thermal effects.

Within the US health care system, burn center criteria indicate that patients with significant burns or compounding injuries should be treated at a burn center with a specialized care team.[18] However, across the entire country, there are approximately 300 burn surgeons whose teams cover approximately 2,000 burn beds.[19] Further, the average burn center in the US has just 15 beds,[19,151] and recent research suggests burn centers operate at 95% capacity on average.[154] Therefore, a typical burn center has, on average, 0.75 beds available for incoming patients. Even if the burn center implements their surge plan and expands their bed capacity by a factor of 1.5,[86] a typical burn center may only be able to take eight patients before becoming overwhelmed. Incidents with multiple burn injuries often present with more than eight patients, so burn centers in other states would be called upon to treat additional patients. However, at any given moment in the US, there are approximately 90 available burn beds across the entire country on average.[154] The bed capacity challenges described above for an individual burn center also apply to the entire burn care system in the US. Even if every burn center in the US could increase their bed capacity by a factor of 1.5 in a no-notice event, there would only be 3,000 burn beds total. Within Bell and Dallas' model of an Atlanta detonation,[17] this leaves an estimated 11,500 individuals who would need care at a burn center but would lack access.

Beyond the burn care capacity, a disaster of such scope would incapacitate the Georgia health care system. A recent analysis[20] suggests that in a no-notice event (such as a nuclear detonation), the Atlanta-area hospitals could treat 499 adult patients and 96 pediatric patients

total. Of these patients, the system can only treat 55 adult and eight pediatric critical patients.[20] Furthermore, according to the American Hospital Directory,[21] 17 of the state's 113 non-federal, acute-care, short-term hospitals are in Atlanta, Georgia, comprising 30% of the staffed beds available in the state. In the event of a nuclear detonation in Atlanta, few if any of these facilities would escape destruction and be available to treat patients, leaving only 70% of the state's typical operating volume responsible for handling the possible tens of thousands of patients. Moreover, when Harris et al.[22] conducted a chemical release exercise with Atlanta-area hospitals, the researchers received significant pressure to modify the scenario in such a way to lower the severity and magnitude of the simulated event. This experience suggests that health care providers are unprepared to respond to a severe chemical disaster, let alone a larger and more catastrophic nuclear disaster. Therefore, there exists a significant area of opportunity to inform local and state organizations about the estimated impacts of a nuclear device detonation and provide them with assistance in increasing preparedness for such an incident.

5.1.4. Study Objective

Increasing the accuracy of casualty estimates in nuclear simulations will better support local and state agencies in their plan development. A dearth of real-world data causes modeling limitations; however, adjusting the methodology for estimating the thermal and radiation effects in addition to choosing representative weather conditions allows for an increased accuracy in casualty estimates. As such, the primary objective of this study is to leverage the improved modeling framework described in Chapter 4 to realistically characterize the estimated casualties in the aftermath of an improvised nuclear device (IND) detonation in Atlanta, Georgia (GA). This study also aimed to understand the health care capacity in GA to respond to such an incident.

5.2. Materials & Methods

5.2.1. Study Area & Time Period

This study focuses on a simulated IND detonation at 10:00 am local time on four days in 2019 in Atlanta, Georgia (GA). The four days for this study (Table 4.1) are the four medoids identified in the cluster analysis described in Chapter 3: November 26 (Medoid 1), November 25 (Medoid 2), July 2 (Medoid 3), and August 19 (Medoid 4). Atlanta was chosen as the site of the simulated nuclear detonation for numerous reasons, including its moderate climate,[36] population and size of a typical major city,[42,43] and plausibility as a target.[38,40,41] Moreover, the health care resources in the state of GA are an average representation of all states in the US. According to an analysis conducted by the Kaiser Family Foundation,[44] the US averaged 2.40 total hospital beds per 1,000 people in 2019. In that same analysis, the state of GA averaged 2.34 total hospital beds per 1,000 people and was the closest state to the national average.[44] The combination of these factors makes Atlanta an ideal sample location to consider the population-level health care impacts in the aftermath of an IND detonation.

5.2.2. Nuclear Detonation Simulation

A simulated 15 kiloton (kt) tactical nuclear weapon was detonated at 40 meters (m) in downtown Atlanta, GA at 10:00 am local time on each of the four chosen days, using the methodology described in Chapter 4 (Section 4.2), with one modification for population estimates. The population data was captured via the Oak Ridge National Laboratory's (ORNL's) LandScan USA 2019 dataset.[184] LandScan USA uses a daysmetric population distribution model to estimate nighttime and daytime population data at 3 arc-second (~90m) resolution.[184] Under the daysymetric method, the model combines high resolution imagery, transportation infrastructure, lidar and automated building extractions, and parcels to refine census block-level

data.[184] It also includes cultural attractions, academic institutions, prisons, shopping malls, and other commercial areas.[184]

However, LandScan USA is a raster dataset, and the documentation suggests careful consideration must be taken prior to converting it to a vector dataset, due to the methodology behind its development.[276] After consulting with the developers of LandScan USA,[277] this study followed their proposed vector analytical framework for population modeling.[278] Because LandScan USA uses a building-based population model, the population within each grid of the raster was assigned to the buildings within that grid, based on the proportional building footprint for all buildings in the raster cell. Additionally, 10% of the entire building population was estimated to be outside, based on prior studies.[279] This population modeling was conducted during the building data integration step in Figure 4.1.

5.2.3. Health Effects Thresholds

5.2.3.1. Blast Effects

The full impact of the blast effect in a modern city is currently unknown, but the thresholds utilized in this study (Table 5.1) were informed by various models and guidance documents.[16,64,65,73,78,120,280] Even though dynamic pressure contributes to the blast effect, these thresholds are typically quantified by the overpressure alone, in pounds per square inch (psi).[7,64,65] While there is evidence to suggest that the severe damage zone would begin closer to 5.0 psi, rather than 8.0 psi,[7,8,64] the designation of the damage zones is derived from Federal Emergency Management Agency (FEMA) documentation and guidance.[280] The estimated probabilities for fatality, survival, surviving with an injury, and surviving without an injury are derived from prior publicly available nuclear detonation models estimating human casualties.[7,16]

Connecting the blast injuries to the physical characteristics of the explosion is challenging as injury correlates are confined to animal models.[64] Injuries seen in conflicts or terrorism incidents are used to supplement the results from animal models, but the existing literature cannot precisely establish the physical characteristics of these incidents to confirm specific thresholds.[35] The categories of traumatic injury and associated thresholds are derived from both the overpressure and dynamic pressure effects on the human body.[64,78] In the absence of additional trauma, the human body is relatively resilient to overpressure-induced primary blast injuries, as the minimum threshold for lung damage is 12.0 psi,[8,64,79] and the most vulnerable organ to pressure, the tympanic membrane, requires a minimum of 5.0 psi to rupture.[64] However, overpressure does not occur in a vacuum, which is why the dynamic pressure must be considered when estimating the blast effect on the human body. The strong winds resulting from the dynamic pressure cause the secondary and tertiary blast effects, which additionally further explains increased incidence of secondary and tertiary blast effects in the aftermath of an explosion.[64,77,78]

5.2.3.2. Thermal Effects

Thermal radiation emitted by a nuclear detonation causes burn injuries either through flash burns from the thermal radiation energy or from secondary fires ignited by the burst or mass fire phenomenon.[8,9,58,64] Similar to the blast effect, connecting the thermal injuries to the physical characteristics of a nuclear explosion is challenging and is rarely fully discussed in the literature. Table 5.2 provides thresholds of thermal fluence required to create each burn depth category for a 15kt nuclear detonation.[64] Burn depth is classified into three primary categories: superficial, partial thickness, and full thickness.[81,82] Superficial burns, also known as as 1st degree burns, involve only the epidermis of the skin.[84,85] On average, superficial burns heal

without scarring and minimal medical attention within 5 to 10 days.[81,86] Partial thickness burns, also known as 2nd degree burns, penetrate the epidermis and involve part of the dermis.[81,83,85] There are two types of 2nd degree burns: superficial partial-thickness and deep partial-thickness. Superficial partial-thickness burns involve only the superficial dermis.[86] The pain associated with superficial partial-thickness burns is severe and healing typically occurs within three weeks with minimal scarring and moderate medical attention.[81,83,86] Deep partial-thickness burns penetrate deeper into the dermis.[81,84] The pain associated with deep partial-thickness burns is minimal due to decreased sensation, and healing typically occurs within three to eight weeks with scarring present and medical intervention.[81,83,84,86] For the purposes of this study, 2nd degree burns were not differentiated between superficial partial-thickness and deep partial-thickness, due to a lack of available data in relation to the associated thermal fluence to cause each type of 2nd degree burn. Lastly, full thickness burns, also known as 3rd degree burns, involve the entirety of skin and subcutaneous structures.[84,86] The pain associated with a full thickness burn is likely nonexistent and healing requires significant medical care, including surgical intervention.[81,86] The risk of mass fires was also considered, based on the significant research into the mass fire phenomenon.[9,16,35,45]

5.2.3.3. Radiation Effects

The syndrome that causes mortality from acute radiation exposure, ARS, is characterized by the development of a group of signs and symptoms that are manifestations of damage to tissues and organs by ionizing radiation.[102,104] However, individuals exposed to radiation will only develop ARS if the following four conditions are met: 1) the radiation dose was high, 2) the radiation was penetrating (i.e., only X-rays or gamma-rays), 3) the individual's entire body received the dose, and 4) the radiation was received over a short period of time.[99,102] The

syndrome has four stages: prodromal, latent, manifest illness, and recovery or death.[104,105] The prodromal phase, which lasts up to the first 48 hours after exposure, results as the immediate effect of cell membrane damage.[104,105] In this phase, patients present with anorexia, nausea, vomiting, lymphopenia, diarrhea, fever, and granulocytosis.[104,105] As the patient transitions to the latent phases, which lasts between hours and 21 days, the prodromata becomes absent or diminished.[104,105] The manifest illness phase, which is the most critical phase, can begin just hours after exposure or can present up to 30 days after exposure.[104,105] In this phase, there are four subsyndromes of ARS that vary with dose and host factors: hematopoietic, gastrointestinal, cutaneous, and neurovascular.[104,105] Table 5.3 summarizes the estimated absorbed ionizing radiation dose thresholds for each subsyndrome.[105] It is important to note that Cutaneous Radiation Syndrome (CRS) can also result from exposure of skin to beta-radiation, causing beta burns.[105,106] Unlike ARS that results from the highly penetrating gamma-radiation, beta burns are rarely deeper than the skin, due to the reduced penetrating power of beta-radiation.[106] However, presentation of beta burns worsens prognosis for patients also presenting with ARS.[104–106] Mortality from acute radiation exposure via ARS is tightly associated with whole-body dose and presentation of acute symptoms, as also described in Table 5.3. The probability of vomiting within four hours of exposure was used as a proxy for acute radiation injury, in alignment with other publications.[102,103,280] The probability of fatality and survival from acute radiation exposure was based on data from the Hiroshima bombing in 1945,[186] further supplemented by additional guidance from the CDC's toxicological profile for ionizing radiation.[187]

5.2.3.4. Triage Category Designations

Given the indications that the health care system will be overwhelmed, it will be imperative to transition to population-level patient care by employing disaster triage practices. Coming from

Table 5.1. Blast effect thresholds for human health impacts.[16,64,78,280] Abbreviations: psi = pounds per square inch.

Overpressure (psi)	Damage Zone	Probability of Fatality	Probability of Survival	Probability of Surviving with Injury	Probability of Surviving with No Injury	Trauma Category
0.5	Light	0%	100%	2%	98%	Minimal
1	Light	0%	100%	5%	95%	Minimal
2	Light	0%	100%	7%	93%	Moderate
3	Moderate	0%	100%	10%	90%	Severe
3.8	Moderate	3%	98%	30%	70%	Severe
4.9	Moderate	5%	95%	35%	65%	Severe
5	Moderate	5%	95%	35%	65%	Severe
7.1	Moderate	10%	90%	70%	30%	Severe
8	Severe	10%	90%	70%	30%	Severe
8.1	Severe	50%	50%	85%	15%	Severe
10	Severe	85%	15%	100%	0%	Severe
12	Severe	85%	15%	100%	0%	Severe
17.5	Severe	85%	15%	100%	0%	Severe
25	Severe	85%	15%	100%	0%	Severe
32.5	Severe	85%	15%	100%	0%	Severe

Table 5.2. Thermal effect thresholds for human health impacts.[9,16,35,45,64] Abbreviations: cal = calories; cm = centimeters.

Thermal Fluence (cal/cm^2)	Thermal Effect	Probability
1.40	No Burn	82%
1.40	1st Degree Burns	18%
2.40	1st Degree Burns	50%
3.53	1st Degree Burns	82%
3.53	2nd Degree Burns	18%
4.77	2nd Degree Burns	50%
6.00	2nd Degree Burns	82%
6.00	3rd Degree Burns	18%
7.37	3rd Degree Burns	50%
8.67	3rd Degree Burns	82%
10.00	Mass Fires Likely	10 - 50%
12.00	Mass Fires Probable	>50%
23.00	Mass Fires Highly Probable	>90%

Table 5.3. Radiation effect thresholds for human health impacts.[102–104,186,187] Abbreviations: ARS = Acute Radiation Sickness; S = Subclinical; H = Hematopoietic; HGC = Hematopoietic/Gastrointestinal/Cutaneous; HGCN = Hematopoietic/Gastrointestinal/Cutaneous/ Neurovascular.

Radiation Dose (rad)	ARS Subsyndrome(s)	Probability of Fatality	Probability of Survival	Probability of Vomiting
0 to <50	S	0%	100%	0%
≥50 to <100	S	9%	91%	0%
≥100 to <200	S	34%	66%	19%
≥200 to <300	H	46%	54%	35%
≥300 to <400	H	68%	32%	54%
≥400 to <500	H	63%	37%	72%
≥500 to <600	H	67%	34%	86%
≥600 to <700	HGC	81%	19%	94%
≥700 to <800	HGC	90%	10%	98%
≥800 to <900	HGC	90%	10%	99%
≥900 to <1000	HGC	90%	10%	100%
≥1000	HGCN	100%	0%	100%

the French word “trier,” meaning “to sort,” a health care provider triages potential patients by using an established system or plan to determine a treatment priority for each patient.[162] Regardless of the specific algorithm, there are typically four possible disaster triage categories: minimal, delayed, immediate, and expectant.[281–285] Assigned the color green, the minimal category includes patients who have injuries that would require minor or no medical intervention and who are expected to survive with or without care.[281–285] Assigned the color yellow, the delayed category includes patients who have serious injuries that require medical care but that care can be delayed without increasing mortality.[281–285] Assigned the color red, the immediate category includes patients that have immediate life-threatening problems but also have high potential for survival.[281–285] Lastly, assigned the color black, expectant patients are unlikely to survive given the available health care resources.[281–285] In order of priority, immediate patients are transported and treated first, followed by delayed and then minimal patients, with comfort care and treatment provided to expectant patients as resources allow following treatment of all other patients.[281–285]

Historically, triage systems are tailored to trauma etiologies, as the preponderance of mass casualty care is derived from military experiences.[163,164] Therefore, for the purposes of this study, the designation of triage categories was based on the triage algorithm specifically developed for the Radiation Triage, Treat, and Transport System (RTR).[281] Adapted by federal guidance,[280] the RTR triage algorithm assigns the four triage categories based on radiation dose, combined injury severity, and resource availability.[281] The absorbed radiation dose categories are: <50 rad; ≥50 rad to <200 rad; ≥200 rad to <600 rad; ≥600 rad to <1,000 rad; and ≥1,000 rad.[281] The injury severity is primarily based on trauma, designated as minimal, moderate, or severe.[281] However, if the burn covers more than 20% of the patient’s total body surface area

(TBSA), the triage category drops one to two levels, lowering the priority of the patient.[281] Based on work to characterize burn injury severity profiles for North Atlantic Treaty Organization (NATO) resources,[275,286,287] this study assumed the severity of a second or third degree burn covering ≥5% TBSA is comparable to ≥20% TBSA within the context of required health care resources and likelihood of survival. Within the modeling workflow for this study, the qualifying burn injury for the RTR triage algorithm included those who were burned with ≥4.77 cal/cm^2. Based on the guidance included in the RTR triage algorithm[281] and indications the health care system would be overwhelmed,[17,19,132] this study used the RTR triage categories associated with poor resource availability and crisis standards of care.

5.2.4. Georgia Hospital Data

While a nuclear detonation would eventually necessitate a response from all levels of the government, federal planning documents suggest full support may not arrive until 48 to 72 hours post detonation.[280] Therefore, this study focuses on the first 48 hours post-detonation and the health care resources that would be available on the local and state levels. To assess health care resource availability in GA, data regarding staffed bed capacity and availability for emergency department, critical care, and general beds were collected daily from April 7, 2020 to April 19, 2021 for 138 hospitals across the state. A map of these facilities and their associated health care coalitions can be found in Appendix E. These coalitions are groups of health care organizations, public safety, and public health partners within a geographic region that work together to prepare health care systems to respond to emergencies and disasters, ultimately increasing local and regional resilience.[288] The fourteen coalitions in GA are designed to facilitate planning, communication, and coordination at the local level, so that all resources are exhausted before calling upon regional, state, and/or federal partners.[289] Because staffed bed capacities and

availabilities change daily, a seven-day average capacity and availability was calculated for inclusion in this study. To avoid confounding with the COVID-19 pandemic, the seven day period of April 7, 2020 to April 13, 2020 was used for this calculation, as it had the lowest reported onset of COVID-19 cases and reported hospitalizations during the period of data collection.[290] This time frame also was the closest available data to the time periods of the simulated detonations. The surge capacity was defined as 1.2 times each coalition's capacity, in alignment with the documentation for the medical response and surge exercise (MRSE) that all health care coalitions are required to complete annually.[291]

5.2.5. Software

The nuclear weapon detonation simulation, blast effects, prompt radiation effects, and fallout radiation plumes were generated in HPAC (v6.8).[134] The thermal attenuation model was developed in Blender,[268] using the Blender-OSM[271] and Blender-GIS addons.[268] All spatial data integration and analysis was conducted in ArcGIS Pro (v3.0).[185]

5.3. Results

5.3.1. Overview of Casualty Estimates

A simulated IND with a 15 kt yield was detonated in downtown, Atlanta, GA for four representative days in 2019 (Table 4.1). The spatial distributions of the effects are described and illustrated throughout Chapter 4 (Section 4.3). Table 5.4 provides an overview of the casualty estimates after 48 hours in the "unwarned" scenario, which is the most likely scenario. It assumes the affected population did not have enough warning to seek effective shelter and thus assumes an even distribution of people within each building and 10% of the population remaining outdoors. The casualty estimates for the blast, thermal, and radiation effects included

all individuals who were affected in each category, meaning an individual exposed to all three effects would appear in all three columns in the table.

The blast effects remained relatively consistent across each simulation. While most of the burn injury estimates were also similar, medoid 4 had approximately 6,000 more individuals with 1st degree burns than the other simulations. Radiation fatalities were highest on the simulation dates of medoids 1 and 4, which likely corresponds with the respective increased total population affected. However, the injuries caused by radiation were highest in medoid 1, and the radiation injury estimates in medoid 4 more closely matched the radiation injury estimates in medoids 2 and 3.

Even though radiation affected the largest area, the radiation effects did not always cause the greatest number of casualties. In medoid 1, the thermal effects caused approximately 25,000 more casualties than the radiation effects when 1st degree burns are included. Conversely, as patients with 1st degree burns likely to survive and are unlikely to require health care resources to treat, the radiation effects caused approximately 12,000 more casualties than the thermal effects in medoid 1 when casualties resulting from 1st degree burns are excluded. A similar trend occurs in medoid 4, albeit dampened, as the thermal effects caused approximately 43,000 more casualties than the radiation effects when 1st degree burns are included. When 1st degree burns are excluded from the casualty estimates, the radiation effects caused approximately 2,000 more casualties than the thermal effects. However, in medoids 2 and 3, the thermal effects still cause more casualties than the radiation effects, even when 1st degree burns are not included in the casualty estimates. The thermal effects caused approximately 50,000 more casualties than the radiation effects when 1st degree burns are included and 10,000 more casualties when 1st degree burns are excluded in medoids 2 and 3.

The thermal effects consistently caused more casualties than the blast effect across all simulations. When 1st degree burns were included, the thermal effects caused approximately 45,000 more casualties than the blast effects and approximately 5,000 more casualties than the blast effects when 1st degree burns were excluded. In medoid 1, the radiation effects caused approximately 17,000 more casualties than the blast effect, and in medoid 4, the radiation effects caused approximately 8,500 more casualties than the blast effect. Conversely, in medoids 2 and 3, the blast effect caused approximately 4,500 more casualties than the radiation effects.

Table 5.5 further examines the casualty estimates in each medoid by examining the overlap between the various mechanisms of injury among affected individuals, again within the "unwarned" scenario. Unlike in Table 5.4, each affected individual appears in only one column, corresponding to all the effects by which they were injured. The casualties resulting from the thermal effects include all possible burn severities (1st degree, 2nd degree, and 3rd degree).

The thermal effects were contained within the blast effects and therefore there were no patients with only thermal injuries. Across all four simulations, more casualties were caused by the blast and burn effects with no radiation than the radiation effects alone. A comparable number of casualties were created by only the blast effect and by the combined blast and radiation effects with no thermal effects. Even though the number of casualties resulting from all three effects remained approximately constant across all four simulations, medoid 1 had the greatest number of casualties resulting from only radiation (18,000). The remaining simulations had approximately 10,000 casualties resulting from only radiation effects. Conversely, medoid 1 had the least number of casualties resulting from blast and thermal effects (approximately 19,000), while the remaining simulations had an additional 8-10,000 casualties resulting from

Table 5.4. Overview of casualty estimations after 48 hours, following a 15kt IND in downtown Atlanta, GA at 10:00 am local time. The included radiation injuries only reflect the "unwarned" scenario, which assumes an even distribution of people within each building. Casualty estimates for the blast, thermal, and radiation effects include all individuals who were affected in each category, meaning an individual exposed to all three effects would appear in all three columns in the table.

			Blast		Thermal			Radiation	
Medoid	Date	Population Exposed	Fatalities	Injuries	1st Degree	2nd Degree	3rd Degree	Fatalities	Injuries
1	11/26/2019	1,278,070	106,464	42,515	37,095	15,073	139,041	135,420	30,824
2	11/25/2019	697,731	106,449	42,818	38,618	16,654	138,581	120,365	24,161
3	7/2/2019	678,073	106,461	42,698	37,201	15,853	138,058	120,785	23,890
4	8/19/2019	1,014,526	106,426	43,830	44,968	17,207	139,509	133,239	25,442

Table 5.5. Estimated casualties by each nuclear effect after 48 hours, following a 15kt IND in downtown Atlanta, GA at 10:00 am local time. The included radiation injuries only reflect the "unwarned" scenario, which assumes an even distribution of people within each building. Fatalities and injuries are combined into one estimate. Casualty estimates are based on each possible combination of mechanism(s) of injury, meaning each affected individual appears in only one column, corresponding to all the effects by which they were injured.

Medoid	Date	Population Affected	Thermal Only	Blast & Thermal Only	Radiation Only	Blast & Radiation Only	Blast, Thermal & Radiation
1	11/26/2019	1,278,070	1,346	19,423	18,642	1,645	154,702
2	11/25/2019	697,731	2,814	30,891	10,042	2,522	149,623
3	7/2/2019	678,073	2,827	28,236	9,075	2,098	151,166
4	8/19/2019	1,014,526	3,031	30,184	10,223	3,643	153,614

only blast and thermal effects. Appendices F – N provide additional breakdowns of casualty estimates.

5.3.2. Mass Casualty Management

5.3.2.1. Triage Category Estimates

The RTR triage algorithm was applied to both the unwarned and warned scenarios, the results of which are described in Table 5.6. Figures 5.1 – 5.4 illustrate the spatial distribution of the casualties in the unwarned scenario for each simulation. Across all simulations in the unwarned scenario, approximately 190,000 patients would not be expected to survive their injuries. Approximately 43,000 patients are estimated to require immediate health care, while only approximately 1,000 would be triaged to receive delayed care. Medoid 2 had the fewest minimally injured patients (approximately 435,000), while medoid 1 had the greatest number of minimally injured patients (approximately 1,025,000).

The impact of the warned scenario varied across the simulations. The warned scenario reduced the number of expectant patients by as few as 1,178 (medoid 3) and as many as 8,391 (medoid 4). While the number of expectant patients in medoid 1 only decreased by approximately 1,500 patients, the number of immediate patients decreased by almost 10,000. Medoid 3 had the second largest decrease in immediate patients (7,443), while the number of immediate patients in medoids 2 and 4 only decreased by approximately 1,500 patients. Medoid 1 was the only simulation that had a decrease in delayed patients (1,774), whereas the remaining simulations had an increase in delayed patients. The number of minimally injured patients increased significantly across all simulations, ranging from 17,601 (medoid 2) to 33,531 (medoid 1). This shift in increasing the number of delayed and minimally injured patients while decreasing the number of immediate and expectant patients would have a dramatic effect on the

Table 5.6. Estimated casualties by RTR triage category after 48 hours, following a 15kt IND in downtown Atlanta, GA at 10:00 am local time. The unwarned scenario reflects a uniform distribution of people within each building, while the warned scenario assumes the affected individuals had adequate time to seek shelter within the most interior room of the building.

RTR Triage Category	Medoid 1		Medoid 2		Medoid 3		Medoid 4	
	Unwarned	Warned	Unwarned	Warned	Unwarned	Warned	Unwarned	Warned
Minimal	1,024,915	1,058,446	453,939	471,540	434,671	455,856	754,720	781,308
Delayed	3,563	1,789	76	160	197	233	207	356
Immediate	41,455	31,939	40,998	39,875	43,384	35,941	46,668	44,716
Expectant	187,415	185,896	190,273	186,156	187,221	186,043	196,537	188,146

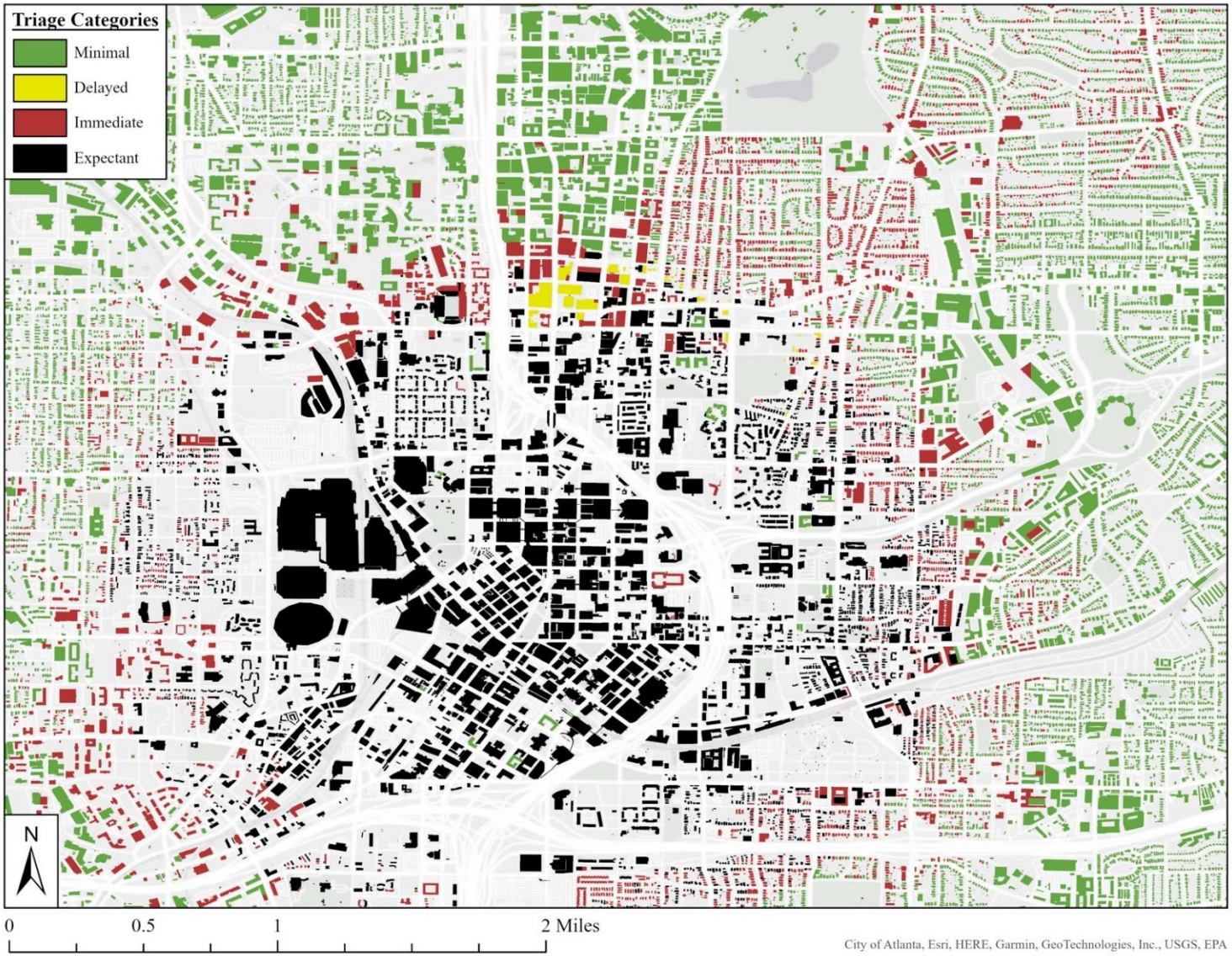

Figure 5.1. Distribution of RTR triage categories in the unwarned scenario after 48 hours, following a 15kt IND in downtown Atlanta, GA at 10:00 am local time on November 26, 2019 (Medoid 1).

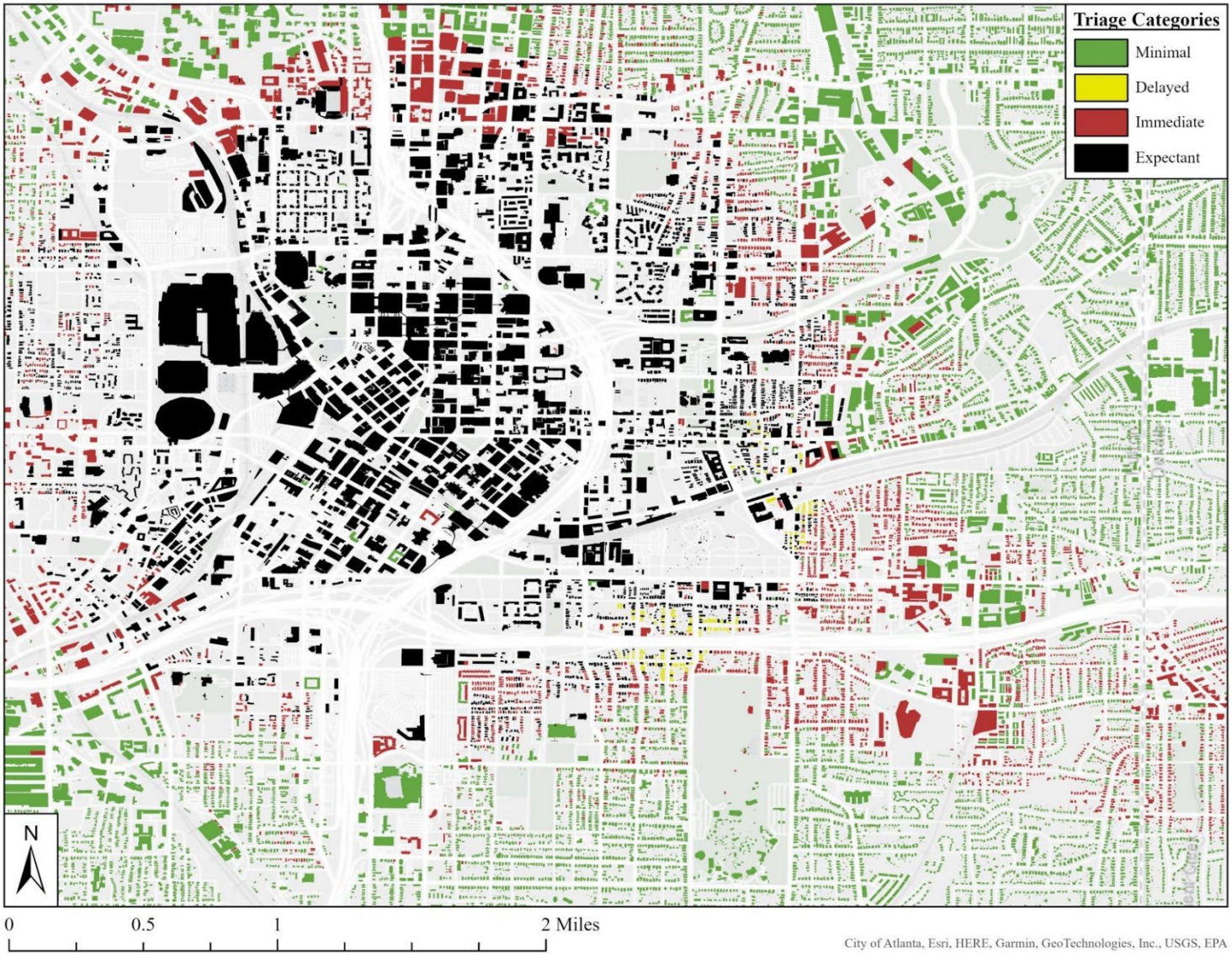

Figure 5.2. Distribution of RTR triage categories in the unwarned scenario after 48 hours, following a 15kt IND in downtown Atlanta, GA at 10:00 am local time on November 25, 2019 (Medoid 2).

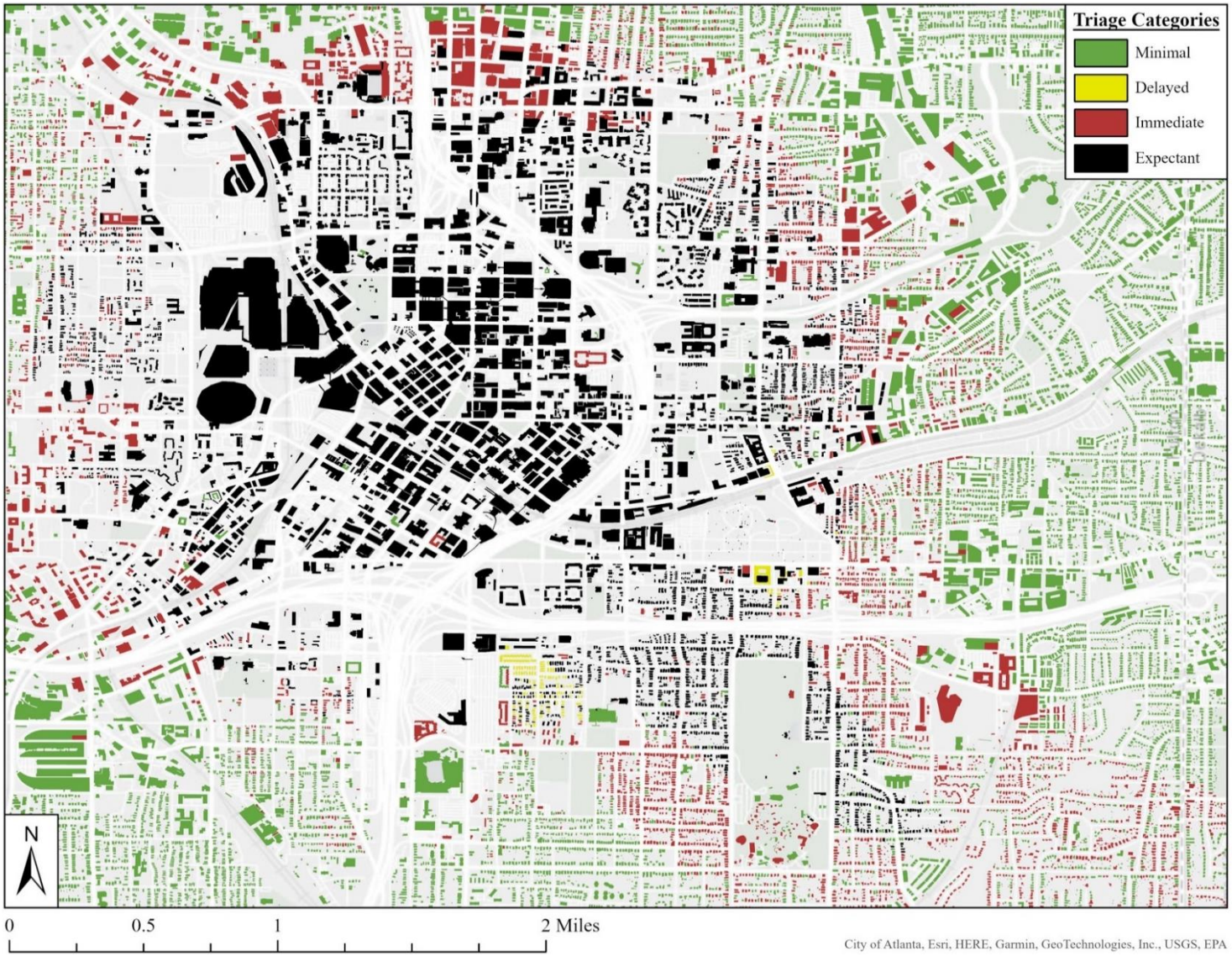

Figure 5.3. Distribution of RTR triage categories in the unwarned scenario after 48 hours, following a 15kt IND in downtown Atlanta, GA at 10:00 am local time on July 2, 2019 (Medoid 3).

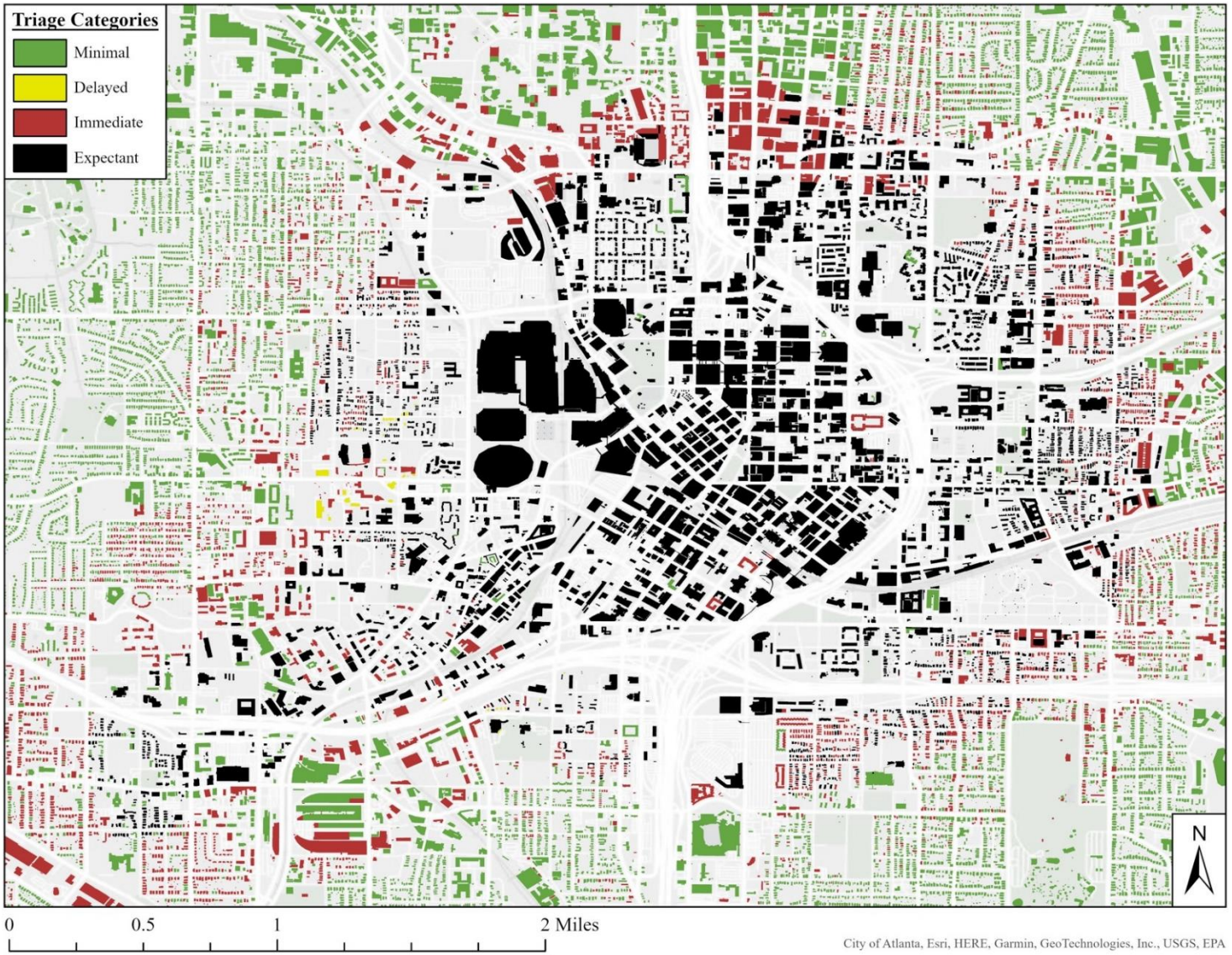

Figure 5.4. Distribution of RTR triage categories in the unwarned scenario after 48 hours, following a 15kt IND in downtown Atlanta, GA at 10:00 am local time on August 19, 2019 (Medoid 4).

health care response.

5.3.2.2. Injury Profiles within Triage Categories

Tables 5.7 – 5.10 provide a closer examination of the patients within each triage category under the unwarned scenario. Appendix O provides the same breakdown in the warned scenario. Only 2nd and 3rd degree burns are included in the estimations, given 1st degree burns are unlikely to require medical attention. Within the minimally injured category, subclinical ARS with no trauma and no burn was the most common injury profile in medoids 1, 2, and 4. However, in medoid 3, the most common injury profile was subclinical ARS with minimal trauma and no burn. Within the delayed category, the most common injury profile was hematopoietic ARS with moderate trauma but no burn across all four simulations. Within the immediate category, also across all four simulations, the most common injury profile was predominantly moderate trauma (subclinical ARS with moderate trauma but no burn). However, in simulations 1 and 4, the second most common injury profile was hematopoietic ARS with no trauma and no burn, whereas in medoids 2 and 3, the second most common injury profile was predominantly significant burns (subclinical ARS with minimal trauma and burn).

5.3.3. Health Care Resources

5.3.3.1. Directly Affected Health Care Resources

The simulated IND detonations not only affected people, but also the health care infrastructure as well. Figures 5.5 – 5.8 and Tables 5.11 – 5.14 respectively, illustrate and describe the hospitals in GA that would be affected by the simulated detonation. Across all four simulations, five facilities were consistently within the damage zones: Children's Healthcare of Atlanta – Hughes Spalding, Emory University Hospital – Midtown, Grady Health System, Piedmont Atlanta Hospital, and WellStar Atlanta Medical Center. These five facilities comprise 9.2% of the statewide

Table 5.7. Estimated casualties by RTR triage category in the unwarned scenario after 48 hours, following a 15kt IND in downtown Atlanta, GA at 10:00 am local time on November 26, 2019 (Medoid 1). Abbreviations: ARS = Acute Radiation Sickness

		No Burn	Burn	**Total**
Minimal				**1,024,915**
Subclinical ARS	No Trauma	805,234	0	805,234
	Minimal Trauma	217,383	2,154	219,537
Hematopoietic ARS	Minimal Trauma	144	0	144
Delayed				**3,563**
Hematopoietic ARS	Moderate Trauma	3,548	15	3,563
Immediate				**41,455**
Subclinical ARS	Minimal Trauma	6,789	7,369	14,158
	Moderate Trauma	13,527	729	14,256
Hematopoietic ARS	No Trauma	9,126	0	9,126
	Minimal Trauma	3,641	270	3,911
	Moderate Trauma	4	0	4
Expectant				**187,415**
Subclinical ARS	Moderate Trauma	5,544	8,043	13,587
	Severe Trauma	6,542	19,241	25,783
Hematopoietic ARS	Moderate Trauma	341	542	883
	Severe Trauma	17,700	66,685	84,385
Gastrointestinal/Cutaneous ARS	No Trauma	596	0	596
	Minimal Trauma	462	41	503
	Moderate Trauma	596	214	810
	Severe Trauma	5,027	20,637	25,664
Neurovascular ARS	No Trauma	277	0	277
	Minimal Trauma	205	27	232
	Moderate Trauma	372	141	513
	Severe Trauma	6,173	28,009	34,182

Table 5.8. Estimated casualties by RTR triage category in the unwarned scenario after 48 hours, following a 15kt IND in downtown Atlanta, GA at 10:00 am local time on November 25, 2019 (Medoid 2). Abbreviations: ARS = Acute Radiation Sickness.

		No Burn	Burn	**Total**
Minimal				**453,939**
Subclinical ARS	No Trauma	226,496	0	226,496
	Minimal Trauma	224,995	2,384	227,379
Hematopoietic ARS	Minimal Trauma	64	0	64
Delayed				**76**
Hematopoietic ARS	Moderate Trauma	71	5	76
Immediate				**40,998**
Subclinical ARS	Minimal Trauma	7,570	8,652	16,222
	Moderate Trauma	18,159	792	18,951
Hematopoietic ARS	No Trauma	1,407	0	1,407
	Minimal Trauma	4,289	123	4,412
	Moderate Trauma	6	0	6
Expectant				**190,273**
Subclinical ARS	Moderate Trauma	6,162	8,577	14,739
	Severe Trauma	8,124	22,421	30,545
Hematopoietic ARS	Moderate Trauma	0	170	170
	Severe Trauma	16,525	61,471	77,996
Gastrointestinal/Cutaneous ARS	No Trauma	3,724	0	3,724
	Minimal Trauma	418	12	430
	Moderate Trauma	197	180	377
	Severe Trauma	4,366	18,697	23,063
Neurovascular ARS	No Trauma	698	0	698
	Minimal Trauma	109	15	124
	Moderate Trauma	12	64	76
	Severe Trauma	6,655	31,676	38,331

Table 5.9. Estimated casualties by RTR triage category in the unwarned scenario after 48 hours, following a 15kt IND in downtown Atlanta, GA at 10:00 am local time on July 2, 2019 (Medoid 3). Abbreviations: ARS = Acute Radiation Sickness.

		No Burn	Burn	**Total**
Minimal				**434,671**
Subclinical ARS	No Trauma	208,624	0	208,624
	Minimal Trauma	223,646	2,388	226,034
Hematopoietic ARS	Minimal Trauma	13	0	13
Delayed				**197**
Hematopoietic ARS	Moderate Trauma	195	2	197
Immediate				**43,384**
Subclinical ARS	Minimal Trauma	6,923	7,603	14,526
	Moderate Trauma	18,975	795	19,770
Hematopoietic ARS	No Trauma	5,069	0	5,069
	Minimal Trauma	3,926	93	4,019
	Moderate Trauma	0	0	0
Expectant				**187,221**
Subclinical ARS	Moderate Trauma	6,410	8,766	15,176
	Severe Trauma	8,516	24,987	33,503
Hematopoietic ARS	Moderate Trauma	33	204	237
	Severe Trauma	15,531	55,579	71,110
Gastrointestinal/Cutaneous ARS	No Trauma	50	0	50
	Minimal Trauma	554	28	582
	Moderate Trauma	204	122	326
	Severe Trauma	4,166	18,950	23,116
Neurovascular ARS	No Trauma	981	0	981
	Minimal Trauma	321	41	362
	Moderate Trauma	43	42	85
	Severe Trauma	7,380	34,313	41,693

Table 5.10. Estimated casualties by RTR triage category in the unwarned scenario after 48 hours, following a 15kt IND in downtown Atlanta, GA at 10:00 am local time on August 19, 2019 (Medoid 4). Abbreviations: ARS = Acute Radiation Sickness.

		No Burn	Burn	**Total**
Minimal				**754,720**
Subclinical ARS	No Trauma	501,851	0	501,851
	Minimal Trauma	250,046	2,799	252,845
Hematopoietic ARS	Minimal Trauma	24	0	24
Delayed				**207**
Hematopoietic ARS	Moderate Trauma	201	6	207
Immediate				**46,668**
Subclinical ARS	Minimal Trauma	5,134	5,777	10,911
	Moderate Trauma	24,023	1,136	25,159
Hematopoietic ARS	No Trauma	6,256	0	6,256
	Minimal Trauma	4,107	235	4,342
	Moderate Trauma	0	0	0
Expectant				**196,537**
Subclinical ARS	Moderate Trauma	6,438	9,198	15,636
	Severe Trauma	7,450	19,923	27,373
Hematopoietic ARS	Moderate Trauma	125	555	680
	Severe Trauma	15,198	56,946	72,144
Gastrointestinal/Cutaneous ARS	No Trauma	1,021	0	1,021
	Minimal Trauma	4,425	1,771	6,196
	Moderate Trauma	278	322	600
	Severe Trauma	6,347	25,380	31,727
Neurovascular ARS	No Trauma	472	0	472
	Minimal Trauma	1,199	359	1,558
	Moderate Trauma	149	114	263
	Severe Trauma	6,668	32,199	38,867

emergency department (ED) capacity, 9.7% of the statewide critical care capacity, and 8.3% of the statewide general medical bed capacity. These estimates do not differentiate between adult and pediatric beds, due to a lack of available data. However, Children's Healthcare of Atlanta – Hughes Spalding is one of only a few pediatric hospitals in the state. Furthermore, Grady Health System has one of three burn centers in the state, comprising approximately 10% of the statewide burn care capacity.

Medoid 1 had the most significant impact on health care infrastructure. Fifteen hospitals across three health care coalitions were directly affected by the detonation and fallout radiation plume. These 15 facilities comprise 17.8% of the statewide ED capacity, 27.2% of the statewide critical care capacity, and 18.9% of the statewide general medical bed capacity, cumulatively affecting almost 20% of the total bed capacity in the state. Critically, Medoid 1 affected Children's Healthcare of Atlanta – Egleston, which is the only level I trauma center in the state, as well as Emory University Hospital, which is one of two hospitals in the state in the Radiation Injury Treatment Network (RITN). Medoid 2 directly affected 11 hospitals across three health care coalitions. These eleven facilities comprise 12.7% of the statewide ED capacity, 10.8% of the statewide critical care capacity, and 10.5% of the statewide general medical bed capacity, cumulatively affecting approximately 10% of the total bed capacity in the state. Similarly, Medoid 4 directly affected eight hospitals across two health care coalitions. These eight facilities comprise 11.9% of the statewide ED capacity, 12.2% of the critical care capacity, and 9.8% of the statewide general med bed capacity, cumulatively affecting 10.5% of the total bed capacity in the state. Medoid 3 had the least significant impact on the health care infrastructure in the state, as only one small acute care facility with a total bed capacity of 10 was affected beyond the damage zone. However, the fallout radiation plume crosses I-20, which would complicate access

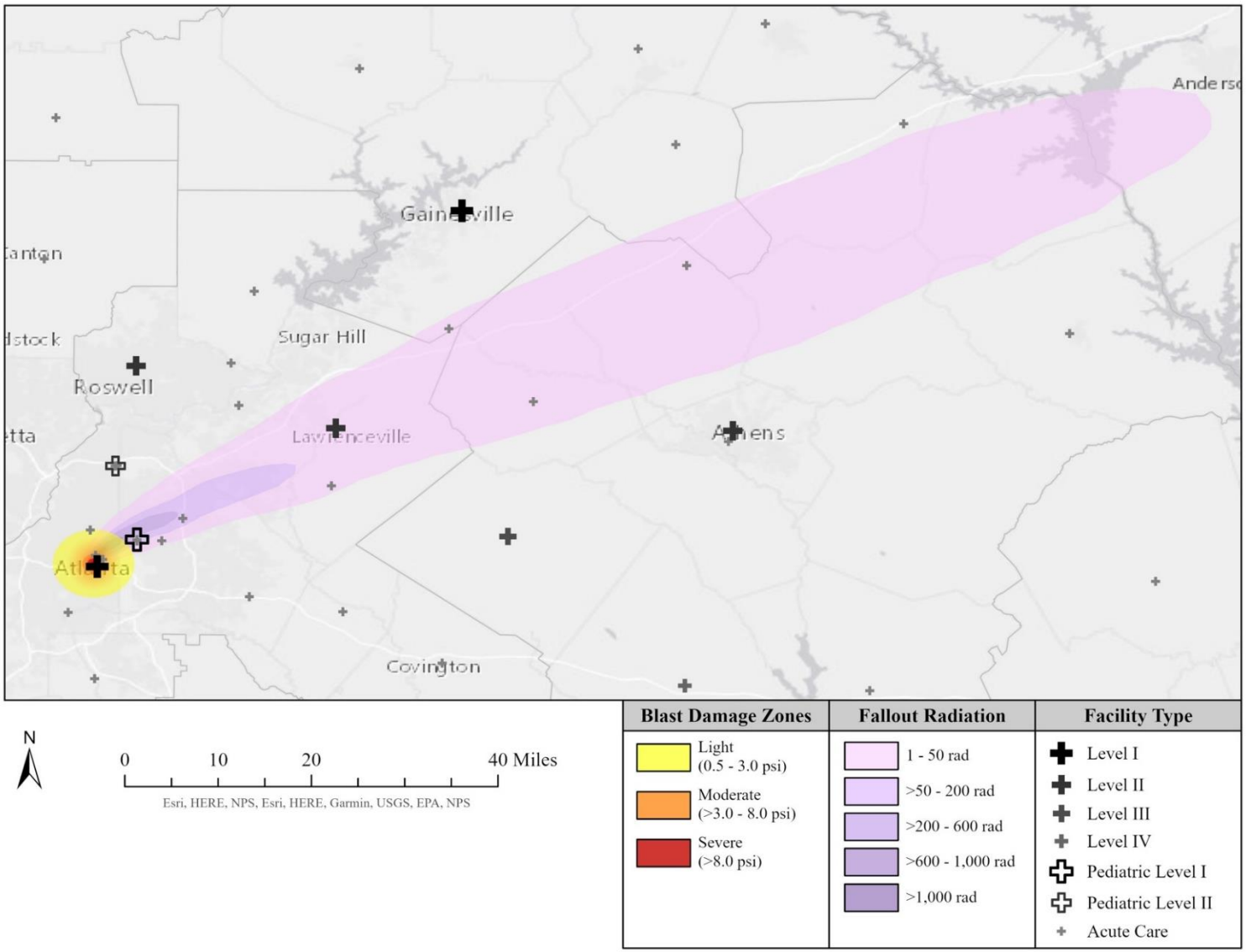

Figure 5.5. Directly impacted health care facilities 48 hours following a 15kt IND detonation in downtown Atlanta, GA at 10:00 am local time on November 26, 2019 (Medoid 1).

Table 5.11. Facilities directly impacted in the first 48 hours following a 15kt IND detonation in downtown Atlanta, GA at 10:00 am local time on November 26, 2019 (Medoid 1). Abbreviations: ED = emergency department; Cap. = capacity; Avail. = available.

Facility Name	Facility Type	ED		Critical Care		General		Total	
		Cap.	Avail.	Cap.	Avail.	Cap.	Avail.	Cap.	Avail.
Region B Health Care Coalition									
Northeast Georgia Medical Center - Braselton	Acute Care	21	13	20	8	134	53	175	74
% of Region B Resources		11.4%	9.5%	14.4%	14.3%	19.3%	18.4%	17.2%	15.4%
Region D Health Care Coalition									
Children's Healthcare of Atlanta - Egleston	Pediatric Level I	53	52	127	35	194	87	374	174
Children's Healthcare of Atlanta - Hughes Spalding	Acute Care	36	35	1	1	24	22	61	58
Eastside Medical Center	Acute Care	37	29	55	9	126	67	218	105
Emory Decatur Hospital	Acute Care	54	34	52	22	261	90	367	146
Emory Rehab Hospital	Acute Care	0	0	0	0	15	1	15	1
Emory University Hospital	Acute Care	30	23	158	48	476	250	664	321
Emory University Hospital - Midtown	Acute Care	57	40	86	38	453	266	596	344
Emory University Orthopaedics and Spine Hospital	Acute Care	0	0	0	0	24	19	24	19
Grady Health System	Level I	88	0	90	8	220	4	398	12
Northside Hospital Gwinnett	Level II	65	48	68	31	239	51	372	130
Piedmont Atlanta Hospital	Acute Care	86	62	40	12	198	80	324	154
WellStar Atlanta Medical Center	Acute Care	30	16	55	5	263	120	348	141
% of Region D Resources		54.6%	52.5%	65.7%	59.9%	58.3%	59.4%	59.1%	57.9%
Region E Health Care Coalition									
Northeast Georgia Medical Center - Barrow	Acute Care	9	7	10	10	25	16	44	33
Northridge Medical Center	Acute Care	9	9	0	0	0	0	9	9
% of Region E Resources		12.7%	13.4%	12.2%	41.7%	4.2%	5.7%	6.5%	9.9%
Total Affected		575	368	762	227	2,652	1,126	3,989	1,721
% of statewide resources		17.8%	15.4%	27.2%	26.3%	18.9%	19.3%	19.9%	18.9%

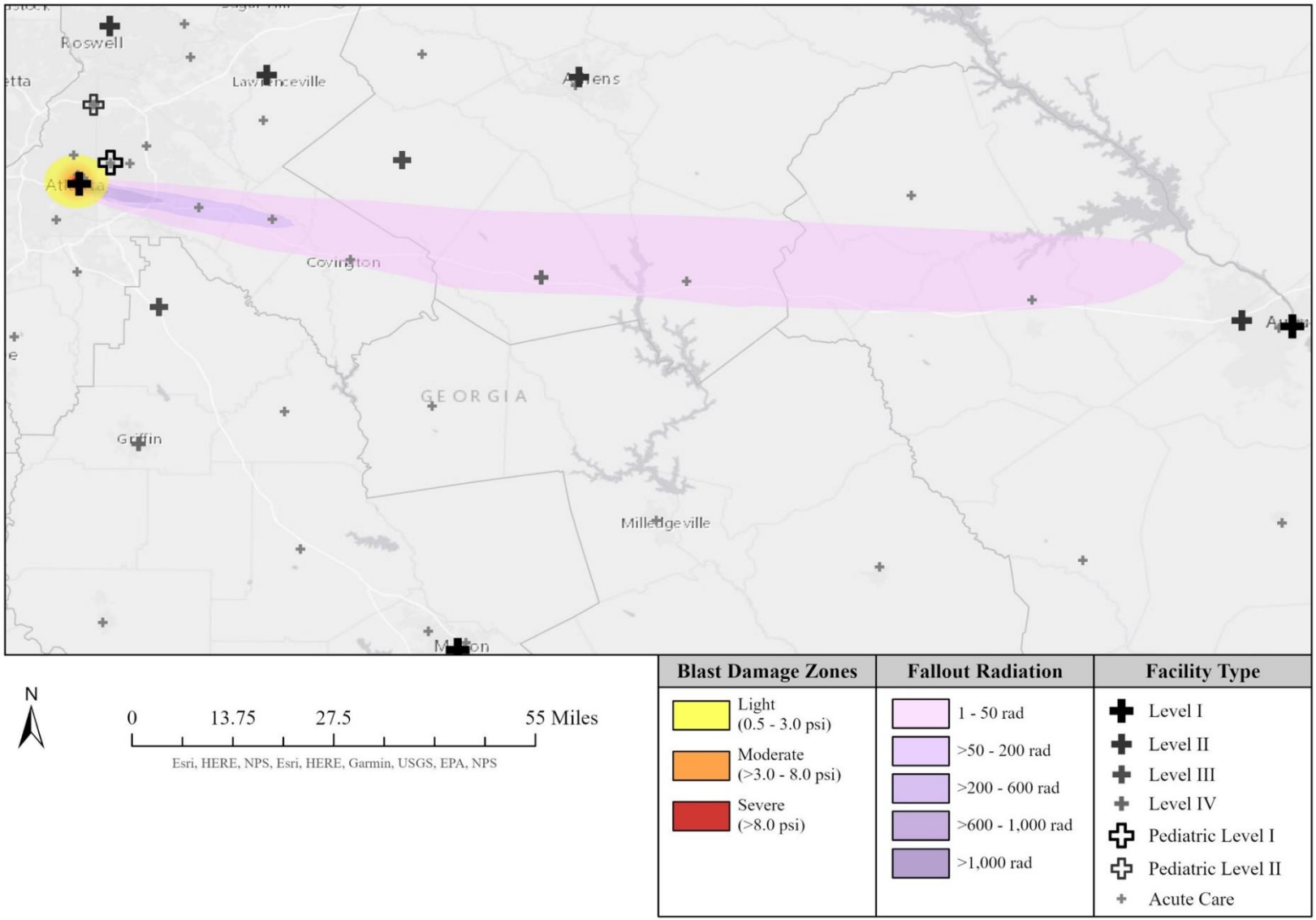

Figure 5.6. Directly impacted health care facilities 48 hours following a 15kt IND detonation in downtown Atlanta, GA at 10:00 am local time on November 25, 2019 (Medoid 2).

Table 5.12. Facilities directly impacted in the first 48 hours following a 15kt IND detonation in downtown Atlanta, GA at 10:00 am local time on November 25, 2019 (Medoid 2). Abbreviations: ED = emergency department; Cap. = capacity; Avail. = available.

Facility Name	Facility Type	ED		Critical Care		General		Total	
		Cap.	Avail.	Cap.	Avail.	Cap.	Avail.	Cap.	Avail.
Region D Health Care Coalition									
Children's Healthcare of Atlanta - Hughes Spalding	Acute Care	36	35	1	1	24	22	61	58
Emory Hillandale Hospital	Acute Care	31	19	14	9	93	36	138	64
Emory University Hospital - Midtown	Acute Care	57	40	86	38	453	266	596	344
Grady Health System	Level I	88	0	90	8	220	4	398	12
Piedmont Atlanta Hospital	Acute Care	86	62	40	12	198	80	324	154
Piedmont Newton Hospital	Acute Care	30	28	0	0	60	31	90	59
Piedmont Rockdale Hospital	Acute Care	25	18	15	6	90	41	130	65
WellStar Atlanta Medical Center	Acute Care	30	16	55	5	263	120	348	141
% of Region D Resources		39.0%	33.7%	27.0%	22.6%	32.8%	33.7%	32.7%	32.3%
Region E Health Care Coalition									
Morgan Medical Center	Level IV	8	7	0	0	25	19	33	26
St. Mary's Good Samaritan Hospital	Acute Care	9	9	1	0	25	11	35	20
% of Region E Resources		12.0%	13.4%	1.2%	0.0%	8.4%	10.8%	8.3%	10.9%
Region G Health Care Coalition									
University Hospital - McDuffie	Acute Care	12	10	0	0	25	10	37	20
% of Region G Resources		5.7%	6.1%	0.0%	0.0%	2.1%	2.1%	2.3%	2.9%
Total Affected		412	244	302	79	1,476	640	2,190	963
% of Statewide Resources		12.7%	10.2%	10.8%	9.1%	10.5%	11.0%	10.9%	10.6%

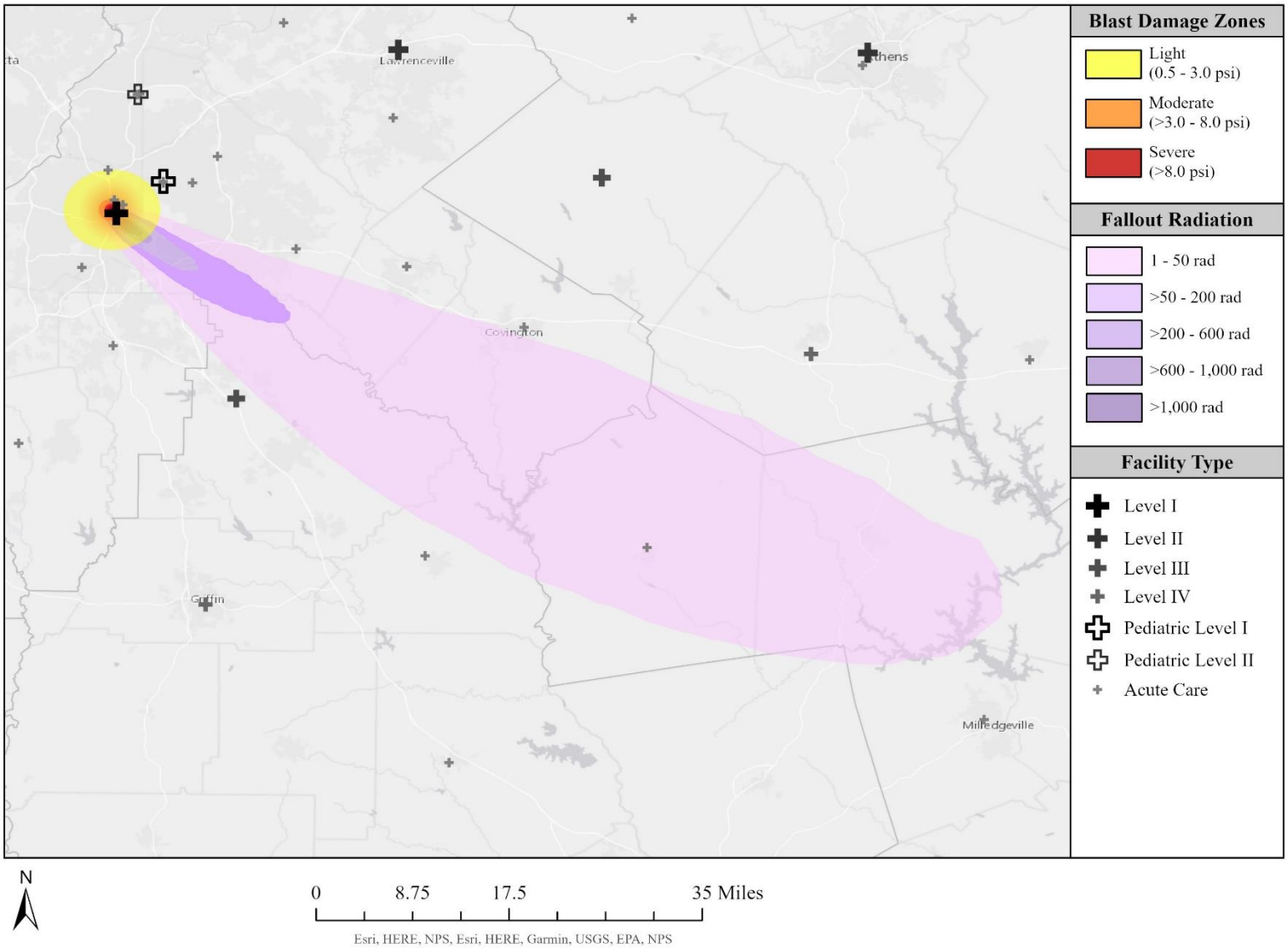

Figure 5.7. Directly impacted health care facilities 48 hours following a 15kt IND detonation in downtown Atlanta, GA at 10:00 am local time on July 2, 2019 (Medoid 3).

Table 5.13. Facilities directly impacted in the first 48 hours following a 15kt IND detonation in downtown Atlanta, GA at 10:00 am local time on July 2, 2019 (Medoid 3). Abbreviations: ED = emergency department; Cap. = capacity; Avail. = available.

Facility Name	Facility Type	ED		Critical Care		General		Total	
		Cap.	Avail.	Cap.	Avail.	Cap.	Avail.	Cap.	Avail.
Region D Health Care Coalition									
Children's Healthcare of Atlanta - Hughes Spalding	Acute Care	36	35	1	1	24	22	61	58
Emory University Hospital - Midtown	Acute Care	57	40	86	38	453	266	596	344
Grady Health System	Level I	88	0	90	8	220	4	398	12
Piedmont Atlanta Hospital	Acute Care	86	62	40	12	198	80	324	154
WellStar Atlanta Medical Center	Acute Care	30	16	55	5	263	120	348	141
% of Region D Resources		30.3%	23.7%	24.4%	18.3%	27.1%	27.7%	27.1%	25.6%
Region H Health Care Coalition									
Jasper Memorial Hospital	Acute Care	3	3	0	0	7	4	10	7
% of Region H Resources		3.4%	4.5%	0.0%	0.0%	2.6%	2.7%	2.5%	3.1%
Total Affected		300	156	272	64	1,165	496	1,737	716
% of Statewide Resources		9.3%	6.5%	9.7%	7.4%	8.3%	8.5%	8.7%	7.9%

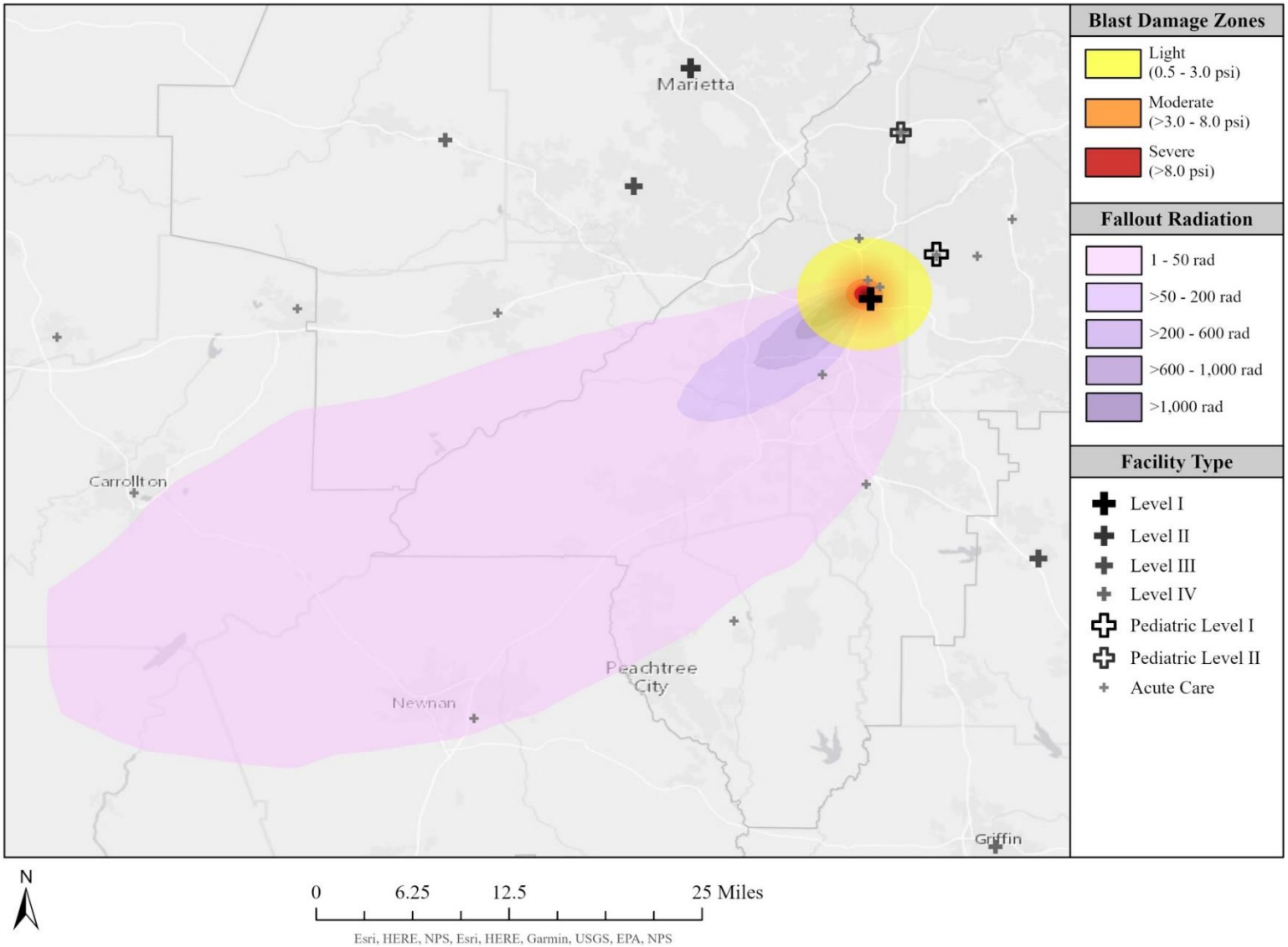

Figure 5.8. Directly impacted health care facilities 48 hours following a 15kt IND detonation in downtown Atlanta, GA at 10:00 am local time on August 19, 2019 (Medoid 4).

Table 5.14. Facilities directly impacted in the first 48 hours following a 15kt IND detonation in downtown Atlanta, GA at 10:00 am local time on August 19, 2019 (Medoid 4). Abbreviations: ED = emergency department; Cap. = capacity; Avail. = available.

Facility Name	Facility Type	ED		Critical Care		General		Total	
		Cap.	Avail.	Cap.	Avail.	Cap.	Avail.	Cap.	Avail.
Region C Health Care Coalition									
Piedmont Newnan	Acute Care	28	24	33	16	86	24	147	64
% of Region C Resources		14.7%	15.3%	19.0%	28.6%	11.3%	7.6%	13.0%	12.1%
Region D Health Care Coalition									
Children's Healthcare of Atlanta - Hughes Spalding	Acute Care	36	35	1	1	24	22	61	58
Emory University Hospital-Midtown	Acute Care	57	40	86	38	453	266	596	344
Grady Health System	Level I	88	0	90	8	220	4	398	12
Southern Regional Medical Center	Acute Care	30	14	12	2	54	24	96	40
WellStar Atlanta Medical Center - South	Acute Care	31	22	26	3	71	28	128	53
Piedmont Atlanta Hospital	Acute Care	86	62	40	12	198	80	324	154
WellStar Atlanta Medical Center	Acute Care	30	16	55	5	263	120	348	141
% of Region D Resources		36.5%	29.3%	27.8%	19.8%	30.0%	30.6%	30.6%	28.9%
Total Affected		386	213	343	85	1,369	568	2,098	866
% of statewide resources		11.9%	8.9%	12.2%	9.8%	9.8%	9.7%	10.5%	9.5%

to other supporting facilities, including the largest burn center in the state.

5.3.3.2. Remaining Health Care Resources

Table 5.15 summarizes the average staffed bed capacity, availability, and surge capacity by health care coalitions across the state. Tables 5.16 – 5.19 describe the remaining staffed bed capacity and availability 48 hours following the detonation in each simulation.

The total bed staffed bed capacity in the state of GA is 20,075, which could plausibly be surged up to 24,090. Across the simulations, there is not a significant difference in the lack of available resources within the context of the number of casualties. In medoid 1, there are almost 9,000 beds occupied in the remaining facilities and approximately 10,500 beds available including the surge capacity. There are only enough beds for approximately 25% of the immediate patients, leaving more than 34,500 immediate or delayed patients without a hospital bed. In medoid 2, there are approximately 10,000 beds occupied in the remaining facilities and approximately 11,500 beds available including the surge capacity. There are only enough beds for approximately 29% of the immediate patients, leaving almost 30,000 immediate or delayed patients without a hospital bed. In medoid 3, there are approximately 10,000 beds occupied in the remaining facilities and approximately 12,000 beds available including the surge capacity. There are only enough beds for approximately 28% of the immediate patients, leaving approximately 31,500 immediate or delayed patients without a hospital bed. Similarly, in medoid 4, there are approximately 10,000 beds occupied in the remaining facilities and approximately 12,000 beds available including the surge capacity. There are only enough beds for 25% of the immediate patients, leaving approximately 35,000 immediate or delayed patients without a hospital bed.

Table 5.15. Reported seven-day average staffed bed capacity, availability, and surge capacity by health care coalitions across the state of GA. Abbreviations: Cap. = capacity; Avail. = available.

Health Care Coalition	ED			Critical Care			General			Total		
	Cap.	Avail.	Surge	Cap.	Avail.	Surge	Cap.	Avail.	Surge	Cap.	Avail.	Surge
Region A	125	97	150	53	27	63	447	250	536	624	373	749
Region B	185	137	222	139	56	167	696	288	835	1,020	481	1,224
Region C	191	157	230	174	56	209	763	317	915	1,128	529	1,354
Region D	981	646	1,177	1,114	349	1,337	4,273	1,778	5,127	6,368	2,773	7,641
Region E	142	119	171	82	24	98	596	279	716	820	423	984
Region F	286	219	343	217	19	260	1,546	500	1,855	2,049	738	2,458
Region G	209	164	251	193	62	232	1,209	474	1,451	1,611	701	1,933
Region H	89	67	106	40	12	48	267	146	321	396	225	475
Region I	143	95	172	110	23	132	673	285	808	926	403	1,112
Region J	294	240	352	202	68	242	943	426	1,131	1,438	734	1,726
Region K	163	127	195	132	40	158	587	193	704	882	361	1,058
Region L	95	74	113	64	18	77	426	202	511	585	294	702
Region M	81	58	97	59	38	71	314	158	377	454	254	545
Region N	256	190	307	222	72	266	1,296	535	1,555	1,774	796	2,129
Total	**3,239**	**2,389**	**3,887**	**2,801**	**864**	**3,361**	**14,035**	**5,831**	**16,842**	**20,075**	**9,083**	**24,090**

Table 5.16. Estimated staffed bed capacity, availability, and surge capacity by health care coalitions across the state of GA, 48 hours post-IND detonation in downtown Atlanta, GA at 10:00 am local time on November 26, 2019 (Medoid 1). The coalitions directly impacted by the detonation are highlighted in yellow. Abbreviations: Cap. = capacity; Avail. = available.

Health Care Coalition	ED			Critical Care			General			Total		
	Cap.	Avail.	Surge	Cap.	Avail.	Surge	Cap.	Avail.	Surge	Cap.	Avail.	Surge
Region A	125	97	150	53	27	63	447	250	536	624	373	749
Region B	164	124	197	119	48	143	562	235	674	845	407	1,014
Region C	191	157	230	174	56	209	763	317	915	1,128	529	1,354
Region D	445	307	534	382	140	458	1,780	721	2,136	2,607	1,168	3,128
Region E	124	103	149	72	14	86	571	263	685	767	380	920
Region F	286	219	343	217	19	260	1,546	500	1,855	2,049	738	2,458
Region G	209	164	251	193	62	232	1,209	474	1,451	1,611	701	1,933
Region H	89	67	106	40	12	48	267	146	321	396	225	475
Region I	143	95	172	110	23	132	673	285	808	926	403	1,112
Region J	294	240	352	202	68	242	943	426	1,131	1,438	734	1,726
Region K	163	127	195	132	40	158	587	193	704	882	361	1,058
Region L	95	74	113	64	18	77	426	202	511	585	294	702
Region M	81	58	97	59	38	71	314	158	377	454	254	545
Region N	256	190	307	222	72	266	1,296	535	1,555	1,774	796	2,129
Total	**2,664**	**2,021**	**3,197**	**2,039**	**637**	**2,447**	**11,383**	**4,704**	**13,660**	**16,086**	**7,362**	**19,304**

Table 5.17. Estimated staffed bed capacity, availability, and surge capacity by health care coalitions across the state of GA, 48 hours post-IND detonation in downtown Atlanta, GA at 10:00 am local time on November 25, 2019 (Medoid 2). The coalitions directly impacted by the detonation are highlighted in yellow. Abbreviations: Cap. = capacity; Avail. = available.

Health Care Coalition	ED			Critical Care			General			Total		
	Cap.	Avail.	Surge	Cap.	Avail.	Surge	Cap.	Avail.	Surge	Cap.	Avail.	Surge
Region A	125	97	150	53	27	63	447	250	536	624	373	749
Region B	185	137	222	139	56	167	696	288	835	1,020	481	1,224
Region C	191	157	230	174	56	209	763	317	915	1,128	529	1,354
Region D	598	428	718	813	270	976	2,872	1,178	3,446	4,283	1,876	5,140
Region E	125	103	150	81	24	97	546	249	655	752	376	902
Region F	286	219	343	217	19	260	1,546	500	1,855	2,049	738	2,458
Region G	197	154	236	193	62	232	1,184	464	1,421	1,574	680	1,889
Region H	89	67	106	40	12	48	267	146	321	396	225	475
Region I	143	95	172	110	23	132	673	285	808	926	403	1,112
Region J	294	240	352	202	68	242	943	426	1,131	1,438	734	1,726
Region K	163	127	195	132	40	158	587	193	704	882	361	1,058
Region L	95	74	113	64	18	77	426	202	511	585	294	702
Region M	81	58	97	59	38	71	314	158	377	454	254	545
Region N	256	190	307	222	72	266	1,296	535	1,555	1,774	796	2,129
Total	**2,827**	**2,145**	**3,392**	**2,499**	**784**	**2,999**	**12,559**	**5,190**	**15,071**	**17,885**	**8,120**	**21,462**

Table 5.18. Estimated staffed bed capacity, availability, and surge capacity by health care coalitions across the state of GA, 48 hours post-IND detonation in downtown Atlanta, GA at 10:00 am local time on July 2, 2019 (Medoid 3). The coalitions directly impacted by the detonation are highlighted in yellow. Abbreviations: Cap. = capacity; Avail. = available.

Health Care Coalition	ED			Critical Care			General			Total		
	Cap.	Avail.	Surge	Cap.	Avail.	Surge	Cap.	Avail.	Surge	Cap.	Avail.	Surge
Region A	125	97	150	53	27	63	447	250	536	624	373	749
Region B	185	137	222	139	56	167	696	288	835	1,020	481	1,224
Region C	191	157	230	174	56	209	763	317	915	1,128	529	1,354
Region D	684	493	821	842	285	1,010	3,115	1,286	3,738	4,641	2,064	5,569
Region E	142	119	171	82	24	98	596	279	716	820	423	984
Region F	286	219	343	217	19	260	1,546	500	1,855	2,049	738	2,458
Region G	209	164	251	193	62	232	1,209	474	1,451	1,611	701	1,933
Region H	86	64	103	40	12	48	260	142	312	386	218	463
Region I	143	95	172	110	23	132	673	285	808	926	403	1,112
Region J	294	240	352	202	68	242	943	426	1,131	1,438	734	1,726
Region K	163	127	195	132	40	158	587	193	704	882	361	1,058
Region L	95	74	113	64	18	77	426	202	511	585	294	702
Region M	81	58	97	59	38	71	314	158	377	454	254	545
Region N	256	190	307	222	72	266	1,296	535	1,555	1,774	796	2,129
Total	**2,940**	**2,234**	**3,528**	**2,528**	**800**	**3,034**	**12,870**	**5,335**	**15,444**	**18,338**	**8,368**	**22,006**

Table 5.19. Estimated staffed bed capacity, availability, and surge capacity by health care coalitions across the state of GA, 48 hours post-IND detonation in downtown Atlanta, GA at 10:00 am local time on August 19, 2019 (Medoid 4). The coalitions directly impacted by the detonation are highlighted in yellow. Abbreviations: Cap. = capacity; Avail. = available.

Health Care Coalition	ED			Critical Care			General			Total		
	Cap.	Avail.	Surge	Cap.	Avail.	Surge	Cap.	Avail.	Surge	Cap.	Avail.	Surge
Region A	125	97	150	53	27	63	447	250	536	624	373	749
Region B	185	137	222	139	56	167	696	288	835	1,020	481	1,224
Region C	163	133	196	141	40	169	677	293	812	981	466	1,177
Region D	623	457	748	804	280	965	2,990	1,234	3,588	4,417	1,971	5,300
Region E	142	119	171	82	24	98	596	279	716	820	423	984
Region F	286	219	343	217	19	260	1,546	500	1,855	2,049	738	2,458
Region G	209	164	251	193	62	232	1,209	474	1,451	1,611	701	1,933
Region H	89	67	106	40	12	48	267	146	321	396	225	475
Region I	143	95	172	110	23	132	673	285	808	926	403	1,112
Region J	294	240	352	202	68	242	943	426	1,131	1,438	734	1,726
Region K	163	127	195	132	40	158	587	193	704	882	361	1,058
Region L	95	74	113	64	18	77	426	202	511	585	294	702
Region M	81	58	97	59	38	71	314	158	377	454	254	545
Region N	256	190	307	222	72	266	1,296	535	1,555	1,774	796	2,129
Total	**2,853**	**2,177**	**3,424**	**2,458**	**779**	**2,949**	**12,667**	**5,263**	**15,200**	**17,977**	**8,218**	**21,572**

5.4. Discussion

This study simulated four 15 kt IND detonation simulations in Atlanta, GA at 10:00 am local time across four days in the year 2019 to consider the population-level health care consequences in the aftermath of the detonation. An estimated 185,896 to 196,537 individuals would not survive their injuries, and an additional 31,939 to 46,668 patients would require immediate health care. An additional 454,015 to 1,060,235 individuals would require delayed or minimal health care.

5.4.1. Casualty Estimates

Few other models have reported specific casualty estimates,[37,58,120,280] and even fewer have reported specific injuries.[126,128] In a simulation of nuclear war, one study estimated 1-3 nuclear warheads, each with a 250 kt yield, detonated on the Atlanta metro area would cause 300,000 fatalities and 600,000 injuries.[126] Even though the current study used a weapon with 1/16th of the yield, the fatality estimates were approximately half those reported in the nuclear war study. Another study estimated a 10 kt detonation in New York City would cause 213,430 injuries and 103,000 fatalities.[128] Scaled for the metro-Atlanta population, this would be comparable to 153,546 injuries and 74,101 fatalities. The results from the current study far exceed these estimations, likely due to differences in the modeling methodology. Both the nuclear war simulation and the New York City simulation utilized NukeMap, a web-based nuclear detonation simulator.[123,126,128] However, for acute casualties, NukeMap only considers blast effects and ignores the thermal and radiation effects in estimating casualties.[130] The improved methodology used in this study to account for the thermal and radiation effects explains the discrepancy in these results. Therefore, future modeling efforts must consider the

acute thermal and radiation effects in order to accurately characterize the casualties following an IND detonation.

In perhaps the most comprehensive publicly available model previously published, Bell & Dallas[17] conducted a 20 kt IND detonation simulation in Atlanta, GA. The authors reported 63,814 casualties from the blast effects, 36,256 casualties from the thermal effects, and 160,224 casualties from fallout radiation where mortality was greater than 0.5%. Bell & Dallas also reported 207,025 casualties from fallout radiation and blast effects, and 182,717 casualties from fallout radiation and thermal effects. Across all four simulations in the current study, the casualties from radiation were roughly comparable to those previously reported, but this study reported far more casualties from the blast and thermal effects. This study reported a range of 153,911 to 156,716 casualties from the thermal effects, and a range of 148,979 to 150,256 casualties from the blast effects. These discrepancies can likely be attributed to changes in the population. Bell & Dallas originally published their work in 2007, at which point the population of metro-Atlanta was approximately 4.2 million, whereas the population of metro-Atlanta in 2019 was approximately 5.7 million.[42] Any remaining discrepancies can be attributed to improvements in the modeling workflow to account for the thermal effects in the urban environment, as well as the blast effect modeling in HPAC.

The preponderance of previously published studies have modeled nuclear detonations to estimate blast, thermal, and radiation casualties separately, ignoring the role of combined injuries.[272] The current study provides an unprecedented glimpse into predicted injury profiles within triage categories. Within the minimally injured category, subclinical ARS with no trauma and no burn was the most common injury profile, and within the delayed category, the most common injury profile was hematopoietic ARS with moderate trauma but no burn. Within the

immediate category, also across all four simulations, the most common injury profile was predominantly moderate trauma (subclinical ARS with moderate trauma but no burn). However, in simulations 1 and 4, the second most common injury profile was hematopoietic ARS with no trauma and no burn, whereas in medoids 2 and 3, the second most common injury profile was predominantly significant burns (subclinical ARS with minimal trauma and burn). Given the available resources, it is unlikely that patients in the upper end of the dose range for hematopoietic ARS and no trauma or burn injuries would survive. While the lethal dose for 50% of the exposed population at 60 days ($LD_{50/60}$) in patients treated with medical care is 600 rads, this threshold decreases to approximately 450 rads in untreated patients.[8,64] As such, it is likely that some of the patients presenting with hematopoietic ARS (indicative of a radiation dose between 200 and 600 rads) would not survive.

Across the four simulations included in this study, the variation in weather conditions and associated plume direction did not have appear to have a significant impact on the estimated casualties requiring medical care. In the unwarned scenario, approximately 190,000 patients would not be expected to survive their injuries. Approximately 43,000 patients are estimated to require immediate health care, while only approximately 1,000 would be triaged to receive delayed care. Under the warned scenario, there were differences in the estimated casualties requiring care. However, these perturbations are more indicative of the changes in protection offered by buildings from radiation, rather than changes in the weather conditions, as further supported by the results in Chapter 4. The difference in weather conditions and associated fallout radiation plumes most significantly impacted the geospatial distribution of these casualties, as well as the volume of minimally injured patients, who would not require care. These patients, however, are important to consider in planning efforts, as such patients are likely to report first to

health care facilities out of fear or concern, complicating access to care for the immediate and delayed patients.[292–294] It is important to note that these results are unique to the parameters in this study, particularly in a land-locked major metropolitan area. Future studies should consider alternative locations of detonation, as it is plausible the weather conditions may have a more pronounced impact on casualties requiring care for coastal regions, which would impact the fallout radiation patterns,[37] or rural areas, which would impact the volume of casualties.

5.4.2. Health Care Resources

This study strongly supports previously published reports speculating that the health care infrastructure would be incapacitated in the aftermath of an IND detonation.[17,132,272,280] Even if none of the health care facilities were directly affected, the state of GA does not have the resources to effectively respond.

Losing the key facilities in the damage zone, as well as those affected by the fallout radiation, in any of the simulation only furthers this strain. The state's total staffed bed capacity including surge capacity is 24,090 beds, of which just more than one-third are available at any given time. Even among the simulations, there is not a significant difference in the lack of available resources within the context of the number of casualties. Across the four simulated detonations, even with surge capacity, there are only enough staffed beds for approximately 25% of the patients requiring immediate health care. This estimation assumes all of the available beds would be capable of providing the specialty care that the immediate patients would require, which is unlikely to be true, given prior research.[20] Future studies should further examine the surge capability (rather than just capacity) in the state in more detail, as it is plausible that limitations on staff and supplies would even further limit the state's ability to respond.

While the debate surrounding the likelihood of mass fires continues,[9,17,35,120,280,295] even without the consideration of mass fires, burn health care resources would be incapacitated. In the state of GA, there are three burn centers, two of which are accredited by the ABA.[296] Grady Memorial Hospital, the mainstay of the Grady Health System, has a burn center with 28 staffed beds, in addition to being widely recognized as one of the busiest level I trauma centers in the country.[297] In all four simulations, Grady would be completely destroyed in the severe damage zone. The state's largest burn center and the nation's largest private burn center, the Joseph M. Still Burn center in Augusta, has approximately 199 staffed beds, and their associated center, located at WellStar Cobb Hospital, has approximately 33 staffed beds. While neither facility was directly impacted by any of the simulations, the fallout radiation plume in medoid 3 covers I-20, the interstate connecting Atlanta and Augusta. Furthermore, the modeled plume only included the cumulative radiation over the first 48 hours. It is likely the cumulative radiation plume would extend to cover Augusta within the first 72 hours, prompting evacuation and/or shelter-in-place procedures in compliance with the Environmental Protection Agency's (EPA's) Protective Action Guide (PAG).

These combined 232 beds are not enough to treat the burn patients in the aftermath of a nuclear detonation. Even if every burn center across the US could increase their bed capacity by a factor of 1.5 in a no-notice event, there would only be 3,000 burn beds total, while this study estimated at least 10,000 patients would require care at a burn center. Furthermore, the US National Bioterrorism Hospital Preparedness Program states that a burn center should plan to care for at least 50 burn cases per million people in a facility's service area in the event of a disaster.[157] However, Dai et al.[158] found that few, if any, centers responding to burn mass casualty incidents (BMCIs) occurring between 1990 – 2015 had this capacity, let alone

capability. Therefore, future studies should consider the optimization of burn care resources in such a scenario.

5.4.3. Implications for Preparedness Measures

The overwhelming and catastrophic nature of an IND detonation in Atlanta, GA necessitates comprehensive and preemptive planning and preparedness considerations. These measures should range from planning efforts to include ancillary medical groups (such as pharmacists, dentists, and veterinarians) and volunteer agencies (such as the Medical Reserve Corps) to planning efforts to increase health care capacity. While the federal government would provide additional resources, planning efforts to effectively integrate all levels of the response, and their associated resources, must be made. Due to the associated threat to national security, the Federal Bureau of Investigation (FBI) would send a Weapons of Mass Destruction (WMD) coordinator to the scene to develop a unified command structure.[128] However, confusion remains on how the chain of command would function. Participants in previous exercises and workshops have indicated persistent confusion regarding what federal resources would be available and how command of the scene would function.[272] While it is not possible to plan for all contingencies in such a complex incident, realistic exercises are vital to the success of the response to an IND detonation.[128] As such, future research, in coordination with training and exercises, should endeavor to include all members of the emergency management community in planning efforts to coalesce the enormously complex response.

An IND detonation is so overwhelming that some experts have gone so far as to suggest there is no point in trying to increase our collective preparedness for such an incident. Gale and Armitage[13] go so far as to argue existing medical preparedness efforts are “obviously useless” in the context of a nuclear device detonation. Saur and Thakur determined “no society can ever be

prepared for such a scenario" when analyzing the number of critical care beds required in the aftermath of a nuclear detonation. This study illustrated pronouncements are incorrect. While it will not be possible to save every single patient, it will be possible to save a significant proportion through proactive preparedness efforts. Education surrounding the importance of sheltering is perhaps one of the most straightforward preparedness measures to implement. This study showed that effectively sheltering-in-place for 48 hours could save between 4,384 and 10,453 lives, just among those who were only exposed to radiation (and not blast or thermal effects). This would be the equivalent of saving between 1.5 and 3.5 times the number of lives lost in the September 11th attacks. Furthermore, sheltering caused a reduction of 1,952 to 9,516 patients requiring immediate health care who would place the greatest strain on the health care system. This reduction is comparable to the total number of available beds across the entire state and therefore clearly plays a critical role in planning an effective response.

Additionally, while the local and state health care resources would be overwhelmed in such an incident, the resources available across the country would be leveraged to support such a response. In 2019, the US had an estimated 919,559 staffed beds across 6,090 hospitals, with an average occupancy rate of 64.4%.[298] This suggests that, on average, there are approximately 327,363 staffed beds available across the country, which would far exceed the need demonstrated in this study. Even though this study focused on the first 48 hours post-detonation, federal resources, including Disaster Medical Assistance Teams (DMATs) under the National Disaster Medical System (NDMS), would arrive to support the response by 72 hours post-detonation. DMATs and other NDMS resources would work to redistribute any surviving patients still in need of medical treatment. Planning efforts to include and optimize these

invaluable resources are a crucial example of preparedness measures that will be invaluable in ensuring the success of the response.

The misconception that preparedness is useless is further highlighted within the context of other hazards upon which the emergency management and public health communities continually focus preparedness measures. The total estimated fatalities in this study across all four simulations are less than any prior pandemic in the 20th and 21st centuries, including the Spanish Influenza and COVID-19 pandemics.[299] Even though the COVID-19 pandemic in particular overwhelmed the health care system by almost every measure,[300] the emergency management and health care communities continued their dedication into responding as effectively as possible, given the resources available. Moreover, the overall lack of preparedness due to a lack of threat recognition is often cited in criticisms in the success of the US' response to the COVID-19 pandemic.[301,302] The COVID-19 pandemic should be regarded as a cautionary example of how poor assumptions regarding the importance of planning and preparedness efforts can have dire consequences.

This study demonstrated there remains a tremendous opportunity for increasing preparedness measures, prior to the detonation of an IND in an urban environment. Certain measures, like increasing public awareness of the "Get Inside, Stay Inside, Stay Tuned" campaign[280] or cross-training medical providers, are more straightforward than others, such as strategically placing resources on the north side of the city (where the fallout radiation is least likely to occur) or focusing on biological research for mass treatment of burn injuries and ARS. Fundamentally, the emergency management, public health, and health care communities have an obligation to prepare the public and infrastructure for such a catastrophic incident.

5.4.4. Limitations and Areas for Future Research

As with any model of such complexity for an unprecedented incident, there are many sources of uncertainty in the input parameters and limitations in the various models included in this study. The limitations of the modeling framework were previously elucidated in Chapter 4 (Section 4.4). Within the specifications of this study, the most significant limitation resides in the approximation of the thermal injuries. Due to a lack of available data, this study was not able to include estimations of %TBSA, a critical measure in predicting the mortality of patients with burn injuries.[303,304] Furthermore, the thresholds considered for thermal effects only considered the risk of flash burn from the fireball; these thresholds did not consider flame burns from secondary burns or inhalation injuries. Federal guidance documents predict significant smoke in the moderate damage zone,[280] and injury from smoke inhalation dramatically affects the likelihood of survival.[150,304,305] As such, future studies should endeavor to identify methods to connect the modeling workflow to these specific health effects. Future studies should also consider incorporating demographic data for the affected population, as evidence suggests thermal burn severity varies by skin color[64] and radiation affects various age groups differently.[188]

Lastly, the data regarding the hospital bed capacity and occupancy were collected during the COVID-19 pandemic. While measures were taken to minimize conflation associated with the increased strain on the health care system during the period, it is possible this study underestimates the true availability of beds in the state. The seven day window used to estimate bed availability corresponds to the beginning of the pandemic, and several studies have shown a substantial decline in the patient volume during that period relative to 2019.[306–312] Future studies should endeavor to collect bed availability data during non-pandemic periods in order to

accurately assess the health care resource availability. Furthermore, future work should also consider how mass panic may affect access and utilization of health care resources, given the significant number of minimally injured patients who will primarily require emotional comfort and guidance.

5.4.5. Conclusions

In conclusion, this study leveraged improved modeling workflow to more realistically characterize the estimated casualties in the aftermath of an IND detonation in a major US city. Including the RTR triage categories and granular descriptions of the injury profiles within each triage category provided an unprecedented insight into the anticipated casualties. This study also clearly demonstrated that the health care resources in the state, as well as specialty resources like burn centers would be almost immediately overwhelmed in the event of such an incident. This discrepancy between available resources and anticipated needs functions as a call to action for the emergency management and health care communities to increase planning efforts, including training and exercises, to more effectively prepare for such a catastrophic incident.

CHAPTER 6

SUMMARY AND CONCLUSIONS

6.1. Summary of the Problem

Despite the increasing risk of a nuclear attack on United States (US) soil, most organizations, but especially local and state agencies, remain largely unprepared for a nuclear disaster.[4–6] Furthermore, the federal planning guidance for response to a nuclear detonation[8] states that federal resources may take up to 72 hours to arrive following a nuclear disaster. This delay leaves local and state officials responsible for managing the aftermath for the first three days, when rescue and treatment efforts are the most urgent. As such, efforts to increase the understanding of, and preparedness for, the threat and impacts of a nuclear disaster at local and state levels are essential for future successful responses.

Models and simulations provide the only feasible mechanism to allow comprehension of the magnitude and complexity of such an event. Given the rare nature of such incidents, it is imperative that researchers continually expand upon existing modeling methodology to increase the accuracy and validity of nuclear models to better support the emergency management, health care, and public health communities in their preparedness efforts for a nuclear detonation.

This dissertation is comprised of three studies that take measured steps towards such a goal, by using sample simulated 15 kiloton (kt) improvised nuclear device (IND) detonations in Atlanta, Georgia (GA). The first aim characterized the possible distribution of, and clustered the fallout radiation plumes resulting from, simulated IND detonations throughout the year 2019. The second aim expanded upon the modeling framework to account for thermal and radiation

effects in an urban environment. The third and final aim consolidated the results of the previous aims to estimate the casualties resulting from the detonation and to understand the health care systems' capacity to respond to such an incident.

6.2. Characterization of Fallout Radiation Patterns

To better understand the variation in fallout radiation distribution following an IND detonation in Atlanta, GA, this study leveraged historical surface-level and three-dimensional (3D) weather data to generate and characterize simulated fallout radiation plumes corresponding to detonation at 10:00 am local time each day of the year 2019. The resulting mean plume extended 160.25 kilometers (km) east from the detonation site, covering 3,174.44 km^2 and placing nearly 3.7 million people at risk for radiation exposure. The majority of the plumes extended in the NE to SE direction, with a small secondary peak of plumes extending SW from the detonation site. Within the fallout radiation plume, nearly two-thirds (61%) of the affected population resided within the lowest risk radiation dose category (0 – 100 rad), where risk of developing acute radiation sickness (ARS) is extremely limited.

The fallout plumes were then classified into four clusters, following the application of a partition around medoids (PAM) clustering algorithm on the spatial patterns and affected populations in the plumes. In evaluation of the optimum number of clusters, selecting fewer than four clusters did not accurately capture the variation in the cumulative fallout radiation plume angle and distance after 48 hours, while affected population estimates within the survivability categories overlapped significantly with additional clusters. The four medoids of the assigned clusters were used as the simulated dates of detonation in the subsequent aims of this dissertation to capture the possible geospatial variation in impact of the nuclear effects. This inclusion provides a critical opportunity to understand the breadth of possible impacts following an IND

detonation; an aspect that has previously been largely ignored in the published literature.[58,132,295,313,314]

As the last component of this study, four machine learning (ML) algorithms were constructed as the first of their kind to predict the fallout radiation plume classification from surface-level weather conditions. Among the compared decision tree (DT), random forest (RF), least absolute shrinkage and selection operator (LASSO), and elastic net (EN) models, the RF had the best performance, with an accuracy of 51.16% and an AUC ROC of 0.76. The RF model identified relative humidity, cloud coverage, and sea level pressure at time of detonation, as well as daily dew point high and dew point range, as the five most important predictors of the plume clusters. As discussed below, future research should endeavor to identify relationships with accessible weather data to increase the accuracy of these prediction models far beyond the 50% accuracy found in this study for such models to be applicable in practical settings.

6.3. Modeling Thermal and Radiation Effects in an Urban Environment

This study introduced the integration of building-specific architectural attributes into the nuclear modeling framework to improve the accuracy of models for the thermal and radiation effects of a nuclear detonation in an urban environment, as increasing the accuracy of models is an imperative step in better understanding the true impact of nuclear detonations. The results of this adaptation of the modeling workflow highlight the importance of building-specific characterizations. Under the thermal attenuation model, approximately half of the buildings that would have previously been assumed to have been exposed to enough thermal fluence to cause either burns or mass fires were shadowed by the surrounding environment and therefore were no longer exposed to such levels of thermal radiation. This suggests the thermal effects in an urban environment can neither be assumed to be uniform nor be ignored in comprehensive nuclear

models. Even with the thermal attenuation model, more than 18,000 buildings would be exposed to enough thermal fluence to cause at least 50% probability of second- or third-degree burns, nearly half of which would likely receive enough thermal fluence for the occurrence of mass fires. Such effects would easily overwhelm the existing firefighting and burn health care resources,[19] further emphasizing the need for preparedness efforts among the emergency management communities.

This study also improved upon the existing Regional Shelter Analysis (RSA) methodology[34] for protection factors (PFs) by incorporating building-specific PF estimates for both fallout and prompt radiation. The introduction of building-by-building evaluation of PFs further highlighted the importance of preparedness measures by showing the efficacy of sheltering from radiation. In all four simulations under a warned scenario, in which members of the public would have time to seek shelter in a basement or in the most interior room of a building, more than 90% of buildings that were externally exposed to more than 200 rads of fallout radiation actually received less than 200 rads internally due to the protection offered by building characteristics, such as construction material, height, and the presence of a basement. While some argue that any warning is unlikely to be feasible in such a scenario,[272] even an unwarned scenario, which assumes an even distribution of people throughout a building, demonstrated significant reductions in radiation dose when considering building-specific PFs. In three of the four simulations under an unwarned scenario, more than 90% of buildings that were exposed to more than 600 rads of fallout radiation actually received less than 600 rads inside the buildings. Therefore, the introduction of building-specific architectural attributes to account for the protection offered from radiation effects by buildings, as well as the attenuation of the

thermal effects released by the fireball, crucially highlighted the role shelters play in health outcomes.

6.4. Casualty Estimates and Scarcity of Health Resources

The final model in this dissertation built upon the previous studies to realistically characterize the casualties resulting from the detonation and to understand the health care capacity to respond to such an incident. Few other models have reported specific casualty estimates,[37,58,120,280] and even fewer have reported specific injuries.[126,128] Across the four simulated detonations, an estimated 185,896 to 196,537 individuals would not survive their injuries, and an additional 31,939 to 46,668 patients would require immediate health care. An additional 454,015 to 1,060,235 individuals would require delayed or minimal health care. This study also provided an unprecedented insight into the predicted injury profiles within triage categories, assigned by the Radiation Triage, Treat, and Transport System (RTR) algorithm. Among the minimally injured category, the most common injury profiles were subclinical ARS with and without minimal trauma. Among the delayed category, the most common injury profile was hematopoietic ARS and moderate trauma. However, among patients who would require immediate health care, the majority would present with moderate trauma (and minimal radiation injury and no burn). These results suggest a critical point of education for first responders and health care providers: most of the patients they will treat will have injuries similar to injuries they treat every day.

While the hundreds of thousands of casualties resulting from a nuclear weapon detonation would overwhelm the health care infrastructure, this strain would be further exacerbated by losing health care facilities directly to the effects of the detonation. Across the four simulated detonations, even when considering surge capacity, there are only enough staffed

beds in GA for approximately 25% of the patients requiring immediate health care. These limitations are particularly pronounced for patients presenting with predominantly burn injuries, as the 232 unaffected, staffed burn beds in GA would not be able to accommodate the estimated 6,913 to 9,444 patients with predominantly burn injuries resulting from the detonation. Even if every burn center across the US could increase their bed capacity by a factor of 1.5 in a no-notice event, there would only be 3,000 burn beds available, which would cover less than half of the patients requiring immediate burn care. Therefore, as discussed below, future research should consider methods to optimize limited health care, and particularly burn care, resources in such a scenario.

An IND detonation is so overwhelming that some experts have gone so far as to suggest there is no point in trying to increase our collective preparedness for such an incident.[13,127] This study clearly illustrated that these pronouncements are incorrect. Education surrounding the importance of sheltering is perhaps one of the most straightforward preparedness measures to implement. Effectively sheltering-in-place for 48 hours could save between 4,384 and 10,453 lives, just among those who were only exposed to radiation (and not blast or thermal effects). This would be the equivalent of saving between 1.5 and 3.5 times the number of lives lost in the September 11th attacks. Furthermore, sheltering would cause a reduction of 1,952 to 9,516 patients requiring immediate health care who would place the greatest strain on the health care system. This reduction is a significant proportion of the total number of available beds across the entire state and therefore clearly plays a critical role in planning an effective response.

6.5. Future Work

Several aspects of this work should be expanded upon in the future. As it relates to the fallout radiation patterns and synoptic weather analyses, future studies should examine a longer

study period or alternative cities, to account for climatological perturbations. Future work should also focus on identifying other sources of accessible weather data that may be more closely associated with likely fallout patterns, such as upper-level atmospheric weather data or an air mass classification system that captures upper-level atmospheric conditions. Accurately tuning the prediction of the fallout radiation plume clusters could plausibly support operational decision making for local responders until federal or military assets mobilize to predict the plume with real-time modeling capabilities.

Continuing to improve the nuclear modeling workflow will be essential to better support planners in the emergency management, health care, and public health communities. Future work on the thermal effects model should examine the protective role of buildings and/or vehicles from thermal effects and determine ways to include alternative consequences of the thermal effect, such as secondary fires and mass fires. Future studies focusing on the radiation effects should include a sensitivity analysis on the PF estimates, which may have implications for shelter-in-place versus evacuation decisions. Additionally, future work should consider the variation of PFs within a building, perhaps by applying the RSA methodology to a building-level resolution. To further understand the distribution of casualties, future models should also consider incorporating demographic information, as demographic characteristics may have a significant impact on the type and the geospatial distribution of predicted injuries.

There remain many limitations on the resources required for mass casualty management in the aftermath of an IND, including specialized beds for patients with burn injuries, pharmaceutical interventions, respiratory therapy, and mass decontamination. Future work should consider identifying alternative sources that could relieve the strain on the health care infrastructure, including the resources that may be available on a federal level, including the

National Disaster Medical System (NDMS). Future studies could also leverage ML and predictive modeling to optimize the limited resources. One example of such a study could use ML to predict the likelihood of mortality among burn patients, given prehospital presentations. Furthermore, operational research (OR) methods could be used to identify specific points of strain in the health care system, which would help identify key opportunities for preparedness measures. OR methods could also be used to validate proposed triage models, such as the RTR algorithm or the American Burn Association (ABA) triage tables. Lastly, OR methods could be used to better understand the role of community reception centers, mass care sites, and points of dispensing that could augment the limited health care resources. A broad range of modeling and simulation methods could be used to further support the emergency management, health care, and public health communities in their preparedness efforts.

While it will not be possible to plan for all contingencies in such a complex incident, realistic training and exercises will be vital to the success of a response. It will be crucial for all levels of responders, from local to federal to military, to understand how the various responding agencies will integrate to form a clear incident command system and the availability and timeline of resources to support the response. Training and exercises dedicated to informing health care responders about the most likely patients and correcting misinformation or fear about radiation are necessary to ensure the health care system responds as best as possible, given the resources available during such an incident. Proactive, robust, and innovative training and exercises among federal agencies, military resources, local and state responders, and academic institutions, based on increasingly accurate models and simulations, will be imperative for a successful response to an IND detonation in the US.

REFERENCES

1. Douple EB, Mabuchi K, Cullings HM, et al. Long-term Radiation-Related Health Effects in a Unique Human Population: Lessons Learned from the Atomic Bomb Survivors of Hiroshima and Nagasaki. *Disaster Med Public Health Prep*. 2011;5(S1):S122-S133. doi:10.1001/dmp.2011.21
2. The Manhattan Engineer District. *The Atomic Bombings of Hiroshima and Nagasaki | Historical Documents*. United States Department of the Army; 1946:102. Accessed March 23, 2023. https://www.atomicarchive.com/resources/documents/med/index.html
3. Perry WJ, Collina TZ. *The Button: The New Nuclear Arms Race and Presidential Power from Truman to Trump*. Vol 1. 1st ed. BenBella Books; 2020.
4. Malus K. Nuclear disaster: How prepared are we? In: Columbia University; 2018. Accessed September 16, 2021. https://k1project.columbia.edu/content/nuclear-disaster-how-prepared-are-we
5. Davis M, Proctor M, Shageer B. A Systems-Of-Systems Conceptual Model and Live Virtual Constructive Simulation Framework for Improved Nuclear Disaster Emergency Preparedness, Response, and Mitigation. *J Homel Secur Emerg Manag*. 2016;13(3):367-393. doi:10.1515/jhsem-2015-0051
6. Hauer JM. US cities are not medically prepared for a nuclear detonation. *Bull At Sci*. 2017;73(4):215-219. doi:10.1080/00963402.2017.1338003
7. Desai SP, Bell WC, Harris C, Burkle FM, Dallas CE. Human Consequences of Multiple Nuclear Detonations in New Delhi (India): Interdisciplinary Requirements in Triage

Management. *Int J Environ Res Public Health*. 2021;18(4):1740. doi:10.3390/ijerph18041740

8. National Security Staff, Interagency Policy Coordination Subcommittee for Preparedness & Response to Radiological and Nuclear Threats. *Planning Guidance for Response to a Nuclear Detonation*. 2nd ed. Homeland Security Council Interagency Policy Coordination Subcommittee for Preparedness and Response to Radiological and Nuclear Threats; 2010. https://irp.fas.org/threat/detonation.pdf
9. Eden L. *Whole World on Fire: Organizations, Knowledge, & Nuclear Weapons Devastation*. 1st ed. Cornell University Press; 2006.
10. Armbruster P. Nuclear structure in cold rearrangement processes in fission and fusion. *Rep Prog Phys*. 1999;62(4):465-525. doi:10.1088/0034-4885/62/4/001
11. Centers for Disease Control and Prevention, National Cancer Institute. *Report on the Feasibility of a Study of the Health Consequences to the American Population from Nuclear Weapons Tests Conducted by the United States and Other Nations.*; 2005. https://www.cdc.gov/nceh/radiation/fallout/default.htm
12. Kim JH. Three principles for radiation safety: time, distance, and shielding. *Korean J Pain*. 2018;31(3):145-146. doi:10.3344/kjp.2018.31.3.145
13. Gale RP, Armitage JO. Are We Prepared for Nuclear Terrorism? *N Engl J Med*. 2018;378(13):1246-1254. doi:10.1056/NEJMsr1714289
14. DeLia D, Wood E. The dwindling supply of empty beds: implications for hospital surge capacity. *Health Aff Proj Hope*. 2008;27(6):1688-1694. doi:10.1377/hlthaff.27.6.1688
15. Blumenthal D, Fowler EJ, Abrams M, Collins SR. Covid-19 — Implications for the Health Care System. *N Engl J Med*. 2020;383(15):1483-1488. doi:10.1056/NEJMsb2021088

16. Dallas CE, Bell WC, Stewart DJ, Caruso A, Burkle FM. Nuclear war between Israel and Iran: lethality beyond the pale. *Confl Health*. 2013;7(1):10. doi:10.1186/1752-1505-7-10

17. Bell WC, Dallas CE. Vulnerability of populations and the urban health care systems to nuclear weapon attack – examples from four American cities. *Int J Health Geogr*. 2007;6(1):5. doi:10.1186/1476-072X-6-5

18. Al-Mousawi AM, Mecott-Rivera GA, Jeschke MG, Herndon DN. Burn Teams and Burn Centers: The Importance of a Comprehensive Team Approach to Burn Care. *Clin Plast Surg*. 2009;36(4):547-554. doi:10.1016/j.cps.2009.05.015

19. Kearns RD, Bettencourt AP, Hickerson WL, et al. Actionable, Revised (Version 3), and Amplified American Burn Association Triage Tables for Mass Casualties: A Civilian Defense Guideline. *J Burn Care Res*. 2020;41(Supplement_1):S65-S66. doi:10.1093/jbcr/iraa024.103

20. Shartar S. Region D & Region N Mass Casualty Incident ED Surge Capacity Tool. Published online March 25, 2016.

21. American Hospital Directory. Individual Hospital Statistics for Georgia. Individual Hospital Statistics for Georgia. Published July 26, 2021. Accessed September 19, 2021. https://www.ahd.com/states/hospital_GA.html

22. Harris C, McCarthy K, Liu EL, et al. Expanding Understanding of Response Roles: An Examination of Immediate and First Responders in the United States. *Int J Environ Res Public Health*. 2018;15(3):534. doi:10.3390/ijerph15030534

23. Department of Defense. U.S. Department of Defense - About. U.S. Department of Defense. Accessed September 19, 2021. https://www.defense.gov/Our-Story/

24. Defense Threat Reduction Agency. DTRA - About Us. About Us. Accessed September 19, 2021. https://www.dtra.mil/About/

25. Defense Threat Reduction Agency. Nuclear Enterprise Directorate. Nuclear-Enterprise. Accessed September 19, 2021. https://www.dtra.mil/Mission/Mission-Directorates/Nuclear-Enterprise/

26. Government Accountability Office. Nuclear Weapons: Emergency Preparedness Planning for Accidents Can Be Better Coordinated. Published online February 10, 1987. https://www.gao.gov/assets/nsiad-87-15.pdf

27. Redlener I. *Americans at Risk: Why We Are Not Prepared for Megadisasters and What We Can Do*. 1st ed. Knopf; 2006.

28. Dahlman O, Svein M, Haak H. *Nuclear Test Ban: Converting Political Visions to Reality*. 1st ed. Springer Netherlands; 2009. https://www.springer.com/gp/book/9781402068836

29. Federation of American Scientists. Status of World Nuclear Forces. Federation Of American Scientists. Accessed September 19, 2021. https://fas.org/issues/nuclear-weapons/status-world-nuclear-forces/

30. Joint Chiefs of Staff. Joint Nuclear Operations. Published online April 17, 2020. Accessed September 16, 2021. https://irp.fas.org/doddir/dod/jp3_72_2020.pdf

31. Kristensen HM, Norris RS. United States nuclear forces, 2018. *Bull At Sci*. 2018;74(2):120-131. doi:10.1080/00963402.2018.1438219

32. Federal Emergency Management Agency. IS-3: Radiological Emergency Management. https://training.fema.gov/emiweb/downloads/is3_is3all.pdf

33. The Committee for the Compilation of Materials on Damage Caused by the Atomic Bombs in Hiroshima and Nagasaki. Hiroshima and Nagasaki: The Physical, Medical, and Social

Effects of Atomic Bombings. *Am Polit Sci Rev*. 1982;76(2):474-474. doi:10.1017/S0003055400187957

34. Dillon MB, Dennison D, Kane J, Walker H, Miller P. *Regional Shelter Analysis Methodology*. Lawrence Livermore National Lab. (LLNL); 2015:63. https://www.osti.gov/servlets/purl/1236135
35. Institute of Medicine (US) Steering Committee for the Symposium on the Medical Implications of Nuclear War. *The Medical Implications of Nuclear War*. (Solomon F, Marston RQ, eds.). National Academies Press (US); 1986. Accessed March 7, 2022. http://www.ncbi.nlm.nih.gov/books/NBK219152/
36. Diem JE, Hursey MA, Morris IR, Murray AC, Rodriguez RA. Upper-Level Atmospheric Circulation Patterns and Ground-Level Ozone in the Atlanta Metropolitan Area. *J Appl Meteorol Climatol*. 2010;49(11):2185-2196.
37. Buddemeier B, Dillon MB. Key Response Planning Factors for the Aftermath of Nuclear Terrorism. Published online August 2009. https://www.osti.gov/servlets/purl/966550
38. Dixon PG, Mote TL. Patterns and Causes of Atlanta's Urban Heat Island–Initiated Precipitation. *J Appl Meteorol Climatol*. 2003;42(9):1273-1284. doi:10.1175/1520-0450(2003)042<1273:PACOAU>2.0.CO;2
39. Feliciano DV, Anderson Jr GV, Rozycki GS, et al. Management of casualties from the bombing at the Centennial Olympics - ScienceDirect. *Am J Surg*. 1998;176(6):538-543.
40. Federal Emergency Management Agency. *Risks & Hazards: A State by State Guide (FEMA-196)*. Federal Emergency Management Agency (FEMA); 1990. http://archive.org/details/Risks_hazards_A_State_by_State_Guide_FEMA196

41. Federal Emergency Management Agency. *Nuclear Attack Planning Base - 1990*. Federal Emergency Management Agency (FEMA); 1987. Accessed March 1, 2023. https://nuke.fas.org/guide/usa/napb-90/
42. U.S. Census Bureau. Geography Profile for Atlanta city, Georgia. Census - Geography Profile. Published December 2020. Accessed September 19, 2021. https://data.census.gov/cedsci/profile?g=1600000US1304000
43. O'Shea B. Population in Atlanta: How large is metro Atlanta? *The Atlanta Journal-Constitution*. July 11, 2021.
44. Kaiser Family Foundation. *Total Hospital Beds*. Kaiser Family Foundation; 2022. Accessed March 18, 2023. https://www.kff.org/other/state-indicator/total-hospital-beds/
45. Binninger G, Hodge JK, Wright S, Holl S. *Development of a Fire Prediction Model for Use within HPAC*. L3 Titan Corp; 2003:86.
46. Badash L, Hodes E, Tiddens A. Nuclear Fission: Reaction to the Discovery in 1939. *Proc Am Philos Soc*. 1986;130(2):196-231.
47. Gosling FG. *The Manhattan Project: Making the Atomic Bomb*. DIANE Publishing; 1999.
48. Cirincione J. *Bomb Scare: The History and Future of Nuclear Weapons*. Columbia University Press; 2007.
49. Serber R. *The Los Alamos Primer: The First Lectures on How to Build an Atomic Bomb, Updated with a New Introduction by Richard Rhodes*. University of California Press; 2020. doi:10.1525/9780520374331
50. Hoddeson L, Henriksen PW, Meade RA, Westfall C. *Critical Assembly: A Technical History of Los Alamos during the Oppenheimer Years, 1943 - 1945*. Vol 1. 1st ed. Cambridge University Press; 2004.

51. U.S. Department of Energy. *United States Nuclear Tests: July 1945 through September 1992*. U.S. Department of Energy; 1993:38.

52. Johnson JD. *Truman's Atomic Bomb Decision. An Attack on Japan's Center of Gravity.* ARMY WAR COLL CARLISLE BARRACKS PA; 1996. Accessed May 1, 2022. https://apps.dtic.mil/sti/citations/ADA308515

53. Kawai K. Mokusatsu, Japan's Response to the Potsdam Declaration. *Pac Hist Rev*. 1950;19(4):409-414. doi:10.2307/3635822

54. Ishikawa E, Swain DL. *Hiroshima and Nagasaki: The Physical, Medical, and Social Effects of the Atomic Bombings*. Basic Books, Inc, Publishers; 1981.

55. Leffler MP, Westad OA. *The Cambridge History of the Cold War*. Cambridge University Press; 2010.

56. Fuhrmann M, Lupu Y. Do Arms Control Treaties Work? Assessing the Effectiveness of the Nuclear Nonproliferation Treaty 1. *Int Stud Q*. 2016;60(3):530-539. doi:10.1093/isq/sqw013

57. Popp R, Horovitz L, Wenger A. *Negotiating the Nuclear Non-Proliferation Treaty: Origins of the Nuclear Order*. Taylor & Francis; 2016.

58. Shubayr NAM. *Planning Guidance for Emergency Response to a Hypothetical Nuclear Attack on Riyadh, Saudi Arabia*. Ph.D. University of Massachusetts Lowell. Accessed April 20, 2022. https://www.proquest.com/docview/1929235843/abstract/B64C5DDD918C4B7APQ/1

59. Bunn M. How Nuclear Bombs Work. Lecture presented at: September 10, 2013; Harvard Kennedy School.

60. Bunn M. Making the Essential Ingredients of Nuclear Weapons. Lecture presented at: September 12, 2013; Harvard Kennedy School.
61. Schmitz R. Introduction to Nuclear Physics: Structure of Matter, Basic Nuclear Phenomenology, and Nuclear Stability and Decay. Lecture presented at: May 31, 2007; University of Washington. http://depts.washington.edu/uwmip/
62. O'Brien J. *Nuclear Physics and Reactor Theory*. Vol 1. U.S. Department of Energy; 2015.
63. Leachman RB. Emission of Prompt Neutrons from Fission. *Phys Rev*. 1956;101(3):1005-1011. doi:10.1103/PhysRev.101.1005
64. Glasstone S, Dolan PJ. *The Effects of Nuclear Weapons. Third Edition*. Department of Defense, Washington, D.C. (USA); Department of Energy, Washington, D.C. (USA); 1977. doi:10.2172/6852629
65. Dolan PJ. *Capabilities of Nuclear Weapons - Defense Nuclear Agency Effects Manual Number One*. Defense Nuclear Agency; 1972.
66. McQuarrie DA, Simon JD. *Physical Chemistry: A Molecular Approach*. 1st ed. University Science Books; 1997.
67. Richardt A, Hülseweh B, Niemeyer B, Sabath F. *CBRN Protection: Managing the Threat of Chemical, Biological, Radioactive and Nuclear Weapons*. John Wiley & Sons; 2013.
68. Burns RD, Siracusa JM. *A Global History of the Nuclear Arms Race: Weapons, Strategy, and Politics [2 Volumes]: Weapons, Strategy, and Politics*. ABC-CLIO; 2013.
69. Federal Emergency Management Agency. Nuclear/Radiological Incident Annex to the Response and Recovery Federal Interagency Operational Plans. Published online October 2016.

70. Bellamy RF, Zajtchuk R. *Conventional Warfare: Ballistic, Blast, and Burn Injuries*. Walter Reed Army Institute of Research, Walter Reed Army Medical Center; 1991.
71. US Department of Commerce N. Speed of Sound Calculator. Accessed May 1, 2022. https://www.weather.gov/epz/wxcalc_speedofsound
72. Buddemeier B, Valentine J, Millage K, Brandt L. National Capital Region Key Response Planning Factors for the Aftermath of Nuclear Terrorism. Published online November 2011.
73. Defense Threat Reduction Agency. Exercise Vista Forge: 10kT IND in Atlanta, GA. Published online January 27, 2022.
74. Mathews ZR, Koyfman A. Blast Injuries. *J Emerg Med*. 2015;49(4):573-587. doi:10.1016/j.jemermed.2015.03.013
75. Kirkman E, Watts S, Cooper G. Blast injury research models. *Philos Trans R Soc B Biol Sci*. 2011;366(1562):144-159. doi:10.1098/rstb.2010.0240
76. Jorolemon MR, Lopez RA, Krywko DM. Blast Injuries. In: *StatPearls*. StatPearls Publishing; 2022. Accessed May 1, 2022. http://www.ncbi.nlm.nih.gov/books/NBK430914/
77. Departments of the Army, the Navy, and the Air Force. *NATO Handbook on the Medical Aspects of NBC Defensive Operations AMedP-6(B)*. United States. Department of the Army; 1996:442. Accessed March 7, 2022. https://www.hsdl.org/?abstract&did=459640
78. Sartori L. Effects of nuclear weapons. *Phys Today*. 1983;83(9).
79. Walker RI, Cerveny TJ, eds. *Textbook of Military Medicine, Part 1: Warfare, Weaponry, and the Casualty, Volume 2: Medical Consequences of Nuclear Warfare*. Vol 2. TMM Publications, Office of the Surgeon General; 1989.

80. Walker PF, Buehner MF, Wood LA, et al. Diagnosis and management of inhalation injury: an updated review. *Crit Care*. 2015;19(1):351. doi:10.1186/s13054-015-1077-4

81. Jeschke MG, Kamolz LP, Sjoberg F, Wolf SE. *Handbook of Burns: Acute Burn Care*. Vol 1. 2nd ed. Springer; 2020.

82. Toussaint J, Singer AJ. The evaluation and management of thermal injuries: 2014 update. *Clin Exp Emerg Med*. 2014;1(1):8-18. doi:10.15441/ceem.14.029

83. Evers LH, Bhavsar D, Mailänder P. The biology of burn injury. *Exp Dermatol*. 2010;19(9):777-783. doi:10.1111/j.1600-0625.2010.01105.x

84. Warby R, Maani CV. Burn Classification. In: *StatPearls*. StatPearls Publishing; 2022. Accessed March 29, 2022. http://www.ncbi.nlm.nih.gov/books/NBK539773/

85. Tolles J. Emergency department management of patients with thermal burns. *Emerg Med Pract*. 2018;20(2):1-24.

86. American Burn Association. Advanced Burn Life Support Course Provider Manual. Published online 2018.

87. Lee S, Rahul, Ye H, et al. Real-time Burn Classification using Ultrasound Imaging. *Sci Rep*. 2020;10(1):5829. doi:10.1038/s41598-020-62674-9

88. Eisenbeiß W, Marotz J, Schrade JP. Reflection-optical multispectral imaging method for objective determination of burn depth. *Burns*. 1999;25(8):697-704. doi:10.1016/S0305-4179(99)00078-9

89. Hoeksema H, Van de Sijpe K, Tondu T, et al. Accuracy of early burn depth assessment by laser Doppler imaging on different days post burn. *Burns*. 2009;35(1):36-45. doi:10.1016/j.burns.2008.08.011

90. McGill DJ, Sørensen K, MacKay IR, Taggart I, Watson SB. Assessment of burn depth: A prospective, blinded comparison of laser Doppler imaging and videomicroscopy. *Burns*. 2007;33(7):833-842. doi:10.1016/j.burns.2006.10.404

91. American Burn Association. Burn Center Referral Criteria. Accessed April 9, 2022. https://ameriburn.org/public-resources/burn-center-referral-criteria/

92. Armstrong JR, Willand L, Gonzalez B, Sandhu J, Mosier MJ. Quantitative Analysis of Estimated Burn Size Accuracy for Transfer Patients. *J Burn Care Res*. 2017;38(1):e30-e35. doi:10.1097/BCR.0000000000000460

93. Parvizi D, Kamolz LP, Giretzlehner M, et al. The potential impact of wrong TBSA estimations on fluid resuscitation in patients suffering from burns: Things to keep in mind. *Burns*. 2014;40(2):241-245. doi:10.1016/j.burns.2013.06.019

94. McCulloh C, Nordin A, Talbot LJ, Shi J, Fabia R, Thakkar RK. Accuracy of Prehospital Care Providers in Determining Total Body Surface Area Burned in Severe Pediatric Thermal Injury. *J Burn Care Res*. 2018;39(4):491-496. doi:10.1093/jbcr/irx004

95. Fajardo LF, Berthrong M, Anderson RE. *Radiation Pathology*. Oxford University Press; 2001.

96. Morita M. Nuclear Excitation by Electron Transition and Its Application to Uranium 235 Separation. *Prog Theor Phys*. 1973;49(5):1574-1586.

97. Humans IWG on the E of CR to. *Neutrons*. International Agency for Research on Cancer; 2000. Accessed May 10, 2022. https://www.ncbi.nlm.nih.gov/books/NBK401333/

98. Bickel JH. Module 3: Neutron Induced Reactions. Lecture presented at: Fundamentals of Nuclear Engineering; USA.

99. Assistant Secretary for Preparedness and Response. *A Decision Makers Guide: Medical Planning and Response for a Nuclear Detonation*. Assistant Secretary for Preparedness and Response; 2017:212. Accessed March 7, 2022. https://remm.hhs.gov/decisionmakersguide.htm
100. Ghita G. Prompt Radiation Protection Factors. Published online February 2018:35.
101. Stricklin D, Prins R, Zaru-Roque I, Bellman J. Modification of Acute Radiation Response in Different Demographic Age Groups. Published online October 2017.
102. Waselenko JK, MacVittie TJ, Blakely WF, et al. Medical management of the acute radiation syndrome: recommendations of the Strategic National Stockpile Radiation Working Group. *Ann Intern Med*. 2004;140(12):1037-1051. doi:10.7326/0003-4819-140-12-200406150-00015
103. Radiation Emergency Assistance Center / Training Site. *The Medical Aspects of Radiation Incidents*. 4th ed. Oak Ridge Associated Universities; 2017.
104. Fliedner TM, Friesecke I, Beyrer K. *Medical Management of Radiation Accidents: Manual on the Acute Radiation Syndrome*. British Inst of Radiology; 2001.
105. López M, Martín M. Medical management of the acute radiation syndrome. *Rep Pract Oncol Radiother J Gt Cancer Cent Poznan Pol Soc Radiat Oncol*. 2011;16(4):138-146. doi:10.1016/j.rpor.2011.05.001
106. Waghmare CM. Radiation burn—From mechanism to management. *Burns*. 2013;39(2):212-219. doi:10.1016/j.burns.2012.09.012
107. Fernández-Villaverde J, Levintal O. Solution methods for models with rare disasters. *Quant Econ*. 2018;9(2):903-944. doi:10.3982/QE744

108. Miller A. *A Comparison in the Accuracy of Mapping Nuclear Fallout Patterns Using HPAC, HYSPLIT, DELFIC FPT and an AFIT FORTRAN95 Fallout Deposition Code*. Air Force Institute of Technology; 2011. https://scholar.afit.edu/etd/1465

109. Pirhalla M. Dispersion Modeling Systems Relevant to Homeland Security Preparedness and Response. Published online October 21, 2020. https://cfpub.epa.gov/si/si_public_record_Report.cfm?dirEntryId=349940&Lab=CESER

110. Zhang XL, Chen JG, Su GF, Yuan HY. Study on Source Inversion Technology for Nuclear Accidents Based on Gaussian Puff Model and EnKF.

111. De Haan P, Rotach MW. A novel approach to atmospheric dispersion modelling: The Puff-Particle Model. *Q J R Meteorol Soc*. 1998;124(552):2771-2792. doi:10.1002/qj.49712455212

112. Hansen OR, Hinze P, Engel D, Davis S. Using computational fluid dynamics (CFD) for blast wave predictions. *J Loss Prev Process Ind*. 2010;23(6):885-906. doi:10.1016/j.jlp.2010.07.005

113. Clutter JK, Mathis JT, Stahl MW. Modeling environmental effects in the simulation of explosion events. *Int J Impact Eng*. 2007;34(5):973-989. doi:10.1016/j.ijimpeng.2006.03.003

114. Garces M. Explosion Source Models. In: Le Pichon A, Blanc E, Hauchecorne A, eds. *Infrasound Monitoring for Atmospheric Studies: Challenges in Middle Atmosphere Dynamics and Societal Benefits*. Springer International Publishing; 2019:273-345. doi:10.1007/978-3-319-75140-5_8

115. Price MA, Nguyen VT, Hassan O, Morgan K. An approach to modeling blast and fragment risks from improvised explosive devices. *Appl Math Model*. 2017;50:715-731. doi:10.1016/j.apm.2017.06.015

116. Nartu MK, Kumar M. Blast Response of Single-Degree-of-Freedom Systems Including Fluid-Structure Interaction. *J Struct Eng*. 2021;147(1):04020296. doi:10.1061/(ASCE)ST.1943-541X.0002878

117. Sisemore C, Babuška V. Single Degree-of-Freedom Systems. In: Sisemore C, Babuška V, eds. *The Science and Engineering of Mechanical Shock*. Springer International Publishing; 2020:45-85. doi:10.1007/978-3-030-12103-7_3

118. Ellobody E, Feng R, Young B. Chapter 3 - Finite Element Modeling. In: Ellobody E, Feng R, Young B, eds. *Finite Element Analysis and Design of Metal Structures*. Butterworth-Heinemann; 2014:31-55. doi:10.1016/B978-0-12-416561-8.00003-2

119. Martin SB. Fire Setting by Nuclear Explosion: A Revisit and Use in Nonnuclear Applications. *J Fire Prot Eng*. 2004;14(4):283-297. doi:10.1177/1042391504044541

120. Buddemeier BR, Dillon MB. *Key Response Planning Factors for the Aftermath of Nuclear Terrorism*. Lawrence Livermore National Lab. (LLNL), Livermore, CA (United States); 2011. doi:10.2172/966550

121. Parker A. A Science-Based Tool for Emergency Planning. Lawrence Livermore National Laboratory: Science & Technology Review. Published October 2018. Accessed March 1, 2023. https://str.llnl.gov/2018-10/alai

122. Stellar. FEMA Planning Tools: Introduction to the City Planner Resource (CPR). Presented at: October 17, 2018. https://rrt5.org/Portals/0/docs/Stellar%20-%20FEMA_chemCPR_Overview_EPA_RRT4_2018-10-10.pdf

123. NUKEMAP by Alex Wellerstein. Accessed April 29, 2022. https://nuclearsecrecy.com/nukemap/

124. Wellerstein A. The psychological power of nuclear weapons. *Bull At Sci*. 2016;72(5):298-303. doi:10.1080/00963402.2016.1216508

125. Eaves E. NUKEMAP creator Alex Wellerstein puts nuclear risk on the radar. *Bull At Sci*. 2017;73(4):211-214. doi:10.1080/00963402.2017.1338001

126. Gellert G. Hippocratic Values in an Era of Nuclear Asymmetry: Should U.S. Public Health Prepare for Nuclear War with North Korea? *J Health Ethics*. 2019;15(2). doi:10.18785/ojhe.1502.06

127. Sauer T, Thakur R. How Many Intensive Care Beds Will a Nuclear Weapon Explosion Require? Published online May 2020.

128. McDonald K, McLees T, Connolly S, McNulty J, Wasserman L, Prins. Modeling Megacity Medical System Response to a CBRNE Event. *Ind Syst Eng Rev*. 2016;4(2). Accessed May 2, 2022. https://core.ac.uk/reader/322516730

129. Sagan SD. The Korean Missile Crisis: Why Deterrence Is Still the Best Option Essays. *Foreign Aff*. 2017;96(6):[i]-82.

130. Montoya NG. *No Winning Moves: Calculated Casualties and Damages of a Nuclear Attack on the United States by Russia for First and Second Strike Scenarios*. Thesis. Massachusetts Institute of Technology; 2021. Accessed May 2, 2022. https://dspace.mit.edu/handle/1721.1/139236

131. NUKEMAP. 404 Not Found. Accessed May 2, 2022. https://nukemap.org/faq/#casualties

132. Dallas CE, Bell WC. Prediction modeling to determine the adequacy of medical response to urban nuclear attack. *Disaster Med Public Health Prep*. 2007;1(2):80-89. doi:10.1097/DMP.0b013e318159a9e3

133. Hill A. Using the Hazard Prediction and Assessment Capability (HPAC) Hazard Assessment Program for Radiological Scenarios Relevant to the Australian Defense Force. Published online March 2003.

134. Defense Threat Reduction Agency. Hazard Prediction and Assessment Capability. Published online 2022.

135. Plante D. An Evaluation of the Hazard Prediction and Assessment Capability (HPAC) Software's Ability to Model the Chornobyl Accident. *Theses Diss*. Published online March 1, 2002. https://scholar.afit.edu/etd/4508

136. Pace K. Terrain and Spatial Effects on Hazard Prediction and Assessment Capability (HPAC) Software Dose-Rate Contour Plot Predictions as Compared to a Sample of Local Fallout Data from Test Detonations in the Continental United States, 1945-1962. *Theses Diss*. Published online March 6, 2006. https://scholar.afit.edu/etd/3371

137. Auxier JP, Auxier JD, Hall HL. Review of current nuclear fallout codes. *J Environ Radioact*. 2017;171:246-252. doi:10.1016/j.jenvrad.2017.02.010

138. Coleman CN, Sullivan JM, Bader JL, et al. Public Health and Medical Preparedness for a Nuclear Detonation: The Nuclear Incident Medical Enterprise. *Health Phys*. 2015;108(2):149-160. doi:10.1097/HP.0000000000000249

139. Parikh N, Hayatnagarkar HG, Beckman RJ, Marathe MV, Swarup S. A comparison of multiple behavior models in a simulation of the aftermath of an improvised nuclear

detonation. *Auton Agents Multi-Agent Syst*. 2016;30(6):1148-1174. doi:10.1007/s10458-016-9331-y

140. Ross JR, Case C, Confer D, et al. Radiation Injury Treatment Network (RITN): Healthcare professionals preparing for a mass casualty radiological or nuclear incident. *Int J Radiat Biol*. 2011;87(8):748-753. doi:10.3109/09553002.2011.556176
141. Kearns RD, Cairns BA, Hickerson WL, Holmes JH 4th. ABA Southern Region Burn Disaster Plan: The Process of Creating and Experience with the ABA Southern Region Burn Disaster Plan. *J Burn Care Res*. 2014;35(1):e43-e48. doi:10.1097/BCR.0b013e3182957468
142. Cairns C, Kang K. *National Hospital Ambulatory Medical Care Survey: 2019 Emergency Department Summary Tables*. National Center for Health Statistics (U.S.); 2022. doi:10.15620/cdc:115748
143. Kearns RD, Hubble MW, Holmes JamesH IV, Lord GC, Helminiak RAC, Cairns BA. Advanced Burn Life Support for Day-to-Day Burn Injury Management and Disaster Preparedness: Stakeholder Experiences and Student Perceptions Following 56 Advanced Burn Life Support Courses. *J Burn Care Res*. 2015;36(4):455-464. doi:10.1097/BCR.0000000000000155
144. Saffle JR, Gibran N, Jordan M. Defining the Ratio of Outcomes to Resources for Triage of Burn Patients in Mass Casualties. *J Burn Care Res*. 2005;26(6):478-482. doi:10.1097/01.bcr.0000185452.92833.c0
145. Evans EI, Purnell OJ, Robinett PW, Batchelor A, Martin M. Fluid and Electrolyte Requirements in Severe Burns. *Ann Surg*. 1952;135(6):804-815.

146. Church D, Elsayed S, Reid O, Winston B, Lindsay R. Burn Wound Infections. *Clin Microbiol Rev*. 2006;19(2):403-434. doi:10.1128/CMR.19.2.403-434.2006

147. Goldman L, Schafer A. *Goldman's Cecil Medicine*. Vol 1. 24th ed. Saunders; 2011. Accessed September 22, 2020. https://www.elsevier.com/books/goldmans-cecil-medicine/9781437716047

148. National Burn Data Standard. National Burn Data Standard: Data Dictionary. Published online June 2015.

149. Taylor S, Curri T, Lawless M, Sen S, Greenhalgh DG, Palmieri TL. Predicting Resource Utilization in Burn Treatment. *J Burn Care Res*. 2014;35(suppl_2):S235-S246. doi:10.1097/BCR.0000000000000076

150. Ryan CM, Schoenfeld DA, Thorpe WP, Sheridan RL, Cassem EH, Tompkins RG. Objective Estimates of the Probability of Death from Burn Injuries. *N Engl J Med*. 1998;338(6):362-366. doi:10.1056/NEJM199802053380604

151. American Burn Assoication. *National Burn Repository 2019 Update*. American Burn Association; 2019:141.

152. Peck MD, Mantelle L, Ward CG. Comparison of Length of Hospital Stay to Mortality Rate in a Regional Burn Center. *J Burn Care Rehabil*. 1996;17(1):39-44. doi:10.1097/00004630-199601000-00010

153. Shields BJ, Comstock RD, Fernandez SA, Xiang H, Smith GA. Healthcare Resource Utilization and Epidemiology of Pediatric Burn-Associated Hospitalizations, United States, 2000. *J Burn Care Res*. 2007;28(6):811-826. doi:10.1097/BCR.0b013e3181599b51

154. Carter JE, Amani H, Carter D, et al. Evaluating Real-World National and Regional Trends in Definitive Closure in U.S. Burn Care: A Survey of U.S. Burn Centers. *J Burn Care Res*. 2022;43(1):141-148. doi:10.1093/jbcr/irab151

155. Pfuntner A, Wier L, Stocks C. Most Frequent Procedures Performed in U.S. Hospitals, 2011: Statistical Brief #165. In: ; 2013.

156. American Burn Association. Burn Center Regional Map – American Burn Association. Published 2020. Accessed April 13, 2022. https://ameriburn.org/public-resources/burn-center-regional-map/

157. US Department of Health and Human Services. National Bioterrorism Hospital Preparedness Program FY 2005 Continuation Guidance. Published online 2005.

158. Dai A, Carrougher GJ, Mandell SP, Fudem G, Gibran NS, Pham TN. Review of Recent Large-Scale Burn Disasters Worldwide in Comparison to Preparedness Guidelines. *J Burn Care Res*. 2017;38(1):36-44. doi:10.1097/BCR.0000000000000441

159. Institute of Medicine. *Crisis Standards of Care: A Systems Framework for Catastrophic Disaster Response: Volume 1: Introduction and CSC Framework*. National Academies Press; 2012.

160. Leider JP, DeBruin D, Reynolds N, Koch A, Seaberg J. Ethical Guidance for Disaster Response, Specifically Around Crisis Standards of Care: A Systematic Review. *Am J Public Health*. 2017;107(9):e1-e9. doi:10.2105/AJPH.2017.303882

161. Taylor S, Jeng J, Saffle JR, Sen S, Greenhalgh DG, Palmieri TL. Redefining the Outcomes to Resources Ratio for Burn Patient Triage in a Mass Casualty. *J Burn Care Res*. 2014;35(1):41-45. doi:10.1097/BCR.0000000000000034

162. Iserson KV, Moskop JC. Triage in Medicine, Part I: Concept, History, and Types. *Ann Emerg Med*. 2007;49(3):275-281. doi:10.1016/j.annemergmed.2006.05.019

163. Bazyar J, Farrokhi M, Salari A, Khankeh HR. The Principles of Triage in Emergencies and Disasters: A Systematic Review. *Prehospital Disaster Med*. 2020;35(3):305-313. doi:10.1017/S1049023X20000291

164. Lidal IB, Holte HH, Vist GE. Triage systems for pre-hospital emergency medical services - a systematic review. *Scand J Trauma Resusc Emerg Med*. 2013;21(1):28. doi:10.1186/1757-7241-21-28

165. Ng CJ, You SH, Wu IL, et al. Introduction of a mass burn casualty triage system in a hospital during a powder explosion disaster: a retrospective cohort study. *World J Emerg Surg*. 2018;13(1):38. doi:10.1186/s13017-018-0199-9

166. Jenkins JL, McCarthy ML, Sauer LM, et al. Mass-Casualty Triage: Time for an Evidence-Based Approach. *Prehospital Disaster Med*. 2008;23(1):3-8. doi:10.1017/S1049023X00005471

167. McKee CH, Heffernan RW, Willenbring BD, et al. Comparing the Accuracy of Mass Casualty Triage Systems When Used in an Adult Population. *Prehosp Emerg Care*. 2020;24(4):515-524. doi:10.1080/10903127.2019.1641579

168. Heller AR, Salvador N, Frank M, Schiffner J, Kipke R, Kleber C. Diagnostic precision of triage algorithms for mass casualty incidents. English version. *Anaesthesist*. 2019;68(1):15-24. doi:10.1007/s00101-017-0352-y

169. Lee CWC, McLeod SL, Aarsen KV, Klingel M, Franc JM, Peddle MB. First Responder Accuracy Using SALT during Mass-casualty Incident Simulation. *Prehospital Disaster Med*. 2016;31(2):150-154. doi:10.1017/S1049023X16000091

170. Robertson-Steel I. Evolution of triage systems. *Emerg Med J EMJ*. 2006;23(2):154-155. doi:10.1136/emj.2005.030270

171. Dillon MB, Kane SR. *Estimating Fallout Building Protection Attributes from Architectural Features and Global Earthquake Model (GEM) Building Descriptions*. Lawrence Livermore National Laboratory (LLNL); 2017:184.

172. Rolph GD, Ngan F, Draxler RR. Modeling the fallout from stabilized nuclear clouds using the HYSPLIT atmospheric dispersion model. *J Environ Radioact*. 2014;136:41-55. doi:10.1016/j.jenvrad.2014.05.006

173. Eisenbud M, Gesell TF. *Environmental Radioactivity from Natural, Industrial and Military Sources: From Natural, Industrial and Military Sources*. Elsevier; 1997.

174. Reisner J, D'Angelo G, Koo E, et al. Climate Impact of a Regional Nuclear Weapons Exchange: An Improved Assessment Based On Detailed Source Calculations. *J Geophys Res Atmospheres*. 2018;123(5):2752-2772. doi:10.1002/2017JD027331

175. Weather Underground. Atlanta, GA Weather Conditions | Weather Underground. Accessed May 9, 2022. https://www.wunderground.com/weather/us/ga/atlanta/KGAATLAN783

176. weather.us. Cloud Coverage Observations. Weather.us. Published 2023. Accessed June 2, 2022. https://weather.us/observations/0f3ea5fcf71ec68aaf88a8167b2560f4/total-cloud-coverage/20190101-1800z.html

177. Monteith J, Unsworth M. *Principles of Environmental Physics*. 3rd ed. Academic Press; 2017.

178. Sheridan SC. The redevelopment of a weather-type classification scheme for North America. *Int J Climatol*. 2002;22(1):51-68. doi:10.1002/joc.709

179. Sheridan SC. Spatial Synoptic Classification v3.0. Spatial Synoptic Classification v3.0. Accessed June 28, 2022. http://sheridan.geog.kent.edu/ssc3.html

180. Gelaro R, McCarty W, Suárez MJ, et al. The Modern-Era Retrospective Analysis for Research and Applications, Version 2 (MERRA-2). *J Clim*. 2017;30(14):5419-5454. doi:10.1175/JCLI-D-16-0758.1

181. National Academies of Sciences E, Division H and M, Policy B on HS, et al. *Federal Planning for Nuclear Incidents*. National Academies Press (US); 2019. Accessed May 12, 2022. https://www.ncbi.nlm.nih.gov/books/NBK543068/

182. Sykes RI, Gabruk RS. A Second-Order Closure Model for the Effect of Averaging Time on Turbulent Plume Dispersion. *J Appl Meteorol Climatol*. 1997;36(8):1038-1045. doi:10.1175/1520-0450(1997)036<1038:ASOCMF>2.0.CO;2

183. Sykes RI, Cerasoli CP, Henn DS. The representation of dynamic flow effects in a Lagrangian puff dispersion model. *J Hazard Mater*. 1999;64(3):223-247. doi:10.1016/S0304-3894(98)00271-4

184. Moehl J, Weber E, Sims K, Trombley N, Weston S, Rose A. LandScan USA 2019.

185. Esri Inc. ArcGIS Pro. Published online 2022.

186. Fujita S, Kato H, Schull WJ. The LD50 associated with exposure to the atomic bombing of Hiroshima and Nagasaki. *J Radiat Res (Tokyo)*. 1991;32 Suppl:154-161. doi:10.1269/jrr.32.supplement_154

187. Agency for Toxic Substances and Disease Registry. *Toxicological Profile for Ionizing Radiation: Draft*. U.S. Department of Health and Human Services, Public Health Service, Agency for Toxic Substances and Disease Registry; 1997. https://books.google.com/books?id=JUDvcSRsUyUC&dq=Ionizing+radiation+is+a+form+

of+radiation+with+sufficient+energy+to+remove+electrons+from+their+atomic+or+molecular+orbital+shells+in+the+tissues+they+penetrate+(Borek+1993)&source=gbs_navlinks_s

188. Stricklin D, Prins R, Bellman J. Development of age-dependent dose modification factors for acute radiation lethality. *Int J Radiat Biol*. 2020;96(1):67-80. doi:10.1080/09553002.2018.1547438

189. Kaufman L, Rousseeuw PJ. *Finding Groups in Data: An Introduction to Cluster Analysis*. John Wiley & Sons; 2009.

190. Botyarov M, Miller EE. Partitioning around medoids as a systematic approach to generative design solution space reduction. *Results Eng*. 2022;15:100544. doi:10.1016/j.rineng.2022.100544

191. Van der Laan M, Pollard K, Bryan J. A new partitioning around medoids algorithm. *J Stat Comput Simul*. 2003;73(8):575-584. doi:10.1080/0094965031000136012

192. Kuhn K, Shah A, Skeels C. Characterizing and classifying historical days based on weather and air traffic. In: *2015 IEEE/AIAA 34th Digital Avionics Systems Conference (DASC)*. ; 2015:1C3-1-1C3-12. doi:10.1109/DASC.2015.7311341

193. Kodinariya T, Makwana P. Review on Determining of Cluster in K-means Clustering. *Int J Adv Res Comput Sci Manag Stud*. 2013;1:90-95.

194. Hidalgo J, Jougla R. On the use of local weather types classification to improve climate understanding: An application on the urban climate of Toulouse. *PLOS ONE*. 2018;13(12):e0208138. doi:10.1371/journal.pone.0208138

195. Suwanda R, Syahputra Z, Zamzami E. Analysis of Euclidean Distance and Manhattan Distance in the K-Means Algorithm for Variations Number of Centroid K. *J Phys Conf Ser*. 2020;1566:012058. doi:10.1088/1742-6596/1566/1/012058

196. Nisbet R, Elder J, Miner G. Part II - The Algorithms in Data Mining and Text Mining, the Organization of the Three Most Common Data Mining Tools, and Selected Specialized Areas Using Data Mining. In: Nisbet R, Elder J, Miner G, eds. *Handbook of Statistical Analysis and Data Mining Applications*. Academic Press; 2009:119-120. doi:10.1016/B978-0-12-374765-5.00052-8

197. Nainggolan R, Perangin-angin R, Simarmata E, Tarigan AF. Improved the Performance of the K-Means Cluster Using the Sum of Squared Error (SSE) optimized by using the Elbow Method. *J Phys Conf Ser*. 2019;1361(1):012015. doi:10.1088/1742-6596/1361/1/012015

198. Hubert LJ, Levin JR. A general statistical framework for assessing categorical clustering in free recall. *Psychol Bull*. 1976;83:1072-1080. doi:10.1037/0033-2909.83.6.1072

199. Rousseeuw PJ. Silhouettes: A graphical aid to the interpretation and validation of cluster analysis. *J Comput Appl Math*. 1987;20:53-65. doi:10.1016/0377-0427(87)90125-7

200. Tibshirani R, Walther G, Hastie T. Estimating the number of clusters in a data set via the gap statistic. *J R Stat Soc Ser B Stat Methodol*. 2001;63(2):411-423. doi:10.1111/1467-9868.00293

201. Yuan C, Yang H. Research on K-Value Selection Method of K-Means Clustering Algorithm. *J*. 2019;2(2):226-235. doi:10.3390/j2020016

202. Othman SA, Ali HTM. Improvement of the Nonparametric Estimation of Functional Stationary Time Series Using Yeo-Johnson Transformation with Application to Temperature Curves. *Adv Math Phys*. 2021;2021:e6676400. doi:10.1155/2021/6676400

203. Yeo IK, Johnson RA. A New Family of Power Transformations to Improve Normality or Symmetry. *Biometrika*. 2000;87(4):954-959.

204. James G, Witten D, Hastie T, Tibshirani R. *An Introduction to Statistical Learning with Applications in R*. 2nd ed. Springer; 2021.

205. Hastie T, Tibshirani R, Friedman J. *The Elements of Statistical Learning: Data Mining, Inference, and Prediction*. 2nd ed. Springer; 2016.

206. Somvanshi M, Chavan P, Tambade S, Shinde SV. A review of machine learning techniques using decision tree and support vector machine. In: *2016 International Conference on Computing Communication Control and Automation (ICCUBEA)*. ; 2016:1-7. doi:10.1109/ICCUBEA.2016.7860040

207. Navada A, Ansari AN, Patil S, Sonkamble BA. Overview of use of decision tree algorithms in machine learning. In: *2011 IEEE Control and System Graduate Research Colloquium*. ; 2011:37-42. doi:10.1109/ICSGRC.2011.5991826

208. Boehmke B, Greenwell BM. *Hands-On Machine Learning with R*. Routledge; 2019. Accessed November 29, 2021. https://www.routledge.com/Hands-On-Machine-Learning-with-R/Boehmke-Greenwell/p/book/9781138495685

209. Breiman L. Random Forests. *Mach Learn*. 2001;45(1):5-32. doi:10.1023/A:1010933404324

210. Qi Y. Random Forest for Bioinformatics. In: Zhang C, Ma Y, eds. *Ensemble Machine Learning: Methods and Applications*. Springer US; 2012:307-323. doi:10.1007/978-1-4419-9326-7_11

211. Roth V. The generalized LASSO. *IEEE Trans Neural Netw*. 2004;15(1):16-28. doi:10.1109/TNN.2003.809398

212. Zou H, Hastie T. Regularization and variable selection via the elastic net. *J R Stat Soc Ser B Stat Methodol*. 2005;67(2):301-320. doi:10.1111/j.1467-9868.2005.00503.x

213. Chintalapudi N, Angeloni U, Battineni G, et al. LASSO Regression Modeling on Prediction of Medical Terms among Seafarers' Health Documents Using Tidy Text Mining. *Bioengineering*. 2022;9(3):124. doi:10.3390/bioengineering9030124

214. Jeong B, Cho H, Kim J, et al. Comparison between Statistical Models and Machine Learning Methods on Classification for Highly Imbalanced Multiclass Kidney Data. *Diagnostics*. 2020;10(6):415. doi:10.3390/diagnostics10060415

215. Ibrahim AU, Ozsoz M, Serte S, Al-Turjman F, Yakoi PS. Pneumonia Classification Using Deep Learning from Chest X-ray Images During COVID-19. *Cogn Comput*. Published online January 4, 2021. doi:10.1007/s12559-020-09787-5

216. Al-Haija QA, Gharaibeh M, Odeh A. Detection in Adverse Weather Conditions for Autonomous Vehicles via Deep Learning. *AI*. 2022;3(2):303-317. doi:10.3390/ai3020019

217. Tharwat A. Classification assessment methods. *Appl Comput Inform*. 2020;17(1):168-192. doi:10.1016/j.aci.2018.08.003

218. Sokolova M, Japkowicz N, Szpakowicz S. Beyond Accuracy, F-Score and ROC: A Family of Discriminant Measures for Performance Evaluation. In: Sattar A, Kang B ho, eds. *AI 2006: Advances in Artificial Intelligence*. Lecture Notes in Computer Science. Springer; 2006:1015-1021. doi:10.1007/11941439_114

219. Florkowski CM. Sensitivity, Specificity, Receiver-Operating Characteristic (ROC) Curves and Likelihood Ratios: Communicating the Performance of Diagnostic Tests. *Clin Biochem Rev*. 2008;29(Suppl 1):S83-S87.

220. Fan J, Upadhye S, Worster A. Understanding receiver operating characteristic (ROC) curves. *Can J Emerg Med*. 2006;8(1):19-20. doi:10.1017/S1481803500013336

221. Hand DJ, Till RJ. A Simple Generalisation of the Area Under the ROC Curve for Multiple Class Classification Problems. *Mach Learn*. 2001;45(2):171-186. doi:10.1023/A:1010920819831

222. R Core Team. R: A language and environment for statistical computing. Published online 2022. https://www.R-project.org/

223. Robinson D, Hayes A, Couch S. broom: Convert statistical objects into tidy tibbles. Published online 2022. https://CRAN.R-project.org/package=broom

224. Bolker B, Robinson D. broom.mixed: Tidying methods for mixed models. Published online 2022. https://CRAN.R-project.org/package=broom.mixed

225. Agostinelli C, Lund U. R package <tt>: Circular statistics (version 0.4-95)</tt>. Published online 2022. https://r-forge.r-project.org/projects/circular/

226. Maechler M, Rousseeuw P, Struyf A, Hubert M, Hornik K. cluster: Cluster analysis basics and extensions. Published online 2022. https://CRAN.R-project.org/package=cluster

227. Corporation M, Weston S. doParallel: Foreach parallel adaptor for the "parallel" package. Published online 2022. https://CRAN.R-project.org/package=doParallel

228. Chang W. extrafont: Tools for using fonts. Published online 2022. https://CRAN.R-project.org/package=extrafont

229. Kassambara A, Mundt F. factoextra: Extract and visualize the results of multivariate data analyses. Published online 2020. https://CRAN.R-project.org/package=factoextra

230. Schloerke B, Cook D, Larmarange J, et al. GGally: Extension to "ggplot2." Published online 2021. https://CRAN.R-project.org/package=GGally

231. Kassambara A. ggpubr: "ggplot2" based publication ready plots. Published online 2020. https://CRAN.R-project.org/package=ggpubr

232. Friedman J, Hastie T, Tibshirani R. Regularization paths for generalized linear models via coordinate descent. *J Stat Softw*. 2010;33(1):1-22. doi:10.18637/jss.v033.i01

233. Sjoberg DD, Whiting K, Curry M, Lavery JA, Larmarange J. Reproducible summary tables with the gtsummary package. *R J*. 2021;13(1):570-580. doi:10.32614/RJ-2021-053

234. Müller K. here: A Simpler Way to Find Your Files. Published online 2020. https://CRAN.R-project.org/package=here

235. Grolemund G, Wickham H. Dates and times made easy with lubridate. *J Stat Softw*. 2011;40(3):1-25.

236. Wright MN, Ziegler A. ranger: A fast implementation of random forests for high dimensional data in C++ and R. *J Stat Softw*. 2017;77(1):1-17. doi:10.18637/jss.v077.i01

237. Wickham H, Bryan J. readxl: Read excel files. Published online 2022. https://CRAN.R-project.org/package=readxl

238. Milborrow S. rpart.plot: Plot "rpart" Models: An Enhanced Version of "plot.rpart." Published online 2022. https://CRAN.R-project.org/package=rpart.plot

239. Wickham H, Seidel D. scales: Scale functions for visualization. Published online 2022. https://CRAN.R-project.org/package=scales

240. Waring E, Quinn M, McNamara A, de la Rubia EA, Zhu H, Ellis S. skimr: Compact and flexible summaries of data. Published online 2022. https://CRAN.R-project.org/package=skimr

241. Wickham H, Averick M, Bryan J, et al. Welcome to the tidyverse. *J Open Source Softw*. 2019;4(43):1686. doi:10.21105/joss.01686

242. Kuhn M, Wickham H. Tidymodels: a collection of packages for modeling and machine learning using tidyverse principles. Published online 2020. https://www.tidymodels.org

243. Greenwell BM, Boehmke BC. Variable importance Plots—An introduction to the vip package. *R J*. 2020;12(1):343-366.

244. Garnier, Simon, Ross, et al. viridis - colorblind-friendly color maps for R. Published online 2021. doi:10.5281/zenodo.4679424

245. Ooms J. writexl: Export data frames to excel "xlsx" format. Published online 2021. https://CRAN.R-project.org/package=writexl

246. Tasian GE, Pulido JE, Gasparrini A, et al. Daily Mean Temperature and Clinical Kidney Stone Presentation in Five U.S. Metropolitan Areas: A Time-Series Analysis. *Environ Health Perspect*. 2014;122(10):1081-1087. doi:10.1289/ehp.1307703

247. Winquist A, Grundstein A, Chang HH, Hess J, Sarnat SE. Warm season temperatures and emergency department visits in Atlanta, Georgia. *Environ Res*. 2016;147:314-323. doi:10.1016/j.envres.2016.02.022

248. McLeod J, Shepherd M, Konrad CE. Spatio-temporal rainfall patterns around Atlanta, Georgia and possible relationships to urban land cover. *Urban Clim*. 2017;21:27-42. doi:10.1016/j.uclim.2017.03.004

249. Reesman C, Miller P, D'Antonio R, Gilmore K, Schott B, Bannan C. Areal Probability of Precipitation in Moist Tropical Air Masses for the United States. *Atmosphere*. 2021;12(2):255. doi:10.3390/atmos12020255

250. Bentley ML, Ashley WS, Stallins JA. Climatological radar delineation of urban convection for Atlanta, Georgia. *Int J Climatol*. 2010;30(11):1589-1594. doi:10.1002/joc.2020

251. Perkins DR. Using synoptic weather types to predict visitor attendance at Atlanta and Indianapolis zoological parks. *Int J Biometeorol*. 2018;62(1):127-137. doi:10.1007/s00484-016-1142-y

252. Hu Y, Chang ME, Russell AG, Odman MT. Using synoptic classification to evaluate an operational air quality forecasting system in Atlanta. *Atmospheric Pollut Res*. 2010;1(4):280-287. doi:10.5094/APR.2010.035

253. Mote TL, Lacke MC, Shepherd JM. Radar signatures of the urban effect on precipitation distribution: A case study for Atlanta, Georgia. *Geophys Res Lett*. 2007;34(20). doi:10.1029/2007GL031903

254. Khajure S, Mohod SW. Future Weather Forecasting Using Soft Computing Techniques. *Procedia Comput Sci*. 2016;78:402-407. doi:10.1016/j.procs.2016.02.081

255. Ghita G. *Prompt Radiation Protection Factors*. Defense Threat Reduction Agency; 2018:35. https://apps.dtic.mil/sti/pdfs/AD1050039.pdf

256. Yoshida-Ohuchi H, Matsuda N, Saito K. Review of reduction factors by buildings for gamma radiation from radiocaesium deposited on the ground due to fallout. *J Environ Radioact*. 2018;187:32-39. doi:10.1016/j.jenvrad.2018.02.006

257. Dillon MB, Kane J, Nasstrom J, Homann S, Pobanz B. *Summary of Building Protection Factor Studies for External Exposure to Ionizing Radiation*. Lawrence Livermore National Lab. (LLNL); 2016:78. https://www.osti.gov/servlets/purl/1256433

258. Thatcher TL, Layton DW. Deposition, resuspension, and penetration of particles within a residence. *Atmos Environ*. 1995;29(13):1487-1497. doi:10.1016/1352-2310(95)00016-R

259. Wallace L. Indoor particles: a review. *J Air Waste Manag Assoc 1995*. 1996;46(2):98-126. doi:10.1080/10473289.1996.10467451

260. Chao CYH, Tung TC. An empirical model for outdoor contaminant transmission into residential buildings and experimental verification. *Atmos Environ*. 2001;35:1585-1596. doi:10.1016/S1352-2310(00)00458-1

261. Lee MH, Yang W, Chae N, Choi S. Performance assessment of HEPA filter against radioactive aerosols from metal cutting during nuclear decommissioning. *Nucl Eng Technol*. 2020;52(5):1043-1050. doi:10.1016/j.net.2019.10.017
262. Black S. Supplemental Material. Published online December 20, 2022.
263. ONEGEO. 3DBuildings. Published online 2022. https://onegeo.co/data/
264. Lutz N, Lehman W, Ryan A, Nguyen T, Goss R. National Structure Inventory. Published online 2022. https://www.hec.usace.army.mil/confluence/nsi
265. National Structure Inventory. Mission, Vision, and Goals. About Us. Published 2023. Accessed March 11, 2023. https://www.hec.usace.army.mil/confluence/nsi/nsio/mission-vision-and-goals
266. Office of Radiation and Indoor Air Radiation Protection Division. PAG Manual: Protective Action Guides and Planning Guidance for Radiological Incidents. Published online January 2017.
267. Hrdina CM, Coleman CN, Bogucki S, et al. The "RTR" medical response system for nuclear and radiological mass-casualty incidents: a functional TRiage-TReatment-TRansport medical response model. *Prehospital Disaster Med*. 2009;24(3):167-178. doi:10.1017/s1049023x00006774
268. Blender Online Community. Blender - a 3D modelling and rendering package. Published online 2022. http://www.blender.org
269. Klepeis NE, Nelson WC, Ott WR, et al. The National Human Activity Pattern Survey (NHAPS): a resource for assessing exposure to environmental pollutants. *J Expo Sci Environ Epidemiol*. 2001;11(3):231-252. doi:10.1038/sj.jea.7500165

270. Brode HL. Review of Nuclear Weapons Effects. *Annu Rev Nucl Sci*. 1968;18(1):153-202. doi:10.1146/annurev.ns.18.120168.001101

271. Prochitecture. Blender-OSM: OpenStreetMap and Terrain for Blender. Published online 2022. https://prochitecture.gumroad.com/l/blender-osm

272. Medicine I of. *Assessing Medical Preparedness to Respond to a Terrorist Nuclear Event: Workshop Report*. (Benjamin GC, McGeary M, McCutchen SR, eds.). The National Academies Press; 2009. doi:10.17226/12578

273. Federal Emergency Management Agency. Radiation Emergencies. Ready.gov. Published February 8, 2023. Accessed March 12, 2023. https://www.ready.gov/radiation

274. Severson K. Atlanta Officials Gamble on Storm and Lose, and Others Pay the Price. *The New York Times*. https://www.nytimes.com/2014/01/30/us/ice-storm-southern-united-states.html. Published January 29, 2014. Accessed March 12, 2023.

275. Oxford SM. *NATO Allied Medical Publication 7.5 (AMedP 7.5) NATO Planning Guide for the Estimation of CBRN Casualties*. Institute for Defense Analyses; 2016. Accessed March 12, 2023. https://apps.dtic.mil/sti/citations/AD1039443

276. Oak Ridge National Laboratory. About LandScan. Published 2022. Accessed May 12, 2022. https://landscan.ornl.gov/about

277. Moehl J. LandScan USA and NSI. Published online November 16, 2022.

278. Moehl J, Weber E, McKee J. *A VECTOR ANALYTICAL FRAMEWORK FOR POPULATION MODELING*. Vol XLVI-4/W2-2021. Oak Ridge National Lab. (ORNL), Oak Ridge, TN (United States); 2021. doi:10.5194/isprs-archives-XLVI-4-W2-2021-103-2021

279. Klepeis NE, Nelson WC, Ott WR, et al. The National Human Activity Pattern Survey (NHAPS): a resource for assessing exposure to environmental pollutants. *J Expo Sci Environ Epidemiol*. 2001;11(3):231-252. doi:10.1038/sj.jea.7500165

280. Federal Emergency Management Agency. *Planning Guidance for Response to a Nuclear Detonation*. Federal Emergency Management Agency (FEMA); 2022. https://www.fema.gov/sites/default/files/documents/fema_nuc-detonation-planning-guide.pdf

281. Coleman CN, Weinstock DM, Casagrande R, et al. Triage and treatment tools for use in a scarce resources-crisis standards of care setting after a nuclear detonation. *Disaster Med Public Health Prep*. 2011;5 Suppl 1:S111-121. doi:10.1001/dmp.2011.22

282. No authors listed. SALT mass casualty triage: concept endorsed by the American College of Emergency Physicians, American College of Surgeons Committee on Trauma, American Trauma Society, National Association of EMS Physicians, National Disaster Life Support Education Consortium, and State and Territorial Injury Prevention Directors Association. *Disaster Med Public Health Prep*. 2008;2(4):245-246. doi:10.1097/DMP.0b013e31818d191e

283. Benson M, Koenig KL, Schultz CH. Disaster triage: START, then SAVE--a new method of dynamic triage for victims of a catastrophic earthquake. *Prehospital Disaster Med*. 1996;11(2):117-124. doi:10.1017/s1049023x0004276x

284. Lerner EB, Cone DC, Weinstein ES, et al. Mass casualty triage: an evaluation of the science and refinement of a national guideline. *Disaster Med Public Health Prep*. 2011;5(2):129-137. doi:10.1001/dmp.2011.39

285. Cone DC, Koenig KL. Mass casualty triage in the chemical, biological, radiological, or nuclear environment. *Eur J Emerg Med Off J Eur Soc Emerg Med*. 2005;12(6):287-302. doi:10.1097/00063110-200512000-00009

286. Curling CA, Todd S. *Parameters for Estimation of Casualties from First and Third Degree Flash Burns*. Institute for Defense Analyses; 2017. Accessed March 17, 2023. https://www.jstor.org/stable/resrep22792

287. Oxford SM, LaViolet LA, Bishop KA, et al. *Technical Reference Manual to Allied Medical Publication 7.5 (AMedP-7.5) NATO Planning Guide for the Estimation of CBRN Casualties*. Institute for Defense Analyses; 2018:622. https://www.coemed.org/files/stanags/03_AMEDP/AMedP-7.5-1_EDA_V1_E_SRD_2553.pdf

288. Assistant Secretary for Preparedness and Response. Health Care Coalitions (HCCs). Published online April 2021. https://aspr.hhs.gov/HealthCareReadiness/HealthCareReadinessNearYou/Documents/HCC-FactSheet-April2021-508.pdf

289. Harris C, Waltz T, O'Neal JP, Nadeau K, Crumpton M, Ervin S. Conceptualization of a Health Care Coalition Framework in Georgia Based on the Existing Regional Coordinating Hospital Infrastructure. *Disaster Med Public Health Prep*. 2016;10(1):174-179. doi:10.1017/dmp.2015.153

290. Georgia Department of Public Health. COVID-19 Status Report. Georgia Department of Public Health. Published January 2023. Accessed January 17, 2023. https://dph.georgia.gov/covid-19-status-report

291. Hospital Preparedness Program. Medical Response & Surge Exercise (MRSE) Situation Manual. Published online September 2021. https://aspr.hhs.gov/HealthCareReadiness/guidance/MRSE/Documents/mrse-situational-manual-508.pdf

292. Stone FP. *The "Worried Well" Response to CBRN Events: Analysis and Solutions*. USAF Conterproliferation Center; 2007:64. Accessed March 23, 2023. https://apps.dtic.mil/sti/citations/ADA475818

293. Beaton R, Stergachis A, Oberle M, Bridges E, Nemuth M, Thomas T. The Sarin Gas Attacks on the Tokyo Subway - 10 years later/Lessons Learned. *Traumatology*. 2005;11(2):103-119. doi:10.1177/153476560501100205

294. Rea ME, Gougelet RM, Nicolalde RJ, Geiling JA, Swartz HM. PROPOSED TRIAGE CATEGORIES FOR LARGE-SCALE RADIATION INCIDENTS USING HIGH-ACCURACY BIODOSIMETRY METHODS. *Health Phys*. 2010;98(2):136. doi:10.1097/HP.0b013e3181b2840b

295. Dallas CE, Bell WC, Stewart DJ, Caruso A, Burkle FM. Nuclear war between Israel and Iran: lethality beyond the pale. *Confl Health*. 2013;7(1):10. doi:10.1186/1752-1505-7-10

296. Georgia Department of Public Health. Designated Trauma & Specialty Care Centers. Georgia Department of Public Health. Published February 21, 2023. Accessed March 18, 2023. https://dph.georgia.gov/EMS/specialty-care-centers-cardiac-trauma-stroke/designated-trauma-specialty-care-centers

297. LeValley C, Page L. 20 Largest Public Hospitals in the United States. Published November 21, 2011. Accessed March 18, 2023. https://www.beckershospitalreview.com/lists-and-statistics/20-largest-public-hospitals-in-the-united-states.html

298. Organization for Economic Co-Operation and Development. OECD Statistics. OECD Statistics. Published 2019. Accessed March 23, 2023. https://stats.oecd.org/#

299. Sampath S, Khedr A, Qamar S, et al. Pandemics Throughout the History. *Cureus*. 13(9):e18136. doi:10.7759/cureus.18136

300. Tangcharoensathien V, Bassett MT, Meng Q, Mills A. Are overwhelmed health systems an inevitable consequence of covid-19? Experiences from China, Thailand, and New York State. *BMJ*. 2021;372:n83. doi:10.1136/bmj.n83

301. Funk C, Tyson A. *Lack of Preparedness Among Top Reactions Americans Have to Public Health Officials' COVID-19 Response*. Rew Research Center; 2022:35. https://www.pewresearch.org/science/wp-content/uploads/sites/16/2022/10/PS_2022.10.05_covid-response-views_REPORT.pdf

302. Baum F, Freeman T, Musolino C, et al. Explaining covid-19 performance: what factors might predict national responses? *BMJ*. 2021;372:n91. doi:10.1136/bmj.n91

303. Dahal P, Ghimire S, Maharjan NK, Rai SM. Baux's and Abbreviated Burn Severity Score for the Prediction of Mortality in Patients with Acute Burn Injury. *J Coll Med Sci-Nepal*. 2015;11(4):24-27. doi:10.3126/jcmsn.v11i4.14321

304. Roberts G, Lloyd M, Parker M, et al. The Baux score is dead. Long live the Baux score: A 27-year retrospective cohort study of mortality at a regional burns service. *J Trauma Acute Care Surg*. 2012;72(1):251-256. doi:10.1097/TA.0b013e31824052bb

305. Taylor RA, Pare JR, Venkatesh AK, et al. Prediction of In-hospital Mortality in Emergency Department Patients With Sepsis: A Local Big Data–Driven, Machine Learning Approach. *Acad Emerg Med*. 2016;23(3):269-278. doi:10.1111/acem.12876

306. Nourazari S, Davis SR, Granovsky R, et al. Decreased hospital admissions through emergency departments during the COVID-19 pandemic. *Am J Emerg Med*. 2021;42:203-210. doi:10.1016/j.ajem.2020.11.029

307. Hartnett KP, Kite-Powell A, DeVies J, et al. Impact of the COVID-19 Pandemic on Emergency Department Visits — United States, January 1, 2019–May 30, 2020. *Morb Mortal Wkly Rep*. 2020;69(23):699-704. doi:10.15585/mmwr.mm6923e1

308. Birkmeyer JD, Barnato A, Birkmeyer N, Bessler R, Skinner J. The Impact Of The COVID-19 Pandemic On Hospital Admissions In The United States. *Health Aff (Millwood)*. 2020;39(11):2010-2017. doi:10.1377/hlthaff.2020.00980

309. Jeffery MM, D'Onofrio G, Paek H, et al. Trends in Emergency Department Visits and Hospital Admissions in Health Care Systems in 5 States in the First Months of the COVID-19 Pandemic in the US. *JAMA Intern Med*. 2020;180(10):1328-1333. doi:10.1001/jamainternmed.2020.3288

310. Baum A, Schwartz MD. Admissions to Veterans Affairs Hospitals for Emergency Conditions During the COVID-19 Pandemic. *JAMA*. 2020;324(1):96-99. doi:10.1001/jama.2020.9972

311. Westgard BC, Morgan MW, Vazquez-Benitez G, Erickson LO, Zwank MD. An Analysis of Changes in Emergency Department Visits After a State Declaration During the Time of COVID-19. *Ann Emerg Med*. 2020;76(5):595-601. doi:10.1016/j.annemergmed.2020.06.019

312. Kim HS, Cruz DS, Conrardy MJ, et al. Emergency Department Visits for Serious Diagnoses During the COVID-19 Pandemic. *Acad Emerg Med*. 2020;27(9):910-913. doi:10.1111/acem.14099

313. Bell WC, Dallas CE. Vulnerability of populations and the urban health care systems to nuclear weapon attack – examples from four American cities. *Int J Health Geogr*. 2007;6(1):5. doi:10.1186/1476-072X-6-5

314. Desai SP, Bell WC, Harris C, Burkle FM, Dallas CE. Human Consequences of Multiple Nuclear Detonations in New Delhi (India): Interdisciplinary Requirements in Triage Management. *Int J Environ Res Public Health*. 2021;18(4):1740. doi:10.3390/ijerph18041740

APPENDIX A

ACRONYMS AND ABBREVIATIONS

3D	three-dimensional
A%	aperture percent
ABA	American Burn Association
ACS	Acute Coronary Syndrome
AH	absolute humidity
AMI	Acute Myocardial Infarction
ARS	Acute Radiation Syndrome
AUC-ROC	Area Under the Curve of Receiver Operator Characteristic
avail	availability
BC	burn center
BMCI	Burn Mass Casualty Incidents
Bq	becquerel
C/kg	Coulomb per kilogram
cal/cm^2	calories per square centimeter
cap	capacity
CART	Classification and Regression Tree
CBT	Comprehensive Nuclear-Test-Ban Treaty
CBRNE	Chemical, Biological, Radiological, Nuclear, and Explosive

CC	comfort care
CDC	Centers for Disease Control and Prevention
CFD	Computational Fluid Dynamics
Ci	curie
CICU	critical intensive care unit
CN^-	cyanide
CNN	The Cable News Network
CO	carbon monoxide
COPD	Chronic Obstructive Pulmonary Disease
COVID-19	Coronavirus Disease 2019
CRS	Cutaneous Radiation Syndrome
DEM	digital elevation model
DFZ	Dangerous Fallout Zone
DM	dry moderate
DMAT	Disaster Medical Assistance Team
DP	dry polar
DOD	Department of Defense
DT	Decision Tree
DT	dry tropical
DTRA	Defense Threat Reduction Agency
DZ	damage zone
ED	emergency department
EMP	electromagnetic pulse

EMS	emergency medical service
EN	elastic net
EPA	Environmental Protection Agency
eV	electron volts
EW	exterior wall density
FBI	Federal Bureau of Investigation
FEM	finite element
FEMA	Federal Emergency Management Agency
FN	false negative
FP	false positive
GA	Georgia
GAO	Government Accountability Office
GCS	Glasgow Coma Score
GIS	geographic information system
Gy	gray
H	hematopoietic
HAZUS	Hazards – United States
HEPA	high efficiency particulate air
HGC	hematopoietic / gastrointestinal / cutaneous
HGCN	hematopoietic / gastrointestinal / cutaneous / neurovascular
HPAC	Hazard Prediction and Assessment Capability
HVAC	heating, ventilation, and air conditioning
iCPR	Improvised Nuclear Device City Planner Resource

ICU	intensive care unit
IND	improvised nuclear device
IWM	interior wall mass density
K	Kelvin
KNN	K-Nearest Neighbor
kPa	kilopascals
KPI	key performance indicator
kt	kiloton
LASSO	least absolute shrinkage and selection operator
$LD_{50/60}$	lethal dose for 50% of exposed population at 60 days
LLNL	Lawrence Livermore National Library
MBq	megabecquerel
MC	medical center
MCI	mass casualty incident
mCi	millicurie
MDS	meteorological data server
MERRA-2	Modern-Era Retrospective analysis for Research and Applications, version 2
MeV	megaelectron volts
ML	machine learning
MM	moist moderate
MP	moist polar
mph	miles per hour
MRSE	medical response and surge exercise

m/s	meters per second
MT	moist tropical
MT	megaton
NATO	North Atlantic Treaty Organization
NB	no basement
NDMS	National Disaster Medical System
nm	nanometer
NPT	Non-Proliferation Treaty
NSI	National Structure Inventory
NWFIRES	Nuclear Weapon Fires
NwpnSe	nuclear weapon single event
OR	operational research
ORNL	Oak Ridge National Laboratory
OSM	OpenStreetMaps
^{239}P	Plutonium-239
PAG	Protective Action Guide
PAGER	Prompt Assessment of Global Earthquakes for Response
PAM	partition around medoids
PF	protection factor
PPE	personal protective equipment
PPV	positive predictive value
P_s	saturation pressure
psi	pounds per square inch

P_v	vapor pressure
Q	quality factor
R	roentgen
R/h	roentgen per hour
R-Baux	Revised-Baux
RDD	radiological dispersion device
RF	Random Forest
RF	reduction factor
RF	roof/floor density
RITN	Radiation Injury Treatment Network
RSA	regional shelter analysis
RTR	Radiation Triage, Treat, and Transport
S	subclinical
SALT	sort, assess, life-saving interventions, treatment and/or transport
SCIPUFF	second-order closure integrated PUFF
SD	standard deviation
SDOF	single-degree-of-freedom
SIP	shelter-in-place
SME	subject matter expert
SPF	sun protection factor
SOPs	standard operating procedures
SSC	spatial synoptic classification
START	simple triage and rapid treatment

Sv	sievert
TBSA	total body surface area
TEDE	total effective dose equivalent
TF	transmission factor
TN	true negative
TNT	trinitrotoluene
TP	true positive
TR	transition
^{235}U	Uranium-235
USSR	Union of Soviet Socialist Republics
US	United States
USGS	United States Geological Survey
UW	unwarned
WB	with basement
WE	Weapons Effects
WMD	weapons of mass destruction
WSS	within-sum-of-squares
WWII	World War II

APPENDIX B

COMMON TYPES OF RADIATION

Table B.1. Common types of ionizing radiation.

	α - Decay / Radiation	**β^- Decay**	**β^+ Decay**	**γ - Decay / Radiation**
Radiation Type	Particle	Particle	Particle	Electromagnetic
Cause	Radioisotope is too large, contains too many protons	Neutron-to-proton ratio is too high	Neutron-to-proton ratio is too low	Relaxation of an excited nucleus
Emission	He nucleus (2 protons and 2 neutrons)	Electron and antineutrino	Positron and neutrino	Gamma photon
Relative Size	Large	Moderate		Small
Relative Weight	Heavy	Moderate		Light
Charge	Positive	Negative	Negative	Neutral
Electric & Magnetic Fields	Small deflection	Large, opposite deflection due to large charge-to-mass ratio (q/m ratio)	Large, same direction deflection due to large charge-to-mass ratio (q/m ratio)	No interaction
Ionizing Ability	Strong	Moderate		Very weak and indirect (via photoelectric and Compton's effect)
Penetrating Power	Very weak, can be stopped by a sheet of paper	Moderate, stopped by a layer of clothing or thin sheet of aluminum foil		Very strong, stopped by at least lead (dense material)
External health hazard	Cannot penetrate skin	Can partially penetrate skin, causing "beta burns"		Passes easily through entire human body, damaging all cells
Human tissue amplification	Severe (1:20)	Moderate (1:5-20)		No amplification (1:1)

APPENDIX C

RADIATION MEASUREMENTS

Table C.1. Radiation measurements and units.

	Radioactivity	**Exposure**	**Absorbed Dose**	**Dose Equivalent**
Common Units	curie (Ci)	roentgen (R)	rad	rem
SI Units	becquerel (Bq)	Coulomb / kilogram (C/kg)	gray (Gy)	sievert (Sv)

Exposure = a measure of the charge on the ions of one sign (negative or positive) resulting from the interaction of gamma ray and X-ray photons in a specified mass of air

- Reflects the intensity of gamma rays or X-rays and the duration of the exposure

Absorbed Dose = a measure of the amount of radiation energy absorbed per unit mass

- Applies to all types of radiation
- Material specific (e.g. air, water, tissue, lead)

Dose Equivalent = a proxy measure of the long term biological consequences for humans of a given exposure to radiation, calculated as product of the absorbed dose to a given organ or tissue multiplied by a quality factor (Q)

- Q (alpha particles) = 20
- Q (beta particles) = 5 - 20
- Q (gamma rays) = 1

Table C.2. Radiation conversion equivalences.

1 curie = 3.7 x 10^10 disintegrations per second		1 becquerel = 1 disintegration per second
1 millicurie (mCi)	=	37 megabecquerels (MBq)
1 rad	=	0.01 gray (Gy)
1 rem	=	0.01 sievert (Sv)
1 roentgen (R)	=	2.58×10^{-4} Coulomb / kilogram (C/kg)
1 megabecquerel (MBq)	=	0.027 millicurie (mCi)
1 gray (Gy)	=	100 rad
1 sievert (Sv)	=	100 rem
1 Coulomb / kilogram (C/kg)	=	3880 roentgen (R)

APPENDIX D: ASSIGNED PROMPT PROTECTION FACTORS BY BUILDING ATTRIBUTES

Table D.1. Assigned protection factors for prompt radiation, based on building characteristics. Unwarned assumes a median estimate for the entire building, while warned specifically refers to the location with the highest protection. Abbreviations: EW = exterior wall density (psf); RF = roof/floor density (psf); IWM = interior wall mass density (psf); A% = aperture %; UW = unwarned; NB = no basement; WB = with basement.

	Num. Story								Protection Factors		
Construction	Min	Max	Foundation	Occupancy	EW	RF	IWM	A%	UW	Warned (NB)	Warned (WB)
Concrete	1	1	Basement	AGR1	100	100	100	10	7.4	7.4	126.7
Concrete	1	1	Basement	COM1	100	100	100	10	7.4	7.4	126.7
Concrete	1	1	Basement	COM2	100	100	100	10	7.4	7.4	126.7
Concrete	1	1	Basement	COM3	100	100	100	25	7.4	7.4	126.7
Concrete	1	1	Basement	COM4	100	100	100	25	7.4	7.4	126.7
Concrete	1	1	Basement	COM7	100	100	100	25	7.4	7.4	126.7
Concrete	1	1	Basement	COM8	100	100	100	25	7.4	7.4	126.7
Concrete	1	1	Basement	EDU2	100	100	100	10	7.4	7.4	126.7
Concrete	1	1	Basement	GOV1	100	100	100	25	7.4	7.4	126.7
Concrete	1	1	Basement	IND2	100	100	100	10	7.4	7.4	126.7
Concrete	1	1	Basement	IND3	100	100	100	10	7.4	7.4	126.7
Concrete	1	1	Basement	IND5	100	100	100	10	7.4	7.4	126.7
Concrete	1	1	Basement	IND6	100	100	100	10	7.4	7.4	126.7
Concrete	1	1	Basement	REL1	100	100	100	10	7.4	7.4	126.7
Concrete	1	1	Basement	RES1_1SWB	100	100	100	10	7.4	7.4	126.7
Concrete	1	1	Basement	RES1_2SWB	100	100	100	10	7.4	7.4	126.7
Concrete	1	1	Basement	RES1_3SWB	100	100	100	10	7.4	7.4	126.7
Concrete	1	1	Basement	RES3A	100	100	100	10	7.4	7.4	126.7

	Num. Story								Protection Factors		
Construction	Min	Max	Foundation	Occupancy	EW	RF	IWM	A%	UW	Warned (NB)	Warned (WB)
Concrete	1	1	Basement	RES3B	100	100	100	25	7.4	7.4	126.7
Concrete	1	1	Basement	RES3C	100	100	100	25	7.4	7.4	126.7
Concrete	1	1	Basement	RES4	100	100	100	25	7.4	7.4	126.7
Concrete	1	1	Basement	RES6	100	100	100	25	7.4	7.4	126.7
Concrete	1	1	Crawl	RES1_1SNB	100	100	100	10	7.4	7.4	126.7
Concrete	1	1	Crawl	RES3A	100	100	100	10	7.4	7.4	126.7
Concrete	1	1	Crawl	RES3B	100	100	100	25	7.4	7.4	126.7
Concrete	1	1	Crawl	RES3C	100	100	100	25	7.4	7.4	126.7
Concrete	1	1	Crawl	RES3E	100	100	100	25	7.4	7.4	126.7
Concrete	1	1	Crawl	RES6	100	100	100	25	7.4	7.4	126.7
Concrete	1	1	Slab	AGR1	100	100	100	10	7.4	7.4	126.7
Concrete	1	1	Slab	COM1	100	100	100	10	7.4	7.4	126.7
Concrete	1	1	Slab	COM10	100	100	100	25	7.4	7.4	126.7
Concrete	1	1	Slab	COM2	100	100	100	10	7.4	7.4	126.7
Concrete	1	1	Slab	COM3	100	100	100	25	7.4	7.4	126.7
Concrete	1	1	Slab	COM4	100	100	100	25	7.4	7.4	126.7
Concrete	1	1	Slab	COM5	100	100	100	25	7.4	7.4	126.7
Concrete	1	1	Slab	COM6	100	100	100	25	7.4	7.4	126.7
Concrete	1	1	Slab	COM7	100	100	100	25	7.4	7.4	126.7
Concrete	1	1	Slab	COM8	100	100	100	25	7.4	7.4	126.7
Concrete	1	1	Slab	COM9	100	100	100	25	7.4	7.4	126.7
Concrete	1	1	Slab	EDU1	100	100	100	25	7.4	7.4	126.7
Concrete	1	1	Slab	EDU2	100	100	100	10	7.4	7.4	126.7
Concrete	1	1	Slab	GOV1	100	100	100	25	7.4	7.4	126.7
Concrete	1	1	Slab	GOV2	100	100	100	10	7.4	7.4	126.7
Concrete	1	1	Slab	IND1	100	100	100	10	7.4	7.4	126.7
Concrete	1	1	Slab	IND2	100	100	100	10	7.4	7.4	126.7

	Num. Story								Protection Factors		
Construction	Min	Max	Foundation	Occupancy	EW	RF	IWM	A%	UW	Warned (NB)	Warned (WB)
Concrete	1	1	Slab	IND3	100	100	100	10	7.4	7.4	126.7
Concrete	1	1	Slab	IND4	100	100	100	10	7.4	7.4	126.7
Concrete	1	1	Slab	IND5	100	100	100	10	7.4	7.4	126.7
Concrete	1	1	Slab	IND6	100	100	100	10	7.4	7.4	126.7
Concrete	1	1	Slab	REL1	100	100	100	10	7.4	7.4	126.7
Concrete	1	1	Slab	RES1_1SNB	100	100	100	10	7.4	7.4	126.7
Concrete	1	1	Slab	RES1_2SNB	100	100	100	10	7.4	7.4	126.7
Concrete	1	1	Slab	RES3A	100	100	100	10	7.4	7.4	126.7
Concrete	1	1	Slab	RES3B	100	100	100	25	7.4	7.4	126.7
Concrete	1	1	Slab	RES3C	100	100	100	25	7.4	7.4	126.7
Concrete	1	1	Slab	RES4	100	100	100	25	7.4	7.4	126.7
Concrete	1	1	Slab	RES5	100	100	100	25	7.4	7.4	126.7
Concrete	1	1	Slab	RES6	100	100	100	25	7.4	7.4	126.7
Concrete	2	3	Basement	COM1	100	100	100	10	6.1	8.8	86.6
Concrete	2	3	Basement	COM2	100	100	100	10	6.1	8.8	86.6
Concrete	2	3	Basement	COM3	100	100	100	25	6.1	8.8	86.6
Concrete	2	3	Basement	COM4	100	100	100	25	6.1	8.8	86.6
Concrete	2	3	Basement	COM5	100	100	100	25	6.1	8.8	86.6
Concrete	2	3	Basement	COM7	100	100	100	25	6.1	8.8	86.6
Concrete	2	3	Basement	COM8	100	100	100	25	6.1	8.8	86.6
Concrete	2	3	Basement	EDU1	100	100	100	25	6.1	8.8	86.6
Concrete	2	3	Basement	GOV1	100	100	100	25	6.1	8.8	86.6
Concrete	2	3	Basement	IND2	100	100	100	10	6.1	8.8	86.6
Concrete	2	3	Basement	IND3	100	100	100	10	6.1	8.8	86.6
Concrete	2	3	Basement	IND6	100	100	100	10	6.1	8.8	86.6
Concrete	2	3	Basement	REL1	100	100	100	10	6.1	8.8	86.6
Concrete	2	3	Basement	RES1_1SWB	100	100	100	10	6.1	8.8	86.6

	Num. Story								Protection Factors		
Construction	Min	Max	Foundation	Occupancy	EW	RF	IWM	A%	UW	Warned (NB)	Warned (WB)
Concrete	2	3	Basement	RES1_2SWB	100	100	100	10	6.1	8.8	86.6
Concrete	2	3	Basement	RES1_3SWB	100	100	100	10	6.1	8.8	86.6
Concrete	2	3	Basement	RES3A	100	100	100	10	6.1	8.8	86.6
Concrete	2	3	Basement	RES3B	100	100	100	25	6.1	8.8	86.6
Concrete	2	3	Basement	RES3C	100	100	100	25	6.1	8.8	86.6
Concrete	2	3	Basement	RES3E	100	100	100	25	6.1	8.8	86.6
Concrete	2	3	Basement	RES6	100	100	100	25	6.1	8.8	86.6
Concrete	2	3	Crawl	REL1	100	100	100	10	6.1	8.8	86.6
Concrete	2	3	Crawl	RES1_1SNB	100	100	100	10	6.1	8.8	86.6
Concrete	2	3	Crawl	RES1_2SNB	100	100	100	10	6.1	8.8	86.6
Concrete	2	3	Crawl	RES1_3SNB	100	100	100	10	6.1	8.8	86.6
Concrete	2	3	Crawl	RES3A	100	100	100	10	6.1	8.8	86.6
Concrete	2	3	Crawl	RES3B	100	100	100	25	6.1	8.8	86.6
Concrete	2	3	Crawl	RES3C	100	100	100	25	6.1	8.8	86.6
Concrete	2	3	Crawl	RES3E	100	100	100	25	6.1	8.8	86.6
Concrete	2	3	Crawl	RES6	100	100	100	25	6.1	8.8	86.6
Concrete	2	3	Slab	AGR1	100	100	100	10	6.1	8.8	86.6
Concrete	2	3	Slab	COM1	100	100	100	10	6.1	8.8	86.6
Concrete	2	3	Slab	COM10	100	100	100	25	6.1	8.8	86.6
Concrete	2	3	Slab	COM2	100	100	100	10	6.1	8.8	86.6
Concrete	2	3	Slab	COM3	100	100	100	25	6.1	8.8	86.6
Concrete	2	3	Slab	COM4	100	100	100	25	6.1	8.8	86.6
Concrete	2	3	Slab	COM5	100	100	100	25	6.1	8.8	86.6
Concrete	2	3	Slab	COM6	100	100	100	25	6.1	8.8	86.6
Concrete	2	3	Slab	COM7	100	100	100	25	6.1	8.8	86.6
Concrete	2	3	Slab	COM8	100	100	100	25	6.1	8.8	86.6
Concrete	2	3	Slab	COM9	100	100	100	25	6.1	8.8	86.6

	Num. Story								Protection Factors		
Construction	Min	Max	Foundation	Occupancy	EW	RF	IWM	A%	UW	Warned (NB)	Warned (WB)
Concrete	2	3	Slab	EDU1	100	100	100	25	6.1	8.8	86.6
Concrete	2	3	Slab	EDU2	100	100	100	10	6.1	8.8	86.6
Concrete	2	3	Slab	GOV1	100	100	100	25	6.1	8.8	86.6
Concrete	2	3	Slab	IND1	100	100	100	10	6.1	8.8	86.6
Concrete	2	3	Slab	IND2	100	100	100	10	6.1	8.8	86.6
Concrete	2	3	Slab	IND3	100	100	100	10	6.1	8.8	86.6
Concrete	2	3	Slab	IND4	100	100	100	10	6.1	8.8	86.6
Concrete	2	3	Slab	IND5	100	100	100	10	6.1	8.8	86.6
Concrete	2	3	Slab	IND6	100	100	100	10	6.1	8.8	86.6
Concrete	2	3	Slab	REL1	100	100	100	10	6.1	8.8	86.6
Concrete	2	3	Slab	RES1_1SNB	100	100	100	10	6.1	8.8	86.6
Concrete	2	3	Slab	RES1_2SNB	100	100	100	10	6.1	8.8	86.6
Concrete	2	3	Slab	RES1_3SNB	100	100	100	10	6.1	8.8	86.6
Concrete	2	3	Slab	RES3A	100	100	100	10	6.1	8.8	86.6
Concrete	2	3	Slab	RES3B	100	100	100	25	6.1	8.8	86.6
Concrete	2	3	Slab	RES3C	100	100	100	25	6.1	8.8	86.6
Concrete	2	3	Slab	RES3E	100	100	100	25	6.1	8.8	86.6
Concrete	2	3	Slab	RES4	100	100	100	25	6.1	8.8	86.6
Concrete	2	3	Slab	RES5	100	100	100	25	6.1	8.8	86.6
Concrete	2	3	Slab	RES6	100	100	100	25	6.1	8.8	86.6
Concrete	4	7	Basement	COM3	100	100	100	25	9.5	17	107.1
Concrete	4	7	Basement	RES3B	100	100	100	25	9.5	17	107.1
Concrete	4	7	Basement	RES3C	100	100	100	25	9.5	17	107.1
Concrete	4	7	Basement	RES3E	100	100	100	25	9.5	17	107.1
Concrete	4	7	Basement	AGR1	100	100	100	10	11.3	24.5	151.1
Concrete	4	7	Basement	IND2	100	100	100	10	11.3	24.5	151.1
Concrete	4	7	Basement	IND6	100	100	100	10	11.3	24.5	151.1

	Num. Story								Protection Factors		
Construction	Min	Max	Foundation	Occupancy	EW	RF	IWM	A%	UW	Warned (NB)	Warned (WB)
Concrete	4	7	Basement	RES1_1SWB	100	100	100	10	11.3	24.5	151.1
Concrete	4	7	Basement	RES1_2SWB	100	100	100	10	11.3	24.5	151.1
Concrete	4	7	Basement	RES1_3SWB	100	100	100	10	11.3	24.5	151.1
Concrete	4	7	Basement	RES3A	100	100	100	10	11.3	24.5	151.1
Concrete	4	7	Crawl	RES6	100	100	100	25	9.5	17	107.1
Concrete	4	7	Crawl	RES1_1SNB	100	100	100	10	11.3	24.5	151.1
Concrete	4	7	Crawl	RES1_2SNB	100	100	100	10	11.3	24.5	151.1
Concrete	4	7	Slab	COM3	100	100	100	25	9.5	17	107.1
Concrete	4	7	Slab	COM4	100	100	100	25	9.5	17	107.1
Concrete	4	7	Slab	COM5	100	100	100	25	9.5	17	107.1
Concrete	4	7	Slab	COM6	100	100	100	25	9.5	17	107.1
Concrete	4	7	Slab	COM7	100	100	100	25	9.5	17	107.1
Concrete	4	7	Slab	COM8	100	100	100	25	9.5	17	107.1
Concrete	4	7	Slab	COM9	100	100	100	25	9.5	17	107.1
Concrete	4	7	Slab	EDU1	100	100	100	25	9.5	17	107.1
Concrete	4	7	Slab	GOV1	100	100	100	25	9.5	17	107.1
Concrete	4	7	Slab	RES3C	100	100	100	25	9.5	17	107.1
Concrete	4	7	Slab	RES4	100	100	100	25	9.5	17	107.1
Concrete	4	7	Slab	AGR1	100	100	100	10	11.3	24.5	151.1
Concrete	4	7	Slab	COM1	100	100	100	10	11.3	24.5	151.1
Concrete	4	7	Slab	COM2	100	100	100	10	11.3	24.5	151.1
Concrete	4	7	Slab	EDU2	100	100	100	10	11.3	24.5	151.1
Concrete	4	7	Slab	GOV2	100	100	100	10	11.3	24.5	151.1
Concrete	4	7	Slab	IND1	100	100	100	10	11.3	24.5	151.1
Concrete	4	7	Slab	IND2	100	100	100	10	11.3	24.5	151.1
Concrete	4	7	Slab	IND6	100	100	100	10	11.3	24.5	151.1
Concrete	4	7	Slab	REL1	100	100	100	10	11.3	24.5	151.1

	Num. Story								Protection Factors		
Construction	Min	Max	Foundation	Occupancy	EW	RF	IWM	A%	UW	Warned (NB)	Warned (WB)
Concrete	4	7	Slab	RES1_1SNB	100	100	100	10	11.3	24.5	151.1
Concrete	4	7	Slab	RES1_3SNB	100	100	100	10	11.3	24.5	151.1
Concrete	8	30	Basement	RES1_1SWB	100	100	100	10	6.9	10.5	64.7
Concrete	8	30	Basement	RES1_2SWB	100	100	100	10	6.9	10.5	64.7
Concrete	8	30	Basement	RES1_3SWB	100	100	100	10	6.9	10.5	64.7
Concrete	8	30	Slab	AGR1	100	100	100	10	6.9	10.5	64.7
Concrete	8	30	Slab	COM1	100	100	100	10	6.9	10.5	64.7
Concrete	8	30	Slab	COM2	100	100	100	10	6.9	10.5	64.7
Concrete	8	30	Slab	EDU2	100	100	100	10	6.9	10.5	64.7
Concrete	8	30	Slab	IND6	100	100	100	10	6.9	10.5	64.7
Concrete	8	30	Slab	COM3	100	100	100	25	10.4	17.9	114.8
Concrete	8	30	Slab	COM4	100	100	100	25	10.4	17.9	114.8
Concrete	8	30	Slab	COM7	100	100	100	25	10.4	17.9	114.8
Concrete	8	30	Slab	COM8	100	100	100	25	10.4	17.9	114.8
Concrete	8	30	Slab	COM9	100	100	100	25	10.4	17.9	114.8
Concrete	8	30	Slab	GOV1	100	100	100	25	10.4	17.9	114.8
Concrete	8	30	Slab	RES3B	100	100	100	25	10.4	17.9	114.8
Concrete	30	77	Slab	COM3	100	100	100	25	11.8	28.3	258.4
Concrete	30	77	Slab	COM4	100	100	100	25	11.8	28.3	258.4
Manufactured	1	1	Crawl	RES2	1.5	5	10	10	1.6	1.6	5.3
Manufactured	2	3	Crawl	RES2	1.5	10	10	10	1.6	1.8	5.6
Masonry	1	1	Basement	COM3	50	10	100	25	3.7	3.7	9.2
Masonry	1	1	Basement	COM4	50	10	100	25	3.7	3.7	9.2
Masonry	1	1	Basement	COM5	50	10	100	25	3.7	3.7	9.2
Masonry	1	1	Basement	COM7	50	10	100	25	3.7	3.7	9.2
Masonry	1	1	Basement	COM8	50	10	100	25	3.7	3.7	9.2
Masonry	1	1	Basement	EDU1	50	10	100	25	3.7	3.7	9.2

	Num. Story								Protection Factors		
Construction	Min	Max	Foundation	Occupancy	EW	RF	IWM	A%	UW	Warned (NB)	Warned (WB)
Masonry	1	1	Basement	GOV1	50	10	100	25	3.7	3.7	9.2
Masonry	1	1	Basement	RES3B	50	10	100	25	3.7	3.7	9.2
Masonry	1	1	Basement	RES3C	50	10	100	25	3.7	3.7	9.2
Masonry	1	1	Basement	RES3E	50	10	100	25	3.7	3.7	9.2
Masonry	1	1	Basement	RES6	50	10	100	25	3.7	3.7	9.2
Masonry	1	1	Basement	AGR1	50	10	100	10	4.3	4.3	17.1
Masonry	1	1	Basement	COM1	50	10	100	10	4.3	4.3	17.1
Masonry	1	1	Basement	COM2	50	10	100	10	4.3	4.3	17.1
Masonry	1	1	Basement	EDU2	50	10	100	10	4.3	4.3	17.1
Masonry	1	1	Basement	IND2	50	10	100	10	4.3	4.3	17.1
Masonry	1	1	Basement	IND5	50	10	100	10	4.3	4.3	17.1
Masonry	1	1	Basement	IND6	50	10	100	10	4.3	4.3	17.1
Masonry	1	1	Basement	REL1	50	10	100	10	4.3	4.3	17.1
Masonry	1	1	Basement	RES1_1SWB	50	10	100	10	4.3	4.3	17.1
Masonry	1	1	Basement	RES1_2SWB	50	10	100	10	4.3	4.3	17.1
Masonry	1	1	Basement	RES1_3SWB	50	10	100	10	4.3	4.3	17.1
Masonry	1	1	Basement	RES2	50	10	100	10	4.3	4.3	17.1
Masonry	1	1	Basement	RES3A	50	10	100	10	4.3	4.3	17.1
Masonry	1	1	Crawl	COM4	50	10	100	25	3.7	3.7	9.2
Masonry	1	1	Crawl	RES3B	50	10	100	25	3.7	3.7	9.2
Masonry	1	1	Crawl	RES3C	50	10	100	25	3.7	3.7	9.2
Masonry	1	1	Crawl	RES3E	50	10	100	25	3.7	3.7	9.2
Masonry	1	1	Crawl	RES6	50	10	100	25	3.7	3.7	9.2
Masonry	1	1	Crawl	COM1	50	10	100	10	4.3	4.3	17.1
Masonry	1	1	Crawl	RES1_1SNB	50	10	100	10	4.3	4.3	17.1
Masonry	1	1	Crawl	RES1_2SNB	50	10	100	10	4.3	4.3	17.1
Masonry	1	1	Crawl	RES1_3SNB	50	10	100	10	4.3	4.3	17.1

	Num. Story								Protection Factors		
Construction	Min	Max	Foundation	Occupancy	EW	RF	IWM	A%	UW	Warned (NB)	Warned (WB)
Masonry	1	1	Crawl	RES3A	50	10	100	10	4.3	4.3	17.1
Masonry	1	1	Slab	COM10	50	10	100	25	3.7	3.7	9.2
Masonry	1	1	Slab	COM3	50	10	100	25	3.7	3.7	9.2
Masonry	1	1	Slab	COM4	50	10	100	25	3.7	3.7	9.2
Masonry	1	1	Slab	COM5	50	10	100	25	3.7	3.7	9.2
Masonry	1	1	Slab	COM6	50	10	100	25	3.7	3.7	9.2
Masonry	1	1	Slab	COM7	50	10	100	25	3.7	3.7	9.2
Masonry	1	1	Slab	COM8	50	10	100	25	3.7	3.7	9.2
Masonry	1	1	Slab	COM9	50	10	100	25	3.7	3.7	9.2
Masonry	1	1	Slab	EDU1	50	10	100	25	3.7	3.7	9.2
Masonry	1	1	Slab	GOV1	50	10	100	25	3.7	3.7	9.2
Masonry	1	1	Slab	RES3B	50	10	100	25	3.7	3.7	9.2
Masonry	1	1	Slab	RES3C	50	10	100	25	3.7	3.7	9.2
Masonry	1	1	Slab	RES3E	50	10	100	25	3.7	3.7	9.2
Masonry	1	1	Slab	RES4	50	10	100	25	3.7	3.7	9.2
Masonry	1	1	Slab	RES5	50	10	100	25	3.7	3.7	9.2
Masonry	1	1	Slab	RES6	50	10	100	25	3.7	3.7	9.2
Masonry	1	1	Slab	AGR1	50	10	100	10	4.3	4.3	17.1
Masonry	1	1	Slab	COM1	50	10	100	10	4.3	4.3	17.1
Masonry	1	1	Slab	COM2	50	10	100	10	4.3	4.3	17.1
Masonry	1	1	Slab	EDU2	50	10	100	10	4.3	4.3	17.1
Masonry	1	1	Slab	GOV2	50	10	100	10	4.3	4.3	17.1
Masonry	1	1	Slab	IND1	50	10	100	10	4.3	4.3	17.1
Masonry	1	1	Slab	IND2	50	10	100	10	4.3	4.3	17.1
Masonry	1	1	Slab	IND3	50	10	100	10	4.3	4.3	17.1
Masonry	1	1	Slab	IND4	50	10	100	10	4.3	4.3	17.1
Masonry	1	1	Slab	IND5	50	10	100	10	4.3	4.3	17.1

	Num. Story								Protection Factors		
Construction	Min	Max	Foundation	Occupancy	EW	RF	IWM	A%	UW	Warned (NB)	Warned (WB)
Masonry	1	1	Slab	IND6	50	10	100	10	4.3	4.3	17.1
Masonry	1	1	Slab	REL1	50	10	100	10	4.3	4.3	17.1
Masonry	1	1	Slab	RES1_1SNB	50	10	100	10	4.3	4.3	17.1
Masonry	1	1	Slab	RES1_2SNB	50	10	100	10	4.3	4.3	17.1
Masonry	1	1	Slab	RES2	50	10	100	10	4.3	4.3	17.1
Masonry	1	1	Slab	RES3A	50	10	100	10	4.3	4.3	17.1
Masonry	2	3	Basement	COM10	50	10	100	25	4.1	5.3	13.5
Masonry	2	3	Basement	COM3	50	10	100	25	4.1	5.3	13.5
Masonry	2	3	Basement	COM4	50	10	100	25	4.1	5.3	13.5
Masonry	2	3	Basement	COM5	50	10	100	25	4.1	5.3	13.5
Masonry	2	3	Basement	COM7	50	10	100	25	4.1	5.3	13.5
Masonry	2	3	Basement	COM8	50	10	100	25	4.1	5.3	13.5
Masonry	2	3	Basement	COM9	50	10	100	25	4.1	5.3	13.5
Masonry	2	3	Basement	EDU1	50	10	100	25	4.1	5.3	13.5
Masonry	2	3	Basement	GOV1	50	10	100	25	4.1	5.3	13.5
Masonry	2	3	Basement	RES3B	50	10	100	25	4.1	5.3	13.5
Masonry	2	3	Basement	RES3C	50	10	100	25	4.1	5.3	13.5
Masonry	2	3	Basement	RES3E	50	10	100	25	4.1	5.3	13.5
Masonry	2	3	Basement	RES4	50	10	100	25	4.1	5.3	13.5
Masonry	2	3	Basement	RES6	50	10	100	25	4.1	5.3	13.5
Masonry	2	3	Basement	AGR1	50	10	100	10	4.9	7	28.5
Masonry	2	3	Basement	COM1	50	10	100	10	4.9	7	28.5
Masonry	2	3	Basement	COM2	50	10	100	10	4.9	7	28.5
Masonry	2	3	Basement	EDU2	50	10	100	10	4.9	7	28.5
Masonry	2	3	Basement	IND1	50	10	100	10	4.9	7	28.5
Masonry	2	3	Basement	IND2	50	10	100	10	4.9	7	28.5
Masonry	2	3	Basement	IND3	50	10	100	10	4.9	7	28.5

	Num. Story								Protection Factors		
Construction	Min	Max	Foundation	Occupancy	EW	RF	IWM	A%	UW	Warned (NB)	Warned (WB)
Masonry	2	3	Basement	IND5	50	10	100	10	4.9	7	28.5
Masonry	2	3	Basement	IND6	50	10	100	10	4.9	7	28.5
Masonry	2	3	Basement	REL1	50	10	100	10	4.9	7	28.5
Masonry	2	3	Basement	RES1_1SWB	50	10	100	10	4.9	7	28.5
Masonry	2	3	Basement	RES1_2SWB	50	10	100	10	4.9	7	28.5
Masonry	2	3	Basement	RES1_3SWB	50	10	100	10	4.9	7	28.5
Masonry	2	3	Basement	RES2	50	10	100	10	4.9	7	28.5
Masonry	2	3	Basement	RES3A	50	10	100	10	4.9	7	28.5
Masonry	2	3	Crawl	COM4	50	10	100	25	4.1	5.3	13.5
Masonry	2	3	Crawl	RES3B	50	10	100	25	4.1	5.3	13.5
Masonry	2	3	Crawl	RES3C	50	10	100	25	4.1	5.3	13.5
Masonry	2	3	Crawl	RES3E	50	10	100	25	4.1	5.3	13.5
Masonry	2	3	Crawl	RES6	50	10	100	25	4.1	5.3	13.5
Masonry	2	3	Crawl	COM1	50	10	100	10	4.9	7	28.5
Masonry	2	3	Crawl	COM2	50	10	100	10	4.9	7	28.5
Masonry	2	3	Crawl	IND2	50	10	100	10	4.9	7	28.5
Masonry	2	3	Crawl	IND6	50	10	100	10	4.9	7	28.5
Masonry	2	3	Crawl	REL1	50	10	100	10	4.9	7	28.5
Masonry	2	3	Crawl	RES1_1SNB	50	10	100	10	4.9	7	28.5
Masonry	2	3	Crawl	RES1_2SNB	50	10	100	10	4.9	7	28.5
Masonry	2	3	Crawl	RES1_3SNB	50	10	100	10	4.9	7	28.5
Masonry	2	3	Crawl	RES3A	50	10	100	10	4.9	7	28.5
Masonry	2	3	Slab	COM10	50	10	100	25	4.1	5.3	13.5
Masonry	2	3	Slab	COM3	50	10	100	25	4.1	5.3	13.5
Masonry	2	3	Slab	COM4	50	10	100	25	4.1	5.3	13.5
Masonry	2	3	Slab	COM5	50	10	100	25	4.1	5.3	13.5
Masonry	2	3	Slab	COM6	50	10	100	25	4.1	5.3	13.5

	Num. Story								Protection Factors		
Construction	Min	Max	Foundation	Occupancy	EW	RF	IWM	A%	UW	Warned (NB)	Warned (WB)
Masonry	2	3	Slab	COM7	50	10	100	25	4.1	5.3	13.5
Masonry	2	3	Slab	COM8	50	10	100	25	4.1	5.3	13.5
Masonry	2	3	Slab	COM9	50	10	100	25	4.1	5.3	13.5
Masonry	2	3	Slab	EDU1	50	10	100	25	4.1	5.3	13.5
Masonry	2	3	Slab	GOV1	50	10	100	25	4.1	5.3	13.5
Masonry	2	3	Slab	RES3B	50	10	100	25	4.1	5.3	13.5
Masonry	2	3	Slab	RES3C	50	10	100	25	4.1	5.3	13.5
Masonry	2	3	Slab	RES3E	50	10	100	25	4.1	5.3	13.5
Masonry	2	3	Slab	RES4	50	10	100	25	4.1	5.3	13.5
Masonry	2	3	Slab	RES5	50	10	100	25	4.1	5.3	13.5
Masonry	2	3	Slab	RES6	50	10	100	25	4.1	5.3	13.5
Masonry	2	3	Slab	AGR1	50	10	100	10	4.9	7	28.5
Masonry	2	3	Slab	COM1	50	10	100	10	4.9	7	28.5
Masonry	2	3	Slab	COM2	50	10	100	10	4.9	7	28.5
Masonry	2	3	Slab	EDU2	50	10	100	10	4.9	7	28.5
Masonry	2	3	Slab	GOV2	50	10	100	10	4.9	7	28.5
Masonry	2	3	Slab	IND1	50	10	100	10	4.9	7	28.5
Masonry	2	3	Slab	IND2	50	10	100	10	4.9	7	28.5
Masonry	2	3	Slab	IND3	50	10	100	10	4.9	7	28.5
Masonry	2	3	Slab	IND4	50	10	100	10	4.9	7	28.5
Masonry	2	3	Slab	IND5	50	10	100	10	4.9	7	28.5
Masonry	2	3	Slab	IND6	50	10	100	10	4.9	7	28.5
Masonry	2	3	Slab	REL1	50	10	100	10	4.9	7	28.5
Masonry	2	3	Slab	RES1_1SNB	50	10	100	10	4.9	7	28.5
Masonry	2	3	Slab	RES1_2SNB	50	10	100	10	4.9	7	28.5
Masonry	2	3	Slab	RES1_3SNB	50	10	100	10	4.9	7	28.5
Masonry	2	3	Slab	RES3A	50	10	100	10	4.9	7	28.5

	Num. Story								Protection Factors		
Construction	Min	Max	Foundation	Occupancy	EW	RF	IWM	A%	UW	Warned (NB)	Warned (WB)
Masonry	4	7	Basement	COM3	50	10	100	25	8.6	15.3	56.7
Masonry	4	7	Basement	COM4	50	10	100	25	8.6	15.3	56.7
Masonry	4	7	Basement	COM8	50	10	100	25	8.6	15.3	56.7
Masonry	4	7	Basement	RES3B	50	10	100	25	8.6	15.3	56.7
Masonry	4	7	Basement	RES3C	50	10	100	25	8.6	15.3	56.7
Masonry	4	7	Basement	RES3E	50	10	100	25	8.6	15.3	56.7
Masonry	4	7	Basement	RES6	50	10	100	25	8.6	15.3	56.7
Masonry	4	7	Basement	COM1	50	10	100	10	10.1	21.3	76.8
Masonry	4	7	Basement	COM2	50	10	100	10	10.1	21.3	76.8
Masonry	4	7	Basement	IND1	50	10	100	10	10.1	21.3	76.8
Masonry	4	7	Basement	IND6	50	10	100	10	10.1	21.3	76.8
Masonry	4	7	Basement	REL1	50	10	100	10	10.1	21.3	76.8
Masonry	4	7	Basement	RES1_1SWB	50	10	100	10	10.1	21.3	76.8
Masonry	4	7	Basement	RES1_2SWB	50	10	100	10	10.1	21.3	76.8
Masonry	4	7	Basement	RES1_3SWB	50	10	100	10	10.1	21.3	76.8
Masonry	4	7	Basement	RES3A	50	10	100	10	10.1	21.3	76.8
Masonry	4	7	Crawl	COM4	50	10	100	25	8.6	15.3	56.7
Masonry	4	7	Crawl	RES3C	50	10	100	25	8.6	15.3	56.7
Masonry	4	7	Crawl	RES3E	50	10	100	25	8.6	15.3	56.7
Masonry	4	7	Crawl	RES6	50	10	100	25	8.6	15.3	56.7
Masonry	4	7	Crawl	RES1_1SNB	50	10	100	10	10.1	21.3	76.8
Masonry	4	7	Crawl	RES1_2SNB	50	10	100	10	10.1	21.3	76.8
Masonry	4	7	Crawl	RES1_3SNB	50	10	100	10	10.1	21.3	76.8
Masonry	4	7	Crawl	RES3A	50	10	100	10	10.1	21.3	76.8
Masonry	4	7	Slab	COM10	50	10	100	25	8.6	15.3	56.7
Masonry	4	7	Slab	COM3	50	10	100	25	8.6	15.3	56.7
Masonry	4	7	Slab	COM4	50	10	100	25	8.6	15.3	56.7

	Num. Story								Protection Factors		
Construction	Min	Max	Foundation	Occupancy	EW	RF	IWM	A%	UW	Warned (NB)	Warned (WB)
Masonry	4	7	Slab	COM5	50	10	100	25	8.6	15.3	56.7
Masonry	4	7	Slab	COM6	50	10	100	25	8.6	15.3	56.7
Masonry	4	7	Slab	COM7	50	10	100	25	8.6	15.3	56.7
Masonry	4	7	Slab	COM8	50	10	100	25	8.6	15.3	56.7
Masonry	4	7	Slab	COM9	50	10	100	25	8.6	15.3	56.7
Masonry	4	7	Slab	EDU1	50	10	100	25	8.6	15.3	56.7
Masonry	4	7	Slab	GOV1	50	10	100	25	8.6	15.3	56.7
Masonry	4	7	Slab	RES3B	50	10	100	25	8.6	15.3	56.7
Masonry	4	7	Slab	RES3C	50	10	100	25	8.6	15.3	56.7
Masonry	4	7	Slab	RES3E	50	10	100	25	8.6	15.3	56.7
Masonry	4	7	Slab	RES4	50	10	100	25	8.6	15.3	56.7
Masonry	4	7	Slab	RES5	50	10	100	25	8.6	15.3	56.7
Masonry	4	7	Slab	RES6	50	10	100	25	8.6	15.3	56.7
Masonry	4	7	Slab	COM1	50	10	100	10	10.1	21.3	76.8
Masonry	4	7	Slab	COM2	50	10	100	10	10.1	21.3	76.8
Masonry	4	7	Slab	EDU2	50	10	100	10	10.1	21.3	76.8
Masonry	4	7	Slab	GOV2	50	10	100	10	10.1	21.3	76.8
Masonry	4	7	Slab	IND1	50	10	100	10	10.1	21.3	76.8
Masonry	4	7	Slab	IND2	50	10	100	10	10.1	21.3	76.8
Masonry	4	7	Slab	IND3	50	10	100	10	10.1	21.3	76.8
Masonry	4	7	Slab	IND4	50	10	100	10	10.1	21.3	76.8
Masonry	4	7	Slab	IND5	50	10	100	10	10.1	21.3	76.8
Masonry	4	7	Slab	IND6	50	10	100	10	10.1	21.3	76.8
Masonry	4	7	Slab	REL1	50	10	100	10	10.1	21.3	76.8
Masonry	4	7	Slab	RES1_1SNB	50	10	100	10	10.1	21.3	76.8
Masonry	4	7	Slab	RES1_2SNB	50	10	100	10	10.1	21.3	76.8
Masonry	4	7	Slab	RES1_3SNB	50	10	100	10	10.1	21.3	76.8

	Num. Story								Protection Factors		
Construction	Min	Max	Foundation	Occupancy	EW	RF	IWM	A%	UW	Warned (NB)	Warned (WB)
Masonry	4	7	Slab	RES3A	50	10	100	10	10.1	21.3	76.8
Masonry	8	30	Basement	RES1_1SWB	10	10	10	10	2.7	3.9	14.1
Masonry	8	30	Basement	RES1_2SWB	10	10	10	10	2.7	3.9	14.1
Masonry	8	30	Basement	RES1_3SWB	10	10	10	10	2.7	3.9	14.1
Masonry	8	30	Basement	RES3A	10	10	10	10	2.7	3.9	14.1
Masonry	8	30	Basement	COM1	50	10	100	10	6.9	10.5	64.7
Masonry	8	30	Basement	RES1_1SWB	50	10	100	10	6.9	10.5	64.7
Masonry	8	30	Basement	RES1_2SWB	50	10	100	10	6.9	10.5	64.7
Masonry	8	30	Basement	RES1_3SWB	50	10	100	10	6.9	10.5	64.7
Masonry	8	30	Basement	RES3A	50	10	100	10	6.9	10.5	64.7
Masonry	8	30	Basement	COM4	50	10	100	25	10.4	17.9	114.8
Masonry	8	30	Crawl	RES1_1SNB	10	10	10	10	2.7	3.9	14.1
Masonry	8	30	Crawl	RES3A	10	10	10	10	2.7	3.9	14.1
Masonry	8	30	Crawl	RES1_1SNB	50	10	100	10	6.9	10.5	64.7
Masonry	8	30	Crawl	RES3A	50	10	100	10	6.9	10.5	64.7
Masonry	8	30	Crawl	RES3E	50	10	100	25	10.4	17.9	114.8
Masonry	8	30	Slab	AGR1	10	10	10	10	2.7	3.9	14.1
Masonry	8	30	Slab	COM1	10	10	10	10	2.7	3.9	14.1
Masonry	8	30	Slab	COM2	10	10	10	10	2.7	3.9	14.1
Masonry	8	30	Slab	GOV2	10	10	10	10	2.7	3.9	14.1
Masonry	8	30	Slab	IND2	10	10	10	10	2.7	3.9	14.1
Masonry	8	30	Slab	RES1_1SNB	10	10	10	10	2.7	3.9	14.1
Masonry	8	30	Slab	RES1_2SNB	10	10	10	10	2.7	3.9	14.1
Masonry	8	30	Slab	RES3A	10	10	10	10	2.7	3.9	14.1
Masonry	8	30	Slab	COM1	50	10	100	10	6.9	10.5	64.7
Masonry	8	30	Slab	COM2	50	10	100	10	6.9	10.5	64.7
Masonry	8	30	Slab	EDU2	50	10	100	10	6.9	10.5	64.7

	Num. Story								Protection Factors		
Construction	Min	Max	Foundation	Occupancy	EW	RF	IWM	A%	UW	Warned (NB)	Warned (WB)
Masonry	8	30	Slab	GOV2	50	10	100	10	6.9	10.5	64.7
Masonry	8	30	Slab	RES1_1SNB	50	10	100	10	6.9	10.5	64.7
Masonry	8	30	Slab	RES1_2SNB	50	10	100	10	6.9	10.5	64.7
Masonry	8	30	Slab	RES1_3SNB	50	10	100	10	6.9	10.5	64.7
Masonry	8	30	Slab	COM3	50	10	100	25	10.4	17.9	114.8
Masonry	8	30	Slab	COM4	50	10	100	25	10.4	17.9	114.8
Masonry	8	30	Slab	COM6	50	10	100	25	10.4	17.9	114.8
Masonry	8	30	Slab	COM8	50	10	100	25	10.4	17.9	114.8
Masonry	8	30	Slab	COM9	50	10	100	25	10.4	17.9	114.8
Masonry	8	30	Slab	RES3C	50	10	100	25	10.4	17.9	114.8
Masonry	30	77	Crawl	RES1_SNB	50	10	100	10	9.3	25.5	101.3
Masonry	30	77	Slab	COM3	50	10	100	25	6.8	17.7	70.9
Masonry	30	77	Slab	COM4	50	10	100	25	6.8	17.7	70.9
Masonry	30	77	Slab	COM8	50	10	100	25	6.8	17.7	70.9
Masonry	30	77	Slab	COM1	50	10	100	10	9.3	25.5	101.3
Masonry	30	77	Slab	RES1_1SNB	50	10	100	10	9.3	25.5	101.3
Steel	1	1	Basement	COM7	30	30	30	25	2.3	2.3	12.1
Steel	1	1	Basement	COM8	30	30	30	25	2.3	2.3	12.1
Steel	1	1	Basement	COM1	30	30	30	10	2.4	2.4	12.6
Steel	1	1	Basement	COM2	30	30	30	10	2.4	2.4	12.6
Steel	1	1	Basement	IND6	30	30	30	10	2.4	2.4	12.6
Steel	1	1	Basement	REL1	30	30	30	10	2.4	2.4	12.6
Steel	1	1	Crawl	RES3B	30	30	30	25	2.3	2.3	12.1
Steel	1	1	Crawl	RES3C	30	30	30	25	2.3	2.3	12.1
Steel	1	1	Crawl	RES1_1SNB	30	30	30	10	2.4	2.4	12.6
Steel	1	1	Crawl	RES3A	30	30	30	10	2.4	2.4	12.6
Steel	1	1	Slab	COM10	30	30	30	25	2.3	2.3	12.1

	Num. Story								Protection Factors		
Construction	Min	Max	Foundation	Occupancy	EW	RF	IWM	A%	UW	Warned (NB)	Warned (WB)
Steel	1	1	Slab	COM3	30	30	30	25	2.3	2.3	12.1
Steel	1	1	Slab	COM4	30	30	30	25	2.3	2.3	12.1
Steel	1	1	Slab	COM5	30	30	30	25	2.3	2.3	12.1
Steel	1	1	Slab	COM6	30	30	30	25	2.3	2.3	12.1
Steel	1	1	Slab	COM7	30	30	30	25	2.3	2.3	12.1
Steel	1	1	Slab	COM8	30	30	30	25	2.3	2.3	12.1
Steel	1	1	Slab	COM9	30	30	30	25	2.3	2.3	12.1
Steel	1	1	Slab	EDU1	30	30	30	25	2.3	2.3	12.1
Steel	1	1	Slab	GOV1	30	30	30	25	2.3	2.3	12.1
Steel	1	1	Slab	RES3B	30	30	30	25	2.3	2.3	12.1
Steel	1	1	Slab	RES4	30	30	30	25	2.3	2.3	12.1
Steel	1	1	Slab	RES5	30	30	30	25	2.3	2.3	12.1
Steel	1	1	Slab	RES6	30	30	30	25	2.3	2.3	12.1
Steel	1	1	Slab	AGR1	30	30	30	10	2.4	2.4	12.6
Steel	1	1	Slab	COM1	30	30	30	10	2.4	2.4	12.6
Steel	1	1	Slab	COM2	30	30	30	10	2.4	2.4	12.6
Steel	1	1	Slab	EDU2	30	30	30	10	2.4	2.4	12.6
Steel	1	1	Slab	GOV2	30	30	30	10	2.4	2.4	12.6
Steel	1	1	Slab	IND1	30	30	30	10	2.4	2.4	12.6
Steel	1	1	Slab	IND2	30	30	30	10	2.4	2.4	12.6
Steel	1	1	Slab	IND3	30	30	30	10	2.4	2.4	12.6
Steel	1	1	Slab	IND4	30	30	30	10	2.4	2.4	12.6
Steel	1	1	Slab	IND5	30	30	30	10	2.4	2.4	12.6
Steel	1	1	Slab	IND6	30	30	30	10	2.4	2.4	12.6
Steel	1	1	Slab	REL1	30	30	30	10	2.4	2.4	12.6
Steel	1	1	Slab	RES1_3SNB	30	30	30	10	2.4	2.4	12.6
Steel	1	1	Slab	RES3A	30	30	30	10	2.4	2.4	12.6

	Num. Story								Protection Factors		
Construction	Min	Max	Foundation	Occupancy	EW	RF	IWM	A%	UW	Warned (NB)	Warned (WB)
Steel	2	3	Basement	COM3	30	30	30	25	2.7	3.1	27.8
Steel	2	3	Basement	COM6	30	30	30	25	2.7	3.1	27.8
Steel	2	3	Basement	EDU1	30	30	30	25	2.7	3.1	27.8
Steel	2	3	Basement	RES6	30	30	30	25	2.7	3.1	27.8
Steel	2	3	Basement	COM1	30	30	30	10	2.9	3.4	30.3
Steel	2	3	Basement	EDU2	30	30	30	10	2.9	3.4	30.3
Steel	2	3	Basement	RES1_2SWB	30	30	30	10	2.9	3.4	30.3
Steel	2	3	Basement	RES3A	30	30	30	10	2.9	3.4	30.3
Steel	2	3	Crawl	COM8	30	30	30	25	2.7	3.1	27.8
Steel	2	3	Crawl	RES3C	30	30	30	25	2.7	3.1	27.8
Steel	2	3	Crawl	RES3A	30	30	30	10	2.9	3.4	30.3
Steel	2	3	Slab	COM10	30	30	30	25	2.7	3.1	27.8
Steel	2	3	Slab	COM3	30	30	30	25	2.7	3.1	27.8
Steel	2	3	Slab	COM4	30	30	30	25	2.7	3.1	27.8
Steel	2	3	Slab	COM5	30	30	30	25	2.7	3.1	27.8
Steel	2	3	Slab	COM6	30	30	30	25	2.7	3.1	27.8
Steel	2	3	Slab	COM7	30	30	30	25	2.7	3.1	27.8
Steel	2	3	Slab	COM8	30	30	30	25	2.7	3.1	27.8
Steel	2	3	Slab	COM9	30	30	30	25	2.7	3.1	27.8
Steel	2	3	Slab	EDU1	30	30	30	25	2.7	3.1	27.8
Steel	2	3	Slab	GOV1	30	30	30	25	2.7	3.1	27.8
Steel	2	3	Slab	RES3B	30	30	30	25	2.7	3.1	27.8
Steel	2	3	Slab	RES3E	30	30	30	25	2.7	3.1	27.8
Steel	2	3	Slab	RES4	30	30	30	25	2.7	3.1	27.8
Steel	2	3	Slab	RES5	30	30	30	25	2.7	3.1	27.8
Steel	2	3	Slab	RES6	30	30	30	25	2.7	3.1	27.8
Steel	2	3	Slab	AGR1	30	30	30	10	2.9	3.4	30.3

	Num. Story								Protection Factors		
Construction	Min	Max	Foundation	Occupancy	EW	RF	IWM	A%	UW	Warned (NB)	Warned (WB)
Steel	2	3	Slab	COM1	30	30	30	10	2.9	3.4	30.3
Steel	2	3	Slab	COM2	30	30	30	10	2.9	3.4	30.3
Steel	2	3	Slab	EDU2	30	30	30	10	2.9	3.4	30.3
Steel	2	3	Slab	GOV2	30	30	30	10	2.9	3.4	30.3
Steel	2	3	Slab	IND1	30	30	30	10	2.9	3.4	30.3
Steel	2	3	Slab	IND2	30	30	30	10	2.9	3.4	30.3
Steel	2	3	Slab	IND3	30	30	30	10	2.9	3.4	30.3
Steel	2	3	Slab	IND4	30	30	30	10	2.9	3.4	30.3
Steel	2	3	Slab	IND5	30	30	30	10	2.9	3.4	30.3
Steel	2	3	Slab	IND6	30	30	30	10	2.9	3.4	30.3
Steel	2	3	Slab	REL1	30	30	30	10	2.9	3.4	30.3
Steel	2	3	Slab	RES1_1SNB	30	30	30	10	2.9	3.4	30.3
Steel	2	3	Slab	RES1_2SNB	30	30	30	10	2.9	3.4	30.3
Steel	2	3	Slab	RES1_3SNB	30	30	30	10	2.9	3.4	30.3
Steel	2	3	Slab	RES3A	30	30	30	10	2.9	3.4	30.3
Steel	4	7	Basement	COM3	30	30	30	25	5.1	7.6	36.1
Steel	4	7	Basement	COM4	30	30	30	25	5.1	7.6	36.1
Steel	4	7	Basement	COM5	30	30	30	25	5.1	7.6	36.1
Steel	4	7	Basement	COM8	30	30	30	25	5.1	7.6	36.1
Steel	4	7	Basement	RES3B	30	30	30	25	5.1	7.6	36.1
Steel	4	7	Basement	RES3C	30	30	30	25	5.1	7.6	36.1
Steel	4	7	Basement	RES3E	30	30	30	25	5.1	7.6	36.1
Steel	4	7	Basement	RES6	30	30	30	25	5.1	7.6	36.1
Steel	4	7	Basement	COM1	30	30	30	10	5.4	8.5	40.1
Steel	4	7	Basement	IND6	30	30	30	10	5.4	8.5	40.1
Steel	4	7	Basement	REL1	30	30	30	10	5.4	8.5	40.1
Steel	4	7	Basement	RES1_3SWB	30	30	30	10	5.4	8.5	40.1

	Num. Story								Protection Factors		
Construction	Min	Max	Foundation	Occupancy	EW	RF	IWM	A%	UW	Warned (NB)	Warned (WB)
Steel	4	7	Basement	RES3A	30	30	30	10	5.4	8.5	40.1
Steel	4	7	Crawl	RES3B	30	30	30	25	5.1	7.6	36.1
Steel	4	7	Crawl	RES3E	30	30	30	25	5.1	7.6	36.1
Steel	4	7	Crawl	RES6	30	30	30	25	5.1	7.6	36.1
Steel	4	7	Crawl	RES1_3SNB	30	30	30	10	5.4	8.5	40.1
Steel	4	7	Crawl	RES3A	30	30	30	10	5.4	8.5	40.1
Steel	4	7	Slab	COM10	30	30	30	25	5.1	7.6	36.1
Steel	4	7	Slab	COM3	30	30	30	25	5.1	7.6	36.1
Steel	4	7	Slab	COM4	30	30	30	25	5.1	7.6	36.1
Steel	4	7	Slab	COM5	30	30	30	25	5.1	7.6	36.1
Steel	4	7	Slab	COM6	30	30	30	25	5.1	7.6	36.1
Steel	4	7	Slab	COM7	30	30	30	25	5.1	7.6	36.1
Steel	4	7	Slab	COM8	30	30	30	25	5.1	7.6	36.1
Steel	4	7	Slab	COM9	30	30	30	25	5.1	7.6	36.1
Steel	4	7	Slab	EDU1	30	30	30	25	5.1	7.6	36.1
Steel	4	7	Slab	GOV1	30	30	30	25	5.1	7.6	36.1
Steel	4	7	Slab	RES3C	30	30	30	25	5.1	7.6	36.1
Steel	4	7	Slab	RES3E	30	30	30	25	5.1	7.6	36.1
Steel	4	7	Slab	RES4	30	30	30	25	5.1	7.6	36.1
Steel	4	7	Slab	RES6	30	30	30	25	5.1	7.6	36.1
Steel	4	7	Slab	AGR1	30	30	30	10	5.4	8.5	40.1
Steel	4	7	Slab	COM1	30	30	30	10	5.4	8.5	40.1
Steel	4	7	Slab	COM2	30	30	30	10	5.4	8.5	40.1
Steel	4	7	Slab	EDU2	30	30	30	10	5.4	8.5	40.1
Steel	4	7	Slab	GOV2	30	30	30	10	5.4	8.5	40.1
Steel	4	7	Slab	IND1	30	30	30	10	5.4	8.5	40.1
Steel	4	7	Slab	IND2	30	30	30	10	5.4	8.5	40.1

	Num. Story								Protection Factors		
Construction	Min	Max	Foundation	Occupancy	EW	RF	IWM	A%	UW	Warned (NB)	Warned (WB)
Steel	4	7	Slab	IND3	30	30	30	10	5.4	8.5	40.1
Steel	4	7	Slab	IND5	30	30	30	10	5.4	8.5	40.1
Steel	4	7	Slab	IND6	30	30	30	10	5.4	8.5	40.1
Steel	4	7	Slab	REL1	30	30	30	10	5.4	8.5	40.1
Steel	4	7	Slab	RES1_2SNB	30	30	30	10	5.4	8.5	40.1
Steel	4	7	Slab	RES1_3SNB	30	30	30	10	5.4	8.5	40.1
Steel	4	7	Slab	RES3A	30	30	30	10	5.4	8.5	40.1
Steel	8	30	Basement	RES1_1SWB	30	30	30	10	5.1	7.9	38.3
Steel	8	30	Basement	COM4	30	30	30	25	13.5	25.9	163.8
Steel	8	30	Basement	RES3E	30	30	30	25	13.5	25.9	163.8
Steel	8	30	Basement	RES6	30	30	30	25	13.5	25.9	163.8
Steel	8	30	Crawl	RES1_3SNB	30	30	30	10	5.1	7.9	38.3
Steel	8	30	Crawl	RES3E	30	30	30	25	13.5	25.9	163.8
Steel	8	30	Crawl	RES6	30	30	30	25	13.5	25.9	163.8
Steel	8	30	Slab	AGR1	30	30	30	10	5.1	7.9	38.3
Steel	8	30	Slab	COM1	30	30	30	10	5.1	7.9	38.3
Steel	8	30	Slab	COM2	30	30	30	10	5.1	7.9	38.3
Steel	8	30	Slab	EDU2	30	30	30	10	5.1	7.9	38.3
Steel	8	30	Slab	GOV2	30	30	30	10	5.1	7.9	38.3
Steel	8	30	Slab	IND1	30	30	30	10	5.1	7.9	38.3
Steel	8	30	Slab	IND2	30	30	30	10	5.1	7.9	38.3
Steel	8	30	Slab	IND3	30	30	30	10	5.1	7.9	38.3
Steel	8	30	Slab	IND4	30	30	30	10	5.1	7.9	38.3
Steel	8	30	Slab	IND5	30	30	30	10	5.1	7.9	38.3
Steel	8	30	Slab	IND6	30	30	30	10	5.1	7.9	38.3
Steel	8	30	Slab	REL1	30	30	30	10	5.1	7.9	38.3
Steel	8	30	Slab	RES3A	30	30	30	10	5.1	7.9	38.3

	Num. Story								Protection Factors		
Construction	Min	Max	Foundation	Occupancy	EW	RF	IWM	A%	UW	Warned (NB)	Warned (WB)
Steel	8	30	Slab	COM10	30	30	30	25	13.5	25.9	163.8
Steel	8	30	Slab	COM3	30	30	30	25	13.5	25.9	163.8
Steel	8	30	Slab	COM4	30	30	30	25	13.5	25.9	163.8
Steel	8	30	Slab	COM5	30	30	30	25	13.5	25.9	163.8
Steel	8	30	Slab	COM6	30	30	30	25	13.5	25.9	163.8
Steel	8	30	Slab	COM7	30	30	30	25	13.5	25.9	163.8
Steel	8	30	Slab	COM8	30	30	30	25	13.5	25.9	163.8
Steel	8	30	Slab	COM9	30	30	30	25	13.5	25.9	163.8
Steel	8	30	Slab	EDU1	30	30	30	25	13.5	25.9	163.8
Steel	8	30	Slab	GOV1	30	30	30	25	13.5	25.9	163.8
Steel	8	30	Slab	RES4	30	30	30	25	13.5	25.9	163.8
Steel	8	30	Slab	RES6	30	30	30	25	13.5	25.9	163.8
Steel	30	77	Slab	COM10	30	30	30	25	3.6	8.3	40.6
Steel	30	77	Slab	COM3	30	30	30	25	3.6	8.3	40.6
Steel	30	77	Slab	COM4	30	30	30	25	3.6	8.3	40.6
Steel	30	77	Slab	COM5	30	30	30	25	3.6	8.3	40.6
Steel	30	77	Slab	COM7	30	30	30	25	3.6	8.3	40.6
Steel	30	77	Slab	COM8	30	30	30	25	3.6	8.3	40.6
Steel	30	77	Slab	EDU1	30	30	30	25	3.6	8.3	40.6
Steel	30	77	Slab	GOV1	30	30	30	25	3.6	8.3	40.6
Steel	30	77	Slab	COM1	30	30	30	10	4	9.3	45
Steel	30	77	Slab	COM2	30	30	30	10	4	9.3	45
Steel	30	77	Slab	IND1	30	30	30	10	4	9.3	45
Steel	30	77	Slab	IND2	30	30	30	10	4	9.3	45
Steel	30	77	Slab	IND6	30	30	30	10	4	9.3	45
Wood	1	1	Basement	AGR1	10	10	10	10	1.6	1.6	4.9
Wood	1	1	Basement	COM1	10	10	10	10	1.6	1.6	4.9

	Num. Story								Protection Factors		
Construction	Min	Max	Foundation	Occupancy	EW	RF	IWM	A%	UW	Warned (NB)	Warned (WB)
Wood	1	1	Basement	COM2	10	10	10	10	1.6	1.6	4.9
Wood	1	1	Basement	COM3	10	10	10	25	1.6	1.6	4.9
Wood	1	1	Basement	COM4	10	10	10	25	1.6	1.6	4.9
Wood	1	1	Basement	COM5	10	10	10	25	1.6	1.6	4.9
Wood	1	1	Basement	COM6	10	10	10	25	1.6	1.6	4.9
Wood	1	1	Basement	COM7	10	10	10	25	1.6	1.6	4.9
Wood	1	1	Basement	COM8	10	10	10	25	1.6	1.6	4.9
Wood	1	1	Basement	EDU1	10	10	10	25	1.6	1.6	4.9
Wood	1	1	Basement	EDU2	10	10	10	10	1.6	1.6	4.9
Wood	1	1	Basement	GOV1	10	10	10	25	1.6	1.6	4.9
Wood	1	1	Basement	IND2	10	10	10	10	1.6	1.6	4.9
Wood	1	1	Basement	IND5	10	10	10	10	1.6	1.6	4.9
Wood	1	1	Basement	IND6	10	10	10	10	1.6	1.6	4.9
Wood	1	1	Basement	REL1	10	10	10	10	1.6	1.6	4.9
Wood	1	1	Basement	RES1_1SWB	10	10	10	10	1.6	1.6	4.9
Wood	1	1	Basement	RES1_2SWB	10	10	10	10	1.6	1.6	4.9
Wood	1	1	Basement	RES1_3SWB	10	10	10	10	1.6	1.6	4.9
Wood	1	1	Basement	RES2	10	10	10	10	1.6	1.6	4.9
Wood	1	1	Basement	RES3A	10	10	10	10	1.6	1.6	4.9
Wood	1	1	Basement	RES3B	10	10	10	25	1.6	1.6	4.9
Wood	1	1	Basement	RES3C	10	10	10	25	1.6	1.6	4.9
Wood	1	1	Basement	RES3E	10	10	10	25	1.6	1.6	4.9
Wood	1	1	Basement	RES4	10	10	10	25	1.6	1.6	4.9
Wood	1	1	Basement	RES5	10	10	10	25	1.6	1.6	4.9
Wood	1	1	Basement	RES6	10	10	10	25	1.6	1.6	4.9
Wood	1	1	Crawl	COM8	10	10	10	25	1.6	1.6	4.9
Wood	1	1	Crawl	RES1_1SNB	10	10	10	10	1.6	1.6	4.9

	Num. Story								Protection Factors		
Construction	Min	Max	Foundation	Occupancy	EW	RF	IWM	A%	UW	Warned (NB)	Warned (WB)
Wood	1	1	Crawl	RES1_2SNB	10	10	10	10	1.6	1.6	4.9
Wood	1	1	Crawl	RES2	10	10	10	10	1.6	1.6	4.9
Wood	1	1	Crawl	RES3A	10	10	10	10	1.6	1.6	4.9
Wood	1	1	Crawl	RES3B	10	10	10	25	1.6	1.6	4.9
Wood	1	1	Crawl	RES3C	10	10	10	25	1.6	1.6	4.9
Wood	1	1	Crawl	RES6	10	10	10	25	1.6	1.6	4.9
Wood	1	1	Slab	AGR1	10	10	10	10	1.6	1.6	4.9
Wood	1	1	Slab	COM1	10	10	10	10	1.6	1.6	4.9
Wood	1	1	Slab	COM10	10	10	10	25	1.6	1.6	4.9
Wood	1	1	Slab	COM2	10	10	10	10	1.6	1.6	4.9
Wood	1	1	Slab	COM3	10	10	10	25	1.6	1.6	4.9
Wood	1	1	Slab	COM4	10	10	10	25	1.6	1.6	4.9
Wood	1	1	Slab	COM5	10	10	10	25	1.6	1.6	4.9
Wood	1	1	Slab	COM6	10	10	10	25	1.6	1.6	4.9
Wood	1	1	Slab	COM7	10	10	10	25	1.6	1.6	4.9
Wood	1	1	Slab	COM8	10	10	10	25	1.6	1.6	4.9
Wood	1	1	Slab	COM9	10	10	10	25	1.6	1.6	4.9
Wood	1	1	Slab	EDU1	10	10	10	25	1.6	1.6	4.9
Wood	1	1	Slab	EDU2	10	10	10	10	1.6	1.6	4.9
Wood	1	1	Slab	GOV1	10	10	10	25	1.6	1.6	4.9
Wood	1	1	Slab	GOV2	10	10	10	10	1.6	1.6	4.9
Wood	1	1	Slab	IND1	10	10	10	10	1.6	1.6	4.9
Wood	1	1	Slab	IND2	10	10	10	10	1.6	1.6	4.9
Wood	1	1	Slab	IND3	10	10	10	10	1.6	1.6	4.9
Wood	1	1	Slab	IND4	10	10	10	10	1.6	1.6	4.9
Wood	1	1	Slab	IND5	10	10	10	10	1.6	1.6	4.9
Wood	1	1	Slab	IND6	10	10	10	10	1.6	1.6	4.9

	Num. Story								Protection Factors		
Construction	Min	Max	Foundation	Occupancy	EW	RF	IWM	A%	UW	Warned (NB)	Warned (WB)
Wood	1	1	Slab	REL1	10	10	10	10	1.6	1.6	4.9
Wood	1	1	Slab	RES1_1SNB	10	10	10	10	1.6	1.6	4.9
Wood	1	1	Slab	RES1_2SNB	10	10	10	10	1.6	1.6	4.9
Wood	1	1	Slab	RES1_3SNB	10	10	10	10	1.6	1.6	4.9
Wood	1	1	Slab	RES3A	10	10	10	10	1.6	1.6	4.9
Wood	1	1	Slab	RES3B	10	10	10	25	1.6	1.6	4.9
Wood	1	1	Slab	RES3C	10	10	10	25	1.6	1.6	4.9
Wood	1	1	Slab	RES3E	10	10	10	25	1.6	1.6	4.9
Wood	1	1	Slab	RES4	10	10	10	25	1.6	1.6	4.9
Wood	1	1	Slab	RES6	10	10	10	25	1.6	1.6	4.9
Wood	2	3	Basement	AGR1	10	10	10	10	1.5	1.7	5.1
Wood	2	3	Basement	COM1	10	10	10	10	1.5	1.7	5.1
Wood	2	3	Basement	COM10	10	10	10	25	1.5	1.7	5.1
Wood	2	3	Basement	COM2	10	10	10	10	1.5	1.7	5.1
Wood	2	3	Basement	COM3	10	10	10	25	1.5	1.7	5.1
Wood	2	3	Basement	COM4	10	10	10	25	1.5	1.7	5.1
Wood	2	3	Basement	COM5	10	10	10	25	1.5	1.7	5.1
Wood	2	3	Basement	COM6	10	10	10	25	1.5	1.7	5.1
Wood	2	3	Basement	COM7	10	10	10	25	1.5	1.7	5.1
Wood	2	3	Basement	COM8	10	10	10	25	1.5	1.7	5.1
Wood	2	3	Basement	EDU1	10	10	10	25	1.5	1.7	5.1
Wood	2	3	Basement	EDU2	10	10	10	10	1.5	1.7	5.1
Wood	2	3	Basement	GOV1	10	10	10	25	1.5	1.7	5.1
Wood	2	3	Basement	IND1	10	10	10	10	1.5	1.7	5.1
Wood	2	3	Basement	IND2	10	10	10	10	1.5	1.7	5.1
Wood	2	3	Basement	IND5	10	10	10	10	1.5	1.7	5.1
Wood	2	3	Basement	IND6	10	10	10	10	1.5	1.7	5.1

	Num. Story								Protection Factors		
Construction	Min	Max	Foundation	Occupancy	EW	RF	IWM	A%	UW	Warned (NB)	Warned (WB)
Wood	2	3	Basement	REL1	10	10	10	10	1.5	1.7	5.1
Wood	2	3	Basement	RES1_1SWB	10	10	10	10	1.5	1.7	5.1
Wood	2	3	Basement	RES1_2SWB	10	10	10	10	1.5	1.7	5.1
Wood	2	3	Basement	RES1_3SWB	10	10	10	10	1.5	1.7	5.1
Wood	2	3	Basement	RES3A	10	10	10	10	1.5	1.7	5.1
Wood	2	3	Basement	RES3B	10	10	10	25	1.5	1.7	5.1
Wood	2	3	Basement	RES3C	10	10	10	25	1.5	1.7	5.1
Wood	2	3	Basement	RES3E	10	10	10	25	1.5	1.7	5.1
Wood	2	3	Basement	RES4	10	10	10	25	1.5	1.7	5.1
Wood	2	3	Basement	RES6	10	10	10	25	1.5	1.7	5.1
Wood	2	3	Crawl	COM4	10	10	10	25	1.5	1.7	5.1
Wood	2	3	Crawl	COM8	10	10	10	25	1.5	1.7	5.1
Wood	2	3	Crawl	RES1_1SNB	10	10	10	10	1.5	1.7	5.1
Wood	2	3	Crawl	RES1_1SWB	10	10	10	10	1.5	1.7	5.1
Wood	2	3	Crawl	RES1_2SNB	10	10	10	10	1.5	1.7	5.1
Wood	2	3	Crawl	RES1_3SNB	10	10	10	10	1.5	1.7	5.1
Wood	2	3	Crawl	RES3A	10	10	10	10	1.5	1.7	5.1
Wood	2	3	Crawl	RES3B	10	10	10	25	1.5	1.7	5.1
Wood	2	3	Crawl	RES3C	10	10	10	25	1.5	1.7	5.1
Wood	2	3	Crawl	RES3E	10	10	10	25	1.5	1.7	5.1
Wood	2	3	Crawl	RES6	10	10	10	25	1.5	1.7	5.1
Wood	2	3	Slab	AGR1	10	10	10	10	1.5	1.7	5.1
Wood	2	3	Slab	COM1	10	10	10	10	1.5	1.7	5.1
Wood	2	3	Slab	COM10	10	10	10	25	1.5	1.7	5.1
Wood	2	3	Slab	COM2	10	10	10	10	1.5	1.7	5.1
Wood	2	3	Slab	COM3	10	10	10	25	1.5	1.7	5.1
Wood	2	3	Slab	COM4	10	10	10	25	1.5	1.7	5.1

	Num. Story								Protection Factors		
Construction	Min	Max	Foundation	Occupancy	EW	RF	IWM	A%	UW	Warned (NB)	Warned (WB)
Wood	2	3	Slab	COM5	10	10	10	25	1.5	1.7	5.1
Wood	2	3	Slab	COM6	10	10	10	25	1.5	1.7	5.1
Wood	2	3	Slab	COM7	10	10	10	25	1.5	1.7	5.1
Wood	2	3	Slab	COM8	10	10	10	25	1.5	1.7	5.1
Wood	2	3	Slab	COM9	10	10	10	25	1.5	1.7	5.1
Wood	2	3	Slab	EDU1	10	10	10	25	1.5	1.7	5.1
Wood	2	3	Slab	EDU2	10	10	10	10	1.5	1.7	5.1
Wood	2	3	Slab	GOV1	10	10	10	25	1.5	1.7	5.1
Wood	2	3	Slab	GOV2	10	10	10	10	1.5	1.7	5.1
Wood	2	3	Slab	IND1	10	10	10	10	1.5	1.7	5.1
Wood	2	3	Slab	IND2	10	10	10	10	1.5	1.7	5.1
Wood	2	3	Slab	IND3	10	10	10	10	1.5	1.7	5.1
Wood	2	3	Slab	IND4	10	10	10	10	1.5	1.7	5.1
Wood	2	3	Slab	IND5	10	10	10	10	1.5	1.7	5.1
Wood	2	3	Slab	IND6	10	10	10	10	1.5	1.7	5.1
Wood	2	3	Slab	REL1	10	10	10	10	1.5	1.7	5.1
Wood	2	3	Slab	RES1_1SNB	10	10	10	10	1.5	1.7	5.1
Wood	2	3	Slab	RES1_2SNB	10	10	10	10	1.5	1.7	5.1
Wood	2	3	Slab	RES1_3SNB	10	10	10	10	1.5	1.7	5.1
Wood	2	3	Slab	RES3A	10	10	10	10	1.5	1.7	5.1
Wood	2	3	Slab	RES3B	10	10	10	25	1.5	1.7	5.1
Wood	2	3	Slab	RES3C	10	10	10	25	1.5	1.7	5.1
Wood	2	3	Slab	RES3E	10	10	10	25	1.5	1.7	5.1
Wood	2	3	Slab	RES4	10	10	10	25	1.5	1.7	5.1
Wood	2	3	Slab	RES6	10	10	10	25	1.5	1.7	5.1
Wood	4	7	Basement	COM3	10	10	10	25	2.9	3.7	13.1
Wood	4	7	Basement	COM4	10	10	10	25	2.9	3.7	13.1

	Num. Story								Protection Factors		
Construction	Min	Max	Foundation	Occupancy	EW	RF	IWM	A%	UW	Warned (NB)	Warned (WB)
Wood	4	7	Basement	COM7	10	10	10	25	2.9	3.7	13.1
Wood	4	7	Basement	COM8	10	10	10	25	2.9	3.7	13.1
Wood	4	7	Basement	RES3B	10	10	10	25	2.9	3.7	13.1
Wood	4	7	Basement	RES3C	10	10	10	25	2.9	3.7	13.1
Wood	4	7	Basement	RES3E	10	10	10	25	2.9	3.7	13.1
Wood	4	7	Basement	RES6	10	10	10	25	2.9	3.7	13.1
Wood	4	7	Basement	COM1	10	10	10	10	2.8	3.7	13.2
Wood	4	7	Basement	COM2	10	10	10	10	2.8	3.7	13.2
Wood	4	7	Basement	IND6	10	10	10	10	2.8	3.7	13.2
Wood	4	7	Basement	REL1	10	10	10	10	2.8	3.7	13.2
Wood	4	7	Basement	RES1_1SWB	10	10	10	10	2.8	3.7	13.2
Wood	4	7	Basement	RES1_2SWB	10	10	10	10	2.8	3.7	13.2
Wood	4	7	Basement	RES1_3SWB	10	10	10	10	2.8	3.7	13.2
Wood	4	7	Basement	RES3A	10	10	10	10	2.8	3.7	13.2
Wood	4	7	Crawl	RES3B	10	10	10	25	2.9	3.7	13.1
Wood	4	7	Crawl	RES3C	10	10	10	25	2.9	3.7	13.1
Wood	4	7	Crawl	RES3E	10	10	10	25	2.9	3.7	13.1
Wood	4	7	Crawl	RES6	10	10	10	25	2.9	3.7	13.1
Wood	4	7	Crawl	RES1_1SNB	10	10	10	10	2.8	3.7	13.2
Wood	4	7	Crawl	RES1_2SNB	10	10	10	10	2.8	3.7	13.2
Wood	4	7	Crawl	RES1_3SNB	10	10	10	10	2.8	3.7	13.2
Wood	4	7	Crawl	RES3A	10	10	10	10	2.8	3.7	13.2
Wood	4	7	Slab	COM10	10	10	10	25	2.9	3.7	13.1
Wood	4	7	Slab	COM3	10	10	10	25	2.9	3.7	13.1
Wood	4	7	Slab	COM4	10	10	10	25	2.9	3.7	13.1
Wood	4	7	Slab	COM5	10	10	10	25	2.9	3.7	13.1
Wood	4	7	Slab	COM6	10	10	10	25	2.9	3.7	13.1

	Num. Story								Protection Factors		
Construction	Min	Max	Foundation	Occupancy	EW	RF	IWM	A%	UW	Warned (NB)	Warned (WB)
Wood	4	7	Slab	COM7	10	10	10	25	2.9	3.7	13.1
Wood	4	7	Slab	COM8	10	10	10	25	2.9	3.7	13.1
Wood	4	7	Slab	EDU1	10	10	10	25	2.9	3.7	13.1
Wood	4	7	Slab	GOV1	10	10	10	25	2.9	3.7	13.1
Wood	4	7	Slab	RES3B	10	10	10	25	2.9	3.7	13.1
Wood	4	7	Slab	RES3C	10	10	10	25	2.9	3.7	13.1
Wood	4	7	Slab	RES3E	10	10	10	25	2.9	3.7	13.1
Wood	4	7	Slab	RES4	10	10	10	25	2.9	3.7	13.1
Wood	4	7	Slab	RES6	10	10	10	25	2.9	3.7	13.1
Wood	4	7	Slab	AGR1	10	10	10	10	2.8	3.7	13.2
Wood	4	7	Slab	COM1	10	10	10	10	2.8	3.7	13.2
Wood	4	7	Slab	COM2	10	10	10	10	2.8	3.7	13.2
Wood	4	7	Slab	EDU2	10	10	10	10	2.8	3.7	13.2
Wood	4	7	Slab	GOV2	10	10	10	10	2.8	3.7	13.2
Wood	4	7	Slab	IND1	10	10	10	10	2.8	3.7	13.2
Wood	4	7	Slab	IND2	10	10	10	10	2.8	3.7	13.2
Wood	4	7	Slab	IND3	10	10	10	10	2.8	3.7	13.2
Wood	4	7	Slab	IND6	10	10	10	10	2.8	3.7	13.2
Wood	4	7	Slab	REL1	10	10	10	10	2.8	3.7	13.2
Wood	4	7	Slab	RES1_1SNB	10	10	10	10	2.8	3.7	13.2
Wood	4	7	Slab	RES1_2SNB	10	10	10	10	2.8	3.7	13.2
Wood	4	7	Slab	RES1_3SNB	10	10	10	10	2.8	3.7	13.2
Wood	4	7	Slab	RES3A	10	10	10	10	2.8	3.7	13.2
Wood	8	30	Basement	COM4	10	10	10	25	3.7	5.4	24.9
Wood	8	30	Basement	RES3B	10	10	10	25	3.7	5.4	24.9
Wood	8	30	Crawl	COM3	10	10	10	25	3.7	5.4	24.9
Wood	8	30	Crawl	RES6	10	10	10	25	3.7	5.4	24.9

	Num. Story								Protection Factors		
Construction	**Min**	**Max**	**Foundation**	**Occupancy**	**EW**	**RF**	**IWM**	**A%**	**UW**	**Warned (NB)**	**Warned (WB)**
Wood	8	30	Slab	COM3	10	10	10	25	3.7	5.4	24.9
Wood	8	30	Slab	COM4	10	10	10	25	3.7	5.4	24.9
Wood	8	30	Slab	COM5	10	10	10	25	3.7	5.4	24.9
Wood	8	30	Slab	COM7	10	10	10	25	3.7	5.4	24.9
Wood	8	30	Slab	COM8	10	10	10	25	3.7	5.4	24.9
Wood	8	30	Slab	RES3B	10	10	10	25	3.7	5.4	24.9
Wood	8	30	Slab	RES4	10	10	10	25	3.7	5.4	24.9
Wood	8	30	Slab	RES6	10	10	10	25	3.7	5.4	24.9
Wood	30	77	Slab	COM1	10	10	10	10	1.4	3.4	7.7
Wood	30	77	Slab	COM3	10	10	10	25	1.4	3.4	7.7
Wood	30	77	Slab	COM8	10	10	10	25	1.4	3.4	7.7
Wood	30	77	Slab	RES1_1SNB	10	10	10	10	1.4	3.4	7.7

APPENDIX E

GEORGIA HOSPITALS AND HEALTH CARE COALITIONS

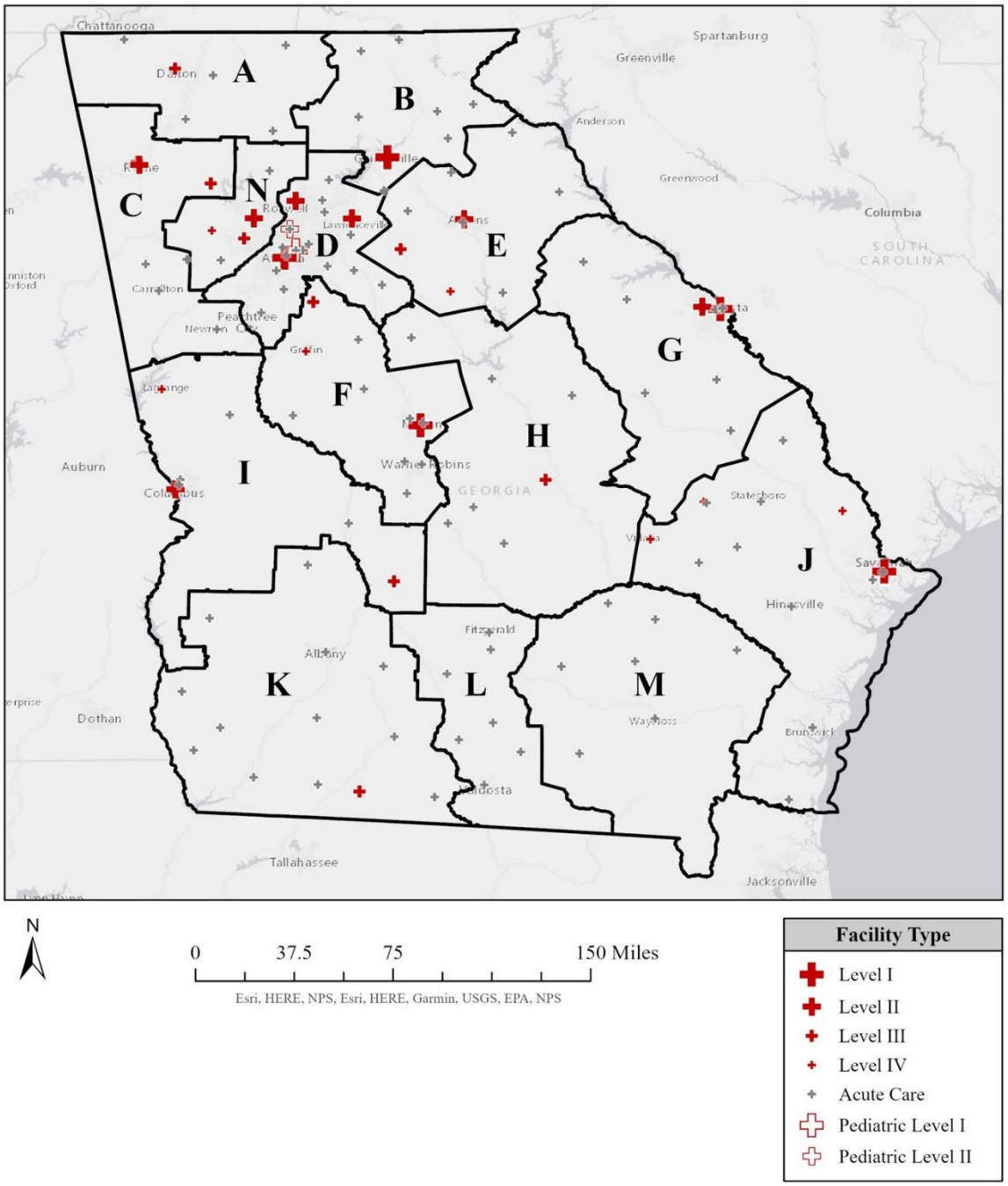

Figure E.1. Georgia hospitals and health care coalitions. Facility type refers to the trauma center designation. The bolded black letters represent each health care coalition in the state.

APPENDIX F

BLAST CASUALTIES

Table F.1. Total estimated casualties resulting from the blast effects after 48 hours, following a 15kt IND detonation in downtown Atlanta, GA at 10:00 am local time for four representative dates of detonation.

	Medoid 1		**Medoid 2**		**Medoid 3**		**Medoid 4**	
Damage Zone	**Fatalities**	**Injuries**	**Fatalities**	**Injuries**	**Fatalities**	**Injuries**	**Fatalities**	**Injuries**
Light	0	8,343	0	8,848	0	8,725	0	9,984
Moderate	1,050	11,711	1,037	11,510	1,048	11,512	1,014	11,385
Severe	105,414	22,461	105,412	22,460	105,413	22,461	105,412	22,461
Total	**106,464**	**42,515**	**106,449**	**42,818**	**106,461**	**42,698**	**106,426**	**43,830**

Table F.2. Estimated casualties resulting from only the blast effects after 48 hours, following a 15kt IND detonation in downtown Atlanta, GA at 10:00 am local time for four representative dates of detonation.

	Medoid 1		**Medoid 2**		**Medoid 3**		**Medoid 4**	
Damage Zone	**Fatalities**	**Injuries**	**Fatalities**	**Injuries**	**Fatalities**	**Injuries**	**Fatalities**	**Injuries**
Light	0	1,346	0	2,814	0	2,826	0	3,030
Moderate	0	0	0	0	0	1	0	1
Severe	0	0	0	0	0	0	0	0
Total	**0**	**1,346**	**0**	**2,814**	**0**	**2,827**	**0**	**3,031**

APPENDIX G

BURN CASUALTIES

Table G.1. Total estimated casualties resulting from the thermal effects after 48 hours, following a 15kt IND detonation in downtown Atlanta, GA at 10:00 am local time for four representative dates of detonation.

Thermal Fluence Range (cal/cm^2)	Description	1st Degree Burn	2nd Degree Burn	3rd Degree Burn
Medoid 1				
<1.4	No burns expected	0	0	0
≥1.4 to <3.53	1st degree burns	27,764	0	0
≥3.53 to <6.00	1st/2nd degree burns	9,331	10,740	0
≥6.00 to <8.67	2nd/3rd degree burns	0	4,333	5,819
≥8.67	3rd degree burns/MF	0	0	133,222
Medoid 1 Total Burns		**37,095**	**15,073**	**139,041**
Medoid 2				
<1.4	No burns expected	0	0	0
≥1.4 to <3.53	1st degree burns	27,764	0	0
≥3.53 to <6.00	1st/2nd degree burns	9,331	10,740	0
≥6.00 to <8.67	2nd/3rd degree burns	0	4,333	5,819
≥8.67	3rd degree burns/MF	0	0	133,222
Medoid 2 Total Burns		**37,095**	**15,073**	**139,041**
Medoid 3				
<1.4	No burns expected	0	0	0
≥1.4 to <3.53	1st degree burns	27,764	0	0
≥3.53 to <6.00	1st/2nd degree burns	9,331	10,740	0
≥6.00 to <8.67	2nd/3rd degree burns	0	4,333	5,819
≥8.67	3rd degree burns/MF	0	0	133,222
Medoid 3 Total Burns		**37,095**	**15,073**	**139,041**

Thermal Fluence Range (cal/cm^2)	Description	1st Degree Burn	2nd Degree Burn	3rd Degree Burn
Medoid 4				
<1.4	No burns expected	0	0	0
≥1.4 to <3.53	1st degree burns	27,764	0	0
≥3.53 to <6.00	1st/2nd degree burns	9,331	10,740	0
≥6.00 to <8.67	2nd/3rd degree burns	0	4,333	5,819
≥8.67	3rd degree burns/MF	0	0	133,222
Medoid 4 Total Burns		**37,095**	**15,073**	**139,041**

APPENDIX H

BLAST/THERMAL ONLY CASUALTIES

Table H.1. Estimated casualties resulting from only the blast and thermal effects after 48 hours, following a 15kt IND detonation in downtown Atlanta, GA at 10:00 am local time for four representative dates of detonation.

	Burn Severity			
Trauma Category	**1st degree**	**2nd degree**	**3rd degree**	**Total Trauma**
Medoid 1				
Minimal Trauma	14,997	3,520	367	18,884
Moderate Trauma	246	7	231	484
Severe Trauma	6	4	45	55
Medoid 1 Total Burns	**15,249**	**3,531**	**643**	**19,423**
Medoid 2				
Minimal Trauma	24,044	5,222	496	29,762
Moderate Trauma	116	92	358	566
Severe Trauma	6	407	150	563
Medoid 2 Total Burns	**24,166**	**5,721**	**1,004**	**30,891**
Medoid 3				
Minimal Trauma	21,671	4,980	471	27,122
Moderate Trauma	104	93	362	559
Severe Trauma	10	410	135	555
Medoid 3 Total Burns	**21,785**	**5,483**	**968**	**28,236**
Medoid 4				
Minimal Trauma	25,072	3,834	217	29,123
Moderate Trauma	186	83	210	479
Severe Trauma	4	59	519	582
Medoid 4 Total Burns	**25,262**	**3,976**	**946**	**30,184**

APPENDIX I

RADIATION CASUALTIES

Table I.1. Total estimated casualties resulting from the radiation effects after 48 hours, following a 15kt IND detonation in downtown Atlanta, GA at 10:00 am local time for four representative dates of detonation.

		Unwarned		Warned	
Radiation Dose (rad)	**ARS Subsyndrome**	**Fatalities**	**Injuries**	**Fatalities**	**Injuries**
Medoid 1					
<50	Subclinical	0	0	0	0
≥50 to <200	Subclinical	16,193	4,572	15,960	4,752
≥200 to <600	Hematopoietic	59,904	22,799	45,197	17,548
≥600 to <1000	Gastrointestinal/Cutaneous	24,119	3,453	18,741	3,255
≥1000	Neurovascular	35,204	0	15,811	0
Medoid 1 Total ARS		**135,420**	**30,824**	**95,709**	**25,555**
Medoid 2					
<50	Subclinical	0	0	0	0
≥50 to <200	Subclinical	9,197	2,449	14,651	4,860
≥200 to <600	Hematopoietic	48,087	18,021	42,053	15,699
≥600 to <1000	Gastrointestinal/Cutaneous	23,852	3,691	12,903	2,046
≥1000	Neurovascular	39,229	0	22,480	0
Medoid 2 Total ARS		**120,365**	**24,161**	**92,087**	**22,605**
Medoid 3					
<50	Subclinical	0	0	0	0
≥50 to <200	Subclinical	9,981	2,926	15,153	5,103
≥200 to <600	Hematopoietic	46,666	17,907	39,903	14,689
≥600 to <1000	Gastrointestinal/Cutaneous	21,017	3,057	12,423	2,235
≥1000	Neurovascular	43,121	0	25,508	0
Medoid 3 Total ARS		**120,785**	**23,890**	**92,987**	**22,027**

Radiation Dose (rad)	ARS Subsyndrome	Unwarned		Warned	
		Fatalities	Injuries	Fatalities	Injuries
Medoid 4					
<50	Subclinical	0	0	0	0
≥50 to <200	Subclinical	9,559	2,626	16,161	5,307
≥200 to <600	Hematopoietic	48,392	17,499	43,397	16,159
≥600 to <1000	Gastrointestinal/Cutaneous	34,128	5,317	17,275	2,959
≥1000	Neurovascular	41,160	0	21,281	0
Medoid 4 Total ARS		**133,239**	**25,442**	**98,114**	**24,425**

Table I.2. Estimated casualties resulting from only the radiation effects after 48 hours, following a 15kt IND detonation in downtown Atlanta, GA at 10:00 am local time for four representative dates of detonation.

		Unwarned		Warned	
Radiation Dose (rad)	**ARS Subsyndrome**	**Fatalities**	**Injuries**	**Fatalities**	**Injuries**
Medoid 1					
<50	Subclinical	0	0	0	0
≥50 to <200	Subclinical	7,522	1,994	3,389	890
≥200 to <600	Hematopoietic	5,823	2,169	285	101
≥600 to <1000	Gastrointestinal/Cutaneous	791	58	290	13
≥1000	Neurovascular	285	0	4	0
Medoid 1 Total ARS		**14,421**	**4,221**	**3,968**	**1,004**
Medoid 2					
<50	Subclinical	0	0	0	0
≥50 to <200	Subclinical	2,663	611	763	155
≥200 to <600	Hematopoietic	1,723	467	3,159	774
≥600 to <1000	Gastrointestinal/Cutaneous	3,503	370	32	4
≥1000	Neurovascular	705	0	123	0
Medoid 2 Total ARS		**8,594**	**1,448**	**4,077**	**933**
Medoid 3					
<50	Subclinical	0	0	0	0
≥50 to <200	Subclinical	1,909	535	1,864	557
≥200 to <600	Hematopoietic	3,981	1,380	717	211
≥600 to <1000	Gastrointestinal/Cutaneous	235	12	60	9
≥1000	Neurovascular	1,023	0	123	0
Medoid 3 Total ARS		**7,148**	**1,927**	**2,764**	**777**
Medoid 4					
<50	Subclinical	0	0	0	0
≥50 to <200	Subclinical	1,997	517	2,148	650
≥200 to <600	Hematopoietic	4,356	1,356	833	248
≥600 to <1000	Gastrointestinal/Cutaneous	1,268	185	121	14
≥1000	Neurovascular	544	0	201	0
Medoid 4 Total ARS		**8,165**	**2,058**	**3,303**	**912**

APPENDIX J

BLAST/RADIATION ONLY CASUALTIES

Table J.1. Estimated casualties resulting from only the blast and radiation effects after 48 hours, following a 15 kt IND detonation in downtown Atlanta, GA at 10:00 am local time for four representative dates of detonation. Abbreviations: ARS = Acute Radiation Sickness; H = Hematopoietic; HGC = Hematopoietic / Gastrointestinal / Cutaneous; HGCN = Hematopoietic / Gastrointestinal / Cutaneous / Neurovascular.

	Unwarned				**Warned**			
	ARS Subsyndrome			**Total**	**ARS Subsyndrome**			**Total**
Trauma Category	**H**	**HGC**	**HGCN**	**Trauma**	**H**	**HGC**	**HGCN**	**Trauma**
Medoid 1								
Minimal Trauma	1,337	113	23	1,473	98	0	0	98
Moderate Trauma	81	37	11	129	35	0	0	35
Severe Trauma	39	0	4	43	32	0	0	32
Medoid 1 Total ARS	**1,457**	**150**	**38**	**1,645**	**165**	**0**	**0**	**165**
Medoid 2								
Minimal Trauma	2,223	170	55	2,448	184	0	0	184
Moderate Trauma	7	23	1	31	6	0	0	6
Severe Trauma	19	22	2	43	34	0	0	34
Medoid 2 Total ARS	**2,249**	**215**	**58**	**2,522**	**224**	**0**	**0**	**224**
Medoid 3								
Minimal Trauma	1,772	192	48	2,012	374	2	0	376
Moderate Trauma	23	17	3	43	4	0	0	4
Severe Trauma	18	3	22	43	14	20	0	34
Medoid 3 Total ARS	**1,813**	**212**	**73**	**2,098**	**392**	**22**	**0**	**414**

	Unwarned				Warned			
	ARS Subsyndrome			Total	ARS Subsyndrome			Total
Trauma Category	**H**	**HGC**	**HGCN**	**Trauma**	**H**	**HGC**	**HGCN**	**Trauma**
Medoid 4								
Minimal Trauma	2,713	363	335	3,411	1,077	0	0	1,077
Moderate Trauma	145	30	7	182	158	0	0	158
Severe Trauma	31	11	8	50	32	2	0	34
Medoid 4 Total ARS	**2,889**	**404**	**350**	**3,643**	**1,267**	**2**	**0**	**1,269**

APPENDIX K

COMBINED EFFECTS CASUALTIES – MEDOID 1

Table K.1. Estimated casualties outside the damage zone resulting from thermal and radiation effects in the unwarned scenario after 48 hours, following a 15 kt IND detonation in downtown Atlanta, GA at 10:00 am local time on November 26, 2019 (Medoid 1).

Thermal Fluence Range (cal/cm^2)	Radiation Dose (rad)	Blast		Thermal			Radiation	
		Fatalities	Injuries	1st degree	2nd degree	3rd degree	Fatalities	Injuries
<1.4	<50	0	0	0	0	0	0	0
	≥50 to <200	0	0	0	0	0	7,393	1,966
	≥200 to <600	0	0	0	0	0	5,340	2,065
	≥600 to <1000	0	0	0	0	0	540	58
	≥1000	0	0	0	0	0	277	0
≥1.4 to <3.53	<50	0	0	0	0	0	0	0
	≥50 to <200	0	0	0	0	0	0	0
	≥200 to <600	0	0	0	0	0	0	0
	≥600 to <1000	0	0	0	0	0	0	0
	≥1000	0	0	0	0	0	0	0
≥3.53 to <6.00	<50	0	0	0	0	0	0	0
	≥50 to <200	0	0	0	0	0	0	0
	≥200 to <600	0	0	0	0	0	0	0
	≥600 to <1000	0	0	0	0	0	0	0
	≥1000	0	0	0	0	0	0	0
≥6.00 to <8.67	<50	0	0	0	0	0	0	0
	≥50 to <200	0	0	0	0	0	0	0
	≥200 to <600	0	0	0	0	0	0	0
	≥600 to <1000	0	0	0	0	0	0	0
	≥1000	0	0	0	0	0	0	0

Thermal Fluence Range (cal/cm^2)	Radiation Dose (rad)	Blast		Thermal			Radiation	
		Fatalities	Injuries	1st degree	2nd degree	3rd degree	Fatalities	Injuries
≥8.67	<50	0	0	0	0	0	0	0
	≥50 to <200	0	0	0	0	0	0	0
	≥200 to <600	0	0	0	0	0	0	0
	≥600 to <1000	0	0	0	0	0	0	0
	≥1000	0	0	0	0	0	0	0
Total		**0**	**0**	**0**	**0**	**0**	**13,550**	**4,089**

Table K.2. Estimated casualties within the light damage zone resulting from thermal and radiation effects in the unwarned scenario after 48 hours, following a 15 kt IND detonation in downtown Atlanta, GA at 10:00 am local time on November 26, 2019 (Medoid 1).

Thermal Fluence Range (cal/cm^2)	Radiation Dose (rad)	Blast		Thermal			Radiation	
		Fatalities	Injuries	1st degree	2nd degree	3rd degree	Fatalities	Injuries
<1.4	<50	0	2,667	0	0	0	0	0
	≥50 to <200	0	92	0	0	0	542	134
	≥200 to <600	0	31	0	0	0	765	232
	≥600 to <1000	0	3	0	0	0	144	6
	≥1000	0	2	0	0	0	34	0
≥1.4 to <3.53	<50	0	2,741	23,361	0	0	0	0
	≥50 to <200	0	222	1,654	0	0	648	140
	≥200 to <600	0	275	2,078	0	0	3,399	982
	≥600 to <1000	0	39	299	0	0	664	80
	≥1000	0	10	90	0	0	168	0
≥3.53 to <6.00	<50	0	1,044	6,003	6,942	0	0	0
	≥50 to <200	0	142	2,340	1,271	0	713	90
	≥200 to <600	0	51	312	358	0	607	178
	≥600 to <1000	0	11	66	73	0	162	18
	≥1000	0	6	231	77	0	418	0
≥6.00 to <8.67	<50	0	457	0	1,828	2,714	0	0
	≥50 to <200	0	167	0	73	729	404	95
	≥200 to <600	0	24	0	112	110	264	105
	≥600 to <1000	0	10	0	69	58	152	23
	≥1000	0	4	0	18	21	65	0
≥8.67	<50	0	246	0	0	3,693	0	0
	≥50 to <200	0	74	0	0	1,044	121	16
	≥200 to <600	0	17	0	0	248	176	77
	≥600 to <1000	0	5	0	0	54	64	8
	≥1000	0	4	0	0	53	60	0
Total		**0**	**8,344**	**36,434**	**10,821**	**8,724**	**9,570**	**2,184**

Table K.3. Estimated casualties within the moderate damage zone resulting from thermal and radiation effects in the unwarned scenario after 48 hours, following a 15 kt IND detonation in downtown Atlanta, GA at 10:00 am local time on November 26, 2019 (Medoid 1).

Thermal Fluence Range (cal/cm^2)	Radiation Dose (rad)	Blast		Thermal			Radiation	
		Fatalities	Injuries	1st degree	2nd degree	3rd degree	Fatalities	Injuries
<1.4	<50	0	4	0	0	0	0	0
	≥50 to <200	0	12	0	0	0	11	2
	≥200 to <600	0	13	0	0	0	22	10
	≥600 to <1000	0	0	0	0	0	0	0
	≥1000	0	1	0	0	0	4	0
≥1.4 to <3.53	<50	0	7	26	0	0	0	0
	≥50 to <200	0	20	59	0	0	29	8
	≥200 to <600	2	66	94	0	0	121	50
	≥600 to <1000	0	11	35	0	0	61	5
	≥1000	3	39	68	0	0	138	0
≥3.53 to <6.00	<50	0	55	5	287	0	0	0
	≥50 to <200	0	196	164	940	0	194	17
	≥200 to <600	46	510	142	523	0	741	407
	≥600 to <1000	1	27	9	101	0	339	18
	≥1000	10	107	60	168	0	383	0
≥6.00 to <8.67	<50	0	54	0	59	231	0	0
	≥50 to <200	23	419	0	1,157	639	693	228
	≥200 to <600	59	736	0	188	859	1,596	665
	≥600 to <1000	23	288	0	689	268	994	109
	≥1000	17	193	0	140	166	642	0
≥8.67	<50	1	69	0	0	690	0	0
	≥50 to <200	158	1,952	0	0	7,693	2,701	908
	≥200 to <600	504	5,151	0	0	10,630	7,512	3,024
	≥600 to <1000	47	476	0	0	1,286	1,349	187
	≥1000	157	1,305	0	0	2,786	3,066	0
Total		**1,051**	**11,711**	**662**	**4,252**	**25,248**	**20,596**	**5,638**

Table K.4. Estimated casualties within the severe damage zone resulting from thermal and radiation effects in the unwarned scenario after 48 hours, following a 15 kt IND detonation in downtown Atlanta, GA at 10:00 am local time on November 26, 2019 (Medoid 1).

Thermal Fluence Range (cal/cm^2)	Radiation Dose (rad)	Blast		Thermal			Radiation	
		Fatalities	Injuries	1st degree	2nd degree	3rd degree	Fatalities	Injuries
<1.4	<50	0	0	0	0	0	0	0
	≥50 to <200	0	0	0	0	0	0	0
	≥200 to <600	0	0	0	0	0	0	0
	≥600 to <1000	0	0	0	0	0	0	0
	≥1000	0	0	0	0	0	0	0
≥1.4 to <3.53	<50	0	0	0	0	0	0	0
	≥50 to <200	0	0	0	0	0	0	0
	≥200 to <600	0	0	0	0	0	0	0
	≥600 to <1000	0	0	0	0	0	0	0
	≥1000	1	1	1	0	0	1	0
≥3.53 to <6.00	<50	0	0	0	0	0	0	0
	≥50 to <200	0	0	0	0	0	0	0
	≥200 to <600	1	1	1	0	0	0	0
	≥600 to <1000	0	0	0	0	0	0	0
	≥1000	0	0	0	0	0	0	0
≥6.00 to <8.67	<50	0	0	0	0	0	0	0
	≥50 to <200	57	44	0	0	22	11	1
	≥200 to <600	9	7	0	0	3	9	3
	≥600 to <1000	0	0	0	0	0	0	0
	≥1000	10	6	0	0	3	16	0
≥8.67	<50	0	0	0	0	0	0	0
	≥50 to <200	7,805	1,412	0	0	7,524	2,733	967
	≥200 to <600	53,611	12,347	0	0	54,483	39,352	15,001
	≥600 to <1000	18,700	3,756	0	0	18,293	19,650	2,941
	≥1000	25,221	4,887	0	0	24,748	29,932	0
Total		**105,415**	**22,461**	**2**	**0**	**105,076**	**91,704**	**18,913**

Table K.5. Estimated casualties outside the damage zone resulting from thermal and radiation effects in the warned scenario after 48 hours, following a 15 kt IND detonation in downtown Atlanta, GA at 10:00 am local time on November 26, 2019 (Medoid 1).

Thermal Fluence Range (cal/cm^2)	Radiation Dose (rad)	Blast		Thermal			Radiation	
		Fatalities	Injuries	1st degree	2nd degree	3rd degree	Fatalities	Injuries
<1.4	<50	0	0	0	0	0	0	0
	≥50 to <200	0	0	0	0	0	3,284	863
	≥200 to <600	0	0	0	0	0	231	93
	≥600 to <1000	0	0	0	0	0	119	13
	≥1000	0	0	0	0	0	0	0
≥1.4 to <3.53	<50	0	0	0	0	0	0	0
	≥50 to <200	0	0	0	0	0	0	0
	≥200 to <600	0	0	0	0	0	0	0
	≥600 to <1000	0	0	0	0	0	0	0
	≥1000	0	0	0	0	0	0	0
≥3.53 to <6.00	<50	0	0	0	0	0	0	0
	≥50 to <200	0	0	0	0	0	0	0
	≥200 to <600	0	0	0	0	0	0	0
	≥600 to <1000	0	0	0	0	0	0	0
	≥1000	0	0	0	0	0	0	0
≥6.00 to <8.67	<50	0	0	0	0	0	0	0
	≥50 to <200	0	0	0	0	0	0	0
	≥200 to <600	0	0	0	0	0	0	0
	≥600 to <1000	0	0	0	0	0	0	0
	≥1000	0	0	0	0	0	0	0
≥8.67	<50	0	0	0	0	0	0	0
	≥50 to <200	0	0	0	0	0	0	0
	≥200 to <600	0	0	0	0	0	0	0
	≥600 to <1000	0	0	0	0	0	0	0
	≥1000	0	0	0	0	0	0	0
Total		**0**	**0**	**0**	**0**	**0**	**3,634**	**969**

Table K.6. Estimated casualties within the light damage zone resulting from thermal and radiation effects in the warned scenario after 48 hours, following a 15 kt IND detonation in downtown Atlanta, GA at 10:00 am local time on November 26, 2019 (Medoid 1).

Thermal Fluence Range (cal/cm^2)	Radiation Dose (rad)	Blast		Thermal			Radiation	
		Fatalities	Injuries	1st degree	2nd degree	3rd degree	Fatalities	Injuries
<1.4	<50	0	2,687	0	0	0	0	0
	≥50 to <200	0	44	0	0	0	250	56
	≥200 to <600	0	4	0	0	0	47	15
	≥600 to <1000	0	0	0	0	0	0	0
	≥1000	0	0	0	0	0	0	0
≥1.4 to <3.53	<50	0	2,465	21,835	0	0	0	0
	≥50 to <200	0	50	519	0	0	645	227
	≥200 to <600	0	2	24	0	0	28	9
	≥600 to <1000	0	0	0	0	0	0	0
	≥1000	0	0	0	0	0	0	0
≥3.53 to <6.00	<50	0	791	6,250	5,606	0	0	0
	≥50 to <200	0	31	259	182	0	143	45
	≥200 to <600	0	0	0	0	0	0	0
	≥600 to <1000	0	0	0	0	0	0	0
	≥1000	0	0	0	0	0	0	0
≥6.00 to <8.67	<50	0	346	0	1,638	2,027	0	0
	≥50 to <200	0	2	0	9	17	13	3
	≥200 to <600	0	6	0	66	27	59	22
	≥600 to <1000	0	0	0	0	0	0	0
	≥1000	0	0	0	0	0	0	0
≥8.67	<50	0	17	0	0	289	0	0
	≥50 to <200	0	0	0	0	0	0	0
	≥200 to <600	0	0	0	0	0	0	0
	≥600 to <1000	0	0	0	0	0	0	0
	≥1000	0	0	0	0	0	0	0
Total		**0**	**6,445**	**28,887**	**7,501**	**2,360**	**1,185**	**377**

Table K.7. Estimated casualties within the moderate damage zone resulting from thermal and radiation effects in the warned scenario after 48 hours, following a 15 kt IND detonation in downtown Atlanta, GA at 10:00 am local time on November 26, 2019 (Medoid 1).

Thermal Fluence Range (cal/cm^2)	Radiation Dose (rad)	Blast		Thermal			Radiation	
		Fatalities	Injuries	1st degree	2nd degree	3rd degree	Fatalities	Injuries
<1.4	<50	0	57	0	0	0	0	0
	≥50 to <200	0	3	0	0	0	17	7
	≥200 to <600	0	1	0	0	0	16	6
	≥600 to <1000	0	0	0	0	0	0	0
	≥1000	0	0	0	0	0	0	0
≥1.4 to <3.53	<50	0	457	3,100	0	0	0	0
	≥50 to <200	0	199	1,170	0	0	814	285
	≥200 to <600	0	115	834	0	0	807	318
	≥600 to <1000	0	0	0	0	0	0	0
	≥1000	0	0	0	0	0	0	0
≥3.53 to <6.00	<50	0	365	2,386	2,365	0	0	0
	≥50 to <200	0	56	7	472	0	125	29
	≥200 to <600	0	9	49	97	0	112	42
	≥600 to <1000	0	0	0	0	0	0	0
	≥1000	0	0	0	0	0	0	0
≥6.00 to <8.67	<50	0	142	0	276	896	0	0
	≥50 to <200	0	144	0	3	572	190	5
	≥200 to <600	0	21	0	108	92	190	65
	≥600 to <1000	0	0	0	0	0	0	0
	≥1000	0	0	0	0	0	0	0
≥8.67	<50	0	265	0	0	3,942	0	0
	≥50 to <200	0	49	0	0	646	95	15
	≥200 to <600	0	14	0	0	201	133	45
	≥600 to <1000	0	1	0	0	13	13	3
	≥1000	0	0	0	0	0	0	0
Total		**0**	**1,898**	**7,546**	**3,321**	**6,362**	**2,512**	**820**

Table K.8. Estimated casualties within the severe damage zone resulting from thermal and radiation effects in the warned scenario after 48 hours, following a 15 kt IND detonation in downtown Atlanta, GA at 10:00 am local time on November 26, 2019 (Medoid 1).

Thermal Fluence Range (cal/cm^2)	Radiation Dose (rad)	Blast		Thermal			Radiation	
		Fatalities	Injuries	1st degree	2nd degree	3rd degree	Fatalities	Injuries
<1.4	<50	0	12	0	0	0	0	0
	≥50 to <200	0	5	0	0	0	4	0
	≥200 to <600	0	12	0	0	0	20	10
	≥600 to <1000	0	0	0	0	0	0	0
	≥1000	0	0	0	0	0	0	0
≥1.4 to <3.53	<50	0	16	37	0	0	0	0
	≥50 to <200	0	50	100	0	0	57	14
	≥200 to <600	2	41	84	0	0	95	37
	≥600 to <1000	3	37	60	0	0	112	12
	≥1000	1	1	1	0	0	2	0
≥3.53 to <6.00	<50	0	229	45	1,174	0	0	0
	≥50 to <200	13	161	253	331	0	170	51
	≥200 to <600	43	473	71	411	0	597	171
	≥600 to <1000	0	25	2	93	0	326	34
	≥1000	1	9	9	9	0	28	0
≥6.00 to <8.67	<50	57	128	0	90	387	0	0
	≥50 to <200	68	743	0	1,362	981	1,165	406
	≥200 to <600	48	608	0	265	606	1,309	515
	≥600 to <1000	18	224	0	516	191	686	143
	≥1000	6	44	0	0	23	136	0
≥8.67	<50	1,542	751	0	0	3,807	0	0
	≥50 to <200	25,277	7,596	0	0	33,216	8,988	2,746
	≥200 to <600	50,393	16,959	0	0	61,390	41,553	16,200
	≥600 to <1000	15,776	3,653	0	0	16,847	17,485	3,050
	≥1000	13,216	2,395	0	0	12,871	15,645	0
Total		**106,464**	**34,172**	**662**	**4,251**	**130,319**	**88,378**	**23,389**

APPENDIX L

COMBINED EFFECTS CASUALTIES – MEDOID 2

Table L.1. Estimated casualties outside the damage zone resulting from thermal and radiation effects in the unwarned scenario after 48 hours, following a 15 kt IND detonation in downtown Atlanta, GA at 10:00 am local time on November 25, 2019 (Medoid 2).

Thermal Fluence Range (cal/cm^2)	Radiation Dose (rad)	Blast		Thermal			Radiation	
		Fatalities	Injuries	1st degree	2nd degree	3rd degree	Fatalities	Injuries
<1.4	<50	0	0	0	0	0	0	0
	≥50 to <200	0	0	0	0	0	2,492	562
	≥200 to <600	0	0	0	0	0	727	259
	≥600 to <1000	0	0	0	0	0	3,352	366
	≥1000	0	0	0	0	0	698	0
≥1.4 to <3.53	<50	0	0	0	0	0	0	0
	≥50 to <200	0	0	0	0	0	0	0
	≥200 to <600	0	0	0	0	0	0	0
	≥600 to <1000	0	0	0	0	0	0	0
	≥1000	0	0	0	0	0	0	0
≥3.53 to <6.00	<50	0	0	0	0	0	0	0
	≥50 to <200	0	0	0	0	0	0	0
	≥200 to <600	0	0	0	0	0	0	0
	≥600 to <1000	0	0	0	0	0	0	0
	≥1000	0	0	0	0	0	0	0
≥6.00 to <8.67	<50	0	0	0	0	0	0	0
	≥50 to <200	0	0	0	0	0	0	0
	≥200 to <600	0	0	0	0	0	0	0
	≥600 to <1000	0	0	0	0	0	0	0
	≥1000	0	0	0	0	0	0	0

Thermal Fluence Range (cal/cm^2)	Radiation Dose (rad)	Blast		Thermal			Radiation	
		Fatalities	Injuries	1st degree	2nd degree	3rd degree	Fatalities	Injuries
≥8.67	<50	0	0	0	0	0	0	0
	≥50 to <200	0	0	0	0	0	0	0
	≥200 to <600	0	0	0	0	0	0	0
	≥600 to <1000	0	0	0	0	0	0	0
	≥1000	0	0	0	0	0	0	0
Total		**0**	**0**	**0**	**0**	**0**	**7,269**	**1,187**

Table L.2. Estimated casualties within the light damage zone resulting from thermal and radiation effects in the unwarned scenario after 48 hours, following a 15 kt IND detonation in downtown Atlanta, GA at 10:00 am local time on November 25, 2019 (Medoid 2).

Thermal Fluence Range (cal/cm^2)	Radiation Dose (rad)	Blast		Thermal			Radiation	
		Fatalities	Injuries	1st degree	2nd degree	3rd degree	Fatalities	Injuries
<1.4	<50	0	3,003	0	0	0	0	0
	≥50 to <200	0	14	0	0	0	224	63
	≥200 to <600	0	33	0	0	0	1,234	417
	≥600 to <1000	0	2	0	0	0	178	15
	≥1000	0	2	0	0	0	56	0
≥1.4 to <3.53	<50	0	3,235	26,941	0	0	0	0
	≥50 to <200	0	65	623	0	0	190	46
	≥200 to <600	0	66	769	0	0	1,218	324
	≥600 to <1000	0	15	116	0	0	300	37
	≥1000	0	2	21	0	0	45	0
≥3.53 to <6.00	<50	0	1,281	8,824	8,682	0	0	0
	≥50 to <200	0	48	386	435	0	116	23
	≥200 to <600	0	13	217	122	0	238	88
	≥600 to <1000	0	2	35	25	0	74	6
	≥1000	0	2	20	24	0	37	0
≥6.00 to <8.67	<50	0	580	0	2,569	3,417	0	0
	≥50 to <200	0	151	0	35	661	258	31
	≥200 to <600	0	1	0	27	39	68	16
	≥600 to <1000	0	0	0	11	6	27	2
	≥1000	0	0	0	4	4	5	0
≥8.67	<50	0	262	0	0	3,783	0	0
	≥50 to <200	0	50	0	0	823	99	23
	≥200 to <600	0	4	0	0	108	45	14
	≥600 to <1000	0	14	0	0	152	141	29
	≥1000	0	4	0	0	48	57	0
Total		**0**	**8,849**	**37,952**	**11,934**	**9,041**	**4,610**	**1,134**

Table L.3. Estimated casualties within the moderate damage zone resulting from thermal and radiation effects in the unwarned scenario after 48 hours, following a 15 kt IND detonation in downtown Atlanta, GA at 10:00 am local time on November 25, 2019 (Medoid 2).

Thermal Fluence Range (cal/cm^2)	Radiation Dose (rad)	Blast		Thermal			Radiation	
		Fatalities	Injuries	1st degree	2nd degree	3rd degree	Fatalities	Injuries
<1.4	<50	0	5	0	0	0	0	0
	≥50 to <200	0	10	0	0	0	5	1
	≥200 to <600	0	7	0	0	0	8	6
	≥600 to <1000	0	6	0	0	0	18	4
	≥1000	0	1	0	0	0	2	0
≥1.4 to <3.53	<50	0	10	42	0	0	0	0
	≥50 to <200	0	27	78	0	0	25	4
	≥200 to <600	5	94	142	0	0	188	69
	≥600 to <1000	0	7	14	0	0	21	1
	≥1000	0	6	6	0	0	12	0
≥3.53 to <6.00	<50	0	112	115	584	0	0	0
	≥50 to <200	10	271	196	1,050	0	447	136
	≥200 to <600	40	456	47	437	0	821	191
	≥600 to <1000	1	11	5	14	0	25	3
	≥1000	6	61	20	65	0	134	0
≥6.00 to <8.67	<50	0	151	0	409	494	0	0
	≥50 to <200	44	750	0	1,802	1,218	1,062	335
	≥200 to <600	41	568	0	194	602	1,315	538
	≥600 to <1000	28	207	0	153	170	398	59
	≥1000	9	130	0	17	115	377	0
≥8.67	<50	0	128	0	0	1,495	0	0
	≥50 to <200	152	2,027	0	0	6,914	2,194	641
	≥200 to <600	582	5,287	0	0	10,598	7,325	2,903
	≥600 to <1000	29	300	0	0	848	888	120
	≥1000	91	878	0	0	2,013	2,111	0
Total		**1,038**	**11,510**	**665**	**4,725**	**24,467**	**17,376**	**5,011**

Table L.4. Estimated casualties within the severe damage zone resulting from thermal and radiation effects in the unwarned scenario after 48 hours, following a 15 kt IND detonation in downtown Atlanta, GA at 10:00 am local time on November 25, 2019 (Medoid 2).

Thermal Fluence Range (cal/cm^2)	Radiation Dose (rad)	Blast		Thermal			Radiation	
		Fatalities	Injuries	1st degree	2nd degree	3rd degree	Fatalities	Injuries
<1.4	<50	0	0	0	0	0	0	0
	≥50 to <200	0	0	0	0	0	0	0
	≥200 to <600	0	0	0	0	0	0	0
	≥600 to <1000	0	0	0	0	0	0	0
	≥1000	0	0	0	0	0	0	0
≥1.4 to <3.53	<50	0	0	0	0	0	0	0
	≥50 to <200	0	0	0	0	0	0	0
	≥200 to <600	1	1	1	0	0	1	0
	≥600 to <1000	0	0	0	0	0	0	0
	≥1000	0	0	0	0	0	0	0
≥3.53 to <6.00	<50	0	0	0	0	0	0	0
	≥50 to <200	0	0	0	0	0	0	0
	≥200 to <600	1	1	1	0	0	0	0
	≥600 to <1000	0	0	0	0	0	0	0
	≥1000	0	0	0	0	0	0	0
≥6.00 to <8.67	<50	0	0	0	0	0	0	0
	≥50 to <200	62	49	0	0	23	15	2
	≥200 to <600	4	3	0	0	1	3	1
	≥600 to <1000	2	0	0	0	0	2	0
	≥1000	8	6	0	0	3	14	0
≥8.67	<50	0	0	0	0	0	0	0
	≥50 to <200	8,630	1,657	0	0	8,432	2,070	582
	≥200 to <600	49,326	10,953	0	0	49,639	34,896	13,195
	≥600 to <1000	17,904	3,564	0	0	17,512	18,428	3,049
	≥1000	29,475	6,227	0	0	29,464	35,681	0
Total		**105,413**	**22,461**	**2**	**0**	**105,074**	**91,110**	**16,829**

Table L.5. Estimated casualties outside the damage zone resulting from thermal and radiation effects in the warned scenario after 48 hours, following a 15 kt IND detonation in downtown Atlanta, GA at 10:00 am local time on November 25, 2019 (Medoid 2).

Thermal Fluence Range (cal/cm^2)	Radiation Dose (rad)	Blast		Thermal			Radiation	
		Fatalities	Injuries	1st degree	2nd degree	3rd degree	Fatalities	Injuries
<1.4	<50	0	0	0	0	0	0	0
	≥50 to <200	0	0	0	0	0	552	95
	≥200 to <600	0	0	0	0	0	2,861	739
	≥600 to <1000	0	0	0	0	0	32	4
	≥1000	0	0	0	0	0	122	0
≥1.4 to <3.53	<50	0	0	0	0	0	0	0
	≥50 to <200	0	0	0	0	0	0	0
	≥200 to <600	0	0	0	0	0	0	0
	≥600 to <1000	0	0	0	0	0	0	0
	≥1000	0	0	0	0	0	0	0
≥3.53 to <6.00	<50	0	0	0	0	0	0	0
	≥50 to <200	0	0	0	0	0	0	0
	≥200 to <600	0	0	0	0	0	0	0
	≥600 to <1000	0	0	0	0	0	0	0
	≥1000	0	0	0	0	0	0	0
≥6.00 to <8.67	<50	0	0	0	0	0	0	0
	≥50 to <200	0	0	0	0	0	0	0
	≥200 to <600	0	0	0	0	0	0	0
	≥600 to <1000	0	0	0	0	0	0	0
	≥1000	0	0	0	0	0	0	0
≥8.67	<50	0	0	0	0	0	0	0
	≥50 to <200	0	0	0	0	0	0	0
	≥200 to <600	0	0	0	0	0	0	0
	≥600 to <1000	0	0	0	0	0	0	0
	≥1000	0	0	0	0	0	0	0
Total		**0**	**0**	**0**	**0**	**0**	**3,567**	**838**

Table L.6. Estimated casualties within the light damage zone resulting from thermal and radiation effects in the warned scenario after 48 hours, following a 15 kt IND detonation in downtown Atlanta, GA at 10:00 am local time on November 25, 2019 (Medoid 2).

Thermal Fluence Range (cal/cm^2)	Radiation Dose (rad)	Blast		Thermal			Radiation	
		Fatalities	Injuries	1st degree	2nd degree	3rd degree	Fatalities	Injuries
<1.4	<50	0	3,008	0	0	0	0	0
	≥50 to <200	0	45	0	0	0	586	184
	≥200 to <600	0	1	0	0	0	94	34
	≥600 to <1000	0	0	0	0	0	0	0
	≥1000	0	0	0	0	0	0	0
≥1.4 to <3.53	<50	0	3,290	27,580	0	0	0	0
	≥50 to <200	0	86	840	0	0	538	180
	≥200 to <600	0	8	50	0	0	116	43
	≥600 to <1000	0	0	0	0	0	0	0
	≥1000	0	0	0	0	0	0	0
≥3.53 to <6.00	<50	0	1,324	9,265	9,114	0	0	0
	≥50 to <200	0	20	209	155	0	105	33
	≥200 to <600	0	1	8	18	0	25	7
	≥600 to <1000	0	0	0	0	0	0	0
	≥1000	0	0	0	0	0	0	0
≥6.00 to <8.67	<50	0	590	0	2,603	3,516	0	0
	≥50 to <200	0	142	0	32	597	190	7
	≥200 to <600	0	0	0	10	13	12	6
	≥600 to <1000	0	0	0	0	0	0	0
	≥1000	0	0	0	0	0	0	0
≥8.67	<50	0	292	0	0	4,279	0	0
	≥50 to <200	0	23	0	0	451	43	1
	≥200 to <600	0	17	0	0	177	113	43
	≥600 to <1000	0	1	0	0	7	6	2
	≥1000	0	0	0	0	0	0	0
Total		**0**	**8,848**	**37,952**	**11,932**	**9,040**	**1,828**	**540**

Table L.7. Estimated casualties within the moderate damage zone resulting from thermal and radiation effects in the warned scenario after 48 hours, following a 15 kt IND detonation in downtown Atlanta, GA at 10:00 am local time on November 25, 2019 (Medoid 2).

Thermal Fluence Range (cal/cm^2)	Radiation Dose (rad)	Blast		Thermal			Radiation	
		Fatalities	Injuries	1st degree	2nd degree	3rd degree	Fatalities	Injuries
<1.4	<50	0	12	0	0	0	0	0
	≥50 to <200	0	5	0	0	0	3	0
	≥200 to <600	0	12	0	0	0	20	12
	≥600 to <1000	0	0	0	0	0	0	0
	≥1000	0	0	0	0	0	0	0
≥1.4 to <3.53	<50	0	23	71	0	0	0	0
	≥50 to <200	0	51	102	0	0	60	17
	≥200 to <600	5	68	106	0	0	138	46
	≥600 to <1000	0	0	0	0	0	0	0
	≥1000	0	2	2	0	0	6	0
≥3.53 to <6.00	<50	0	196	129	1,039	0	0	0
	≥50 to <200	17	248	216	695	0	380	122
	≥200 to <600	39	466	37	413	0	760	167
	≥600 to <1000	0	0	1	0	0	1	0
	≥1000	0	0	0	1	0	1	0
≥6.00 to <8.67	<50	0	170	0	422	563	0	0
	≥50 to <200	86	1,056	0	2,095	1,432	1,372	447
	≥200 to <600	10	358	0	57	412	900	357
	≥600 to <1000	26	217	0	0	190	390	51
	≥1000	1	6	0	0	3	20	0
≥8.67	<50	35	451	0	0	2,690	0	0
	≥50 to <200	399	3,688	0	0	9,516	3,038	1,274
	≥200 to <600	392	4,175	0	0	8,785	6,293	2,520
	≥600 to <1000	26	292	0	0	845	890	134
	≥1000	1	14	0	0	32	39	0
Total		**1,037**	**11,510**	**664**	**4,722**	**24,468**	**14,311**	**5,147**

Table L.8. Estimated casualties within the severe damage zone resulting from thermal and radiation effects in the warned scenario after 48 hours, following a 15 kt IND detonation in downtown Atlanta, GA at 10:00 am local time on November 25, 2019 (Medoid 2).

Thermal Fluence Range (cal/cm^2)	Radiation Dose (rad)	Blast		Thermal			Radiation	
		Fatalities	Injuries	1st degree	2nd degree	3rd degree	Fatalities	Injuries
<1.4	<50	0	0	0	0	0	0	0
	≥50 to <200	0	0	0	0	0	0	0
	≥200 to <600	0	0	0	0	0	0	0
	≥600 to <1000	0	0	0	0	0	0	0
	≥1000	0	0	0	0	0	0	0
≥1.4 to <3.53	<50	0	0	0	0	0	0	0
	≥50 to <200	0	0	0	0	0	0	0
	≥200 to <600	1	1	1	0	0	1	0
	≥600 to <1000	0	0	0	0	0	0	0
	≥1000	0	0	0	0	0	0	0
≥3.53 to <6.00	<50	0	0	0	0	0	0	0
	≥50 to <200	0	0	0	0	0	0	0
	≥200 to <600	1	1	1	0	0	0	0
	≥600 to <1000	0	0	0	0	0	0	0
	≥1000	0	0	0	0	0	0	0
≥6.00 to <8.67	<50	57	48	0	0	20	0	0
	≥50 to <200	12	6	0	0	6	6	3
	≥200 to <600	4	3	0	0	1	3	1
	≥600 to <1000	2	0	0	0	0	2	0
	≥1000	0	0	0	0	0	0	0
≥8.67	<50	5,425	976	0	0	5,217	0	0
	≥50 to <200	26,530	4,892	0	0	25,746	7,778	2,497
	≥200 to <600	43,816	10,435	0	0	44,673	30,717	11,724
	≥600 to <1000	11,313	2,200	0	0	11,074	11,582	1,855
	≥1000	18,251	3,898	0	0	18,336	22,292	0
Total		**105,412**	**22,460**	**2**	**0**	**105,073**	**72,381**	**16,080**

APPENDIX M

COMBINED EFFECTS CASUALTIES – MEDOID 3

Table M.1. Estimated casualties outside the damage zone resulting from thermal and radiation effects in the unwarned scenario after 48 hours, following a 15 kt IND detonation in downtown Atlanta, GA at 10:00 am local time on July 2, 2019 (Medoid 3).

Thermal Fluence Range (cal/cm^2)	Radiation Dose (rad)	Blast		Thermal			Radiation	
		Fatalities	Injuries	1st degree	2nd degree	3rd degree	Fatalities	Injuries
<1.4	<50	0	0	0	0	0	0	0
	≥50 to <200	0	0	0	0	0	1,824	531
	≥200 to <600	0	0	0	0	0	3,052	1,225
	≥600 to <1000	0	0	0	0	0	45	5
	≥1000	0	0	0	0	0	981	0
≥1.4 to <3.53	<50	0	0	0	0	0	0	0
	≥50 to <200	0	0	0	0	0	0	0
	≥200 to <600	0	0	0	0	0	0	0
	≥600 to <1000	0	0	0	0	0	0	0
	≥1000	0	0	0	0	0	0	0
≥3.53 to <6.00	<50	0	0	0	0	0	0	0
	≥50 to <200	0	0	0	0	0	0	0
	≥200 to <600	0	0	0	0	0	0	0
	≥600 to <1000	0	0	0	0	0	0	0
	≥1000	0	0	0	0	0	0	0
≥6.00 to <8.67	<50	0	0	0	0	0	0	0
	≥50 to <200	0	0	0	0	0	0	0
	≥200 to <600	0	0	0	0	0	0	0
	≥600 to <1000	0	0	0	0	0	0	0
	≥1000	0	0	0	0	0	0	0

Thermal Fluence Range (cal/cm^2)	Radiation Dose (rad)	Blast		Thermal			Radiation	
		Fatalities	Injuries	1st degree	2nd degree	3rd degree	Fatalities	Injuries
≥8.67	<50	0	0	0	0	0	0	0
	≥50 to <200	0	0	0	0	0	0	0
	≥200 to <600	0	0	0	0	0	0	0
	≥600 to <1000	0	0	0	0	0	0	0
	≥1000	0	0	0	0	0	0	0
Total		**0**	**0**	**0**	**0**	**0**	**5,902**	**1,761**

Table M.2. Estimated casualties within the light damage zone resulting from thermal and radiation effects in the unwarned scenario after 48 hours, following a 15 kt IND detonation in downtown Atlanta, GA at 10:00 am local time on July 2, 2019 (Medoid 3).

Thermal Fluence Range (cal/cm^2)	Radiation Dose (rad)	Blast		Thermal			Radiation	
		Fatalities	Injuries	1st degree	2nd degree	3rd degree	Fatalities	Injuries
<1.4	<50	0	3,072	0	0	0	0	0
	≥50 to <200	0	19	0	0	0	183	44
	≥200 to <600	0	30	0	0	0	1,095	323
	≥600 to <1000	0	3	0	0	0	197	15
	≥1000	0	1	0	0	0	51	0
≥1.4 to <3.53	<50	0	3,075	25,420	0	0	0	0
	≥50 to <200	0	93	688	0	0	184	17
	≥200 to <600	0	78	801	0	0	1,406	386
	≥600 to <1000	0	9	154	0	0	354	39
	≥1000	0	7	50	0	0	154	0
≥3.53 to <6.00	<50	0	1,179	8,194	8,322	0	0	0
	≥50 to <200	0	103	913	549	0	224	16
	≥200 to <600	0	14	140	92	0	200	69
	≥600 to <1000	0	4	33	69	0	174	10
	≥1000	0	9	72	51	0	202	0
≥6.00 to <8.67	<50	0	538	0	2,121	3,111	0	0
	≥50 to <200	0	155	0	59	664	272	34
	≥200 to <600	0	0	0	18	14	19	4
	≥600 to <1000	0	0	0	7	29	62	14
	≥1000	0	0	0	6	6	19	0
≥8.67	<50	0	282	0	0	4,070	0	0
	≥50 to <200	0	38	0	0	657	86	18
	≥200 to <600	0	16	0	0	175	118	43
	≥600 to <1000	0	2	0	0	44	52	2
	≥1000	0	1	0	0	21	21	0
Total		**0**	**8,728**	**36,465**	**11,294**	**8,791**	**5,073**	**1,034**

Table M.3. Estimated casualties within the moderate damage zone resulting from thermal and radiation effects in the unwarned scenario after 48 hours, following a 15 kt IND detonation in downtown Atlanta, GA at 10:00 am local time on July 2, 2019 (Medoid 3).

Thermal Fluence Range (cal/cm^2)	Radiation Dose (rad)	Blast		Thermal			Radiation	
		Fatalities	Injuries	1st degree	2nd degree	3rd degree	Fatalities	Injuries
<1.4	<50	0	5	0	0	0	0	0
	≥50 to <200	0	13	0	0	0	6	1
	≥200 to <600	0	6	0	0	0	8	6
	≥600 to <1000	0	1	0	0	0	3	0
	≥1000	0	6	0	0	0	22	0
≥1.4 to <3.53	<50	0	15	60	0	0	0	0
	≥50 to <200	0	30	68	0	0	25	5
	≥200 to <600	7	123	195	0	0	256	82
	≥600 to <1000	1	13	21	0	0	38	2
	≥1000	0	7	8	0	0	14	0
≥3.53 to <6.00	<50	0	111	115	579	0	0	0
	≥50 to <200	10	241	201	905	0	370	111
	≥200 to <600	41	464	43	442	0	818	192
	≥600 to <1000	0	4	5	9	0	17	1
	≥1000	6	57	20	51	0	111	0
≥6.00 to <8.67	<50	0	164	0	409	552	0	0
	≥50 to <200	43	697	0	1,861	967	911	280
	≥200 to <600	44	580	0	135	545	1,308	501
	≥600 to <1000	4	58	0	121	53	176	34
	≥1000	33	286	0	47	257	707	0
≥8.67	<50	0	144	0	0	1,623	0	0
	≥50 to <200	122	1,719	0	0	6,041	1,957	554
	≥200 to <600	544	5,121	0	0	10,452	7,040	2,783
	≥600 to <1000	82	657	0	0	1,556	1,602	267
	≥1000	112	989	0	0	2,149	2,283	0
Total		**1,049**	**11,511**	**736**	**4,559**	**24,195**	**17,672**	**4,819**

Table M.4. Estimated casualties within the severe damage zone resulting from thermal and radiation effects in the unwarned scenario after 48 hours, following a 15 kt IND detonation in downtown Atlanta, GA at 10:00 am local time on July 2, 2019 (Medoid 3).

Thermal Fluence Range (cal/cm^2)	Radiation Dose (rad)	Blast		Thermal			Radiation	
		Fatalities	Injuries	1st degree	2nd degree	3rd degree	Fatalities	Injuries
<1.4	<50	0	0	0	0	0	0	0
	≥50 to <200	0	0	0	0	0	0	0
	≥200 to <600	0	0	0	0	0	0	0
	≥600 to <1000	0	0	0	0	0	0	0
	≥1000	0	0	0	0	0	0	0
≥1.4 to <3.53	<50	0	0	0	0	0	0	0
	≥50 to <200	0	0	0	0	0	0	0
	≥200 to <600	1	1	1	0	0	1	0
	≥600 to <1000	0	0	0	0	0	0	0
	≥1000	0	0	0	0	0	0	0
≥3.53 to <6.00	<50	0	0	0	0	0	0	0
	≥50 to <200	0	0	0	0	0	0	0
	≥200 to <600	1	1	1	0	0	0	0
	≥600 to <1000	0	0	0	0	0	0	0
	≥1000	0	0	0	0	0	0	0
≥6.00 to <8.67	<50	0	0	0	0	0	0	0
	≥50 to <200	62	49	0	0	23	15	2
	≥200 to <600	4	3	0	0	1	3	1
	≥600 to <1000	2	0	0	0	0	2	0
	≥1000	8	6	0	0	3	14	0
≥8.67	<50	0	0	0	0	0	0	0
	≥50 to <200	12,360	2,323	0	0	12,027	3,924	1,313
	≥200 to <600	43,480	9,954	0	0	44,004	31,342	12,292
	≥600 to <1000	17,708	3,353	0	0	17,211	18,295	2,668
	≥1000	31,789	6,772	0	0	31,807	38,542	0
Total		**105,415**	**22,462**	**2**	**0**	**105,076**	**92,138**	**16,276**

Table M.5. Estimated casualties outside the damage zone resulting from thermal and radiation effects in the warned scenario after 48 hours, following a 15 kt IND detonation in downtown Atlanta, GA at 10:00 am local time on July 2, 2019 (Medoid 3).

Thermal Fluence Range (cal/cm^2)	Radiation Dose (rad)	Blast		Thermal			Radiation	
		Fatalities	Injuries	1st degree	2nd degree	3rd degree	Fatalities	Injuries
<1.4	<50	0	0	0	0	0	0	0
	≥50 to <200	0	0	0	0	0	1,767	527
	≥200 to <600	0	0	0	0	0	456	192
	≥600 to <1000	0	0	0	0	0	54	9
	≥1000	0	0	0	0	0	122	0
≥1.4 to <3.53	<50	0	0	0	0	0	0	0
	≥50 to <200	0	0	0	0	0	0	0
	≥200 to <600	0	0	0	0	0	0	0
	≥600 to <1000	0	0	0	0	0	0	0
	≥1000	0	0	0	0	0	0	0
≥3.53 to <6.00	<50	0	0	0	0	0	0	0
	≥50 to <200	0	0	0	0	0	0	0
	≥200 to <600	0	0	0	0	0	0	0
	≥600 to <1000	0	0	0	0	0	0	0
	≥1000	0	0	0	0	0	0	0
≥6.00 to <8.67	<50	0	0	0	0	0	0	0
	≥50 to <200	0	0	0	0	0	0	0
	≥200 to <600	0	0	0	0	0	0	0
	≥600 to <1000	0	0	0	0	0	0	0
	≥1000	0	0	0	0	0	0	0
≥8.67	<50	0	0	0	0	0	0	0
	≥50 to <200	0	0	0	0	0	0	0
	≥200 to <600	0	0	0	0	0	0	0
	≥600 to <1000	0	0	0	0	0	0	0
	≥1000	0	0	0	0	0	0	0
Total		**0**	**0**	**0**	**0**	**0**	**2,399**	**728**

Table M.6. Estimated casualties within the light damage zone resulting from thermal and radiation effects in the warned scenario after 48 hours, following a 15 kt IND detonation in downtown Atlanta, GA at 10:00 am local time on July 2, 2019 (Medoid 3).

Thermal Fluence Range (cal/cm^2)	Radiation Dose (rad)	Blast		Thermal			Radiation	
		Fatalities	Injuries	1st degree	2nd degree	3rd degree	Fatalities	Injuries
<1.4	<50	0	3,094	0	0	0	0	0
	≥50 to <200	0	24	0	0	0	226	75
	≥200 to <600	0	7	0	0	0	182	60
	≥600 to <1000	0	0	0	0	0	2	0
	≥1000	0	0	0	0	0	0	0
≥1.4 to <3.53	<50	0	3,159	26,099	0	0	0	0
	≥50 to <200	0	86	888	0	0	498	171
	≥200 to <600	0	16	126	0	0	245	86
	≥600 to <1000	0	0	0	0	0	2	0
	≥1000	0	0	0	0	0	0	0
≥3.53 to <6.00	<50	0	1,289	9,164	8,896	0	0	0
	≥50 to <200	0	15	164	144	0	70	22
	≥200 to <600	0	2	24	38	0	54	18
	≥600 to <1000	0	2	0	6	0	26	6
	≥1000	0	0	0	0	0	0	0
≥6.00 to <8.67	<50	0	550	0	2,165	3,211	0	0
	≥50 to <200	0	143	0	41	607	181	0
	≥200 to <600	0	0	0	4	6	14	4
	≥600 to <1000	0	0	0	0	0	0	0
	≥1000	0	0	0	0	0	0	0
≥8.67	<50	0	298	0	0	4,368	0	0
	≥50 to <200	0	33	0	0	509	81	15
	≥200 to <600	0	7	0	0	87	50	20
	≥600 to <1000	0	0	0	0	2	2	0
	≥1000	0	0	0	0	0	0	0
Total		**0**	**8,725**	**36,465**	**11,294**	**8,790**	**1,633**	**477**

Table M.7. Estimated casualties within the moderate damage zone resulting from thermal and radiation effects in the warned scenario after 48 hours, following a 15 kt IND detonation in downtown Atlanta, GA at 10:00 am local time on July 2, 2019 (Medoid 3).

Thermal Fluence Range (cal/cm^2)	Radiation Dose (rad)	Blast		Thermal			Radiation	
		Fatalities	Injuries	1st degree	2nd degree	3rd degree	Fatalities	Injuries
<1.4	<50	0	15	0	0	0	0	0
	≥50 to <200	0	5	0	0	0	3	0
	≥200 to <600	0	6	0	0	0	8	6
	≥600 to <1000	0	6	0	0	0	18	2
	≥1000	0	0	0	0	0	0	0
≥1.4 to <3.53	<50	0	28	77	0	0	0	0
	≥50 to <200	0	53	105	0	0	61	16
	≥200 to <600	8	101	164	0	0	216	65
	≥600 to <1000	0	2	3	0	0	5	0
	≥1000	0	2	2	0	0	6	0
≥3.53 to <6.00	<50	0	216	128	1,146	0	0	0
	≥50 to <200	17	196	223	425	0	271	93
	≥200 to <600	39	465	31	413	0	755	166
	≥600 to <1000	0	0	1	1	0	2	0
	≥1000	0	0	0	0	0	0	0
≥6.00 to <8.67	<50	0	183	0	427	621	0	0
	≥50 to <200	86	998	0	2,096	1,143	1,181	377
	≥200 to <600	11	366	0	17	392	903	351
	≥600 to <1000	2	77	0	34	87	256	43
	≥1000	26	162	0	0	130	262	0
≥8.67	<50	35	460	0	0	2,781	0	0
	≥50 to <200	374	3,352	0	0	8,637	2,791	1,183
	≥200 to <600	394	4,366	0	0	9,261	6,491	2,585
	≥600 to <1000	43	349	0	0	880	927	145
	≥1000	13	104	0	0	261	314	0
Total		**1,048**	**11,512**	**734**	**4,559**	**24,193**	**14,470**	**5,032**

Table M.8. Estimated casualties within the severe damage zone resulting from thermal and radiation effects in the warned scenario after 48 hours, following a 15 kt IND detonation in downtown Atlanta, GA at 10:00 am local time on July 2, 2019 (Medoid 3).

Thermal Fluence Range (cal/cm^2)	Radiation Dose (rad)	Blast		Thermal			Radiation	
		Fatalities	Injuries	1st degree	2nd degree	3rd degree	Fatalities	Injuries
<1.4	<50	0	0	0	0	0	0	0
	≥50 to <200	0	0	0	0	0	0	0
	≥200 to <600	0	0	0	0	0	0	0
	≥600 to <1000	0	0	0	0	0	0	0
	≥1000	0	0	0	0	0	0	0
≥1.4 to <3.53	<50	0	0	0	0	0	0	0
	≥50 to <200	0	0	0	0	0	0	0
	≥200 to <600	1	1	1	0	0	1	0
	≥600 to <1000	0	0	0	0	0	0	0
	≥1000	0	0	0	0	0	0	0
≥3.53 to <6.00	<50	0	0	0	0	0	0	0
	≥50 to <200	0	0	0	0	0	0	0
	≥200 to <600	1	1	1	0	0	0	0
	≥600 to <1000	0	0	0	0	0	0	0
	≥1000	0	0	0	0	0	0	0
≥6.00 to <8.67	<50	57	48	0	0	20	0	0
	≥50 to <200	12	6	0	0	6	6	3
	≥200 to <600	4	3	0	0	1	3	1
	≥600 to <1000	2	0	0	0	0	2	0
	≥1000	0	0	0	0	0	0	0
≥8.67	<50	4,984	876	0	0	4,795	0	0
	≥50 to <200	26,295	4,870	0	0	25,520	8,017	2,621
	≥200 to <600	42,658	10,137	0	0	43,493	30,525	11,135
	≥600 to <1000	11,084	2,178	0	0	10,851	11,127	2,030
	≥1000	20,315	4,341	0	0	20,389	24,804	0
Total		**105,413**	**22,461**	**2**	**0**	**105,075**	**74,485**	**15,790**

APPENDIX N

COMBINED EFFECTS CASUALTIES – MEDOID 4

Table N.1. Estimated casualties outside the damage zone resulting from thermal and radiation effects in the unwarned scenario after 48 hours, following a 15 kt IND detonation in downtown Atlanta, GA at 10:00 am local time on August 19, 2019 (Medoid 4).

Thermal Fluence Range (cal/cm^2)	Radiation Dose (rad)	Blast		Thermal			Radiation	
		Fatalities	Injuries	1st degree	2nd degree	3rd degree	Fatalities	Injuries
<1.4	<50	0	0	0	0	0	0	0
	≥50 to <200	0	0	0	0	0	1,829	487
	≥200 to <600	0	0	0	0	0	3,270	1,117
	≥600 to <1000	0	0	0	0	0	858	158
	≥1000	0	0	0	0	0	472	0
≥1.4 to <3.53	<50	0	0	0	0	0	0	0
	≥50 to <200	0	0	0	0	0	0	0
	≥200 to <600	0	0	0	0	0	0	0
	≥600 to <1000	0	0	0	0	0	0	0
	≥1000	0	0	0	0	0	0	0
≥3.53 to <6.00	<50	0	0	0	0	0	0	0
	≥50 to <200	0	0	0	0	0	0	0
	≥200 to <600	0	0	0	0	0	0	0
	≥600 to <1000	0	0	0	0	0	0	0
	≥1000	0	0	0	0	0	0	0
≥6.00 to <8.67	<50	0	0	0	0	0	0	0
	≥50 to <200	0	0	0	0	0	0	0
	≥200 to <600	0	0	0	0	0	0	0
	≥600 to <1000	0	0	0	0	0	0	0
	≥1000	0	0	0	0	0	0	0

Thermal Fluence Range (cal/cm^2)	Radiation Dose (rad)	Blast		Thermal			Radiation	
		Fatalities	Injuries	1st degree	2nd degree	3rd degree	Fatalities	Injuries
≥8.67	<50	0	0	0	0	0	0	0
	≥50 to <200	0	0	0	0	0	0	0
	≥200 to <600	0	0	0	0	0	0	0
	≥600 to <1000	0	0	0	0	0	0	0
	≥1000	0	0	0	0	0	0	0
Total		**0**	**0**	**0**	**0**	**0**	**6,429**	**1,762**

Table N.2. Estimated casualties within the light damage zone resulting from thermal and radiation effects in the unwarned scenario after 48 hours, following a 15 kt IND detonation in downtown Atlanta, GA at 10:00 am local time on August 19, 2019 (Medoid 4).

Thermal Fluence Range (cal/cm^2)	Radiation Dose (rad)	Blast		Thermal			Radiation	
		Fatalities	Injuries	1st degree	2nd degree	3rd degree	Fatalities	Injuries
<1.4	<50	0	3,357	0	0	0	0	0
	≥50 to <200	0	101	0	0	0	432	56
	≥200 to <600	0	50	0	0	0	1,734	566
	≥600 to <1000	0	32	0	0	0	892	117
	≥1000	0	15	0	0	0	393	0
≥1.4 to <3.53	<50	0	3,556	29,258	0	0	0	0
	≥50 to <200	0	195	1,642	0	0	614	151
	≥200 to <600	0	38	285	0	0	640	228
	≥600 to <1000	0	96	591	0	0	1,796	261
	≥1000	0	27	178	0	0	540	0
≥3.53 to <6.00	<50	0	1,256	11,509	8,560	0	0	0
	≥50 to <200	0	84	674	713	0	167	9
	≥200 to <600	0	15	53	164	0	259	94
	≥600 to <1000	0	70	72	608	0	1,207	171
	≥1000	0	14	26	125	0	279	0
≥6.00 to <8.67	<50	0	290	0	1,349	2,178	0	0
	≥50 to <200	0	270	0	308	1,247	480	41
	≥200 to <600	0	18	0	54	89	243	105
	≥600 to <1000	0	94	0	578	462	1,584	217
	≥1000	0	25	0	98	126	480	0
≥8.67	<50	0	229	0	0	3,456	0	0
	≥50 to <200	0	79	0	0	1,102	199	45
	≥200 to <600	0	40	0	0	489	398	106
	≥600 to <1000	0	25	0	0	444	472	65
	≥1000	0	9	0	0	124	129	0
Total		**0**	**9,985**	**44,288**	**12,557**	**9,717**	**12,938**	**2,232**

Table N.3. Estimated casualties within the moderate damage zone resulting from thermal and radiation effects in the unwarned scenario after 48 hours, following a 15 kt IND detonation in downtown Atlanta, GA at 10:00 am local time on August 19, 2019 (Medoid 4).

Thermal Fluence Range (cal/cm^2)	Radiation Dose (rad)	Blast		Thermal			Radiation	
		Fatalities	Injuries	1st degree	2nd degree	3rd degree	Fatalities	Injuries
<1.4	<50	0	4	0	0	0	0	0
	≥50 to <200	0	14	0	0	0	19	7
	≥200 to <600	0	11	0	0	0	19	9
	≥600 to <1000	0	1	0	0	0	2	0
	≥1000	0	2	0	0	0	11	0
≥1.4 to <3.53	<50	0	10	52	0	0	0	0
	≥50 to <200	0	22	69	0	0	25	3
	≥200 to <600	5	94	148	0	0	190	62
	≥600 to <1000	0	11	12	0	0	35	5
	≥1000	0	9	15	0	0	26	0
≥3.53 to <6.00	<50	0	146	112	773	0	0	0
	≥50 to <200	10	271	167	1,119	0	402	104
	≥200 to <600	40	469	57	460	0	884	217
	≥600 to <1000	1	21	26	19	0	52	9
	≥1000	6	60	23	54	0	117	0
≥6.00 to <8.67	<50	0	87	0	67	365	0	0
	≥50 to <200	45	714	0	1,916	983	940	292
	≥200 to <600	55	547	0	108	577	1,039	412
	≥600 to <1000	14	236	0	127	156	660	103
	≥1000	8	82	0	10	60	222	0
≥8.67	<50	0	217	0	0	2,164	0	0
	≥50 to <200	87	1,394	0	0	5,772	1,836	499
	≥200 to <600	508	4,964	0	0	10,187	6,830	2,682
	≥600 to <1000	90	764	0	0	1,795	1,897	272
	≥1000	146	1,240	0	0	2,662	2,868	0
Total		**1,015**	**11,390**	**681**	**4,653**	**24,721**	**18,074**	**4,676**

Table N.4. Estimated casualties within the severe damage zone resulting from thermal and radiation effects in the unwarned scenario after 48 hours, following a 15 kt IND detonation in downtown Atlanta, GA at 10:00 am local time on August 19, 2019 (Medoid 4).

Thermal Fluence Range (cal/cm^2)	Radiation Dose (rad)	Blast		Thermal			Radiation	
		Fatalities	Injuries	1st degree	2nd degree	3rd degree	Fatalities	Injuries
<1.4	<50	0	0	0	0	0	0	0
	≥50 to <200	0	0	0	0	0	0	0
	≥200 to <600	0	0	0	0	0	0	0
	≥600 to <1000	0	0	0	0	0	0	0
	≥1000	0	0	0	0	0	0	0
≥1.4 to <3.53	<50	0	0	0	0	0	0	0
	≥50 to <200	0	0	0	0	0	0	0
	≥200 to <600	1	1	1	0	0	1	0
	≥600 to <1000	0	0	0	0	0	0	0
	≥1000	0	0	0	0	0	0	0
≥3.53 to <6.00	<50	0	0	0	0	0	0	0
	≥50 to <200	0	0	0	0	0	0	0
	≥200 to <600	1	1	1	0	0	0	0
	≥600 to <1000	0	0	0	0	0	0	0
	≥1000	0	0	0	0	0	0	0
≥6.00 to <8.67	<50	0	0	0	0	0	0	0
	≥50 to <200	57	48	0	0	20	13	1
	≥200 to <600	8	4	0	0	4	6	2
	≥600 to <1000	2	0	0	0	0	2	0
	≥1000	7	6	0	0	3	14	0
≥8.67	<50	0	0	0	0	0	0	0
	≥50 to <200	6,888	1,348	0	0	6,746	2,603	931
	≥200 to <600	45,056	10,187	0	0	45,608	32,879	11,899
	≥600 to <1000	23,652	4,849	0	0	23,284	24,671	3,939
	≥1000	29,741	6,017	0	0	29,410	35,609	0
Total		**105,413**	**22,461**	**2**	**0**	**105,075**	**95,798**	**16,772**

Table N.5. Estimated casualties outside the damage zone resulting from thermal and radiation effects in the warned scenario after 48 hours, following a 15 kt IND detonation in downtown Atlanta, GA at 10:00 am local time on August 19, 2019 (Medoid 4).

Thermal Fluence Range (cal/cm^2)	Radiation Dose (rad)	Blast		Thermal			Radiation	
		Fatalities	Injuries	1st degree	2nd degree	3rd degree	Fatalities	Injuries
<1.4	<50	0	0	0	0	0	0	0
	≥50 to <200	0	0	0	0	0	2,022	623
	≥200 to <600	0	0	0	0	0	441	175
	≥600 to <1000	0	0	0	0	0	119	14
	≥1000	0	0	0	0	0	197	0
≥1.4 to <3.53	<50	0	0	0	0	0	0	0
	≥50 to <200	0	0	0	0	0	0	0
	≥200 to <600	0	0	0	0	0	0	0
	≥600 to <1000	0	0	0	0	0	0	0
	≥1000	0	0	0	0	0	0	0
≥3.53 to <6.00	<50	0	0	0	0	0	0	0
	≥50 to <200	0	0	0	0	0	0	0
	≥200 to <600	0	0	0	0	0	0	0
	≥600 to <1000	0	0	0	0	0	0	0
	≥1000	0	0	0	0	0	0	0
≥6.00 to <8.67	<50	0	0	0	0	0	0	0
	≥50 to <200	0	0	0	0	0	0	0
	≥200 to <600	0	0	0	0	0	0	0
	≥600 to <1000	0	0	0	0	0	0	0
	≥1000	0	0	0	0	0	0	0
≥8.67	<50	0	0	0	0	0	0	0
	≥50 to <200	0	0	0	0	0	0	0
	≥200 to <600	0	0	0	0	0	0	0
	≥600 to <1000	0	0	0	0	0	0	0
	≥1000	0	0	0	0	0	0	0
Total		**0**	**0**	**0**	**0**	**0**	**2,779**	**812**

Table N.6. Estimated casualties within the light damage zone resulting from thermal and radiation effects in the warned scenario after 48 hours, following a 15 kt IND detonation in downtown Atlanta, GA at 10:00 am local time on August 19, 2019 (Medoid 4).

Thermal Fluence Range (cal/cm^2)	Radiation Dose (rad)	Blast		Thermal			Radiation	
		Fatalities	Injuries	1st degree	2nd degree	3rd degree	Fatalities	Injuries
<1.4	<50	0	3,470	0	0	0	0	0
	≥50 to <200	0	44	0	0	0	479	151
	≥200 to <600	0	42	0	0	0	673	231
	≥600 to <1000	0	0	0	0	0	0	0
	≥1000	0	0	0	0	0	0	0
≥1.4 to <3.53	<50	0	3,746	30,849	0	0	0	0
	≥50 to <200	0	40	356	0	0	169	43
	≥200 to <600	0	125	748	0	0	1,495	599
	≥600 to <1000	0	0	0	0	0	0	0
	≥1000	0	0	0	0	0	0	0
≥3.53 to <6.00	<50	0	1,346	12,196	9,353	0	0	0
	≥50 to <200	0	31	88	262	0	91	21
	≥200 to <600	0	62	49	554	0	819	335
	≥600 to <1000	0	0	0	0	0	0	0
	≥1000	0	0	0	0	0	0	0
≥6.00 to <8.67	<50	0	432	0	1,684	2,939	0	0
	≥50 to <200	0	148	0	48	606	198	4
	≥200 to <600	0	117	0	653	556	1,433	507
	≥600 to <1000	0	0	0	1	0	1	0
	≥1000	0	0	0	0	0	0	0
≥8.67	<50	0	275	0	0	4,144	0	0
	≥50 to <200	0	80	0	0	1,027	274	80
	≥200 to <600	0	23	0	0	392	271	93
	≥600 to <1000	0	3	0	0	51	49	12
	≥1000	0	0	0	0	0	0	0
Total		**0**	**9,984**	**44,286**	**12,555**	**9,715**	**5,952**	**2,076**

Table N.7. Estimated casualties within the moderate damage zone resulting from thermal and radiation effects in the warned scenario after 48 hours, following a 15 kt IND detonation in downtown Atlanta, GA at 10:00 am local time on August 19, 2019 (Medoid 4).

Thermal Fluence Range (cal/cm^2)	Radiation Dose (rad)	Blast		Thermal			Radiation	
		Fatalities	Injuries	1st degree	2nd degree	3rd degree	Fatalities	Injuries
<1.4	<50	0	12	0	0	0	0	0
	≥50 to <200	0	7	0	0	0	6	1
	≥200 to <600	0	11	0	0	0	20	10
	≥600 to <1000	0	1	0	0	0	2	0
	≥1000	0	0	0	0	0	0	0
≥1.4 to <3.53	<50	0	21	69	0	0	0	0
	≥50 to <200	0	34	82	0	0	45	7
	≥200 to <600	5	88	139	0	0	166	63
	≥600 to <1000	0	1	3	0	0	5	0
	≥1000	0	1	3	0	0	5	0
≥3.53 to <6.00	<50	0	306	124	1,567	0	0	0
	≥50 to <200	17	177	199	424	0	235	81
	≥200 to <600	39	481	61	431	0	816	186
	≥600 to <1000	0	1	0	1	0	2	0
	≥1000	0	1	0	1	0	3	0
≥6.00 to <8.67	<50	0	104	0	82	436	0	0
	≥50 to <200	76	937	0	2,124	1,106	1,131	359
	≥200 to <600	46	480	0	22	495	912	352
	≥600 to <1000	0	134	0	0	96	309	95
	≥1000	0	10	0	0	8	33	0
≥8.67	<50	19	417	0	0	2,998	0	0
	≥50 to <200	361	3,295	0	0	9,129	2,855	1,190
	≥200 to <600	328	3,965	0	0	8,486	5,989	2,419
	≥600 to <1000	87	653	0	0	1,418	1,463	253
	≥1000	36	248	0	0	548	666	0
Total		0	12	0	0	0	0	0

Table N.8. Estimated casualties within the severe damage zone resulting from thermal and radiation effects in the warned scenario after 48 hours, following a 15 kt IND detonation in downtown Atlanta, GA at 10:00 am local time on August 19, 2019 (Medoid 4).

Thermal Fluence Range (cal/cm^2)	Radiation Dose (rad)	Blast		Thermal			Radiation	
		Fatalities	Injuries	1st degree	2nd degree	3rd degree	Fatalities	Injuries
<1.4	<50	0	0	0	0	0	0	0
	≥50 to <200	0	0	0	0	0	0	0
	≥200 to <600	0	0	0	0	0	0	0
	≥600 to <1000	0	0	0	0	0	0	0
	≥1000	0	0	0	0	0	0	0
≥1.4 to <3.53	<50	0	0	0	0	0	0	0
	≥50 to <200	0	0	0	0	0	0	0
	≥200 to <600	1	1	1	0	0	1	0
	≥600 to <1000	0	0	0	0	0	0	0
	≥1000	0	0	0	0	0	0	0
≥3.53 to <6.00	<50	0	0	0	0	0	0	0
	≥50 to <200	0	0	0	0	0	0	0
	≥200 to <600	1	1	1	0	0	0	0
	≥600 to <1000	0	0	0	0	0	0	0
	≥1000	0	0	0	0	0	0	0
≥6.00 to <8.67	<50	57	48	0	0	20	0	0
	≥50 to <200	11	6	0	0	5	6	3
	≥200 to <600	4	3	0	0	1	3	1
	≥600 to <1000	2	0	0	0	0	2	0
	≥1000	0	0	0	0	0	0	0
≥8.67	<50	1,555	284	0	0	1,498	0	0
	≥50 to <200	30,090	5,505	0	0	29,148	8,650	2,744
	≥200 to <600	41,717	10,252	0	0	42,894	30,358	11,188
	≥600 to <1000	14,818	3,129	0	0	14,752	15,323	2,585
	≥1000	17,156	3,232	0	0	16,756	20,377	0
Total		**105,412**	**22,461**	**2**	**0**	**105,074**	**74,720**	**16,521**

APPENDIX O

INJURY PROFILES WITHIN TRIAGE CATEGORIES FOR THE WARNED SCENARIO

Table O.1. Estimated casualties by RTR triage category in the warned scenario after 48 hours, following a 15kt IND in downtown Atlanta, GA at 10:00 am local time on November 26, 2019 (Medoid 1). Abbreviations: ARS = Acute Radiation Sickness.

		No Burn	Burn	**Total**
Minimal				**1,058,446**
Subclinical ARS	No Trauma	829,175	0	829,175
	Minimal Trauma	227,023	2,244	229,267
Hematopoietic ARS	Minimal Trauma	4	0	4
Delayed				**1,789**
Hematopoietic ARS	Moderate Trauma	1,778	11	1,789
Immediate				**31,939**
Subclinical ARS	Minimal Trauma	6,990	7,524	14,514
	Moderate Trauma	15,989	768	16,757
Hematopoietic ARS	No Trauma	392	0	392
	Minimal Trauma	183	93	276
Expectant				**185,896**
Subclinical ARS	Moderate Trauma	5,984	8,404	14,388
	Severe Trauma	12,664	41,348	54,012
Hematopoietic ARS	Moderate Trauma	267	487	754
	Severe Trauma	16,149	62,672	78,821
Gastrointestinal/Cutaneous ARS	No Trauma	132	0	132
	Moderate Trauma	3	13	16
	Severe Trauma	4,315	17,647	21,962
Neurovascular ARS	Severe Trauma	2,908	12,903	15,811

Table O.2. Estimated casualties by RTR triage category in the warned scenario after 48 hours, following a 15kt IND in downtown Atlanta, GA at 10:00 am local time on November 25, 2019 (Medoid 2). Abbreviations: ARS = Acute Radiation Sickness.

		No Burn	Burn	**Total**
Minimal				**471,540**
Subclinical ARS	No Trauma	233,927	0	233,927
	Minimal Trauma	235,154	2,440	237,594
Hematopoietic ARS	Minimal Trauma	17	2	19
Delayed				**160**
Hematopoietic ARS	Moderate Trauma	159	1	160
Immediate				**39,875**
Subclinical ARS	Minimal Trauma	7,666	8,723	16,389
	Moderate Trauma	18,119	798	18,917
Hematopoietic ARS	No Trauma	4,252	0	4,252
	Minimal Trauma	297	20	317
Expectant				**186,156**
Subclinical ARS	Moderate Trauma	6,399	8,786	15,185
	Severe Trauma	15,173	49,441	64,614
Hematopoietic ARS	Moderate Trauma	36	195	231
	Severe Trauma	14,302	54,341	68,643
Gastrointestinal/Cutaneous ARS	No Trauma	132	0	36
	Moderate Trauma	3	7	8
	Severe Trauma	2,850	12,109	14,959
Neurovascular ARS	No Trauma	122	0	122
	Severe Trauma	3,986	18,372	22,358

Table O.3. Estimated casualties by RTR triage category in the warned scenario after 48 hours, following a 15kt IND in downtown Atlanta, GA at 10:00 am local time on July 2, 2019 (Medoid 3). Abbreviations: ARS = Acute Radiation Sickness.

		No Burn	Burn	**Total**
Minimal				**455,856**
Subclinical ARS	No Trauma	220,109	0	220,109
	Minimal Trauma	233,264	2,458	235,722
Hematopoietic ARS	Minimal Trauma	25	0	25
Delayed				**233**
Hematopoietic ARS	Moderate Trauma	228	5	233
Immediate				**35,941**
Subclinical ARS	Minimal Trauma	6,998	7,674	14,672
	Moderate Trauma	18,984	810	19,794
Hematopoietic ARS	No Trauma	726	0	726
	Minimal Trauma	728	21	749
Expectant				**186,043**
Subclinical ARS	Moderate Trauma	6,679	8,999	15,678
	Severe Trauma	14,543	47,617	62,160
Hematopoietic ARS	Moderate Trauma	25	109	134
	Severe Trauma	14,283	53,577	67,860
Gastrointestinal/Cutaneous ARS	No Trauma	63	0	63
	Minimal Trauma	4	0	4
	Moderate Trauma	26	8	34
	Severe Trauma	2,749	11,853	14,602
Neurovascular ARS	No Trauma	122	0	122
	Severe Trauma	4,606	20,780	25,386

Table O.4. Estimated casualties by RTR triage category in the warned scenario after 48 hours, following a 15kt IND in downtown Atlanta, GA at 10:00 am local time on August 19, 2019 (Medoid 4). Abbreviations: ARS = Acute Radiation Sickness.

		No Burn	Burn	**Total**
Minimal				**781,308**
Subclinical ARS	No Trauma	518,491	0	518,491
	Minimal Trauma	259,950	2,833	262,783
Hematopoietic ARS	Minimal Trauma	34	0	34
Delayed				**356**
Hematopoietic ARS	Moderate Trauma	344	12	356
Immediate				**44,716**
Subclinical ARS	Minimal Trauma	5,643	6,193	11,836
	Moderate Trauma	23,738	1,144	24,882
Hematopoietic ARS	No Trauma	841	0	841
	Minimal Trauma	5,244	1,913	7,157
Expectant				**188,146**
Subclinical ARS	Moderate Trauma	6,846	9,893	16,739
	Severe Trauma	14,578	48,537	63,115
Hematopoietic ARS	Moderate Trauma	110	230	340
	Severe Trauma	14,037	52,329	66,366
Gastrointestinal/Cutaneous ARS	No Trauma	133	0	133
	Moderate Trauma	10	52	62
	Severe Trauma	3,843	16,267	20,110
Neurovascular ARS	No Trauma	197	0	197
	Severe Trauma	3,771	17,313	21,084